Holographic conformal field theories and their flat-space structures

Yue-Zhou Li

Department of Physics

McGill University, Montréal

October, 2023

A thesis submitted to McGill University in partial fulfillment of the requirements of the degree of

Doctor of Philosophy

Declaration of Authorship

The present thesis is based on three of the projects that I have worked on during my Ph.D.:

- Chapter 3 is a reproduction of [1] that was written on my own. This project unofficially began during the completion of my paper [2] collaborated with my supervisor Professor Simon Caron-Huot. At that time, I was reading and reviewing the "bulk-point limit" for writing [2], and realized the relevant literature was messy for me because there are different ways to perform the limit. I started straightening the literature by learning the detailed derivations and writing notes on the "flat-space limit". A discussion with my supervisor Professor Simon Caron-Huot on a section of [3] was insightful. The authors of [3] demonstrated that their proposal could be recast into a known one by saddle point analysis. I immediately realized the saddle point was the key and promptly finished this project by connecting all known frameworks using the saddle point analysis.

- Chapter 4 is a reproduction of [2] that was written in collaboration with my supervisor Professor Simon Caron-Huot. This project requires advanced knowledge of harmonic analysis, the Lorentzian inversion formula, and scattering amplitudes. I made a very insightful observation that allowed me to avoid the technical and abstract sessions of harmonic analysis and correctly obtain the OPE for spinning operators of mean-field theory. This mainly contributed to the results recorded in sections 4.3.1 and 4.3.2. After that, I became more familiar with the goal and tools of this project, such as the Lorentzian inversion formula. Independent of Professor Simon Caron-Huot, I developed the integration-by-part trick to turn the spinning bootstrap into the scalar bootstrap and computed anomalous dimensions appending to my supervisor's results, which partially contributed to section 4.4. Surprisingly, I also understood my supervisor's idea of producing the flat-space limit and thus worked out section 4.5. I wrote most sections of the draft of this paper, and Professor Simon Caron-Huot made modifications and added some new understanding and results based on my rough draft.

- Chapter 5 is a reproduction of [4] that was written in collaboration with my supervisor Professor Simon Caron-Huot, Dr. Julio Parra-Martinez who is a postdoc from Caltech and Professor David Simmons-Duffin who is a professor from Caltech. Our original target was photon scattering, for which I used projectors of conformal blocks from another paper to construct photon partial waves relevant to our purpose. The efficiency of this method was pretty slow, and Professor Simon Caron-Huot suggested inviting Professor David Simmons-Duffin to join because he is an expert on group representation theory and semi-definite programming, both essential ingredients of this project. Later, Professor David Simmons-Duffin invited Dr. Julio Parra-Martinez to join because of his expertise in scattering amplitudes. Professor David Simmons-Duffin's weight-shifting methods could quickly reproduce my previous results for the photon case, and we even proceeded to construct graviton partial waves in all dimensions $D \geq 4$. On the other hand, Professor Simon Caron-Huot constructed all dispersive sum rules and low energy amplitudes for photon and graviton scattering, and Julio Parra-Martinez and myself made nontrivial double-checks. Finally, we moved to the stage where we should gather all ingredients and program them to obtain our rigorous bounds for low-energy EFT using SDPB. During this period, I learned to use SDPB and high-performance computing. I modified the Haskell codes made by David Simmons-Duffin to investigate different bounds and analyze the functionals. This project was highly competitive; thus, we put out a paper soon with our $D = 4$ graviton results [5]. We organized our results for higher dimensional graviton four months later and wrote [4]. I wrote parts of section 5.2 and the interpretation of central charge in 5.4 and some of the Appendices.

- Chapter 6 is a reproduction of [6] that was written on my own. This project began in 2020, as many researchers are looking for a double copy relation in AdS. As trained by the project of Chapter 4, I believe I have expertise in spinning correlators in CFTs, which can benefit this direction. Nevertheless, this project is challenging and highly competitive. At first, I immediately observed how to differentially represent simple contact diagrams in AdS. However, I did not find a way to generalize my findings to the diagrams with spinning particles being exchanged. The discussion with Jiajie Mei drew my attention to [7], letting me know the differential representation. While collaborating with Jiajie on another project, I realized that the essence of differential representation is the Casimir equation of single-trace conformal block. As the Casimir equation eliminates the single-trace operator, the resulting correlator contains pure double-trace and is organized as effective contact diagrams. This is a universal fact in CFTs regardless of whether the operator carries spin; my previous observation can represent the effective contact diagrams. During my visit to the Hong Kong University of Science and Technology, invited by Professor Yi Wang from November 2022 to December 2022, I started to work out the details.

These articles have only been modified to agree with the McGill thesis format and to fix apparent typos.

It is common practice in theoretical high-energy physics to list authors alphabetically. I have been an important, integral, and contributing part in each of these projects in all steps, from defining the problems to writing the papers.

The rest of the thesis is a review of previous literature, and a discussion of the works reproduced here.

Abstract

In this thesis, we discuss some novel and hidden structures and constraints of Anti de-Sitter space (AdS) and holographic conformal field theories (CFT). First, we review different frameworks for taking the flat-space limit of holographic CFT correlators in the literature. Using the saddle point analysis, we point out that different descriptions of the flat-space limit share the same origin from the holographic reconstruction as saddle points of smearing the boundary dynamics. Second, we focus on CFTs in three dimensions and describe the construction of the helicity basis for orthogonally organizing spinning conformal correlators. Using this basis, we apply the harmonic analysis and the Lorentzian inversion formula to study holographic four-point correlators of conserved currents. We also explore the bulk-point limit for the anomalous dimensions of double-twist operators and prove they coincide with the flat-space phase shift. Third, we provide group theoretical methods to construct the partial waves of flat-space graviton scattering amplitudes in dimensions higher than four. Combining the unitarity and causality, we provide sharp bounds on the size of higher-derivative curvature corrections in terms of the mass of new higher-spin states. In five dimensions, we describe the uplift of our sharp bounds to central charge bound in four-dimensional holographic CFTs. Finally, we find the differential representation of gluon and graviton amplitude in AdS, allowing us to uplift the flat-space amplitudes to AdS. The differential representation is powerful in revealing the hidden structures of AdS and holographic CFTs, as we manifestly prove the three-point doubly copy relation. Using the conformal generators, we also prove the differential Bern-Carrasco-Johansson (BCJ) for four-point Yang-Mills amplitudes in AdS.

Abrégé

Dans cette thèse, nous discutons de certaines structures et contraintes nouvelles et cachées de l'espace Anti-de Sitter (AdS) et des théories de champs conformes holographiques (CFT). Tout d'abord, nous passons en revue différents cadres pour prendre la limite d'espace plat des corrélateurs CFT holographiques dans la littérature. En utilisant l'analyse du point de selle, nous soulignons que différentes descriptions de la limite d'espace plat partagent la même origine que la reconstruction holographique en tant que points de selle de lissage de la dynamique de la frontière. Deuxièmement, nous nous concentrons sur les CFT en trois dimensions et décrivons la construction de la base d'hélicité pour organiser orthogonalement les corrélateurs conformes tournants. En utilisant cette base, nous appliquons l'analyse harmonique et la formule d'inversion lorentzienne pour étudier les corrélateurs holographiques à quatre points de courants conservés. Nous explorons également la limite du point de volume pour les dimensions anormales des opérateurs à double torsion et prouvons qu'elles coïncident avec le déphasage d'espace plat. Troisièmement, nous proposons des méthodes de groupe théorique pour construire les ondes partielles des amplitudes de diffusion de graviton d'espace plat dans des dimensions supérieures à quatre. En combinant l'unitarité et la causalité, nous fournissons des limites précises sur la taille des corrections de courbure à dérivées supérieures en termes de la masse de nouveaux états de spin supérieurs. En cinq dimensions, nous décrivons l'élévation de nos limites précises à la limite de charge centrale dans les CFT holographiques en quatre dimensions. Enfin, nous trouvons la représentation différentielle de l'amplitude de gluon et de graviton dans AdS, ce qui nous permet de hisser les amplitudes d'espace plat à AdS. La représentation différentielle est puissante pour révéler les structures cachées d'AdS et des CFT holographiques, car nous prouvons manifestement la relation de double copie à trois points. En utilisant les générateurs conformes, nous prouvons également le BCJ différentiel pour les amplitudes de Yang-Mills à quatre points dans AdS.

Acknowledgements

I would like to sincerely thank my supervisor Professor Simon Caron-Huot for all his great help and support since 2019 throughout my studies. I am pleased and excited to be his Ph.D. student and have the chance to work with him. I learn a lot from him, not only knowledge of high-energy physics but also coding skills and way of thinking, etc. I am also grateful for his tolerance of my stupidity and mistakes throughout our contact.

I would like to thank my supervisory committee members, Professor Alexander Maloney and Professor Keshav Dasgupta, for their review, questions, and encouragement during each progress tracking report.

I would also like to thank my collaborator Professor David Simmons-Duffin for his guidance on the research project. I always have the great pleasure of talking to and discussing with him, and I am also grateful for his patience in tolerating my stupidness sometimes.

I would also like to thank my collaborators: Junyu Liu, Hong Lu, Liang Ma, Jiajie Mei, and Julio Parra-Martinez. I have learned a lot from their discussions and collaborations, and I am grateful for their encouragement.

I also want to thank my friends Wenliang Li, Jiaxin Qiao, Cheng Shang, Yuan Xin, Xiang Zhao, and Zechuan Zheng, as well as my colleagues at McGill University Vincent Dumont, Mathieu Giroux, Viraj Meruliya, Beatrix Muehlmann, Keivan Namjou, and Zahra Zahraee, for all the discussions and chats with them when I felt overwhelming.

Finally, I would love to thank my parents, Li Li and Juan Yue, and my girlfriend, Jian-Hua Ren, for their love and support during my Ph.D. I am especially grateful to Jian-Hua, my beloved, who is always on my back with all her love and encouragement.

Contents

List of Tables

List of Figures

Chapter 1

Introduction

Local quantum field theories (QFT) are essential in understanding fundamental particles. In the framework of QFTs, the building blocks are fields spreading over the whole space, and the particles are created once the fields are excited. In this framework, particles can be created, annihilated, and interact with each other by exchanging particular types of particles, as governed by the dynamics of fields. Since last century, tremendous progress has been made on QFT in the flat Minkowski space. The flat Minkowski space is a uniform and flat spacetime not shaped by the gravity field. Throughout this thesis, we refer to this spacetime as the flat-space. These profound developments drove the establishment of the standard model (SM) of particles in the flat-space, which successfully predicts and explains exciting phenomena with high precision regarding particles' existence and behavior discovered and verified by the large colliders [8].

However, General Relativity, an extraordinary and successful theory of gravity, states that any matter and energy can bend spacetime away from the flat-space. Heavier matters come with more curved space. Therefore, the actual situation is that fundamental particles are propagating and interacting in a curved space. For example, the broadest picture of this kind is our Universe. Our Universe is not flat; it behaves like an expanding balloon that can be approximated by a de Sitter (dS) space. This fact leads to one crucial question: why and how can the SM, a model that is built upon the flat-space QFT, accurately predict the colliding experiments performed in a generally curved space? Our ordinary life provides an intuitive answer: the surface of the Earth is a sphere, but we walk as in a flat plane because the scale of our activities and horizon is extremely short compared to the radius of the Earth. A similar logic applies to the colliding particles: when the colliding happens in a region small enough compared to the "radius" of the curved space (that is the inverse of the curvature), the curvature effects can be neglected, and the particles' behavior can be locally described by the flat-space QFT.

Nonetheless, it is hard to quantitatively prove the aforementioned intuitive picture from the general frameworks of QFTs in curved space. The colliding experiments involve initially preparing particles and finally detecting the final particles. From the fundamental principle of quantum mechanics, this process can be mathematically packaged by a matrix between initial and final states. This matrix is phrased as the S-matrix, where the word "S" refers to the "scattering" because particles are deflected from their original path via colliding with other particles. S-matrix is a broad and complete description of a scattering process, and its individual coefficients, known as the scattering amplitudes, are already sufficient to represent specific scattering events detected in the experiments. Therefore, a sharp proof of the intuitive picture mentioned above requires deducing the flat-space S-matrix or scattering amplitudes from the scattering process in a curved space by localizing the process into a small and local region, which is tremendously difficult to come by.

A less ambitious step is restricting the scattering process to a maximally symmetric space. Sphere and hyperbolic space are maximally symmetric spaces in the Euclidean signature (i.e., no real-time direction). As Wick rotates to the Lorentzian signature, i.e., including the time direction, they are called the dS and Anti de-Sitter (AdS) space. This space contains a large number of isometry that may help improve the understanding of the scattering on it. Although our Universe is approximately a dS space, we consider AdS throughout this thesis for the reason we shall explain shortly. Therefore, the essential question to ask is

Q1: Can the scattering process in AdS define S-matrix or scattering amplitudes in the flat Minkowski spacetime at the limit of large AdS

radius?

Why AdS? Generally speaking, it is not straightforward to have well-defined in and out states in the curved space for the scattering events, as the notions for creating and annihilating particles are ambiguously defined. Therefore, finding an appropriate definition of unitary “S-matrix” or “amplitudes” parallel to flat-space is generally hard. For our purpose in this thesis, fortunately, “scattering amplitudes” can be naturally defined in AdS because of the AdS/CFT correspondence [9, 10, 11].

In 1997, Juan Maldacena first came up with AdS/CFT correspondence [9]. This profound conjecture remarkably establishes a bridge to connect the quantum gravity in $D = d + 1$ dimensional AdS and d-dimensional conformal field theories (CFT) on the boundary of AdS without gravity, where CFTs are special QFTs that embrace more symmetry such as the scale invariance. The conjecture of AdS/CFT correspondence states that all physics behind the quantum gravity in AdS and the CFTs on its boundary is essentially equivalent. The mathematical description of this correspondence can be formulated by equating the partition function Z on both sides because the partition function is defined by summing over all possible states of the system and therefore encodes the complete information of the underlying theory

$$Z_{\text{grav}} = Z_{\text{CFT}}\,. \tag{1.1}$$

The significance of AdS/CFT correspondence must be emphasized. The quantum description of gravity is still far from being reached as reflected by, e.g., the irreconcilability of Ultra-Violet (UV) divergence (a catastrophe of quantum gravity at the very short distance), and the mysterious physics of black holes. Surprisingly, CFTs, theories with enhanced symmetry but no gravity, provide a complete and nonperturbative description of underlying quantum gravity, in principle, through the AdS/CFT correspondence.

Essential building blocks of CFTs are the correlation functions. According to the picture of AdS/CFT correspondence, the scattering process in AdS should be equivalently described by certain correlation functions on the CFT side. These correlation

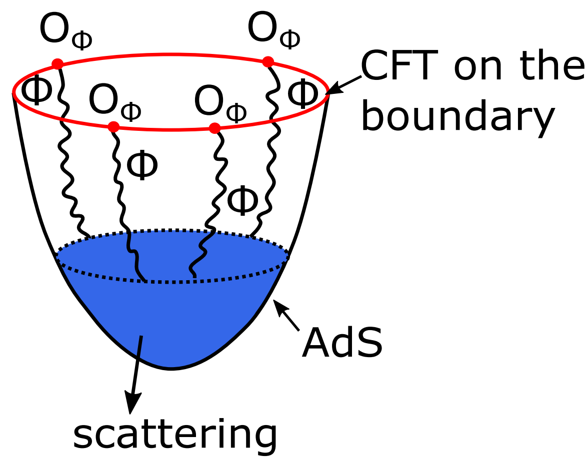

Figure 1.1: An illustration of AdS scattering in terms of AdS/CFT. The hyperboloid refers to the AdS, and the red circle refers to the boundary of the AdS space where the holographic CFTs live. The operators $\mathcal{O}_\phi$ on the boundary reconstruct the fields ϕ in AdS that are shot from the boundary to scatter in the blue region.

functions enjoy strong constraints from the conformal symmetry and crossing symmetry (see, e.g., [12, 13] for quick reviews), which help understand the AdS scattering. To be more precise, the weakly coupled AdS amplitudes constructed from bulk field ϕ, where the quantum effects of gravitational fluctuation are highly suppressed, can be naturally defined by correlation functions of the operator $\mathcal{O}_\phi$ in the CFT with large degrees of freedom (that is known as the large-N limit). Such CFTs are usually phrased as holographic CFTs because they are the hologram of the AdS space. Their correlation functions can be computed in AdS using the holographic dictionary [10, 11], a mathematical framework to identify the AdS quantities with the CFT quantities in one-to-one correspondence. According to the dictionary, CFTs' operators on the boundary somehow induce the ripples near the boundary that play roles like in and out states to be scattered in the AdS. See Fig 1.1.

How to set the local scattering experiments in AdS that are effectively described by flat-space physics? Wave packets with high enough frequencies will focus on a local region around the middle of AdS [14, 15, 16, 17, 18]. Such set-ups restrict holographic CFTs to specialized kinematic configurations, where techniques of CFT efficiently allow the reconstruction of flat-space scattering data [19, 20, 21, 22, 23, 24, 3, 25, 26], as shown in Fig 1.2. These exciting findings strongly suggest a novel route to define

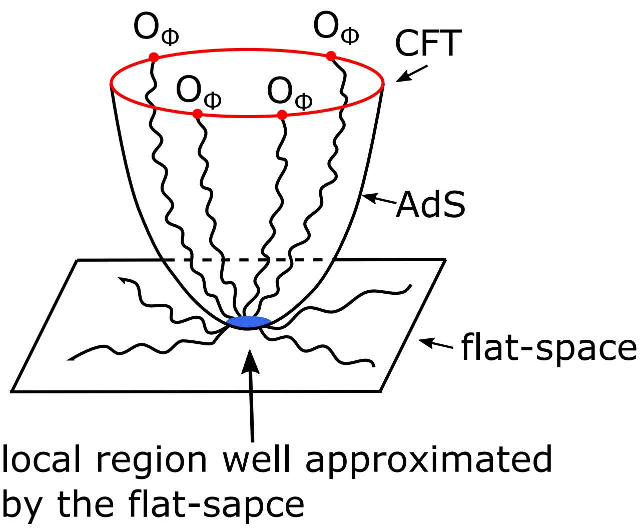

Figure 1.2: As the AdS scattering happens in the small region (blue) compared to the AdS radius, it can be well described by the flat-space scattering.

the axiomatic S-matrix from holographic CFTs [27], where the axioms of CFT might benefit more rigorous understandings of analytic aspects of S-matrix that are hard to prove nonperturbatively using the asymptotic creation and annihilation of particles (see, e.g., [28] for a review).

It may not be surprising that the flat-space limit of AdS amplitudes gives rise to amplitudes in flat Minkowski space. However, the relevant studies seem to suggest a positive answer to another crucial question

Q2: Can the locally flat scattering experiments make predictions for observers at the asymptotic infinity in a curved spacetime such as AdS?

The answer is positive, at least for perturbative low-energy effective field theories (EFTs), where the heavy modes are integrated out. One example is what we will show in Chapter 4 (i.e., [2]); we can follow the intuition about the helicity of massless spinning particles in flat-space, a local quantity that describes the component of particles' spin along the direction of motion, to define the concept of helicity that allows to satisfactorily describe the spinning amplitudes in AdS beyond the flat-space limit. More surprisingly, [29, 30, 31, 7, 32, 6, 7] pointed out that there exists a remarkable representation of AdS amplitudes, known as the differential representation, which manifests the flat-space limit of tree-level correlators, and surprisingly allows

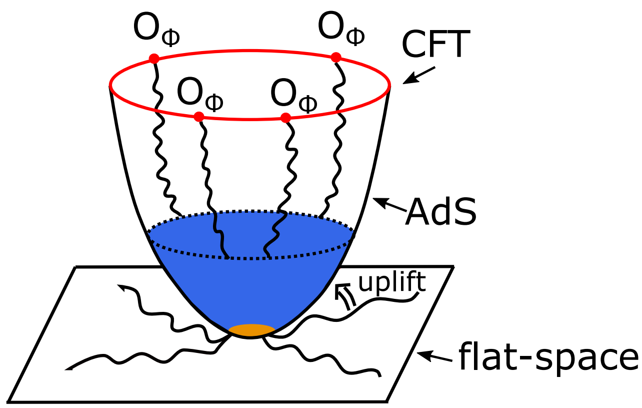

Figure 1.3: The differential representation allows the uplift of flat-space scattering to the scattering in AdS (the blue region) that is beyond the local orange region.

the direct uplift of flat-space amplitudes to AdS, as demonstrated in Fig 1.3. The uplift can also be extended to other observables that encode the UV information, such as the Wilson coefficients of infra-red (IR) EFTs, provided that observables are measured in the small region [33].

This thesis is devoted to gaining a deeper understanding and providing the application of local scattering in holographic CFTs.

In Chapter 2 of this thesis, we will provide a comprehensive review of subjects and tools that are relevant and needed to understand this thesis.

In Chapter 3 of this thesis, we will review different frameworks for taking and observing the flat-space limit of holographic CFTs (for scalar operators). Those frameworks all work nicely for reproducing flat-space data in different representations from AdS/CFT, which are not manifestly related to each other. We will explain how the connections between different frameworks of flat-space limit can be established by localizing the AdS amplitudes into the saddle points of the transform between the representations in the large AdS radius limit.

In Chapter 4 of this thesis, we will describe new constructions of spinning correlators. The new basis corresponds to the helicity basis of the flat-space S-matrix. This helicity basis allows us to cleanly extract the generalized free operator expansion (OPE) coefficients for conserved currents and the tree-level anomalous dimensions of double-twist operators constructed from the conserved current. We will verify that the large-twist limit of anomalous dimensions precisely predicts the flat-space phase shift of gluon scattering amplitudes at tree-level. Our results first verify the flat-space limit for four-point spinning correlators.

In Chapter 5 of this thesis, we will study higher dimension gravitational EFT in flat-space. We will describe our methods for constructing the graviton partial waves in higher dimensions and explain how to establish the dispersion relations that connect low-energy EFT to UV data of graviton scattering. We will build rigorous bounds on low-lying Wilson coefficients and describe the uplift of our sharp bounds to constraints on central charges of holographic CFTs.

In Chapter 6 of this thesis, we will study the three-point and four-point AdS scattering amplitudes of gluon and graviton from Yang-Mills theory and Einstein gravity. We construct the differential representation of gluon and graviton amplitudes by proposing new differential operators using the weight-shifting operators. The differential representation allows us to uplift the flat-space gluon and graviton amplitudes to AdS. Using the differential representation, we also prove the three-point double copy relation in AdS, as well as the BCJ relation of gluon amplitudes in AdS.

In Chapter 7 of this thesis, we discuss all our findings relevant to this thesis by making broad outlooks. We conclude the thesis in Chapter 8.

Chapter 2

Preliminaries

This Chapter reviews the basic aspects of conformal field theory (CFT), AdS geometry, AdS/CFT correspondence, and the S-matrix dispersion relation. The first three parts will be helpful for understanding Chapter 3, 4 and 6, and the last part is essential for understanding Chapter 5.

2.1 CFT and the bootstrap program

As the views go from the microscopic to the macroscopic world, tiny and heavy excitations are coarse-grained. This intuitive picture can be physically described by the renormalization group (RG) flow from Ultra-Violet (UV) to Infra-Red (IR) energy scales. The reason is that the high energy of UV excitations have short wave length, which allows for probing the short distance physics. Along the RG flow, the effective descriptions of physical systems alter. CFTs can be thought of as starting point to understand the RG flow because CFTs describe the physical systems at the fixed point where the RG flow ends. The picture of RG flow is depicted in Fig 2.1.

CFTs are invariant under the enhanced conformal group, which is powerfully constraining for organizing and understanding the dynamics of a theory. Their dynamics can build QFTs away from the fixed point and thus potentially provides a UV-completed definition of QFTs.

Microscopic systems can flow to their critical points, for example, the critical point

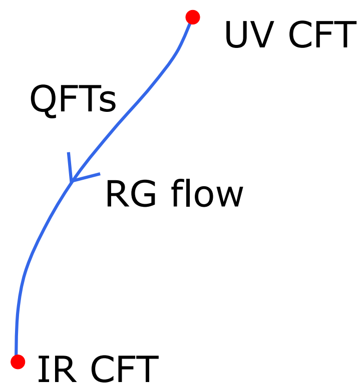

Figure 2.1: The RG flow from UV CFT to IR CFT, where the red dots represent the fixed points where CFTs emerge. Away from the fixed points, there are QFTs.

of the phase transition between liquid and gas. These critical points are RG fixed points described above because the correlation length at the critical points extends to infinity, and the systems' behavior remains invariant under scaling. Therefore, physical systems at critical points can be described by CFTs. Saliently, different microscopic systems can flow to the same IR CFT. This fact is known as the critical universality [34]. For example, the critical point of liquid-gas phase transition and the uniaxial ferromagnetic around the Currie temperature is universally described by the $3d$ Ising model at long distances, which give rise to the same IR CFT arising from ϕ^4 bosonic QFT [35]. For this reason, CFTs are well-studied with broad interests from different areas of physics, e.g., statistical physics, condensed matter physics, high-energy physics, and string theory.

Perhaps the most interesting class of CFTs is the strongly coupled systems, for which the standard perturbation theory does not work well. An intriguing proposal, phrased as "bootstrap", was initiated by Ferrara, Grillo, Gatto [36] and Polyakov [37] independently in the last century. The bootstrap program aims to use symmetry and other consistency conditions, such as unitarity, to constrain and even solve a theory like CFTs and S-matrix. In recent decades, this bootstrap program applying to CFTs, known as the conformal bootstrap, has revived and is currently booming for both numerical [38, 39] and analytic [40, 41, 42, 43] developments due to the enhanced power of computer and the more profound understanding of analytic structures.

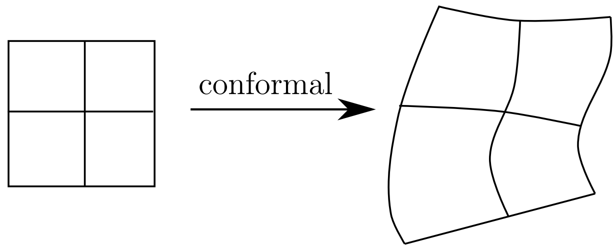

Figure 2.2: A rectangular grid (left) and its image under the conformal transformation (right). The conformal transformation stretches the shape and size of the grid but preserving the angles of intersecting lines to be 90°.

2.1.1 Conformal group

We consider CFTs in d dimensional Euclidean space $\mathbb{R}^d$. The conformal symmetry is the coordinate transformation that lead to the conformal transformation of the metric $g_{\mu\nu}$, i.e., consider $x \to \tilde{x}$, then we shall have

$$\tilde{g}_{\mu\nu}(\tilde{x}) = e^{2\sigma(x)} g_{\mu\nu}(x)\,. \tag{2.1}$$

This is a map that preserves the angles between two curves through x, therefore it is also usually called the angle-preserving transformation, as depicted in Fig 2.2.

We can consider the infinitesimal transformations $x^\mu \to x^\mu + \xi^\mu$ to understand generators of the conformal group, where σ is correspondingly small. The infinitesimal transformation varies the flat metric $\delta_{\mu\nu}$ of $\mathbb{R}^d$

$$\delta_{\mu\nu} \to \delta_{\mu\nu} + 2\partial_{(\mu}\xi_{\nu)}\,. \tag{2.2}$$

To ensure this infinitesimal change induces the conformal transformation (2.1) with infinitesimal σ, ξ has to obey the following equation

$$\partial_{(\mu}\xi_{\nu)} = \frac{1}{d}\partial_\rho \xi^\rho \delta_{\mu\nu}\,. \tag{2.3}$$

The solutions of (2.3) can classify the conformal transformation as follows

(1) Poincare transformations: Translation $\xi^\mu = a^\mu$ and rotation $\xi^\mu = R^\mu_\nu x^\nu$

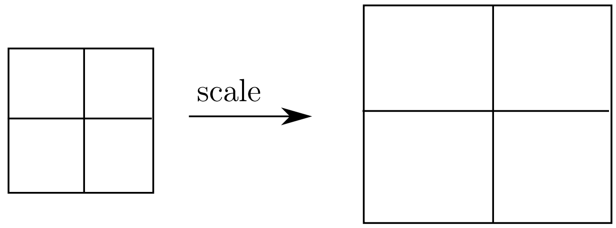

Figure 2.3: The scale transformation zooms out the rectangular grid.

(2) Scale (dilatation) transformations: $\xi^\mu = \lambda x^\mu$

(3) Special conformal transformations: $\xi^\mu = b^\mu x^2 - 2x^\mu\, b\cdot x$

Unsurprisingly, the Poincare transformation exists as a part of the conformal transformation, as the standard QFT is invariant under the Poincare transformation. The scale invariance is a new symmetry. The term "scale transformation" refers to the action of zooming in and out of a view, as shown in Fig 2.3. The invariance under the transformation is reminiscent of the RG fixed point of QFTs, or the critical point of statistical and condensed matter systems. This is why physics at RG fixed point and the critical point is described by CFTs, as people are usually convinced that scale invariance implies the conformal invariance. Nevertheless, it is worth noting that the special conformal transformation is the most nontrivial symmetry, and its emergence from the scale invariance is not a well-established strong statement (except for CFTs in two-dimensions, where there is rigorous proof under well-accepted assumptions [44, 45]). For the relevant discussions regarding "scale invariance vs. conformal invariance", see [46] for an excellent review. The special conformal transformation can be intuitively understood as the inversion that takes a point to its inversion $x \to 1/x$, because it can be operationally obtained by "inversion$\to$ translation $\to$ inversion".

Mathematically, simple algebra allows one to obtain the finite version of the conformal symmetry as follows

(1) Poincare transformations: Translation $\tilde{x}^\mu = x^\mu + a^\mu$ and rotation $\tilde{x}^\mu = R^\mu_\nu x^\nu$

(2) Scale (dilatation) transformations: $\tilde{x}^\mu = \lambda x^\mu$

(3) Special conformal transformations: $\tilde{x}^\mu = \dfrac{x^\mu + b^\mu x^2}{1 + 2b\cdot x + b^2 x^2}$

The generators of the conformal group are as follows

$$
\begin{aligned}
\text{(Translation)} \qquad & P_\mu = -i\partial_\mu \,, \\
\text{(Rotation)} \qquad & L_{\mu\nu} = i(x_\mu \partial_\nu - x_\nu \partial_\mu) \,, \\
\text{(Scale)} \qquad & D = -i x^\mu \partial_\mu \,, \\
\text{(Special Conformal Transformation)} \qquad & K_\mu = -i(2x_\mu x^\nu \partial_\nu - x^2 \partial_\mu) \,.
\end{aligned} \tag{2.4}
$$

which satisfy

$$
\begin{aligned}
& [D, P_\mu] = iP_\mu \,, \qquad [D, K_\mu] = -iK_\mu \,, \qquad [K_\mu, P_\nu] = 2i(\delta_{\mu\nu} D - L_{\mu\nu}) \,, \\
& [K_\rho, L_{\mu\nu}] = i(\delta_{\rho\mu} K_\nu - \delta_{\rho\nu} K_\mu) \,, \qquad [P_\rho, L_{\mu\nu}] = i(\delta_{\rho\mu} P_\nu - \delta_{\rho\nu} P_\mu) \,, \\
& [L_{\mu\nu}, L_{\rho\sigma}] = i(\delta_{\nu\rho} L_{\mu\sigma} + \delta_{\nu\sigma} L_{\nu\rho} - \delta_{\mu\rho} L_{\nu\sigma} - \delta_{\nu\sigma} \; L_{\mu\rho}) \,.
\end{aligned} \tag{2.5}
$$

The conformal group is isomorphic to $\mathrm{SO}(d+1,1)$, which is the Lorentz group of Minkowski space $\mathbb{R}^{d+1,1}$. This fact can be made manifest by redefining

$$
J_{\mu\nu} = L_{\mu\nu} \,, \quad J_{-1\mu} = \frac{1}{2}(P_\mu - K_\mu) \,, \quad J_{-1,0} = D \,, \quad J_{0\mu} = \frac{1}{2}(P_\mu + K_\mu) \,. \tag{2.6}
$$

As a result, the algebra can be rewritten by

$$
[J_{ab}, J_{cd}] = i(\eta_{ad} J_{bc} + \eta_{bc} J_{ad} - \eta_{ac} J_{bd} - \eta_{bd} J_{ac}) \,, \tag{2.7}
$$

where η_{ab} is the Minkowski metric of $\mathbb{R}^{d+1,1}$. The Lorentzian CFT is the CFT in Minkowski spacetime $\mathbb{R}^{d-1,1}$, which can be obtained from the Euclidean CFT by Wick rotating one direction to be the time direction. The conformal group of the Lorentzian CFT is $\mathrm{SO}(d,2)$.

Under the conformal transformation, the operators in CFTs also transform correspondingly

$$
\mathcal{O}(x') \to e^{-\Delta\sigma} R[J_{\mu\nu}] \mathcal{O}(x) \,, \tag{2.8}
$$

where Δ is called the scaling dimension (it is usually the synonym of the conformal dimension) of the operator $\mathcal{O}$, and $R[J_{\mu\nu}]$ is a representation matrix acting on the indices of the spinning operator $\mathcal{O}$. This imposes strong constraints on the correlation functions of operators. For example, the two-point function of the scalar operator is fixed up to a multiplicative constant

$$\langle \mathcal{O}(x_1)\mathcal{O}(x_2)\rangle = \frac{c_{12}}{|x_1 - x_2|^{2\Delta}}\,, \tag{2.9}$$

where the constant c_{12} can be normalized to be 1. Nevertheless, at this stage, the conformal group is highly nonlinear and requires attention to work with more non-trivial spinning operators. In the following subsection, we will briefly introduce the embedding formalism that linearizes the conformal symmetry and largely simplifies many indications.

2.1.2 The embedding formalism

Since the conformal group in d dimensions is isomorphic to the Lorentz group in $d+2$ dimensions, all the implications from the conformal symmetry in $\mathbb{R}^d$ shall be linearly represented by more comprehensive Lorentz invariance in two higher dimensional Minkowski space. This idea is phrased as the embedding formalism [47], since it embeds CFTs in the lightcone of two higher dimensional Minkowski space and uses the Lorentz symmetry to organize the conformal correlators powerfully. We review the construction of the embedding formalism in [47].

To illustrate the idea of embedding formalism, we consider the lightcone coordinates in $\mathbb{R}^{d+1,1}$

$$ds^2 = -dX^+dX^- + \sum_{i=1}^{d}(dX^i)^2\,, \qquad X^{\pm} = X^{-1} \pm X^0\,. \tag{2.10}$$

The construction is restricted on the lightcone $X^2 = 0$. Define the conformal section $X^+ = \lambda$ where λ is an arbitrary constant, and we set it to 1 for simplicity. Consequently, we have $X^- = x^2$, where x denotes the coordinates of $\mathbb{R}^d$ that Euclidean

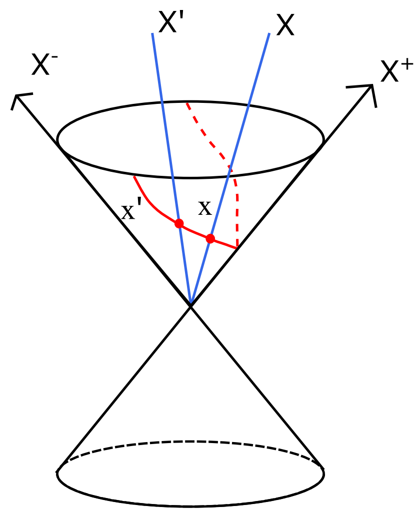

Figure 2.4: The lightcone in the embedding space. Blue lines denote light-rays for X and X'. They are in one-to-one correspondence with the physical space points x and $x\prime$ by intersecting with the conformal section marked as the red curve.

CFT lives in. The induced metric in the conformal section of the lightcone gives rise to the Euclidean space where CFTs are defined. The section can be generally parametrized by

$$X^a = (1, x^2, x^\mu)\,. \tag{2.11}$$

Any points x^μ on the section would define a light-ray. The Lorentz action rotates the embedding coordinates $X'^a = \Lambda^a_b X^b$, which might drive the light-ray to go outside the conformal section, and a scaling factor is required to pull it back. As a result, the action of the Lorentz group on a light-ray moves x^μ to another light-ray x'^μ. From the perspective of the conformal section, this procedure is precisely the conformal transformation

$$\begin{aligned} ds'^2|_{\text{section}} = \eta_{ab}\, d(\Omega(X)X^a)d(\Omega(X)dX^b)|_{\text{section}} = \Big(&d\Omega(X)^2X^2 + 2\Omega(X)\eta_{ab}X^a dX^b d\Omega \\ &+\Omega(X)^2 ds^2\Big)|_{\text{section}} = \Omega(X)^2 ds^2|_{\text{section}}\,, \end{aligned} \tag{2.12}$$

See Fig 2.4 see a visualize picture of the embedding space that is described above.

To describe a CFT, we should also consider how to embed the operators. For example, consider symmetric and traceless primary operators $\mathcal{O}_{a_1a_2\cdots a_\ell}(X)$ as spin-ℓ tensors of $\mathrm{SO}(d+1,1)$, the construction is as follows:

- The operators are assumed to be homogeneous function on $\mathbb{R}^{d+1,1}$

$$\mathcal{O}_{a_1a_2\cdots a_\ell}(\lambda X) = \lambda^{-\Delta}\mathcal{O}_{a_1a_2\cdots a_\ell}(X)\,, \tag{2.13}$$

  where Δ is the homogeneous degree in the embedding space and should be identified with the scaling dimension of CFT operators. The motivation of this property is to ensure the correct scaling behavior of CFT operators.

- The operators with $\ell > 1$ are assumed to be symmetric and traceless, as they should be consistent with the symmetric and traceless primary operators in CFT.

- The operators are assumed to be transverse to the conformal section

$$X^{a_1}\mathcal{O}_{a_1a_2\cdots a_\ell}(X) = 0\,. \tag{2.14}$$

Projecting the operator $\mathcal{O}_{a_1a_2\cdots a_\ell}$ onto the section defines the symmetric operator of the CFT on $\mathbb{R}^d$

$$\mathcal{O}_{\mu_1\mu_2\cdots\mu_\ell} = \Lambda^{a_1}_{\mu_1}\Lambda^{a_2}_{\mu_2}\cdots\Lambda^{a_\ell}_{\mu_\ell}\mathcal{O}_{a_1a_2\cdots a_\ell}\,, \qquad \Lambda^{a_1}_{\mu_1} = \frac{\partial X^{a_1}}{\partial x^{\mu_1}}\,. \tag{2.15}$$

The traceless property of projective operators $\mathcal{O}_{\mu_1\mu_2\cdots\mu_\ell}$ are guaranteed by the traceless and transverse properties of $\mathcal{O}_{a_1a_2\cdots a_\ell}$. It is worth noting that the projection map is not one-to-one. Many seemingly different operators on $\mathbb{R}^{d+1,1}$ can have the same projected operator. In principle, two different operators $\mathcal{O}_{a_1\cdots a_\ell}$ and $\tilde{\mathcal{O}}_{a_1\cdots a_\ell}$ are giving rise to the same CFT operator $\mathcal{O}_{\mu_1\cdot\mu_\ell}$ if $\mathcal{O}$ and $\tilde{\mathcal{O}}$ is different up to pure gauges that are vanishing under the projection onto the conformal section, e.g., a factor X_a.

To well organize the spinning operators, it is insightful to introduce the auxiliary embedding polarizations Z_a, which are vanishing by contract with the embedding coordinates on the conformal section

$$X^2 = Z^2 = X \cdot Z = 0\,. \tag{2.16}$$

The simplification is made by defining

$$\mathcal{O}(X, Z) = \mathcal{O}_{a_1 \cdots a_\ell}(X) Z^{a_1} \cdots Z^{a_\ell}\,, \tag{2.17}$$

Now $\mathcal{O}(X, Z)$ has homogeneous degree ℓ for Z. Restricting Z_a onto the section gives

$$\mathcal{O}(x, \epsilon) = \mathcal{O}_{\mu_1 \cdots \mu_\ell}(x) \epsilon^{\mu_1} \cdots \epsilon^{\mu_\ell} = \tilde{\mathcal{O}}_{a_1 \cdots a_\ell}(X) \Lambda^{a_1}_{\mu_1} \cdots \Lambda^{a_\ell}_{\mu_\ell} \epsilon^{\mu_1} \cdots \epsilon^{\mu_\ell}\,, \tag{2.18}$$

where ϵ is the auxiliary polarization in $\mathbb{R}^d$. Therefore, restricting onto the conformal section gives the parameterization

$$Z^a = (0, 2x \cdot \epsilon, \epsilon^\mu). \tag{2.19}$$

It is worth noting there are many polynomials $\mathcal{O}(X, Z)$ we can use to construct the spinning operators in the CFT; they are allowed to be different up to pure gauges X^2, Z^2 and $X \cdot Z$. For simplicity, we shut down all X^2, Z^2, and $X \cdot Z$.

This formalism allows us to organize two and three-point functions by writing down the Lorentz invariant structures in the embedding space with the identified homogeneous degree. Trivial examples are scalar correlation functions

$$\begin{aligned}
\langle \mathcal{O}(X_1)\mathcal{O}(X_2) \rangle &= \frac{1}{(-2X_1 \cdot X_2)^{\Delta}}\,, \\
\langle \mathcal{O}(X_1)\mathcal{O}(X_2)\mathcal{O}(X_3) \rangle &= \frac{\lambda_{123}}{(-2X_1 \cdot X_2)^{\frac{\Delta_1+\Delta_2-\Delta_3}{2}}(-2X_2 \cdot X_3)^{\frac{\Delta_2+\Delta_3-\Delta_1}{2}}(-2X_1 \cdot X_3)^{\frac{\Delta_1+\Delta_3-\Delta_2}{2}}}\,,
\end{aligned} \tag{2.20}$$

where the coefficient of the three-point function encodes the dynamic information and is called the three-point OPE coefficient for the reason we will discuss soon.

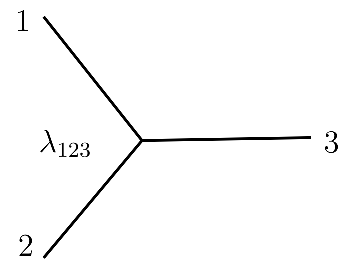

Figure 2.5: A picture for the OPE: two operators fuse to be represented by the third operator.

2.1.3 OPE and conformal blocks

The completeness of the Hilbert space implies that any state can be represented by linear combinations of primaries and descendants. This fact can be formulated as the OPE after using the state-operator correspondence

$$\mathcal{O}_i^a(x_1)\mathcal{O}_j^b(x_2) = \sum_k C_{ijk}^{abc}(x_{12}, \partial_2)\mathcal{O}_k^c(x_2)\,, \tag{2.21}$$

where a, b, c are the spin indices. To illustrate the basic idea, we consider the scalar operators. The simplest exercise is to consider a three-point function (the second line of (2.20)) and evaluate it by performing the OPE for the first two operators. This exercise shows that the OPE kernel C_{ijk} can be determined by conformal symmetry up to overall coefficient λ_{ijk} that also appears in the three-point function

$$C_{ijk} = \frac{\lambda_{ijk}}{|x|^{\Delta_i+\Delta_j-\Delta_k}} F_{ijk}(x, P)\,, \qquad F_{ijk}(x, P) = \sum a_{mn}(ix\cdot P)^m x^{2n}(iP)^{2n}\,, \tag{2.22}$$

where P is the translation operator (2.4). The coefficients a_{mn} are

$$a_{mn} = \frac{\left(\frac{\Delta_{jki}}{2}\right)_n \left(\frac{\Delta_{ikj}}{2}\right)_{n+m}}{(-1)^n 4^n n! m! (\Delta_k)_{m+2n}(\Delta_k - h + 1)_n}\,. \tag{2.23}$$

We use the shorthand notation $\Delta_{ijk} = \Delta_i + \Delta_j - \Delta_k$ and $h = d/2$ in the above. For this reason, λ_{ijk} is called the three-point OPE coefficient. We depict the picture of OPE in Fig 2.5

As performed for studying the four-point function, the OPE ensures conformal block decomposition. Typically, the four-point function can be written by

$$\langle \mathcal{O}_1(x_1)\mathcal{O}_2(x_2)\mathcal{O}_3(x_3)\mathcal{O}_4(x_4)\rangle = \frac{g(u,v)}{(x_{12}^2)^{\frac{\Delta_1+\Delta_2}{2}}(x_{34}^2)^{\frac{\Delta_3+\Delta_4}{2}}}\left(\frac{x_{24}^2}{x_{14}^2}\right)^{\frac{\Delta_{12}}{2}}\left(\frac{x_{14}^2}{x_{13}^2}\right)^{\frac{\Delta_{34}}{2}}, \quad (2.24)$$

where $g(u,v)$ is an unknown function of (u,v) that are known as conformally invariant cross ratios

$$u = \frac{x_{12}^2 x_{34}^2}{x_{13}^2 x_{24}^2}, \quad v = \frac{x_{14}^2 x_{23}^2}{x_{13}^2 x_{24}^2}. \quad (2.25)$$

Performing the OPE for $\mathcal{O}_1\mathcal{O}_2$ and $\mathcal{O}_3\mathcal{O}_4$ simultaneously gives rise to

$$g(u,v) = \sum_{\Delta,J} f_{12\mathcal{O}_{\Delta,J}} f_{34\mathcal{O}_{\Delta,J}}\, G_{\Delta,J}(u,v)\,, \quad (2.26)$$

where $G_{\Delta,J}(u,v)$ is called the conformal block. The conformal block is the kinematic object that can be, in principle, solved by the Casimir equation

$$\mathcal{C}_{12}G_{\Delta,J} = C_{\Delta,J}G_{\Delta,J}\,, \quad C_{\Delta,J} = \Delta(\Delta-d) + J(J+d-2)\,, \quad (2.27)$$

where the Casimir operator $\mathcal{C}_{12}$ is

$$\mathcal{C}_{12} = \frac{1}{2}(J_1+J_2)^2\,, \quad J_i^{\mu\nu} = i\big(X_i^\mu \frac{\partial}{\partial X_i^\nu} - X_i^\nu \frac{\partial}{\partial X_i^\mu}\big)\,. \quad (2.28)$$

In terms of the cross-ratio, it is

$$\begin{aligned}\mathcal{C}_{12} = {} & 2(1-u-v)\frac{\partial}{\partial v}(v\frac{\partial}{\partial v} + a + b) + 2u\frac{\partial}{\partial u}(2u\frac{\partial}{\partial u} - d) \\ & - 2(1+u-v)(u\frac{\partial}{\partial u} + v\frac{\partial}{\partial v} + a)(u\frac{\partial}{\partial u} + v\frac{\partial}{\partial v} + b)\,, \end{aligned} \quad (2.29)$$

where $a = \Delta_{21}/2$, $b = \Delta_{34}/2$.

On the other hand, the coefficients $f_{12\mathcal{O}} f_{34\mathcal{O}} := c_{\Delta,J}$ is usually called the OPE coefficient in the modern bootstrap language, which is theory dependent and thus encodes dynamics.

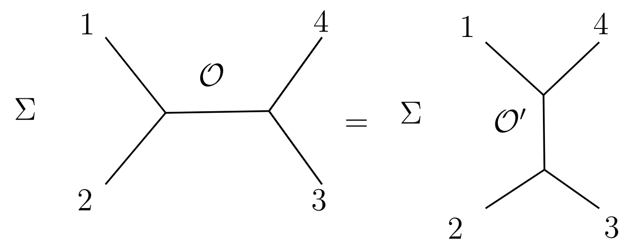

Figure 2.6: Graphic illustration of the crossing symmetry.

2.1.4 Short review on conformal bootstrap

So far, we have only exploited the conformal symmetry itself. What determines a CFT without referring to the microscopic picture? As the conformal symmetry already settles down the kinematic structures such as conformal bocks, the complete knowledge of a CFT then only spans the conformal spectrum (Δ, J) and the three-point OPE coefficients λ_{ijk}, which are known as the conformal data. The goal of conformal bootstrap is to use other consistency conditions to solve for those conformal data.

A strongly constraining consistency condition is the crossing symmetry for a four-point function, which states the equivalence of conformal block expansion for s-channel (OPE for 12 and 34) and t-channel (OPE for 23 and 14), as shown in Fig 2.6.

It is usual to consider a conformal frame, where the conformal symmetry can be used to put the first operator at the origin, the third operator at 1 and the fourth operator at infinity, while keeping the second operator lying on a two-dimensional plane

$$\langle \mathcal{O}_1(0)\mathcal{O}_2(z,\bar{z})\mathcal{O}_3(1)\mathcal{O}(\infty)\rangle \,, \tag{2.30}$$

where $(z, \bar{z})$ is another parameterization of the cross ratios $u = z\bar{z}, v = (1-z)(1-\bar{z})$, as shown in Fig 2.7.

For an identical scalar four-point function, the crossing symmetry gives the fol-

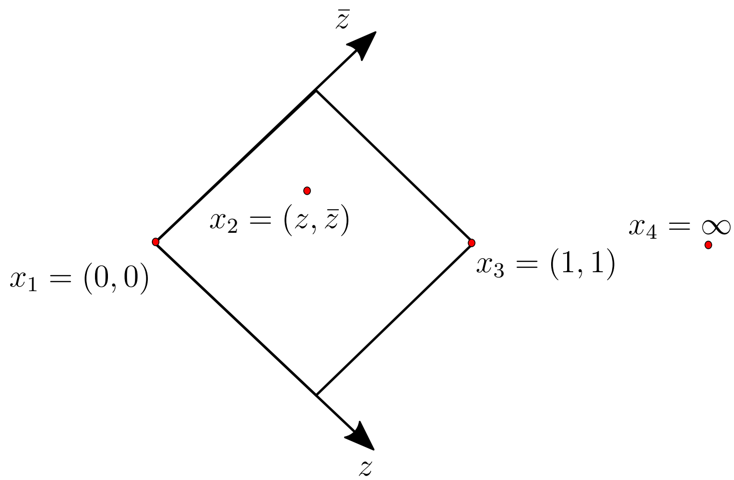

Figure 2.7: The configuration shaped using the conformal symmetry. The four-point function is a function of $(z, \bar{z})$.

lowing equation

$$\sum_{\Delta,J} c_{\Delta,J} G_{\Delta,J}(u,v) = \frac{u^{\Delta_\phi}}{v^{\Delta_\phi}} \sum_{\Delta',J'} c_{\Delta',J'} G_{\Delta',J'}(v,u)\,. \tag{2.31}$$

The essence of the conformal bootstrap is to solve the crossing equation with the help of unitarity (that ensures $c_{\Delta,J} \geq 0$ and other unitary bounds of spectrum (Δ, J) [48]) either numerically or analytically.

The numerical methods for solving the crossing equation were pioneered in [38] using linear programming and were later optimized using the semi-definite-programming [49]. We will not cover numerics in this thesis. However, we would like to highlight how powerful the crossing symmetry is in Fig 2.8 and 2.9, as the numerical bootstrap based on it allowed [50] to locate the kink for $3D$ Ising model and [51] to precisely pinpoint the island of $3D$ Ising model

On the other hand, the analytic method was initiated in [40, 41] by understanding the consistency of singularities appearing in the crossing equation at the lightcone limit $v \ll 1$, which is now known as the lightcone bootstrap. The simplest example to illustrate this idea is to consider the identity exchange in the t-channel and ask

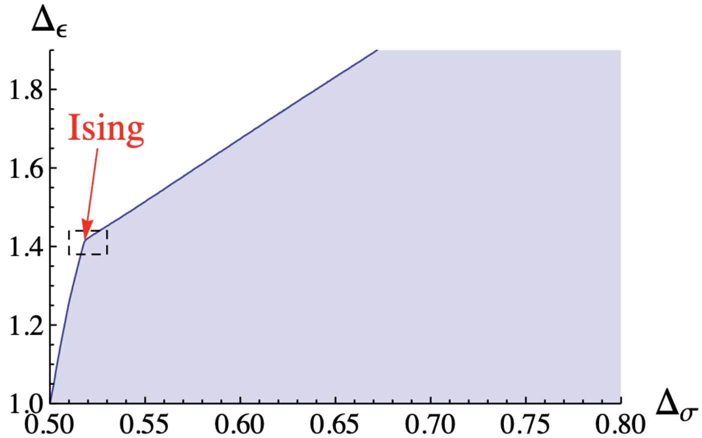

Figure 2.8: The exclusion plot made in [50] using the numerical conformal bootstrap. The shaded region is the allowed space for the scaling dimensions as constrained by the crossing symmetry. $3D$ Ising model lives on the kink.

what operators have to exist to ensure the crossing equation (2.31)

$$\sum_{\Delta,J} c_{\Delta,J} G_{\Delta,J}(u,v) = \frac{u^{\Delta_\phi}}{v^{\Delta_\phi}}. \tag{2.32}$$

At the lightcone limit $v \ll 1$, the RHS develops the singularity $v^{-\Delta_\phi}$ while each term of LHS does not have such a singularity. This implies that there must be an infinite number of terms in the LHS that sum over to produce the singularity, where the large-spin limit dominates the sum. By taking the lightcone limit $v \ll 1$ of the conformal block, [40, 41] shows that (2.32) can only be valid if there is an accumulating tower of double-twist operators with $\Delta = 2\Delta_\phi + J + 2n$ for integer $n \geq 0$ at large J, e.g.,

$$[\phi\phi]_{n,J} = \phi \partial_{\mu_1} \cdots \partial_{\mu_J} \partial^{2n} \phi \,, \tag{2.33}$$

and the OPE coefficients $c_{\Delta,J}$ at the large J limit are bootstrapped by solving (2.32) order by order in the expansion of $u \ll 1$. For example, for leading order of $u \to 0$ but $v \ll u$, the conformal block can be approximated by

$$G_{\Delta,J}(u,v) \simeq \frac{\sqrt{J} 2^{\Delta+J}}{\sqrt{\pi}} u^{\frac{\Delta-J}{2}} K_0(2J\sqrt{v}) \,, \tag{2.34}$$

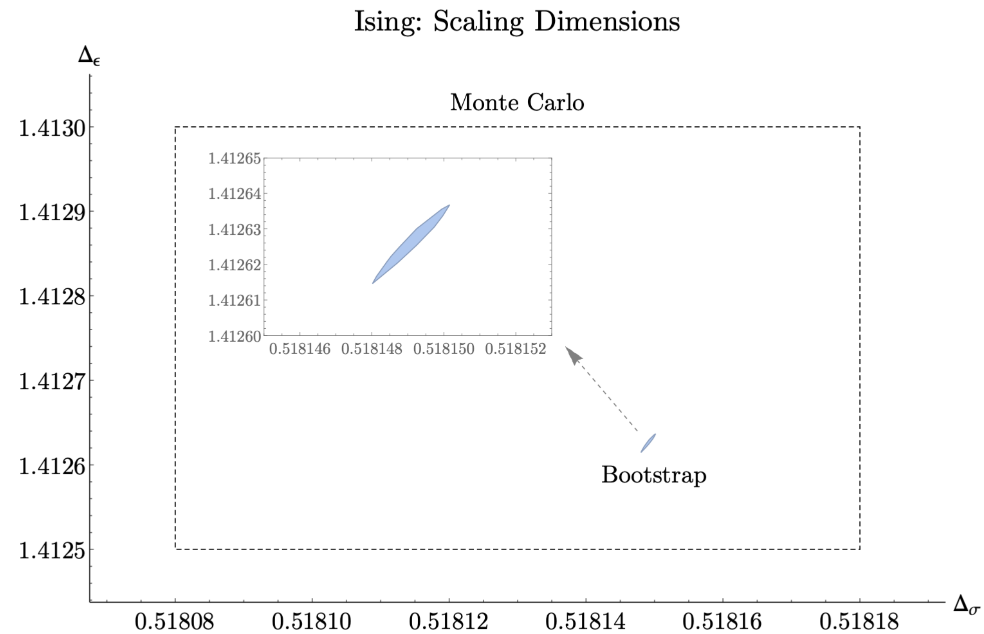

Figure 2.9: The island for the leading scaling dimensions in $3D$ Ising model from [51] using the numerical conformal bootstrap, with the comparison to the best Monte Carlo results (the dashed rectangle) [52] prior to [51].

where K_0 is the modified Bessel function, and the OPE coefficient is

$$c_{\Delta=2\Delta_\phi+J,J} \simeq \frac{\sqrt{\pi}2^{-2\Delta_\phi-2J+2}J^{2\Delta_\phi-\frac{3}{2}}}{\Gamma\left(\Delta_\phi\right)^2}\,, \tag{2.35}$$

which is consistent with the OPE coefficient for mean field theory [53]. This is a limit that can be well described by Fig 2.10.

The existence of the double-twist family (2.33) can be intuitively understood as the analog of a two-particle bound state formed by two individual particles, as shown in Fig 2.11. This is indeed the correct understanding in the holographic theories that we will review shortly.

A more nontrivial application is to consider a single twist τ conformal block at t-channel, and the lightcone bootstrap allows one to extract the large spin anomalous dimensions. These anomalous dimensions can correspondingly be understood as the internal energy of a two-particle bound state in Fig 2.11 perturbatively corrected by interactions. Essentially, the lightcone bootstrap relies on the double lightcone

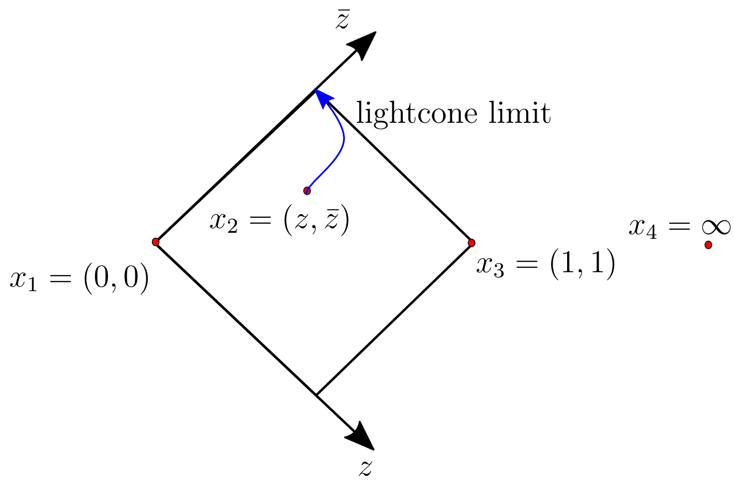

Figure 2.10: The blue arrow denotes the lightcone limit $v \ll u \ll 1$, which is $1 - \bar{z} \ll z \ll 1$ in this picture.

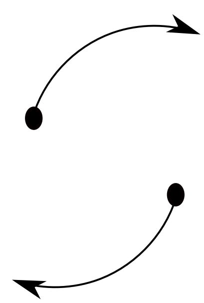

Figure 2.11: An intuitive picture to think of the double-twist operators $[\phi\phi]_{n,J}$ as a two-particle bound state formed by two particles circling each other.

limit $v \ll u \ll 1$: one has to play this game for a higher order of u to obtain OPE coefficients at higher twist n and for a higher order of v to obtain OPE coefficients with $1/J$ corrections [54, 55, 56, 57]. The rigorous setting of this lightcone bootstrap is still actively under exploration [58]. Much progress has been made in understanding the large spin asymptotes in recent years. In particular, the large spin perturbation theory [42] first provided a systematic way for resummation of large spin data in the analytic bootstrap, which is surprisingly valid up to finite low spin [59, 60]. This validity was then explained as the analyticity in spin by Lorentzian inversion formula [43, 61, 62] as long as unitarity is preserved, which is the analog of Froissart-Gribov formula for extracting partial wave coefficients of an S-matrix. The highest spin that the lightcone bootstrap does not work well is then understood as the Regge intercept using the Lorentzian inversion formula, which is still out of reach systematically.

It is worth noting, in contrast with the numerical bootstrap, where the crossing equation is solved as a whole, the analytic bootstrap usually can only address the cross channel by a single conformal block and ask what this conformal block contributes to other channels. This procedure may need to be clarified for any CFTs, since the infinite summation of all conformal blocks may behave very differently, e.g., the new singularity may arise. For this reason, the analytic bootstrap is more suitable for those CFTs with a hierarchy that leads to clear factorization, for which the conformal block expansion can be well organized by the hierarchy, e.g., the identity dominates other conformal blocks. Importantly for this thesis, as we will explain later, holographic CFTs fall into this class, where the relevant hierarchy is the large-N degrees of freedom.

2.2 AdS geometry

Even beyond the scope of AdS/CFT, AdS space is still attractive since it is a maximal symmetric space other than the Minkowski space. For a better description of AdS/CFT in the next section, we give a brief introduction to AdS geometry in this small section.

To make contact with the Euclidean CFT, we consider the Euclidean AdS, which is the hyperbolic space. The AdS$_D$ can be defined by embedding in the $\mathbb{R}^{1,D}$

$$ds^2_{D+1} = -dX_0^2 + \sum_i^D dX_i^2 \,, \tag{2.36}$$

where

$$-X_0^2 + \sum_i^{D-1} X_i^2 = -\ell^2 \,. \tag{2.37}$$

The curvature of this space is negative $\sim -1/\ell^2$. The symmetry of this space consists of D boosts and $D(D-1)/2$ rotations, isomorphic to $\mathrm{SO}(1,D)$ symmetry. It is already worth noting that this symmetry is the same as CFT_{D-1}; this is perhaps the first hint for AdS/CFT. To arrive at the Lorentzian AdS, we should Wick rotate X_1, and the resulting embedding space is $\mathbb{R}^{2,d}$, where the isometry group is $\mathrm{SO}(2, D-1)$.

There are different parameterizations for AdS local coordinates, and they have different purposes in the context of AdS/CFT.

(1) Global coordinates

A simple way to parametrize the coordinates is

$$X_0 = \sqrt{\ell^2 + r^2} \cosh(\tfrac{t}{\ell})\,, \qquad X_1 = \sqrt{\ell^2 + r^2} \sinh(\tfrac{t}{\ell})\,, \qquad \ell^2 = \sum_i X_i^2\,. \quad (2.38)$$

We end up with

$$ds_{\text{global}} = (1 + r^2 \ell^{-2}) dt^2 + \frac{dr^2}{1 + r^2 \ell^{-2}} + r^2 d\Omega_{D-2}^2\,, \quad (2.39)$$

where $r \in (0, \infty)$. This coordinate is called global because it covers the whole AdS space. The AdS boundary is located at $r \to \infty$. It is usually common to redefine r and define the following global coordinate

$$ds_{\text{global}} = \ell^2 (\cosh^2 \rho\, dt^2 + d\rho^2 + \sinh^2 \rho\, d\Omega_{D-2}^2)\,, \quad (2.40)$$

where AdS boundary is located at $\rho \to \infty$. For the Lorentz signature, we can simply Wick rotate τ. See Fig 3.3 for an illustration of this coordinate.

(2) Poincare coordinates

We can also parametrize the coordinates as follows

$$X_0 = \ell \frac{1 + (z^2 + x^2)}{2z}\,, \quad X_1 = \ell \frac{1 - (z^2 + x^2)}{2z}\,, \quad X_{i>1} = \ell \frac{x_{i-1}}{z}\,. \quad (2.41)$$

The Poincare coordinate is then given by

$$ds^2_{\text{Poincare}} = \frac{\ell^2}{z^2} (dt^2 + dz^2 + \delta_{ij} dx^i dx^j)\,, \quad (2.42)$$

where $z \in (0, \infty)$ and $t \in (-\infty, \infty)$, and AdS boundary is located at $z \to 0$, while $z \to \infty$ refers as the Poincare horizon. It is evident that this coordinate does not cover the whole AdS space; it only covers a patch $X_0 + X_D > 0$. For this reason, the Poincare coordinate is usually called the Poincare patch. For an intuitive picture of the Poincare patch, see Fig 3.4. There is another way to write the Poincare patch by simply redefining $z^2 = \ell^2 \rho$

$$ds^2_{\text{FG}} = \frac{\ell^2}{4\rho^2} d\rho^2 + \frac{1}{\rho} \delta_{ij} dx^i dx^j \,, \tag{2.43}$$

where $\rho \to 0$ is the AdS boundary. This coordinate (2.43) is also known as Fefferman-Graham (FG) coordinate, which helps evaluate the holographic counterterms, holographic anomalies, and deriving holographic energy-momentum tensor, and so on, see, e.g., [63, 64, 65, 66].

2.3 Holography and AdS/CFT

The holographic principle is a hypothesized property of quantum gravity that states that all information of a dynamical system involving gravity is encoded by a lower dimensional boundary of the system. This principle was first hypothesized by 't Hooft [67] and was further elaborated in terms of string interpretation by Susskind [68]. The most famous example of the holographic principle is perhaps the entropy of a black hole: the black hole entropy is proportional to the black hole horizon area but counts all microscopic degrees of freedom inside [69, 70].

The prime realization of the holographic principle was constructed by Maldacena in 1997 [9] from Type IIB string theory. This construction relates Type IIB string theory in $\text{AdS}_5 \times \text{S}_5$ and $\mathcal{N} = 4$ super Yang-Mills theory (SYM) in $d = 4$ (which is a CFT with supersymmetry), for this reason, it is phrased as $\text{AdS}_5/\text{CFT}_4$ correspondence. Later on, Gubser, etc. and Witten, etc. provided the mathematically quantitative descriptions for AdS/CFT [10, 11], namely the holographic dictionary, which made it possible for more solid tests of this correspondence by computing physical observables. More explicit examples can be constructed from string, and M theory, e.g., $\mathrm{AdS}_7/\mathrm{CFT}_6$ and $\mathrm{AdS}_4/\mathrm{CFT}_3$ [9, 71]. These examples have clear UV origin as the string and M theory and thus are referred to as top-down holographic models. Nevertheless, people are convinced that AdS/CFT is more broadly applicable without referring to a specific UV completion, such as string theory. A more general statement of AdS/CFT, also known as holography or gauge/gravity duality, claims that quantum gravity in AdS can be equivalently described by a certain CFT on the boundary. There are active studies to investigate the conditions a CFT has to have so that it becomes holographic CFT with a gravity dual, see, e.g., [18].

2.3.1 Maldacena's $\mathrm{AdS}_5/\mathrm{CFT}_4$

The basic idea of Maldacena's construction of $\mathrm{AdS}_5/\mathrm{CFT}_4$ is to consider a stack of N nearly coincidental D3-branes in Type IIB string theory in ten-dimensional Minkowski space and think about the low energy effective descriptions of this system from open string and closed string perspective respectively.

From an open string perspective, the interactions between D3-branes and closed strings can be formulated as open strings ending up on the D3-branes. The coincidental limit of open string modes whose endpoints are attached to D3-branes induces a $\mathrm{SU}(N)$ gauge group. These modes organized by $\mathrm{SU}(N)$ symmetry are dynamical on the branes which is effectively four-dimensional flat Minkowski spacetime, giving rise to a gauged QFT in $d = 4$. More specifically, in the low energy limit where the string length tends to zero, i.e., $\ell_s = \sqrt{\alpha'} \to 0$, such configuration can be effectively described by $d = 4, \mathcal{N} = 4$ SYM with gauge group $\mathrm{SU}(N)$.

From a closed string perspective, N stack of D3-branes bends the space and results in the following geometry

$$ds^2 = \left(1 + \frac{\ell^4}{y^4}\right)^{-\frac{1}{2}} \eta_{ij} dx^i dx^j + \left(1 + \frac{\ell^4}{y^4}\right)^{\frac{1}{2}} \left(dy^2 + y^2 d\Omega_5^2\right) , \tag{2.44}$$

where η_{ij} is the Minkowski metric on D3-branes

$$\ell^4 = 4\pi g_s N \ell_s^4 \,. \tag{2.45}$$

The interaction is mostly dominated by near horizon regime $y \to 0$. The low energy limit around $y = 0$ can be achieved by redefining $z = \ell^2/y$ that is kept fixed at the limit of $y \to 0, \ell_s \to 0$

$$ds^2 = \frac{\ell^2}{z^2}(dz^2 + \eta_{\mu\nu}dx^\mu dx^\nu) + \ell^2 d\Omega_5^2 \,. \tag{2.46}$$

This space is the Lorentzian AdS with internal space as S^5, namely $\mathrm{AdS}_5 \times \mathrm{S}^5$ with the same radius. The number of D3-branes N can be described by the integer flux of the 5-form flow $F_{(5)}$. It is also worth noting that, as we already emphasized in previous sections, the isometry group of AdS_5 matches the conformal group in four dimensions. The isometry SO(6) of S^5, in this case, can be mapped to the global R-symmetry group in super Yang-Mills theory $\mathrm{SU}(4) \sim \mathrm{SO}(6)$ in the bosonic sector. Therefore, the isometry of $\mathrm{AdS}_5 \times S^5$ realizes the maximal bosonic subgroup of the superconformal group $\mathrm{SU}(2,2|4)$, and the completion into the full superconformal group is supplemented by Poincare supersymmetry of N coincidental D3-branes.

These two perspectives should be equivalent (as depicted in Fig 2.12), because they describe the same system: N coincidental D3-branes interacting with closed strings in Type IIB string theory. This duality led Maldacena to conjecture $\mathrm{AdS}_5/\mathrm{CFT}_4$ correspondence, for which the original version was

- Type IIB superstring theory with string length ℓ_s and string coupling g_s on $\mathrm{AdS}_5 \times \mathrm{S}^5$ where the AdS radius and sphere radius are both ℓ is physically equivalent to $\mathcal{N} = 4, d = 4$ SYM with gauge group SU(4) and coupling g_{YM}. The parameters are identified correspondingly

$$g_{\mathrm{YM}}^2 = 2\pi g_s \,, \quad \ell^4 = 4\pi g_s N \ell_s^4 \,. \tag{2.47}$$

However, it is hard to generally prove or simply test this correspondence in a complete set because this requires computations of the same observables on both sides. To acquire further understanding, a certain parametric limit is necessary. One natural limit is to take the large-N expansion of SYM but keep the 't Hoott coupling $\lambda = g_s N$ fixed. At this limit, the AdS side should be described by semi-classical Type IIB string theory on $\mathrm{AdS}_5 \times \mathrm{S}^5$ with underlying string loops expansions in terms of g_s. The correspondence has passed many checks for different regimes of λ at the large-N limit. In particular, agreement of results at different limits of λ for the scaling dimensions of 1/2BPS single-trace operators and their two and three-point functions suggest that these results do not depend on the 't Hooft coupling λ, as protected by supersymmetry [72]. Some observables that preserve enough supersymmetry, such as the sphere partition function [73] and the Wilson loops [74], can also be computed at any λ using the localization. Non-protected single-trace operators can also be probed using the integrability techniques in the planar limit; see, e.g., [75] for an overview. These are all special examples that rely on supersymmetry and integrability.

Perhaps the simplest and well-studied situation is to further take large 't Hooft limit $\lambda \gg 1$, and the dual description would be semi-classical Type IIB supergravity with α' expansions. This regime is often called the strong/weak duality since the SYM is strongly coupled while supergravity is weakly coupled. The broad sense of AdS/CFT is built upon the assumption of strong/weak duality, where the bulk theory is guaranteed to be local, as we will review soon.

2.3.2 Holographic dictionary

The holographic dictionary establishes a quantitative bridge to compare physical quantities on both sides of AdS/CFT [10, 11]. Its essence is the equivalence of partition functions (1.1), from which all the dictionaries could be built in principle. For this thesis, we only introduce the dictionary relevant to the energy scale and the correlation functions. Other dictionaries are developed later for other physical quantities, such as Wilson loops and entanglement entropy, which is, however, irrelevant to this thesis.

The most important dictionary relevant to this thesis is the field-operator duality,

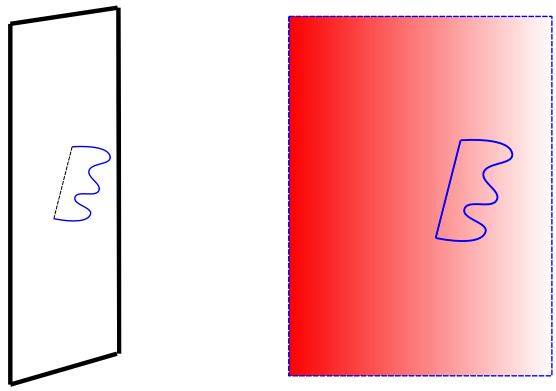

Figure 2.12: (a) Open strings ended on the stacked D3-branes. (b) D3-branes result in a curved background (depicted by a gradient red rectangle) where closed strings propagate.

which states that for any quantum fields ϕ with mass m in AdS, there are corresponding gauge invariant primary operators $\mathcal{O}_\phi$ in CFT, and the boundary values $\phi^{(0)}$ of ϕ correspond to the source coupled to the operator $\mathcal{O}_\phi$. More explicitly, we have

$$Z_{\text{grav}}\big|_{\phi^{(0)}} = \int_{\phi^{(0)}} [D\phi] \exp\big[-S[\phi]\big] = \Big\langle \exp\big[-\int_\partial d^d x\, \phi^{(0)} \mathcal{O}_\phi\big] \Big\rangle_{\text{CFT}}\,, \tag{2.48}$$

where the subscript ∂ refers to the asymptotic AdS boundary, and the expectation value is over CFT path integral. This readily leads to the definition of AdS amplitudes in terms of conformal correlation functions

$$\mathcal{M}_{\text{AdS}} = \langle \mathcal{O}_\phi \cdots \mathcal{O}_\phi \rangle = \big(\prod_{i=1}^{n} \frac{\delta}{\delta\phi^{(0)}}\big)\big(Z_{\text{grav}}\big|_{\phi^{(0)}}\big)\,. \tag{2.49}$$

To better understand this dictionary, it helps to consider the asymptotic solution of free fields in AdS around the AdS boundary $z \to 0$, which admits universal structure

$$\phi \simeq z^{2\alpha}(\phi^{(0)} + \phi^{(2)} z^2 + \cdots (\phi^{(2n)} + \tilde{\phi}^{(2n)} \log z) z^{2n} + \cdots)\,. \tag{2.50}$$

where $\log z$ is a possible anomalous term. α and $\alpha + n$ are two solutions for Δ in

$$\Delta(\Delta - d) = m^2 \ell^2\,, \tag{2.51}$$

Evaluating the AdS action followed by using (2.49) derives that the corresponding operator is actually encoded by $\phi^{(2n)}$

$$\langle \mathcal{O}_\phi \rangle \sim \phi^{(2n)} \,. \tag{2.52}$$

The rescaling of $z \to \lambda z$ that fixes AdS induces a boundary scaling $x \to \lambda x$, as a result, (2.50) then shows precisely $\mathcal{O}_\phi \to \lambda^\Delta \mathcal{O}_\phi$. Thus, for field-operator duality, the mass of the bulk field determines the scaling dimension of the CFT operator via (2.51). This dictionary has salient implications for important fields and operators: gauge field in AdS, such as Yang-Mills, corresponds to conserved spin-1 operator in CFT; graviton in AdS corresponds to the stress-tensor in CFT. This dictionary is served as the stone for Chapter 3, 4 and 6.

There is another important dictionary that is essential for the review in the next subsection: radius-energy duality. This is a duality to answer a simple question: what is the role of the radial direction of AdS in CFT? The answer is $z \sim 1/\mu$ where μ is the energy scale in CFT. For pure AdS, the geometry does not change along z. This then indicates that CFTs do not run along the RG flow. This dictionary plays an important role in understanding the holographic c-theorem [76].

2.3.3 The condition for holographic CFTs

Aside from the explicit AdS/CFT model from string and M theory, it is profound to ask how general AdS/CFT can be without referring to specific CFT models where the holographic dictionary applies. This question can be recast into a simpler one: what condition a CFT has to have so that it is a holographic CFT with a local AdS gravity dual?

This question was addressed by an outstanding work known as HPPS [18]. The basic intuition is to start with the notion of locality by using the radius-energy duality. In particular, the approximate locality in energy on the CFT side implies $\delta\mu/\mu \sim \mathcal{O}(1)$, which then indicates the resolution of the locality of AdS is down to $ds \sim \ell$. The holography at this scale is phrased as the AdS scale holography. The holography is not sharp at this scale because it probes only the spectrum and one-point, two-point and three-point functions, for which the structures are only sensitive to the AdS isometry. In order to build a sharp statement of holography, it is necessary to consider four-point functions, for which the locality of AdS ensures that the scattering of four wave packets can focus on the string scale that is much smaller than the AdS scale. At the scale $ds < \ell$, the holography is sharply sensitive to bootstrap constraints of conformal correlators and is phrased as the sub-AdS holography. Based on this discussion, [18] made a conjecture for the condition that a holographic CFT has to satisfy, which, to my knowledge, updates the understanding of bottom-up AdS/CFT

- Any CFT with a large-N expansion and a large gap $\Delta_{\text{gap}} \gg 1$ of higher spin $J > 2$ single-trace operator has a local dual of weakly coupled AdS gravity.

Here the large-N limit refers to the large central charge limit $N^2 \sim C_T \ll 1$ where C_T is the coefficient of stress-tensor two-point function, and the holographic dictionary relates it to the Newton constant or Plank scale $C_T \sim 1/G_N$. The existence of a large gap for single-trace operator $\Delta_{\text{gap}} \gg 1$ can be translated to the existence of heavy higher spin states with mass $M \gg 1/\ell$ that are integrated out to give bulk gravitational EFT. Typically, being consistent with the EFT validity, bulk higher-derivative corrections are suppressed by $1/M$, thus giving rise to conformal data at the order of $1/\Delta_{\text{gap}}$, e.g., see [18, 77, 78, 79, 33]. For string theory, M would be the string length $M \sim 1/\ell_s$. Thus for the correspondence between $\text{AdS}_5 \times \text{S}^5$ and $\mathcal{N} = 4, d = 4$ SYM with $\text{SU}(N)$, Δ_{gap} is actually $\lambda^{\frac{1}{4}}$.

We should emphasize that the limit $\ell \gg 1/M$ contains more information than the flat-space limit. For flat-space limit, the particles are excited with large frequency within the EFT regime $\omega < M$ to be scattered around the impact parameter $b \sim 1/\omega$ so that the scattering happens at local scale $\ell \gg b > 1/M$. This regime is the bulk-point limit [24, 33]. The AdS locality more broadly covers the regime $\ell \sim b \gg 1/M$, which is the AdS Regge limit [33] and does not produce the flat-space S-matrix. Nevertheless, as we will review in the next section, this regime allows the uplift of rigorous bounds on Wilson coefficients of flat-space to AdS, where the error is suppressed by $1/\Delta_{\mathrm{gap}}$ [33] .

2.4 EFT bootstrap

Effective Field Theories (EFTs) are powerful tools for describing physical systems over a specific range of energy scales, especially when the complete underlying theory is highly intricate or unknown. The basic idea behind EFTs is to separate the physics at different scales and simplify the models by retaining only the most relevant degrees of freedom, while treating less important ones as parameters of the EFTs, known as Wilson coefficients.

A commonly used type of EFTs is the weakly coupled low-energy EFTs, where the traditional perturbative description of QFTs works well. The UV effects enter as higher-dimensional operators in the effective action, suppressed by a UV scale M. One of the most profound questions in theoretical physics is what is the space of EFTs that ensures a consistent UV completion, e.g., the quantum gravity.

Using the causality to constrain the space of EFTs enjoys a long history, qualitative constraints or simple positive conditions of EFT Wilson coefficients are explored by experimenting with scattering processes, e.g., [77, 80, 81]. Recently a series of papers [82, 83, 84, 85, 86, 87, 88] developed a systematic bootstrap algorithm that is able to carve out rigorous allowed space of EFTs. The crucial idea of this algorithm is that the causality relates the low-energy and high-energy physics by establishing the dispersion relation, which allows to systematically express EFT parameters in terms of positive UV data by considering the forward $2 \to 2$ scattering. For example, for identical massless scalar scattering, as long as the Regge boundedness $|\mathcal{M}(s,t)|/|s|^2\big|_{|s|\to\infty} \to 0$ is assumed, the fixed-$t=-p^2$ dispersion relations can be constructed for s

$$B_k(p^2) = \oint_{\infty} \frac{ds}{s} \frac{\mathcal{M}(s,-p^2)}{[s(s-p^2)]^{\frac{k}{2}}} = 0\,, \tag{2.53}$$

where $k \geq 2$ takes even integers. The causality implies that the amplitudes $\mathcal{M}$ are analytic in the upper-half plane $\mathrm{Im}\, s > 0$ for fixed real $t < 0$ and there are only low

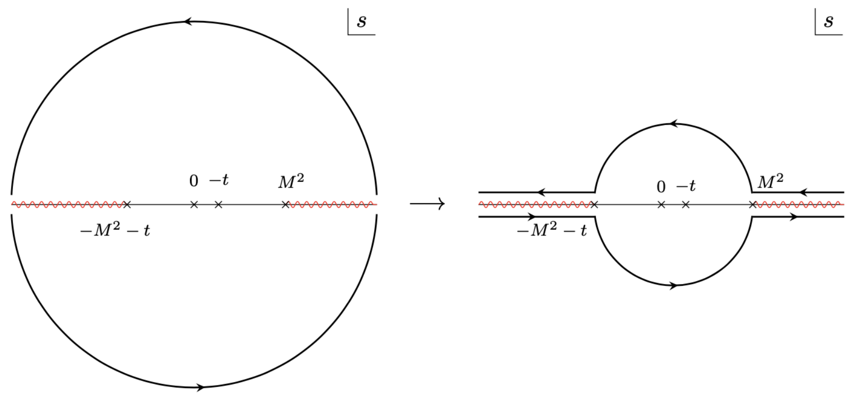

Figure 2.13: The illustration of the contour deformation for the dispersion relations that relates low energy EFT and the UV positivity.

energy poles and the branch cuts starting with the scale M. This condition allows the contour deformation to give (see Fig 2.13)

$$-B_k(p^2)\big|_{\mathrm{IR}} = B_k(p^2)\big|_{\mathrm{UV}} \,. \tag{2.54}$$

The IR part can be evaluated by taking the Residue of pole structures of weakly coupled EFT, while the UV part is a positive sum over the partial wave coefficient. By expanding around the forward limit $p \to 0$, the dispersive sum rule (2.54) allows us to find an optimal positive combination of UV data that bounds the ratio of low energy Wilson coefficients from two-sides. It can give, for example

$$g_0 \geq 0 \,, \qquad \frac{\#_1}{M^a} < \frac{g}{g_0} < \frac{\#_2}{M^a} \,, \tag{2.55}$$

where a counts the dimension of the ratio.

However, this procedure has suffered from a long-standing issue in the presence of gravity because the low-energy graviton pole completely diverges in the forward limit. This problem has been addressed in [33] by measuring the EFT parameters at impact parameter $b \sim 1/M$ rather than the forward limit $p \to 0$. Namely, [33] smears the sum rule (2.54) by wave function $\psi(p)$ so that the sum rule radically decays at large $b \gg 1/M$

$$-\int_0^M dp\,\psi(p)B_k(p^2)\big|_{\rm IR} = \int_0^M dp\,\psi(p)B_k(p^2)\big|_{\rm UV}\,. \tag{2.56}$$

This measurement allows them to find optimal such function $\psi(p)$ that bounds Wilson coefficients in terms of Newton constant G_N, for example

$$\frac{\#_1 G_N}{M^{\dim - D+2}} < g < \frac{\#_2 G_N}{M^{\dim - D+2}}\,, \tag{2.57}$$

where the dimension of g is dim.

This type of bounds was considered in [33] for holographic CFTs with local AdS EFT dual, which sharpens the notion of AdS locality with numerics. The basic idea is to construct the CFT dispersive sum rule along the line of [89] where the IR and UV sectors are separated by $\Delta_{\rm gap}$. It should be emphasized that the AdS locality at the Regge limit $b \gg 1/M$ is guaranteed by flat-space functional as $\psi(p)$ creates functionals localized in impact parameter space. This led [89] to show that the positive flat-space functional can be uplifted to give a positive CFT functional with, at most small corrections. On the other hand, the functional also measures the same Wilson coefficient as in flat-space within the EFT regime up to $1/\Delta_{\rm gap}$ corrections. The whole analysis then suggests that the flat-space bound can give rise to the constraint of holographic CFT

$$\frac{\#_1 G_N}{\Delta_{\rm gap}^{\dim - D+2}}\big(1+\mathcal{O}(\frac{1}{\Delta_{\rm gap}^2})\big) < \frac{g_{\rm AdS}}{\ell^{\dim - D+2}} < \frac{\#_2 G_N}{M^{\dim - D+2}}\big(1+\mathcal{O}(\frac{1}{\Delta_{\rm gap}^2})\big)\,, \tag{2.58}$$

where $g_{\rm AdS}/\ell^{\dim - D+2}$ is associated with some OPE coefficients in CFT.

Chapter 3

Flat-space limit of AdS/CFT

3.1 Introduction

Including negative cosmological constant, gravity theory coupled to other local fields can be formulated as weakly coupled quantum field theory (QFT) by perturbatively expanding the curvatures around the Anti-de Sitter (AdS) background. Although the resulting QFT lives on AdS, we are still able to apply the standard techniques, which utilize the propagators in AdS to calculate the "AdS amplitudes" for local quantum fields. As interpreted by the AdS/CFT correspondence, these AdS amplitudes are corresponding to correlation functions of large-N expanded conformal field theory (CFT) on the AdS boundary [9, 10, 11].

Naively, at the level of effective Lagrangian, we can take the large AdS radius limit $\ell \to \infty$, QFTs on AdS then make no difference from flat-space. We can also easily observe the limit $\ell \to \infty$ reduces AdS background to a flat-space. It is, however, rather nontrivial to incorporate the AdS amplitudes into this flat-space limit, where we expect that AdS amplitudes degrade and give rise to S-matrix or scattering amplitudes of QFT in flat-space. Employing AdS/CFT, the flat-space limit of AdS then suggests that boundary CFT correlation function shall encode the flat-space S-matrix [1].

[1] It is worth noting that the flat-space limit of AdS/CFT is different from flat holography proposal, e.g., [90]. In the flat-space limit of AdS/CFT, we expect CFT encodes one higher dimensional S-matrix, but the S-matrix can not fully encode CFT. While by flat holography, flat-space physics and CFT should be able to be transformed back and forth between each other

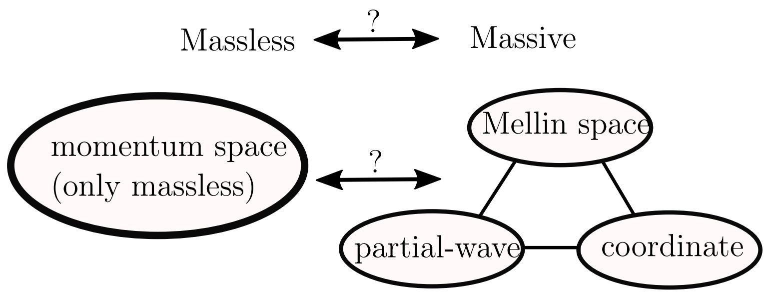

Figure 3.1: The existed frameworks describing the flat-space limit of AdS/CFT, where the question mark denotes the undiscovered relation.

The idea on the flat-space limit of AdS/CFT enjoys a long history [14, 15, 16, 17, 18, 19, 20], and more quantitative and precise maps were established in the recent decade [21, 22, 23, 24, 3, 25, 26]. However, in the literature, there exist several frameworks which work in different representations of CFT: momentum space [26], Mellin space [22, 23, 25], coordinate space [21, 24, 3], and partial-wave expansion (conformal block expansion) [24, 25], as summarised in Figure 3.1. The latter three representations are natural to consider conformal bootstrap [89], so our focus will be mostly on the latter three frameworks, for which the formulas describing massless scattering and massive scattering (defined for external legs) are sharply different. The massless particles are described by operators with finite conformal dimension, while massive particles are described by operators with infinite conformal dimension $\Delta \sim \ell \to \infty$ [2]. The details shall be reviewed in subsection 3.3.1 and here we simply provide a chronological history: the massless formula in coordinate space for four-point case was first proposed in [21] and was reformulated by the proposal of Mellin space [22], which is later known as the bulk-point limit [24], and a contact example of the partial-wave coefficients was provided in [24]; the massive Mellin space formula and the phase-shift formula (which is basically the coefficient of the partial-wave) was later proposed in [25], and the massive formula in the coordinate space was recently conjectured in [3].

Two natural questions that we aim to answer in this paper are:

- What is the origin of these seemingly different frameworks of the flat-space

[2] For the framework in momentum space, as far as we know, only the massless formula was proposed [26]

limit?

- Why do the formulas describing massless scattering and massive scattering look different and how do we unify them?

Considering the Mellin space, coordinate space and partial-wave expansion can be translated to each other, we expect they share the same origin. The origin follows the spirit of the HKLL formula [91, 92], which represents the flat-space S-matrix in terms of boundary correlation function via smearing over the boundary against a scattering smearing kernel. Such scattering smearing kernel for massless scattering was constructed in [20] and was applied to rigorously derive the massless Mellin formula later [23]. A scattering smearing kernel that is generally valid for both massless and massive cases was proposed in [93], which slightly overlaps with this paper. We find, crucially, only the scattering smearing kernel constructed from global AdS can be served as the origin of the flat-space limit in Mellin space, coordinate space, and partial-wave expansion; on the other hand, when we construct the scattering smearing kernel from Poincare AdS, we find it simply performs the Fourier-transform and thus gives rise to the framework of flat-space limit in momentum space. According to subregion duality [94, 95, 96] which states subregion of CFT is encoded in the corresponding subregion of AdS (usually the causal wedge [94] or more generally entanglement wedge [97]), we expect that the Poincare scattering smearing kernel can be transformed to the global smearing kernel, simply because the Poincare patch is a part of the global AdS. We indeed find that the global scattering can be obtained from Poincare scattering, which also suggests a momentum-coordinate duality for CFT at large momentum and conformal dimensions.

Notably, scattering smearing kernels never treat massless and massive scattering distinguishingly, we should be able to unify the massless flat-space limit and massive flat-space limit. In this paper, we find a Mellin formula applying to all masses, which can be easily translated to other frameworks for both massless and massive cases. Typically, in terms of CFT language, the massive scattering is more like a "limit" of massless one, because nonzero masses provide additional large parameters

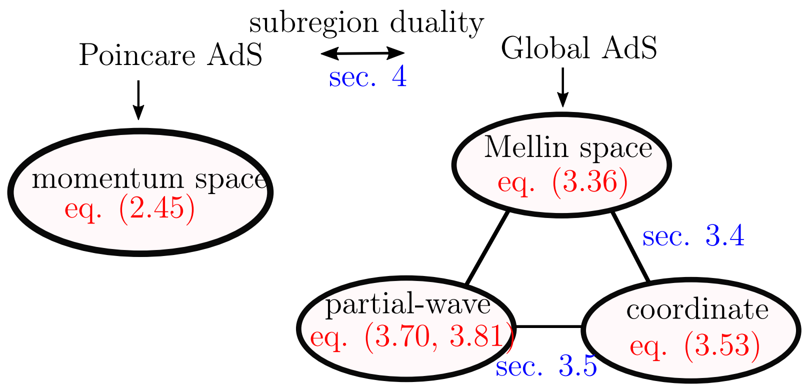

Figure 3.2: Massless and massive unified frameworks of the flat-space limit, where the origins are clarified.

$\Delta \sim \ell \to \infty$ that further dominate the scattering smearing kernel.

The outline of our finding is illustrated in Figure 3.2. This paper is organized as follows. In section 3.2, we take the flat-space limit for bulk reconstruction in both global AdS and Poincare AdS to construct scattering smearing kernels that represent flat-space S-matrix in terms of CFT correlator. The Poincare scattering smearing kernel automatically Fourier-transforms the CFT correlator and gives rise to flat-space limit in momentum space. In section 3.3, we review the existed flat-space limit, include Mellin space, coordinate space, and partial-wave expansion. We start with the global scattering smearing kernel and find saddle-points that dominate the smearing integral. Using the saddle-points, we find a Mellin formula that applies to both massless scattering and massive scattering. We then show this Mellin formula gives rise to the flat-space limit in coordinate space, and then to the partial-wave/phase-shift formula. In section 3.4, use the notion of subregion duality, we propose a momentum-coordinate duality, which relates the flat-space limit in momentum space to global scattering smearing kernel. In section 3.5, we propose a flat-space parameterization of embedding coordinate for spinning operators. We apply our proposal to $\langle VV\mathcal{O}\rangle$ three-point function where V is conserved current, we verify the momentum-coordinate duality as well as a map to flat-space amplitude.

In appendix A.1, we analytically continue the flat-space limit in momentum space to Euclidean CFT, which effectively turns AdS into dS. In appendix A.2, we show how to fix the normalization of scattering smearing kernel. In appendix A.3, we provide

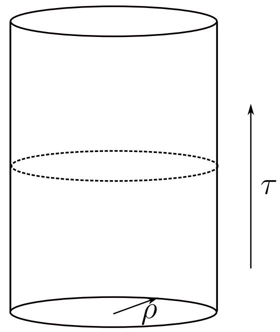

Figure 3.3: Cylinder diagram of global AdS.

more details on derivation of Mellin flat-space limit. In appendix A.4, we compute four-point scalar contact Witten diagram (no derivative) and verify it is equivalent to momentum conservation delta function in the flat-space limit. In appendix A.5, we introduce a new conformal frame, which helps us solve the conformal block at limit $\Delta, \Delta_i \to \infty$. We double-check our conformal block by working explicitly in $d = 2, 4$.

3.2 Quantization and scattering smearing kernel

3.2.1 Global quantization and the flat-space limit

We first consider global Euclidean AdS coordinate

$$ds^2 = \frac{\ell^2}{\cos\rho^2}(d\tau^2 + d\rho^2 + \sin\rho^2 d\Omega_{d-1}^2)\,, \tag{3.1}$$

where its boundary is located at $\rho = \pi/2$. The advantage of global AdS is that it provides a $R \times S_{d-1}$ background for boundary CFT, i.e.,

$$ds^2_{\text{CFT}} = d\tau^2 + d\Omega^2_{d-1}\,, \tag{3.2}$$

which is natural for radial quantization in CFT. This global coordinate is depicted in Fig 3.3. Moreover, to make contact with flat Minkowski space where physical scattering processes happen, we may start with Lorentzian AdS. To do this, we simply wick rotate τ

$$ds^2 = \frac{\ell^2}{\cos\rho^2}(-d\tau^2 + d\rho^2 + \sin\rho^2 d\Omega_{d-1}^2)\,, \tag{3.3}$$

for which the AdS and CFT embedding coordinate X and P are parameterized by

$$X = \frac{\ell}{\cos\rho}(\cos\tau, -i\sin\tau, \sin\rho\,\widehat{r})\,, \quad P = (\cos\tau, -i\sin\tau, \widehat{r})\,, \tag{3.4}$$

respectively.

Let us consider a free scalar with mass m in global AdS, which can be quantized by [19]

$$\phi = \sum_{n,J,m_i} e^{iE_{nJ}\tau} R_{n,J}(\rho) Y_{Jm_i}(\widehat{\rho}) a_{nJm_i} + \text{c.c}\,,$$

$$R_{n,J}(\rho) = \frac{1}{N_{\Delta J}} \sin^J\rho \cos^\Delta\rho\, {}_2F_1\big(-n, \Delta + J + n, J + \frac{d}{2}, \sin\rho^2\big)\,, \tag{3.5}$$

where the energy eigenvalues are discretized as $E_{nJ} = \Delta + J + 2n$, and

$$m^2\ell^2 = \Delta(\Delta - d)\,. \tag{3.6}$$

This spectra correspond to a primary operator $\mathcal{O}$ and all its descendent family $\partial^{2n}\partial_{\mu_1}\cdots\partial_{\mu_J}\mathcal{O}$. The normalization factor $N_{\Delta J}$ can be found by usual quantization procedure

$$[\phi(\vec{x},\tau), \pi(\vec{y},\tau)] = i\frac{\delta(\vec{x}-\vec{y})}{\sqrt{-g}}\,, \quad [a_{nJm_i}, a^\dagger_{n'J'm'_i}] = \delta_{nn'}\delta_{JJ'}\delta_{m_i m'_i}\,, \tag{3.7}$$

which yields [19]

$$N_{\Delta J} = \sqrt{\frac{n!\Gamma(J+\frac{d}{2})^2\Gamma(\Delta + n - \frac{d-2}{2})\ell^{d-1}}{\Gamma(n+J+\frac{d}{2})\Gamma(\Delta+n+J)}}\,. \tag{3.8}$$

Since we are starting with global AdS, we may call this quantization “global quantization".

Now with this preliminary of global quantization, we can move to discuss the flat-space limit. At first, we shall discuss how to take the flat-space limit for coordinates. Our notation of flat-space is

$$ds^2 = -dt^2 + dr^2 + r^2 d\Omega_{d-1}^2 \,. \tag{3.9}$$

We can see now taking the flat-space limit for coordinates is quite trivial, we can take the coordinate transformation

$$\ell \tan\rho = r \,, \quad \tau\ell = t \,, \tag{3.10}$$

and then send $\ell \to \infty$. It immediately follows that to make the Fourier factor $e^{iE\tau}$ in (3.5) valid with flat-space limit, the energy must scale as ℓ, i.e., $E = \omega\ell$, where we denote ω as the energy in flat-space. This fact also indicates that $n \sim \ell$ for massless particles, more specifically we have $\omega = 2n/\ell$. Note also in the context of AdS/CFT, we should be aware of $m \sim \Delta/\ell$. Thus any primary scalar operators with finite conformal dimensions Δ corresponds to massless particles in the flat-space limit [21], and it is necessary to consider scalar operators with large conformal dimensions scaling linear in ℓ to probe massive particles in flat-space [25].

Before we discuss the flat-space limit of quantization, we shall briefly review the quantization of scalar fields in flat-space in spherical coordinates. To avoid confusion, we denote φ as scalars in flat-space. We have

$$\varphi = \sum_{J,m_i} \int d\omega (a_{\omega J m_i} e^{i\omega t} R_{|\vec{p}|,J}(r) Y_{J m_i}(\widehat{r}) + \text{c.c}) \,, \tag{3.11}$$

where Y_{Jm_i} is the spherical harmonics on S^{d-1} (in which m_i denotes all "magnetic" angular momenta), and the radial function $R_{|\vec{p}|,J}(r)$ is given by

$$R_{|\vec{p}|,J}(r) = \frac{1}{\sqrt{2}} r^{\frac{2-d}{2}} J_{\frac{d-2}{2}+J}(|\vec{p}|r) \,. \tag{3.12}$$

The quantization condition is also straightforward

$$[\varphi(\vec{x},t),\pi_\varphi(\vec{y},t)] = i\frac{\delta(\vec{x}-\vec{y})}{\sqrt{-g}}\,, \quad [a_{\omega J m_i}, a^\dagger_{\omega' J' m'_i}] = \delta(\omega-\omega')\delta_{JJ'}\delta_{m_i m'_i}\,. \tag{3.13}$$

Now we can easily take the flat-space limit for radial function and we can observe that

$$R_{n,J}(\rho)\big|_{\ell\to\infty} = \sqrt{\frac{2}{\ell}}R_{|\vec{p}|,J}(r)\,. \tag{3.14}$$

It is also not hard to probe the flat-space limit for creation and annihilation operators by comparing the canonical quantization condition for those operators, i.e.,

$$\begin{aligned}&[a_{njm_i}, a^\dagger_{n'j'm'_i}]\big|_{\ell\to\infty} = \delta(n-n')\delta_{JJ'}\delta_{m_i m'_i} = \delta(\frac{(\omega-\omega')\ell}{2})\delta_{JJ'}\delta_{m_i m'_i}\\ &= \frac{2}{\ell}\delta(\omega-\omega')\delta_{JJ'}\delta_{m_i m'_i} = \frac{2}{\ell}[a_{\omega J m_i}, a^\dagger_{\omega' J' m'_i}]\,.\end{aligned} \tag{3.15}$$

It thus immediately follows

$$a_{njm_i}\big|_{\ell\to\infty} = \sqrt{\frac{2}{\ell}}e^{i\eta}a_{\omega J m_i}\,, \tag{3.16}$$

with an arbitrary phase factor η that is to be fixed by convenience later. Trivially, the Fourier factor is simply $e^{iE\tau} = e^{i\omega t}$, and the flat-space limit of measure in summation over all energy spectra is also consistent

$$\sum_n \to \int d\omega\frac{\ell}{2}\,. \tag{3.17}$$

By including above factors, we are led to

$$\phi\big|_{\ell\to\infty} \simeq \varphi\,. \tag{3.18}$$

In other words, the flat-limit of the quantized scalars in global AdS is equivalent to the quantized scalars in flat-space.

Using the quantization in global AdS, the corresponding primary operator $\mathcal{O}$ that is dual to ϕ can be quantized via

$$\mathcal{O} = \sum_{n,j,m_i} (e^{iE_{nj}\tau} Y_{jm_i}(\widehat{\rho}) a_{njm} + \text{c.c}) N^{\mathcal{O}}_{\Delta,n,j} \,, \tag{3.19}$$

where the normalization can be fixed by normalizing the two-point function [19]

$$N^{\mathcal{O}}_{\Delta,n,j} = \sqrt{\frac{\Gamma(1+\Delta-\frac{d}{2}+n)\Gamma(\Delta+J+n)}{\Gamma(1+n)\Gamma(\frac{d}{2}+J+n)}} \frac{1}{\Gamma(1+\Delta-\frac{d}{2})} \,. \tag{3.20}$$

It then follows that we can represent creation operator by $\mathcal{O}$ via

$$a^{\dagger}_{njm_i} = \int_{-\frac{\pi}{2}-\tau_0}^{\frac{\pi}{2}-\tau_0} \frac{d\tau}{\pi} d\Omega_{d-1} e^{iE_{nj}\tau} \frac{Y_{jm_i}(\widehat{\rho})}{N^{\mathcal{O}}_{\Delta,n,j}} \mathcal{O}(\tau,\widehat{\rho}) \,, \tag{3.21}$$

where τ_0 is the (finite) reference time which can be chosen for convenience and doesn't affect the integral. This reflects the τ translation symmetry. Take the flat-space limit on both sides of above formula, we obtain

$$a^{\dagger}_{\omega J m_i} = \int_{-\frac{\pi}{2}\ell-\tau_0}^{\frac{\pi}{2}\ell-\tau_0} \frac{dt d\Omega_{d-1}}{\sqrt{2\pi^2\ell}} e^{i\omega t} Y_{jm_i}(\widehat{\rho}) 2^{\Delta-\frac{d}{2}} (|\vec{p}|\ell)^{\frac{d}{2}-\Delta} \xi_{\omega\Delta} \Gamma(1+\Delta-\frac{d}{2}) \times e^{-i\eta} \mathcal{O}(\tau,\widehat{\rho}) \,, \tag{3.22}$$

where we define

$$\xi_{\omega\Delta} = \left(\frac{\omega\ell-\Delta}{\omega\ell+\Delta}\right)^{\frac{\omega\ell}{2}} e^{\Delta} = \exp\left[\frac{\omega\ell}{2} \log\left(\frac{\omega\ell-\Delta}{\omega\ell+\Delta}\right) + \Delta\right] , \tag{3.23}$$

which, as an exponent factor, is well-defined for both massive and massless cases. We can readily verify that $\xi_{\omega\Delta}$ is simply 1 at $\ell \to \infty$ limit for massless particles.

Using this formula, we can construct the smearing kernel $K_a(t,\widehat{r})$ that represents scattering states $|p\rangle$ in terms of primary operator in CFT [20]

$$|p\rangle = \int dt d\Omega_{d-1} K_a(t,\widehat{r}) \mathcal{O}(\tau,\widehat{r})|0\rangle \,, \tag{3.24}$$

To find the smearing kernel, we can decompose the momentum eigenstate $|p\rangle$ into angular momentum eigenstate

$$|p\rangle = \sum_{J,m_i} \langle J, m_i|p\rangle |J, m_i\rangle\,, \quad \langle J, m_i|p\rangle = i^J 2^{\frac{d+1}{2}} \pi^{\frac{d}{2}} |\vec{p}|^{\frac{2-d}{2}} Y_{Jm_i}(\widehat{p})\,, \tag{3.25}$$

from which we can derive the smearing kernel

$$\begin{aligned} K_a(t,\widehat{r}) &= e^{i\omega t} \sum_{Jm_i} \ell^{\frac{d-1}{2}-\Delta} \xi_{\omega,\Delta} |\vec{p}|^{1-\Delta} \times 2^{\Delta} \pi^{\frac{d-2}{2}} Y_{Jm_i}(\widehat{r}) Y_{Jm_i}(\widehat{p}) \Gamma(1+\Delta-\frac{d}{2}) \\ &= e^{i\omega t} \ell^{\frac{d-1}{2}-\Delta} \xi_{\omega,\Delta} |\vec{p}|^{1-\Delta} \times 2^{\Delta} \pi^{\frac{d-2}{2}} \Gamma(1+\Delta-\frac{d}{2}) \delta(\widehat{p}-\widehat{r})\,, \end{aligned} \tag{3.26}$$

in which we choose $\eta = -J\pi/2$ to cancel the funny i^J factor. Note this smearing kernel is obtained for a free scalar theory. Nevertheless, we assume it also works whenever the plane-wave state is asymptotically free, which is exactly the scattering states defined at infinite past or future. We can then apply this smearing kernel to establish a formula relating flat-space (n-particle) S-matrix to CFT n-point function (or AdS amplitudes)

$$\begin{aligned} S &= {}_{+\infty}\langle p_1 p_2 \cdots p_k | p_{k+1} \cdots p_n \rangle_{-\infty} = \mathbb{I} + i\delta^{(d+1)}(p_{\text{tot}}) T(p_i) \\ &= \lim_{\ell\to\infty} \int \Big(\prod_i dt_i e^{i\omega_i t_i} \ell^{\frac{d-1}{2}-\Delta_i} \xi_{\omega_i \Delta_i} |\vec{p}_i|^{1-\Delta} 2^{\Delta_i} \pi^{\frac{d-2}{2}} \Gamma(1+\Delta_i - \frac{d}{2}) \Big) \langle \mathcal{O}_1 \cdots \mathcal{O}_n \rangle\,, \end{aligned} \tag{3.27}$$

where $\mathbb{I}$ denotes the disconnected part of S-matrix and T the scattering amplitudes, and in the second line we analytically continue the momenta such that all momenta are in-states before employing the smearing kernel (3.26). The interpretation of eq. (3.27) shall be briefly discussed before we move on. A pure CFT does know nothing about ℓ without the notion of AdS/CFT. One job that AdS/CFT (with large ℓ limit of AdS) does is to provide a specific kernel K_{s} in eq. (3.27). Then we can study a particular CFT correlator in a single CFT and notice that the smeared version (smear over τ) of the CFT correlator with a large ℓ limit of the kernel will approximate the flat-space S-matrix, where Δ/ℓ estimates the masses. However, from the dynamics, to define a flat-space QFT with gravity, we have to take a family of AdS and follow the sequence that ℓ grows. The estimation of flat-space S-matrix by using eq. (3.27) becomes more and more accurate if we have a family of CFTs supported with large N limit and sparse gap Δ_{gap}. Thus to extract S-matrix accurately by using eq. (3.27), one should consider a family of CFTs. We shall call

$$K_{\rm s}=\Big(\prod_i e^{i\omega_i t_i}\ell^{\frac{d-1}{2}-\Delta_i}\xi_{\omega_i\Delta_i}|\vec{p}_i|^{1-\Delta_i}2^{\Delta_i}\pi^{\frac{d-2}{2}}\Gamma(1+\Delta_i-\frac{d}{2})\Big)\,, \tag{3.28}$$

the global scattering smearing kernel. This global scattering smearing kernel generalizes the massless smearing written down in [23], and was also recently obtained by requiring the consistency with HKLL formula [93] (where they take $\Delta\sim m\ell\to\infty$ to simplify the prefactor). Note that the integration range in t is different from [23] for massless case. In [23], the scattering smearing kernel integrates time within $t\in(-\pi/2\ell-\delta t,-\pi/2\ell+\delta t)$, because it was argued that the flat-space physics emerges from the wave packets starting around $\tau=-\pi/2$ [17], and δt exists to make sure the in and out wave packets don't overlap. Here we construct the scattering smearing kernel from the exact free theory and thus the integration range runs over the reasonable range of τ, i.e., $(-\pi/2-\tau_0,\pi/2-\tau_0)$. In the next section, we prove that there is indeed $\tau=-\pi/2$ (for reference point $\tau_0>0$) dominates the scattering smearing kernel and thus effectively gives $t\in(-\pi/2\ell-\delta t,-\pi/2\ell+\delta t)$.

3.2.2 Poincare quantization and the momentum space

We can also consider quantization in Poincare coordinates

$$ds^2=\frac{\ell^2}{z^2}(dz^2-dT^2+\sum_{i=1}^{d-1}dY_i^2)\,, \tag{3.29}$$

which can be depicted as Fig 3.4. It is straightforward to work with the quantization

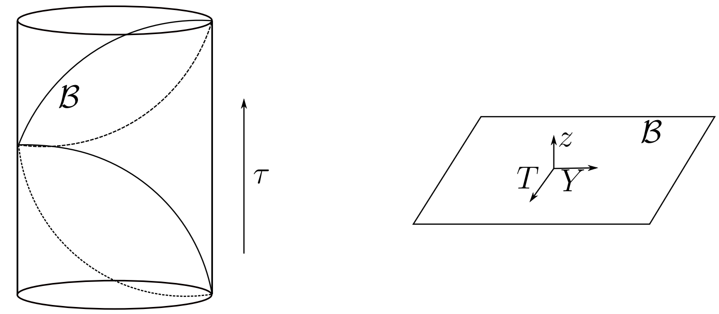

Figure 3.4: Poincare AdS only covers a wedge of global AdS. On LHS, the lines marked $\mathcal{B}$ meet the global AdS boundary. $\mathcal{B}$ is the boundary of Poincare AdS where CFT lives. On the RHS, we depict a local figure near $\mathcal{B}$.

in this coordinate, which gives

$$\phi = \frac{1}{\sqrt{2}\ell^{\frac{d-1}{2}}} \int_{E>|K|} \frac{dE d^{d-1}K}{(2\pi)^{\frac{d-1}{2}}} \left(a_{EK} e^{-iET+i\vec{K}\cdot Y} z^{\frac{d}{2}} J_{\Delta-\frac{d}{2}}(z|\mathbf{K}|) + \text{c.c}\right), \qquad (3.30)$$

where we denote $|\mathbf{K}| = \sqrt{E^2 - K^2} > 0$, and the overall factor is determined by canonical quantization condition

$$[\phi(Y), \pi_\phi(Y')] = i\frac{\delta^{(d)}(Y - Y')}{\sqrt{-g}}, \quad [a_{EK}, a^\dagger_{E'K'}] = \delta(E - E')\delta^{(d-1)}(K - K'). \quad (3.31)$$

Note this quantization is only valid for $E > K$ where the momentum is time-like, which is the necessary condition for the field to have its CFT dual. For the space-like spectrum $E < K$, it is equivalent to consider Euclidean AdS, and this quantization crashes because of the divergence at Poincare horizon $z \to 0$. Instead of the Bessel function of the first kind, the quantization for spatial momentum should be expanded by the modified Bessel function of the second kind K_ν which does, however, not have the appropriate fall-off to admit operator dual. We shall emphasize it does not contradict the Euclidean AdS/CFT, it only indicates that in Euclidean space the quantization of CFT operators is not compatible with the bulk quantization described above if we persist AdS. Nevertheless, [26] established a flat-space limit in the momentum space for spatial momentum, and the price is to have an imaginary momentum in the bulk. We show in appendix A.1 their limit is equivalent to ours but wick rotates $z \to iz$, which in effect analytically continues AdS to dS.

The scalar field in flat-space is standardly quantized via

$$\varphi = \int \frac{d^d k}{(2\pi)^d 2\omega} \left(a_k e^{-i\omega t + \vec{k}\cdot x} + a_k^\dagger e^{i\omega t - i\vec{k}\cdot x} \right) , \tag{3.32}$$

where

$$[\varphi(x), \pi_\varphi(x')] = i\delta^{(d)}(x - x') , \quad [a_k, a_{k'}^\dagger] = (2\pi)^d 2\omega \delta^{(d)}(k - k') . \tag{3.33}$$

Our first goal is thus to understand that how the flat-space limit brings (3.30) to (3.32). For this purpose, we change the variables

$$z = e^{\frac{x_d}{\ell}} , \tag{3.34}$$

such that the limit $\ell \to \infty$ would nicely give rise to Minkowski space

$$ds^2 = -dt^2 + \sum_{i=1}^{d} dx_i^2 , \quad t = \ell T , \quad x_{i<d} = \ell Y_i . \tag{3.35}$$

To fully understand the flat-space limit of quantization, we have to clarify $\ell \to \infty$ limit of mode functions. As before, the Fourier phase factor is trivial, we just need to take the energy and the momenta in AdS scaling as ℓ, i.e., $E = \omega\ell , K = k\ell$. Probing the large ℓ limit of Bessel functions is more technically difficult. We shall first explicitly write down the series representation of Bessel function

$$J_\nu(x) = (\frac{1}{2}x)^\nu \sum_{n=0}^{\infty} (-1)^n \frac{\left(\frac{1}{4}x^2\right)^n}{\Gamma(\nu + n + 1)\Gamma(n + 1)} , \tag{3.36}$$

and we should be interested in its limit at $\nu, x \to \infty$ with ν/x fixed. The strategy is to rewrite this series in terms of a complex integral

$$J_\nu(x) = \int_C \frac{dz}{2\pi i} \frac{\left(\frac{1}{2}x\right)^{2z+\nu}}{\Gamma(\nu + z + 1)\Gamma(z + 1)} \frac{e^{iz\pi}}{e^{2iz\pi} - 1} . \tag{3.37}$$

When we deform the contour to pick up poles located at $z \in \mathbb{Z}^+$, the series repre-

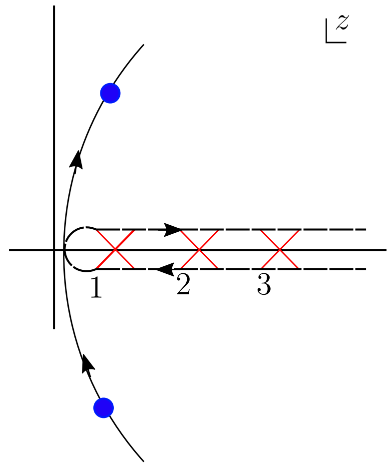

Figure 3.5: The original integral contour of z, as depicted as dotted line, picks up poles denoted as cross at positive integers, which sums to Bessel function. The contour is deformed to pass through the saddle-points in the desired limit.

sentation (3.36) is produced. The trick to find its limit is to notice that the limit exponentiates the integrand, and thus we can deform the integral contour to pick up the saddle-points, which gives

$$J_\nu(x)\Big|_{\nu,x\to\infty,\nu/x\,\text{fixed}} = \frac{e^{-\frac{3i\pi}{4}-i\chi}x^{-i\chi}(\nu-i\chi)^{\frac{1}{2}(i\chi-\nu)}(\nu+i\chi)^{\frac{1}{2}(i\chi+\nu)}}{\sqrt{2\pi}(e^{i\pi\nu-\pi\chi}-1)\chi^{\frac{1}{2}}} + \text{c.c}\,, \tag{3.38}$$

where $\chi = \sqrt{x^2-\nu^2}$. The process is depicted in Fig 3.5. This trick is actually the main tool of this paper, and we will use it to derive the flat-space limit formula in following sections. After simple algebra, we find

$$J_{\Delta-\frac{d}{2}}(|\mathbf{K}|z)|_{\ell\to\infty} = \alpha_{k_d}e^{ik_d x_d} + \alpha^\dagger_{k_d}e^{-ik_d x_d}\,, \tag{3.39}$$

where $k_d = \sqrt{|\mathbf{k}|^2-m^2}$ and

$$\alpha_{k_d} = \frac{e^{i\ell k_d - i\frac{\pi}{4}}(m+ik_d)^{-\frac{\Delta}{2}}(m-ik_d)^{\frac{\Delta}{2}}}{\sqrt{2\pi\ell}k_d^{\frac{1}{2}}}\,. \tag{3.40}$$

Then it is readily to evaluate

$$\phi|_{\ell\to\infty} = \frac{\ell^{\frac{d+1}{2}}}{\sqrt{2}}\int \frac{dk_d d^{d-1}k}{(2\pi)^{\frac{d-1}{2}}}\frac{k_d}{\omega}(a_{EK}\alpha_{k_d}e^{-i\omega t+i\vec{k}\cdot x} + \text{c.c})\,, \tag{3.41}$$

where the covariant momentum now is

$$p^{(d+1)} = (\omega, k) = (\omega, k_{i<d}, k_d) = (p^{(d)}, k_d)\,, \tag{3.42}$$

which satisfies the on-shell condition trivially. We have used on-shell condition to replace $d\omega$ by dk_d with a Jacobian factor k_d/ω, it is then easy to observe that $\alpha_{k_d} = (2\pi\ell k_d)^{-\frac{1}{2}} e^{i\tilde{\alpha}_{k_d} - i\frac{\pi}{4}}$, where $\tilde{\alpha}_{k_d}$ is purely real in the Lorentzian signature and denotes the nontrivial phase. We thus obtain the limit for annihilation (or creation) operator

$$a_{EK}|_{\ell\to\infty} = \frac{1}{\sqrt{2\ell^{d-1}(2\pi)^{d-1}}} \alpha^{\dagger}_{k_d} e^{i(\eta+\frac{\pi}{4})} a_k\,, \tag{3.43}$$

which suggests the same formula (3.18). We can then readily obtain the smearing kernel in Poincare coordinate (we simply choose $\eta = -\pi/4$ to cancel the pure number in the phase)

$$|p\rangle = 2^{1-\frac{d}{2}+\Delta} \ell^{-\Delta} \sqrt{\frac{\Gamma(1+\Delta-\frac{d}{2})}{\Gamma(\frac{d}{2}-\Delta)}} \frac{k_d^{\frac{1}{2}}}{|\mathbf{k}|^{\Delta-\frac{d}{2}}} e^{-i\tilde{\alpha}_{k_d}} \int d^d x e^{ip^{(d)}\cdot x} \mathcal{O}(T,Y)|0\rangle\,. \tag{3.44}$$

We can thus conclude

$$S = \lim_{\ell\to\infty} \int \Big(\prod_i d^d x_i 2^{1-\frac{d}{2}+\Delta_i} \ell^{-\Delta_i} \sqrt{\frac{\Gamma(1+\Delta_i-\frac{d}{2})}{\Gamma(\frac{d}{2}-\Delta_i)}} \frac{k_{id}^{\frac{1}{2}}}{|\mathbf{k}_i|^{\Delta_i-\frac{d}{2}}} e^{-i\tilde{\alpha}_{k_d}} e^{ip_i^{(d)}\cdot x_i} \Big) \langle \mathcal{O}_1 \cdots \mathcal{O}_n \rangle_{\mathrm{L}}\,, \tag{3.45}$$

where the subscript L denotes the Lorentzian correlator. In other words, written in Poincare patch, the flat-space S-matrix is simply the Fourier-transform of correlators, up to prefactors with robust dependence on the momentum. This formula reminds us the flat-space limit in momentum space of AdS proposed in [26] for massless particles, which is actually related to ours by wick rotations to Euclidean CFT and is also shared by dS flat-space limit. We explain the details in appendix A.1, and here we simply

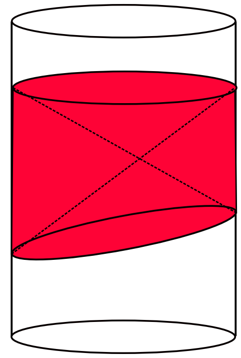

Figure 3.6: The red strip of boundary can reconstruct the bulk fields living in the region enclosed by the red strip.

quote the formula

$$S = \lim_{\ell\to\infty} \int \Big(\prod_i d^d x_i 2^{1-\frac{d}{2}+\Delta_i} \ell^{-\Delta_i} \sqrt{\frac{\Gamma(1+\Delta_i-\frac{d}{2})}{\Gamma(\frac{d}{2}-\Delta_i)}} \frac{\omega_i^{\frac{1}{2}}}{|p_i|^{\Delta_i-\frac{d}{2}}} e^{-i\tilde{\alpha}_\omega} e^{ip_i\cdot x_i} \Big) \langle \mathcal{O}_1 \cdots \mathcal{O}_n \rangle_{\mathrm{E}} \,, \tag{3.46}$$

where p is spatial and satisfies $-\omega^2 + p^2 = -m^2$.

3.2.3 HKLL + LSZ = scattering smearing kernel

In preceding sections, we constructed the scattering smearing kernel for both global AdS and Poincare AdS by quantization procedures. The quantization and mode sum approach is also used to construct the HKLL formula which reconstructs the bulk fields from boundary CFT operators [91, 92]

$$\phi(X) = \int d^d P K(X;P) \mathcal{O}(P) \,, \tag{3.47}$$

where X is bulk coordinate and P boundary coordinate. An illustrative example is depicted in Fig 3.6. Eq. (3.47) is the HKLL formula encoding only the free theory. In order to reconstruct bulk fields with interactions, the HKLL formula should include more terms perturbatively in couplings. Nevertheless, the free theory version above is enough for our purpose as we consider perturbative QFT: the Feynman rules consist of only the free fields supplemented by the form of interaction vertices, while the exact propagator is not necessary. We can expect that the flat-space limit of HKLL formula simply represents flat-space fields in terms of CFT operators. In flat-space, S-matrix can be constructed from correlator of fields through LSZ reduction. For scalars, it reads

$$S=\int\big(\prod_{i=1}^{n}d^{d+1}x_i e^{ip_i\cdot x_i}(p_i^2+m_i^2)\big)\langle \mathrm{T}\phi(x_1)\cdots\phi(x_n)\rangle\,, \tag{3.48}$$

where T refers to time ordering. Thus it is natural that scattering smearing kernel could be constructed by simply combining HKLL formula and LSZ reduction, in a way that we have

$$S=\lim_{\ell\to\infty}\int\big(\prod_{i=1}^{n}d^{d+1}x_i d^d x_i' e^{ip_i\cdot x_i}(p_i^2+m_i^2)K(x_i;x_i')\big)\langle\mathcal{O}(x_1')\cdots\mathcal{O}(x_n')\rangle\,. \tag{3.49}$$

In this subsection, we provide strong evidence that this procedure indeed works for both global smearing and Poincare smearing. For simplicity, we consider HKLL formula in even bulk dimensions, which is then free of logarithmic term. In odd bulk dimensions, although HKLL formula contains a further logarithmic term, we can argue that such a logarithmic term just gives an factor that is naturally absorbed in the normalization.

In both global and Poincare AdS, the smearing function K in HKLL formula eq. (3.47) is written as [92]

$$K(x,\rho;x')=\frac{(-1)^{\frac{d-1}{2}}2^{\Delta-d-1}\Gamma(\Delta-\frac{d}{2}+1)}{\pi^{\frac{d}{2}}\Gamma(\Delta-d+1)}\sigma(x,x')^{\Delta-d}\,, \tag{3.50}$$

where $\sigma(x,x')$ is the geodesic length connecting bulk points x and boundary points x', which reads, respectively for global and Poincare AdS

$$\sigma_{\text{global}}=\cos(\tau-\tau')-\sin\rho\,\widehat{r}\cdot\widehat{r'}\,,\quad \sigma_{\text{Poincare}}=z^2+|Y-Y'|^2-|T-T'|^2\,. \tag{3.51}$$

To derive the scattering smearing kernel, we rewrite $\sigma^{\Delta-d}$ as $\exp[(\Delta-d)\log\sigma]$, then we can first integrate over x_i in eq. (3.49) by picking up the saddle-points of time at large ℓ limit.

Let's first discuss the global smearing, where we have integrands for each x_i as follows

$$\int dt_i d^d x_i \exp[-i\omega_i t_i + i|p_i|\widehat{p_i} \cdot x_i + (\Delta - d)\log \sigma_{\text{global}}] . \tag{3.52}$$

We simply slip off the normalization factor in HKLL formula (3.50). We can use eq. (3.10) and find that there is a saddle-point for time t_i

$$t_i^* = (\arctan(-i\frac{\omega_i}{m_i}) + \tau_i')\ell . \tag{3.53}$$

Expanding the exponents around this saddle-point and integrating t_i yields

$$\int d^d x_i e^{-i\omega_i\tau_i'\ell - i(|p_i|\widehat{p_i}\cdot x_i - \sqrt{\omega_i^2-m_i^2}\widehat{r_i'}\cdot x_i)} \times \sqrt{\ell}\, i^{-\Delta_i+\omega_i\ell+d} m_i^{\Delta_i-d+\frac{1}{2}} \frac{(\omega_i\ell-\Delta_i)^{\frac{\omega_i\ell}{2}}}{(\omega_i\ell+\Delta_i)^{\frac{\omega_i\ell}{2}}}(\omega_i^2-m_i^2)^{\frac{d-\Delta_i}{2}-1} . \tag{3.54}$$

Note that we should not take the on-shell condition $\omega^2 - m^2 = |p|^2$ at this moment, since there is literally not such constraint in AdS, rather we expect

$$|p| \sim \sqrt{\omega^2 - m^2} + \frac{\#}{\ell} . \tag{3.55}$$

On the other hand, keeping $p^2 + m^2 \neq 0$ is helpful for keeping track of how one-particle factor $p_i^2 + m_i^2$ in eq. (3.49) get canceled. In fact, we can observe that there is a Dirac delta function of the on-shell condition coming from the remaining Fourier factor when we integrate over x_i, which can cancel one-particle factor. More precisely, we have

$$\int d^d x_i e^{-i(|p_i|\widehat{p_i}\cdot x_i - \sqrt{\omega^2-m^2}\widehat{r_i'}\cdot x_i)} \sim \delta^{(d-1)}(\widehat{p_i} - \widehat{r_i'})\frac{\delta(|p_i| - \sqrt{\omega_i^2 - m_i^2})}{|p_i|^{d-1}} . \tag{3.56}$$

Now we see the delta function mapping directions appear as in eq. (3.26), and we can directly integrated it out. If we take the on-shell condition, we then have $\delta(0)$, giving the length of radius of our effective flat-space which is of the order ℓ. On the other hand, the one-particle factor gives $p_i^2+m_i^2 \propto 2|p_i|\ell$, we can then argue that one-particle factor and delta function of on-shell condition get canceled, leaving us kinematic factor $2|p_i|$ with some other things to be fixed by normalization. Including additional $|p_i|$ and $1/\Gamma(\Delta-d+1)$ in HKLL formula eq. (3.50), the kinematic factor $e^{i\omega_i t_i}\xi_{\omega_i\Delta_i}|\vec{p}_i|^{1-\Delta}$ in scattering smearing kernel eq. (3.28) is precisely produced! HKLL formula eq. (3.50) also provides the Gamma function $\Gamma(\Delta-d/2+1)$, but we still miss some normalization factors, for example, correct scaling in ℓ. The loss of correct normalization factors is resulted from our rough estimate of the integral where the delta function of on-shell condition arises. The on-shell condition is the saddle-point for $|p|$ at large ℓ limit, and a more careful analysis around this saddle-point may give rise to a function that cancels one-particle factor and includes the correct normalization. Nevertheless, we can fix the normalization by requiring tow-point S-matrix is canonically normalized, as we will show in appendix A.2

$$S_{12} = \langle p_1|p_2\rangle = (2\pi)^d 2\omega\delta^{(d)}(p_1-p_2)\,. \tag{3.57}$$

The Poincare smearing follows similarly. Except now we have

$$\int dT_i d^{d-1}Y_i dx_d \exp[-i\omega_i T_i\ell + i\vec{k}_i\cdot Y_i\ell + i(k_d)_i(x_d)_i + (\Delta-d)\log\sigma_{\text{Poincare}}]\,. \tag{3.58}$$

The saddle-points of T_i and Y_i are

$$T_i - T_i' = -\frac{i\omega_i(m_i+i(k_d)_i)}{|\mathbf{k_i}|}\,,\quad Y_i - Y_i' = -\frac{ik_i(m_i+i(k_d)_i)}{|\mathbf{k_i}|}\,. \tag{3.59}$$

Let's only look into the important exponent. We find, after integrating out T_i and Y_i

$$\int dx_d e^{-ip_i\cdot x_i + i(k_d - \sqrt{|\mathbf{k}|^2-m^2}x_d)} e^{-i\tilde{\alpha}_{k_d}}(\cdots)\,, \tag{3.60}$$

where $(\cdots)$ represents those not-so-essential factors that could be fixed by eq. (3.57). Note the Fourier-transform factor of Poincare smearing kernel (3.45) already appears, while the further integration over x_d gives, as in global case, the on-shell condition that is about to get canceled by one-particle factor.

In odd dimensions, the smearing function is modified by additional factor of $\log\sigma$. However, such logarithmic factor doesn't affect the exponent and the saddle-points. Thus it simply gives a constant $\log\sigma^*$ specified to saddle-points and can be absorbed in the normalization factor.

Now we understand the scattering smearing kernel as the flat-space limit of HKLL bulk reconstruction, the AdS subregion duality [94, 95, 96] then suggests that a local point (where the interactions happen) belongs to the overlap region of global and Poincare AdS can be reconstructed either from global smearing or Poincare smearing. It is thus not surprising that we can transform the Poincare scattering smearing to global scattering smearing, as we will show in section 3.4.

3.3 The flat-space limit from global smearing

3.3.1 Known frameworks of the flat-space limit

We begin with briefly reviewing the existed frameworks of flat-space limit, include Mellin space, coordinate space and partial-wave expansion, from historical point of view without providing very technical details. We will then show these frameworks are originated from global smearing kernel eq. (3.28) in the following subsections and dig in more physical details there. Our focus is always the flat-space limit $\ell\to\infty$, thus we may keep $\ell\to\infty$ implicit in the rest of this paper when there is no confusion.

Mellin space

- Massless

  The Mellin formula (Mellin space will be reviewed shortly in the next subsection) describing the massless scattering in the flat-space limit was first proposed in

[22], it gives

$$T(s_{ij}) = \ell^{\frac{n(d-1)}{2}-d-1}\Gamma(\frac{\Delta_\Sigma - d}{2}) \int_{-i\infty}^{i\infty} \frac{d\alpha}{2\pi i} e^\alpha \alpha^{\frac{d-\Delta_\Sigma}{2}} M(\delta_{ij} = -\frac{\ell^2}{4\alpha} s_{ij}) \,, \quad (3.61)$$

where we use the shorthand notation $\Delta_\Sigma = \sum_{i=1}^n \Delta_i$. This formula was proved in [23] by using the massless scattering smearing kernel (global AdS). We will actually follow the proof [23] in appendix A.3. It also passes verification to work for supersymmetric theories, see e.g., [98, 99, 100, 101, 102, 103, 104].

- Massive

The Mellin formula describing the massive scattering in the flat-space limit was conjectured in [25], and was recently rederived from massive formula in coordinate space [3]. In our conventions, it reads

$$m_1^{\frac{n(d-1)}{2}-d-1} T(s_{ij}) = \Delta_1^{\frac{n(d-1)}{2}-d-1} M\big(\delta_{ij} = \frac{\Delta_i \Delta_j}{\Delta_\Sigma}(1 + \frac{\vec{p}_i \cdot \vec{p}_j}{m_i m_j})\big) \,. \quad (3.62)$$

Coordinate space

- Massless

The massless scattering written in the coordinate space only has the version for four-point function, which first came out in [21] and was rederived from Mellin descriptions in [22]. Analysis of contact terms of Witten diagram also suggests the same expression [24], which also phrases the name “bulk-point limit”.

$$\langle \mathcal{O}_1 \cdots \mathcal{O}_4 \rangle = \prod_{i=1}^4 \frac{\mathcal{C}_{\Delta_i}}{\Gamma(\Delta_i)} \frac{i^{\Delta_\Sigma} \pi^{\frac{d+3}{2}} \ell^{\Delta_\Sigma - d}}{2^{\Delta_\Sigma}} \int ds (\frac{\sqrt{s}}{2})^{\Delta_\Sigma - \frac{d+7}{2}} \xi^{\frac{3-d}{2}} K_{\frac{d-3}{2}}(\sqrt{s}\xi) \frac{iT(s,\sigma)}{2\sqrt{\sigma(1-\sigma)}} \,, \quad (3.63)$$

where

$$\xi^2 = -\lim_{\det P_{ij} \to 0} \frac{\ell^2 \det P_{ij}}{4P_{12}P_{34}\sqrt{P_{13}P_{24}P_{14}P_{23}}} \,, \quad \sigma = \frac{P_{13}P_{24}}{P_{14}P_{23}} \,, \quad (3.64)$$

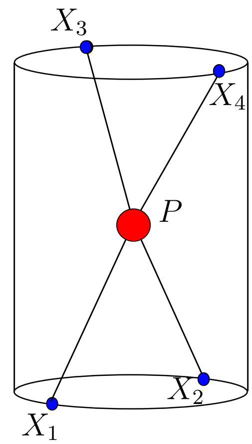

Figure 3.7: Bulk-point kinematics in Lorentzian cylinder of AdS. X_1 and X_2 are at Lorentzian time $-\pi/2$, X_3 and X_4 are at Lorentzian time $\pi/2$, where particles are focused on the bulk-point P.

where $\det P_{ij} \sim (z-\bar{z})^2 \sim 0$ is called the bulk-point limit in [24]. One example of the development of this bulk-point is to start with boundary configuration where the Lorentzian time of $\mathcal{O}_{1,2}$ is $-\pi/2$ and the Lorentzian time of $\mathcal{O}_{3,4}$ is $\pi/2$ [24], see Fig 3.7 (figure directly copied from [2])

- Massive

The flat-space limit for massive scattering was recently conjectured in [3] (the same parameterization was also obtained in [93]), rather straightforward by relating kinematics of flat-space scattering to embedding coordinate of CFT

$$P = (1, -\frac{\omega}{m}, i\frac{\vec{p}}{m})\,, \quad T(s_{ij}) = D\langle \mathcal{O}_1 \cdots \mathcal{O}_n \rangle\,, \tag{3.65}$$

where D denotes the contact diagram in AdS, and it can represent the momentum conserving delta function being absorbed into T to give the S-matrix conjecture [3]

$$S = \langle \mathcal{O}_1 \cdots \mathcal{O}_n \rangle\,. \tag{3.66}$$

Partial-wave expansion/phase-shift formula

The description of flat-space limit in terms of partial-wave expansion only refers to four-point case (where $\Delta_2 = \Delta_3, \Delta_4 = \Delta_1$). The four-point function is expanded in terms of conformal blocks, and the flat-space amplitude is expanded in terms of the partial-waves (where the coefficients are usually named as scattering phase-shift), then one has a map for coefficients of expansions.

- Massless

  Expand eq. (3.63) in terms of conformal blocks and partial-waves for LHS and RHS respectively, one can have access to the formula [24]

$$e^{-i\pi\gamma_{n,J}} \frac{c_{n,J}}{c^{(0)}_{n,J}}\bigg|_{n\to\infty} = e^{2i\delta_J}\,, \quad 4n^2 = \ell^2 s\,. \tag{3.67}$$

  One example of contact diagram at leading order was verified in [24], see [105] for examples of scalar and graviton tree-level exchange. It even passes checks at loop level [106]. Surprisingly, this formula is recently verified to work for gluon scattering, without referring to explicit expression of conformal blocks and partial-waves [2].

- Massive

  The phase-shift formula for massive scattering was proposed in [25]

$$\frac{1}{N_J} \sum_{|\Delta-\sqrt{s}\ell|<\delta E} e^{-i\pi(\Delta-\Delta_1-\Delta_2-J)} \frac{c_{\Delta,J}}{c^{(0)}_{\Delta,J}}\bigg|_{\Delta\to\infty} = e^{2i\delta_J}\,, \tag{3.68}$$

  where N_J is the normalization factor to make sure $e^{2i\delta_J} = 1$ for free theory. Recently, by doing conformal blcok/partial-wave expansion for their flat-space limit in the coordinate space eq. (3.65), [3] managed to derive the same phase-shift formula for identical particles.

It is not hard to see for each framework, the formulas for flat-space limit of massless scattering and massive scattering are quite different. For example, the massless Mellin formula is represented as integral over Mellin amplitudes, but massive Mellin formula doesn't have any integral to perform. We expect that massless scattering and massive scattering should be combined into one formula, as suggested by scattering smearing kernel. Meanwhile, as far as we know, some frameworks, for example, the coordinate framework for massive scattering, still remain as a conjecture with supportive examples [3]. In the following subsection, we will start with the global smearing eq. (3.28) and present how all those existed descriptions of flat-space limit naturally arise around the saddle-points of the scattering smearing kernel.

3.3.2 Mellin space and saddle-points

For our purpose, we factorize out the time dependence of the scattering smearing kernel K_s (3.28) and denote the remaining factor as kinematic factor

$$\prod_i \ell^{\frac{d-1}{2}-\Delta_i}\xi_{\omega_i\Delta_i}|\vec{p}_i|^{1-\Delta}2^{\Delta_i}\pi^{\frac{d-2}{2}}\Gamma(1+\Delta_i-\frac{d}{2})=\mathrm{KI}\,. \tag{3.69}$$

Such a factor play its role when deriving the final formulae, but it is not relevant for saddle-points analysis.

The n-point function in CFT and thus the corresponding AdS amplitudes can be nicely and naturally represented in Mellin space [107, 108, 109, 22] (which is argued to be well-defined non-perturvatively [110])

$$\langle\mathcal{O}_1\cdots\mathcal{O}_n\rangle=\frac{\mathcal{N}}{(2\pi i)^{\frac{n(n-3)}{2}}}\int d\delta_{ij}\prod_{i<j}\Gamma(\delta_{ij})\big(P_{ij}\big)^{-\delta_{ij}}M(\delta_{ij})\,,\quad \sum_{j\neq i}\delta_{ij}=\Delta_i\,, \tag{3.70}$$

where the normalization factor is

$$\mathcal{N}=\frac{\pi^{\frac{d}{2}}}{2}\Gamma\big(\frac{\Delta_\Sigma-d}{2}\big)\prod_{i=1}^{n}\frac{\mathcal{C}_{\Delta_i}}{\Gamma\big(\Delta_i\big)}\,,\quad \mathcal{C}_\Delta=\frac{\Gamma(\Delta)}{2\pi^{\frac{d}{2}}\Gamma\big(\Delta-\frac{d}{2}+1\big)}\,. \tag{3.71}$$

In Mellin space eq. (3.70), δ_{ij} is called the Mellin variables, and their integral contours run parallel to the imaginary axis. Note in our coordinate (3.4), we have

$$-2P_i\cdot P_j:=P_{ij}=2(\cos\tau_{ij}-\widehat{p}_i\cdot\widehat{p}_j)\,, \tag{3.72}$$

where we have already used the fact that $\widehat{r} \to \widehat{p}$ due to the presence of delta function in smearing kernel (3.26). To play with the flat-space limit of Mellin amplitudes, we can redefine $\delta_{ij} = \ell^2\sigma_{ij}$. This redefinition should not be understood as that Mellin variables in CFT depend on ℓ, because a pure CFT correlator does not know about ℓ; rather, as we will show shortly, this redefinition is taken for convenience, because the smearing kernel pushes δ_{ij} to regions that can be parameterized in terms of ℓ. Moreover, to make order counting more obvious and straightforward, we make the following convention

$$\tilde{P}_{ij} = \frac{|p_i||p_j|}{2\sum_k \Delta_k} P_{ij}\,, \tag{3.73}$$

such that $\tilde{P}_{ij}$ is well-defined with no subtlety for taking massless limit, and from now on we would shortly write $|\vec{p}|$ as $|p|$. Such an redefinition is arbitrary and ambiguous as soon as the prefactor is factorized into sum of pair i,j, provided the constraints of δ_{ij}, i.e.,

$$\sum_{i<j}(b_i+b_j)\delta_{ij} = \sum_i b_i\Delta_i\,. \tag{3.74}$$

Such a redefinition does nothing but provide additional prefactors that are not relevant to saddle-points analysis. We make our choice for latter convenience. In the flat-space limit, we can call Stirling approximation for $\Gamma(\delta_{ij})$ and rewrite $P_{ij}^{-\delta_{ij}}$ as an exponent. Then, we can further add the Lagrange multiplier, which is responsible for constraining δ_{ij}, and we will have following exponent

$$\exp[\ell^2\sum_{i<j}(-\sigma_{ij}+\sigma_{ij}\log\sigma_{ij}-\sigma_{ij}\log\tilde{P}_{ij}) + i\ell\sum_i \omega_i\tau_i + i\sum_i\lambda_i(\sum_{j\neq i}\ell^2\sigma_{ij}-\Delta_i)]\,. \tag{3.75}$$

It is instructive to make variable change for λ_i

$$e^{-i\lambda_i} = \beta_i\,, \tag{3.76}$$

which rewrites the exponent as

$$\exp\big[\ell^2\sum_{i<j}(-\sigma_{ij}+\sigma_{ij}\log\sigma_{ij}-\sigma_{ij}\log\tilde{P}_{ij})+i\ell\sum_i\omega_i\tau_i-\ell^2\sum_{i<j}(\log\beta_i+\log\beta_j)\sigma_{ij}+\sum_i\Delta_i\log\beta_i\big]\,. \tag{3.77}$$

We can actually immediately solve the saddle-points of above exponent for σ_{ij}

$$\sigma_{ij}=\beta_i\beta_j\tilde{P}_{ij}\,. \tag{3.78}$$

Substitute this saddle-point into above exponent, we obtain

$$\exp[\ell^2\sum_{i<j}\big(-\frac{\beta_i\beta_j}{\Delta_\Sigma}(\cos\tau_{ij}|p_i||p_j|-\vec{p}_i\cdot\vec{p}_j)\big)+\sum_i\Delta_i\log\beta_i+i\ell\sum_i\omega_i\tau_i]\,. \tag{3.79}$$

we can start from this exponent and go further to solve saddle-points for τ_i and β_i. We assume the momentum conservation, and we can then find a very simple solution to saddle-points equations. We can already notice the difference between massless formula and massive formula comes from the last two terms: they do not contribute for massless case but play their roles for massive case.

- All massless partiales

  For the scattering where all particles are massless, Δ_i is order 1, and thus we could neglect the last two terms to consider the saddle-point analysis. The equation gives below

$$\begin{aligned}\text{vary } \tau_i &\rightarrow -\sum_{i\neq k}\frac{\beta_i\beta_k}{\Delta_\Sigma}\sin\tau_{ik}|p_i||p_k|=0\,,\\ \text{vary } \beta_i &\rightarrow \sum_{i\neq k}\frac{\beta_i}{\Delta_\Sigma}(-\cos\tau_{ik}|p_i||p_k|+\vec{p}_i\cdot\vec{p}_k)=0\,.\end{aligned} \tag{3.80}$$

  It is not hard to find a very simple solution to above equation

$$\sin\tau_{ij}=0\,,\quad \cos\tau_{ij}=\pm1\,,\quad \beta_i=\beta\,, \tag{3.81}$$

where β is arbitrary. There is $\pm$ sign, because we analytically continue the momentum such that all particles are in-going, which implies that energy ω of some particles are negative, i.e., $\omega = -|p|$, to guarantee the energy conservation. The saddle-points obtained above produce the known bulk-point configurations Fig 3.7 where massless scalars start around $\tau_i = \pm\pi/2$ [24].

- All massive particles

For scattering with all massive particles, we should scale $\Delta_i = m_i \ell$, and all terms in the exponent become the same order and participate in the saddle equations

$$\begin{aligned} &\text{vary } \tau_i \rightarrow -\sum_{i\neq k} \frac{\beta_i \beta_k}{m_\Sigma} \sin\tau_{ik} |p_i||p_k| + i\omega_k = 0\,, \\ &\text{vary } \beta_i \rightarrow \sum_{i\neq k} \frac{\beta_i}{m_\Sigma} (-\cos\tau_{ik}|p_i||p_j| + \vec{p}_i\cdot\vec{p}_k) + \frac{m_k}{\beta_k} = 0\,. \end{aligned} \tag{3.82}$$

The simple solution is

$$\sin\tau_{ij} = i\frac{\omega_i m_j - \omega_j m_i}{|p_i||p_j|}\,, \quad \cos\tau_{ij} = \frac{-m_i m_j + \omega_i\omega_j}{|p_i||p_j|}\,, \quad \beta_i = i\,. \tag{3.83}$$

We can easily verify that above solution for $\sin\tau_{ij}$ and $\cos\tau_{ij}$ is consistent on-shell, and there is a simple solution which we can take for convenience

$$\tau_i = \pm \arcsin\frac{\omega_i}{|p_i|}\,. \tag{3.84}$$

It is obvious that trivially shifting every τ_i above by the same constant still satisfies eq. (3.83). Choosing a convenient reference point can be understood as a sort of gauge choice or frame choice associated with τ translation symmetry (which is the constant scaling symmetry of a CFT) subject to saddle constraints eq. (3.83) and the presumed range $\tau \in (-\pi/2-\delta, \pi/2-\delta)$. Amazing part is that the solution of τ_i is continuous without subtlety for massless limit, except that β_i cannot be fully determined for massless case. We can easily show that the solution eq. (3.84) is exactly what [3] suggests for writing the flat-space limit in coordinate space. We only need to scale P by $\cos\tau$

$$P \to (1, -i\tan\tau, \frac{\widehat{r}}{\cos\tau})\,. \tag{3.85}$$

This scaling is allowed, because in embedding space, correlators are homogeneous in scaling P weighted by conformal dimensions [47]. Compare with [3], we can easily find

$$n_0 = -i\tan\tau\,, \quad n_i = \frac{\widehat{r}}{\cos\tau}\,. \tag{3.86}$$

Taking the saddle-points (3.84) (we choose the minus sign, i.e., $\sin\tau = -\omega/|p|$ and $\cos\tau = -im/|p|$), it is easy to find

$$n_0 = -\frac{\omega}{m}\,, \quad n_i = i\frac{\vec{p}}{m}\,, \tag{3.87}$$

which is exactly eq. (2.9) in [3]! The scaling introduces $1/m$, making their parameterization [3] not suitable for addressing massless particles.

- Mixing massless and massive particles

  When external particles have both massless and massive particles, the situation makes no difference from scattering with all massive particles, thanks to analytic property at massless limit of saddle-points τ_i. This fact is quite obvious but surprising: as soon as there is one massive particle, its contribution will make β_i determined!

Some more comments come in order. First, we have to note that above saddle-points analysis assume the energy and momentum conservation, which is, however, not guaranteed in AdS. When taking the flat-space limit, the dominant part of the spacetime is translational symmetric, giving rise to the conservation of the momentum. This fact can be made manifest when we are deriving the flat-space formula of Mellin amplitudes by using global scattering smearing kernel. The original scattering smearing kernel is constructed for the whole S-matrix eq. (3.27), and we can easily subtract the identity $\mathbb{I}$ (which represents the free field theory) to leave only scattering amplitudes T. It is obvious that the free QFT $\mathbb{I}$ corresponds to mean field theory (MFT) of CFT, because MFT factorizes CFT correlators into several pieces of two-point functions multiplied together

$$\langle\mathcal{O}_1\cdots\mathcal{O}_n\rangle=\langle\mathcal{O}_1\mathcal{O}_2\rangle\langle\mathcal{O}_3\mathcal{O}_4\rangle\cdots\langle\mathcal{O}_{n-1}\mathcal{O}_n\rangle+\text{perm}\,, \tag{3.88}$$

which gives rise to a bunch of conserving factors $\delta(p_i+p_j)$

$$\mathbb{I}=S_{12}S_{34}\cdots S_{n-1,n}+\text{perm}=\delta(p_1+p_2)\delta(p_3+p_4)\cdots+\text{perm}\,, \tag{3.89}$$

where S_{ij} is defined in eq. (A.4). Writing in terms of scattering amplitudes, we have

$$T=-i\int d^{d+1}p_{\text{tot}}\int\prod_{i=1}^{n}d\tau_i K_s\langle\mathcal{O}_1\cdots\mathcal{O}_n\rangle_{\text{c}}\,, \tag{3.90}$$

where the subscript "c" denotes the connected part of CFT correlator and we utilize an integral over p_{tot} to eliminate the momentum conservation delta function (without causing confusion, we will ignore the subscript for simplicity). In other words, the momentum conservation can be understood as saddle-points of integration over p_{tot}. More precisely, we can define (we follow [23])

$$p_i=p_i'+q\,,\quad s_{ij}=s_{ij}'+\frac{2n}{n-2}q\cdot(p_i+p_j)-\frac{2n^2}{(n-1)(n-2)}q^2\,,\quad nq=p_{\text{tot}}\,, \tag{3.91}$$

where p_i' and s_{ij}' are the saddle-points of p_i and s_{ij}, satisfying

$$\sum p_i'=0\,,\quad\sum_{j\neq i}s_{ij}'=(n-4)m_i^2+\sum_{j=1}^{n}m_j^2\,. \tag{3.92}$$

Then we could expand β_i, σ_{ij} and τ_i around their saddle-points

$$\beta_i = \beta^* + \delta\beta_i\,, \quad \tilde{P}_{ij} = \frac{1}{2\Delta_\Sigma}\big(s_{ij} - (m_i+m_j)^2 + \delta s_{ij}\big)\,, \quad \sigma_{ij} = \frac{\beta^2}{2\Delta_\Sigma}(s'_{ij} - (m_i+m_j)^2 + \epsilon_{ij})\,, \tag{3.93}$$

where

$$\delta s_{ij} = (-2\sin\tau^*_{ij}\delta\tau_{ij} - \cos\tau^*_{ij}\delta\tau^2_{ij} + \cdots)|p_i||p_j|\,, \tag{3.94}$$

and perform the integral over the fluctuations $q \sim \delta\beta_i \sim \delta\tau_i \sim \epsilon_{ij} \ll 1$. For latter purpose of presenting the flat-space limit in coordinate space, we may do those integral separately. First, we integrate out ϵ_{ij} and $\delta\beta_i$, which is expected to take the form

$$\langle\mathcal{O}_1\cdots\mathcal{O}_n\rangle = \frac{\mathcal{N}}{(2\pi i)^{\frac{n(n-3)}{2}}}\int d\beta\,\mathcal{D}(s_{ij},\beta)e^{S(q,\delta s_{ij},\beta)}M\Big(\delta_{ij} = \frac{\ell^2\beta^2}{2\Delta_\Sigma}\big(s_{ij} - (m_i+m_j)^2\big)\Big)\,. \tag{3.95}$$

We can then expand $S(q,\delta s_{ij},\beta)$ up to $\mathcal{O}(q^2) \sim \mathcal{O}(\delta\tau_i^2)$, and complete the Gaussian integral for $\delta\tau_i$ and $p_{\rm tot}$. The details are recorded in appendix A.3, and in the end we obtain a Mellin formula in flat-space limit that applies to arbitrary external scalar particles

$$T(s_{ij}) = \frac{1}{\mathcal{N}_T}\int_{-i\infty}^{i\infty}\frac{d\alpha}{2i\pi}e^\alpha\alpha^{\frac{d-\Delta_\Sigma}{2}}M\Big(\delta_{ij} = -\frac{\ell^2}{4\alpha}\big(s_{ij} - (m_i+m_j)^2\big)\Big)\,, \tag{3.96}$$

where

$$\mathcal{N}_T = \frac{\ell^{\frac{n(1-d)}{2}+d+1}}{\Gamma\big(\frac{\Delta_\Sigma - d}{2}\big)}\,. \tag{3.97}$$

Let us comment briefly on why this formula governs massless formula eq. (3.61) proposed in [22] and massive formula eq. (3.61) proposed in [25]. For massless scattering, due to $\Delta_i \ll \ell$, we can ignore m_i in Mellin amplitudes and then the formula comes back to eq. (3.61). On the other hand, if there exist one massive parti-

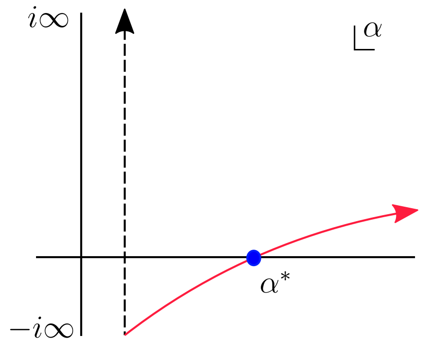

Figure 3.8: We deform the contour of α to pass through along the steepest descent contour.

cle, then Δ_Σ become parametrically large, together with e^α, $\alpha^{\frac{\Delta_\Sigma-d}{2}}$ exponentiates as $\alpha^{\frac{\Delta_\Sigma-d}{2}}=e^{\frac{\Delta_\Sigma-d}{2}\log\alpha}$ to locate the saddle-point of α

$$\alpha^*=\frac{\Delta_\Sigma}{2}\,. \tag{3.98}$$

Thus we can deform the contour of α to pass through α^*, as shown in Fig 3.8. Around this saddle-point α^*, we have

$$\int_{-i\infty}^{i\infty}\frac{d\alpha}{2i\pi}e^{\alpha+\frac{\Delta_\Sigma-d}{2}\log\alpha}f(\alpha)\simeq\frac{e^{\frac{\Delta_\Sigma}{2}}2^{\frac{1}{2}(-d+\Delta_\Sigma-2)}\Delta_\Sigma^{\frac{1}{2}(d-\Delta_\Sigma+1)}}{\sqrt{\pi}}f(\alpha^*)\,, \tag{3.99}$$

where the overall coefficient is precisely the large Δ_Σ limit of $1/\Gamma((\Delta_\Sigma-d)/2)$! Thus we are led to eq. (3.61).

The inverse formula of eq. (3.96) is straightforward and would be useful for going to formula in coordinate space

$$M(\delta_{ij})=\mathcal{N}_T\int d\gamma e^{-\gamma}\gamma^{\frac{\Delta_\Sigma-d}{2}-1}T\Big(s_{ij}=-\frac{4\gamma\delta_{ij}}{\ell^2}+(m_i+m_j)^2\Big)\,. \tag{3.100}$$

The second subtlety is about the effects of Mellin poles on saddle-points, which were posed recently in [3]. For some analytic regions of Maldastam variables, it turns out the deformation of integral contour to go through saddle-points along steepest descent contour would inevitably pick up poles of Mellin amplitudes, as result, the Mellin formula of the flat-space limit might have additional and isolated contribution from those Mellin poles. In terms of perturbative Witten diagram, this subtle phenomenon is corresponding to the existence of Landau pole [3]. A similar phenomenon is also observed in [33] where there exist saddle-points of AdS giving something different from flat-space S-matrix. We do not consider this subtlety in this paper, by appropriately assuming a nice analytic region of Maldastam variables and restricting the Maldastam variables to physical region. Nevertheless, we expect the global smearing kernel eq. (3.27) always works since its construction does not have any subtlety. Thus we would like to think of eq. (3.27) as a definition of a certain S-matrix in terms of a specific CFT correlator, where the underlying CFT theory should be supported with large N limit and large gap Δ_{gap}. The details of the CFT correlator encode the interactions of the corresponding S-matrix, and universal properties of the CFT correlators would also have their landing point in S-matrices. Then we might be able to investigate the novel analytic region by directly studying analytic aspects of eq. (3.27), provided with axioms of CFT e.g., [111]. We leave this interesting question to future research.

3.3.3 Conformal frame subject to saddle-points

Before we move to other space, we would like to comment on the conformal frame subject to the saddle constraints eq. (3.83), which will benefit following subsections.

The saddle-points only constrain $\cos\tau_{ij}$ by eq. (3.83). We can shift τ_i by the same constant or shift τ_{ij} by 2π without changing the saddle-points and the physics. This reminds us the concept of frame choice. Nevertheless, it is quite trivial to shift a constant, which is nothing but choosing a specific starting time. Much more non-trivially, we notice that eq. (3.83) only establishes a dictionary relating the conformal configurations to scattering kinematics. From point view of scattering process, we are allowed to choose different scattering frames which then have different $(\omega_i, \vec{p}_i)$ subject to on-shell condition and the momentum conservation. Constrained by saddle-points eq. (3.83), a choice of scattering frame then corresponds to a choice of conformal frame.

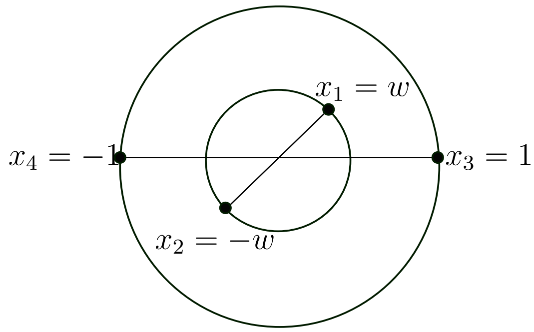

Figure 3.9: Without restriction set by saddle-points, any four points of CFT can be brought to above conformal frame. Constrained by saddle-points of points in CFT, only massless or identical massive four-point function can have access to above conformal frame. Figure comes from [112].

In our choice, we have explicitly

$$P = -\frac{i}{|p|}(m, \omega, i\vec{p})\,. \tag{3.101}$$

The i factor in front of spatial momentum $\vec{p}$ somehow wick rotates the spatial momentum to make $(\omega, i\vec{p})$ map precisely to momentum of scattering. Then straightforwardly, the frame choice of p leads to the corresponding conformal frame P. For instance, we are allowed to take the rest frame where $\vec{p} = 0$ for massive particles, even though P seems to divergent, it can be scaled to give $P \sim (1, -1, 0)$, representing the conformal position at ∞! Let's consider four-point case with $\Delta_3 = \Delta_2, \Delta_4 = \Delta_1$ to gain more insights about conformal frame constrained by eq. (3.83) and prepare for discussions on the partial-wave expansion in subsection 3.3.5.

Consider four-point function in a CFT, it is especially useful to use the radial frame (r, θ) (or to write $w = re^{i\theta}$), which makes Caimir easy to keep track of series expansion of conformal block [112] (see Fig 3.9 for illustration)

$$z\bar{z} = \frac{P_{12}P_{34}}{P_{13}P_{24}} = \frac{16r^2}{(1 + r^2 + 2r\cos\theta)^2}\,, \quad (1-z)(1-\bar{z}) = \frac{P_{14}P_{23}}{P_{13}P_{24}} = \frac{(1 + r^2 + 2r\cos\theta)^2}{(1 + r^2 - 2r\cos\theta)^2}\,. \tag{3.102}$$

Constrained by eq. (3.101), only massless scattering and identical massive scattering can have their CFT descriptions within the radial frame. Non-identical particles do not admit the radial frame! It would be very clear to observe these facts by using the center-of-mass frame for scattering amplitudes.

- **Identical particles**

The center-of-mass frame for identical particles is especially simple

$$p_1 = (\omega, p\widehat{n})\,, \quad p_2 = (\omega, -p\widehat{n})\,, \quad p_3 = (-\omega, p\widehat{n}')\,, \quad p_4 = (-\omega, -p\widehat{n}')\,. \tag{3.103}$$

These kinematic variables (ω, θ) can be related to Maldastam variables

$$\omega = \frac{\sqrt{s}}{2}\,, \quad \cos\theta = 1 + \frac{2t}{s - 4m^2}\,. \tag{3.104}$$

Correspondingly we have

$$P_{12} = P_{34} = 4\,, \quad P_{23} = P_{14} = 2\Big(\frac{4m^2+s}{4m^2-s} + \cos\theta\Big)\,, \quad P_{14} = P_{23} = 2\Big(\frac{4m^2+s}{4m^2-s} - \cos\theta\Big)\,. \tag{3.105}$$

It is not hard to see this configuration allows the radial frame eq. (3.102) by identifying θ to scattering angle and

$$s = \frac{4m^2(r-1)^2}{(r+1)^2}\,, \tag{3.106}$$

where r here can be defined by $r = e^{i\tau_{23}}$. For special case where $m = 0$, it is obvious $r = -1 = e^{-i\pi}$.

- **Non-identical particles**

If $m_1 \neq m_2$, it is then not possible to use the radial frame eq. (3.102). We can still consider the center-of-mass frame, but now it is a bit more complicated in a sense that there must be different kinematic variables

$$p_1 = (\omega_1, p\widehat{n})\,, \quad p_2 = (\omega_2, -p\widehat{n})\,, \quad p_3 = (-\omega_2, p\widehat{n}')\,, \quad p_4 = (-\omega_1, -p\widehat{n}')\,. \tag{3.107}$$

Useful kinematic variables now take the form

$$\omega_1=\frac{s+m_{12}\bar{m}_{12}}{2\sqrt{2}}\,,\quad \omega_2=\frac{s-m_{12}\bar{m}_{12}}{2\sqrt{2}}\,,\quad p=\frac{1}{2}\sqrt{\frac{(s-m_{12}^2)(s-\bar{m}_{12}^2)}{s}}\,,$$
$$\cos\theta=1+\frac{2st}{(s-m_{12}^2)(s-\bar{m}_{12}^2)}\,, \tag{3.108}$$

where $m_{12}=m_1-m_2$ and $\bar{m}_{12}=m_1+m_2$. There is no way to appropriately define r in terms of above variables to reach eq. (3.102). Nevertheless, we still have access to convenient conformal frame, which is particularly useful for solving conformal block at large conformal dimensions Δ,Δ_i (appendix A.5) and then analyzing the partial-wave expansion for non-identical particles (subsection 3.3.5). We only need to identify θ with scattering angle and then slightly generalize eq. (3.106)

$$s=\frac{\bar{m}_{12}^2(r-1)^2}{(r+1)^2}\,,\quad \cos\theta=1+\frac{2st}{(s-m_{12}^2)(s-\bar{m}_{12}^2)}\,. \tag{3.109}$$

For $m_1=m_2$, eq. (3.109) reduces to eq. (3.106). In this case we have

$$P_{12}=P_{34}=\frac{4s}{s-m_{12}^2}\,,\quad P_{13}=P_{24}=\frac{4s(s+t-m_{12}^2)}{(m_{12}^2-s)(s-\bar{m}_{12}^2)}\,,$$
$$P_{23}=\frac{4s(4m_2^2-t)}{(m_{12}^2-s)(s-\bar{m}_{12}^2)}\,,\quad P_{14}=\frac{4s(4m_1^2-t)}{(m_{12}^2-s)(s-\bar{m}_{12}^2)}\,. \tag{3.110}$$

The frame now reads (in terms of (s,t))

$$z\bar{z}=\frac{(s-\bar{m}_{12}^2)^2}{(s+t-\bar{m}_{12}^2)^2}\,,\quad (1-z)(1-\bar{z})=\frac{m_{12}^4+(\bar{m}_{12}^2-t)^2-2m_{12}^2(\bar{m}_{12}^2+t)}{(s+t-\bar{m}_{12}^2)^2}\,. \tag{3.111}$$

We can use eq. (3.108) and eq. (3.109) to explicitly write eq. (3.111) in terms of r and $\cos\theta$, the final expression cannot be simplified to the radial frame eq. (3.102) unless $m_1=m_2$.

3.3.4 From Mellin space to coordinate space

Recently, [3] proposed two conjectures for the (massive) flat-space limit in coordinate space, as we reviewed in subsection 3.3.1, see eqs. (3.65) and (3.66). The key point is the kinematic identification (3.87) that we derived. We could now find a way to derive the flat-space limit in coordinate space by using the inverse Mellin formula (3.100). The idea is to start from Mellin representation of n-point function in CFT (3.70) subject to kinematic identification (3.84) and $\widehat{r} = \widehat{p}$, and work out the integral by picking up the saddle-points $\sigma_{ij} = \beta_i \beta_j \tilde{P}_{ij}$, which can establish a formula relating CFT n-point function to Mellin amplitudes specified to those saddle-points. Next, we use the inverse Mellin formula (3.100) to produce the formula directly relating n-point function in coordinate space to flat-space scattering amplitudes or S-matrix.

Let us start with (3.95) and specify to saddle-points, we now have

$$\langle \mathcal{O}_1 \cdots \mathcal{O}_n \rangle = \frac{\mathcal{N}}{(2\pi i)^{\frac{n(n-3)}{2}}} \int d\beta \, \mathcal{D}(s_{ij}, \beta) e^{S(0,\delta s_{ij},\beta)} M\Big(\delta_{ij} = \frac{\ell^2 \beta^2}{2\Delta_\Sigma}\big(s_{ij} - (m_i + m_j)^2\big)\Big) , \tag{3.112}$$

where we keep δs_{ij} nonzero up to sub-leading order to regulate the integral. We will see later that this regulation is exactly corresponding to bulk-point singularity [24]. Using (3.100) yields

$$\begin{aligned} \langle \mathcal{O}_1 \cdots \mathcal{O}_n \rangle = & \frac{\mathcal{N}\mathcal{N}_T}{(2\pi i)^{\frac{n(n-3)}{2}}} \int d\beta \, \mathcal{D}(s_{ij}, \beta) e^{S(0,\delta s_{ij},\beta)} \int d\gamma e^{-\gamma} \gamma^{\frac{\Delta_\Sigma - d}{2} - 1} \\ & \times T\Big(\frac{2\gamma\beta^2}{\Delta_\Sigma}\big(- s_{ij} + (m_i + m_j)^2\big) + (m_i + m_j)^2\Big) . \end{aligned} \tag{3.113}$$

We shall explain in details on this formula for massive case and massless case separately.

3.3.4.1 All massless particles: bulk-point singularity

For all external particles are massless, we have

$$\langle \mathcal{O}_1 \cdots \mathcal{O}_n \rangle = \frac{\mathcal{N}\mathcal{N}_T}{(2\pi i)^{\frac{n(n-3)}{2}}} \int d\beta\, \mathcal{D}(s_{ij},\beta) e^{S(0,\delta s_{ij},\beta)} \int d\gamma e^{-\gamma} \gamma^{\frac{\Delta_\Sigma - d}{2}-1} \times T\Big(-\frac{2\gamma\beta^2}{\Delta_\Sigma} s_{ij}\Big)\,. \tag{3.114}$$

We can redefine γ by

$$\tilde{\gamma} = -\frac{2\gamma\beta^2}{\Delta_\Sigma} s_{12}\,, \tag{3.115}$$

which gives

$$\langle \mathcal{O}_1 \cdots \mathcal{O}_n \rangle = \frac{\mathcal{N}\mathcal{N}_T}{(2\pi i)^{\frac{n(n-3)}{2}}} \int d\tilde{\gamma} \int d\beta\, \mathcal{D}(s_{ij},\beta) e^{S(0,\delta s_{ij},\beta)+\frac{\Delta_\Sigma \tilde{\gamma}}{2\beta^2 s_{12}}} \big(-\frac{\Delta_\Sigma}{2\beta^2 s_{12}}\big)^{\frac{\Delta_\Sigma - d}{2}} \times \tilde{\gamma}^{\frac{\Delta_\Sigma - d}{2}-1} T(\tilde{\gamma}, \frac{s_{ij}}{s_{12}})\,. \tag{3.116}$$

Now $\tilde{\gamma}$ in the amplitudes play exactly the role as scattering energy s. From appendix A.3, we have

$$\begin{aligned} \mathcal{D}(s_{ij},\beta) &= (-1)^{\frac{1}{4}n(n+1)} \big(\frac{\ell^2}{2\Delta_\Sigma}\big)^{\frac{1}{2}\Delta_\Sigma} (2\pi)^{\frac{1}{2}n(n-1)} \beta^{\Delta_\Sigma - n} \prod_i \omega_i^{\Delta_i} \sqrt{\frac{(2\pi)^{n+1}}{\det A_\beta}}\,,\\ S(0,\delta s_{ij},\beta) &= -\frac{\ell^2\beta^2}{2\Delta_\Sigma} \big(\sum_i \omega_i \delta\tau_i\big)^2\,, \end{aligned} \tag{3.117}$$

where A_β can be found in eq. (A.24). We can integrate out β to have a Bessel function. We obtain

$$\langle \mathcal{O}_1 \cdots \mathcal{O}_n \rangle = \frac{\mathcal{N}\mathcal{N}_T}{(2\pi i)^{\frac{n(n-3)}{2}}} \int d\tilde{\gamma} D\big(s_{ij},\omega_i\big) \delta^{\frac{1}{2}(n-d-1)} \big(\frac{i\ell\sqrt{\tilde{\gamma}}}{\sqrt{s_{12}}}\big)^{\frac{1}{2}(1+d-n)+\Delta_\Sigma - d - 2} \times K_{\frac{d+1-n}{2}}\big(\frac{i\ell\sqrt{\tilde{\gamma}}\delta}{\sqrt{s_{12}}}\big) T(\tilde{\gamma}, \frac{s_{ij}}{s_{12}})\,, \tag{3.118}$$

where

$$D\big(s_{ij},\omega_i\big)=\frac{(-1)^{\frac{1}{4}(n^2+n+2)}2^{\frac{1}{2}((n^2-3n-2)+d-\Delta_\Sigma)}\Delta_\Sigma^{\frac{1-n}{2}}\ell^{n+1}\pi^{\frac{1}{2}(n^2-3n-2)}}{s_{12}}\prod_i\omega_i^{\Delta_i}\sqrt{\frac{(2\pi)^{n+1}}{\det A_\beta}}\,. \tag{3.119}$$

Note we use a shorthand notation $\delta=\sum_i\omega_i\delta\tau_i$. Taking $n=4$, above formula reduces to known massless flat-space limit formula first proposed in [21]. More specifically, we can neaten up eq. (3.118)

$$\langle\mathcal{O}_1\cdots\mathcal{O}_4\rangle=\prod_{i=1}^4\frac{\mathcal{C}_{\Delta_i}}{\Gamma(\Delta_i)}\frac{i\pi^{\frac{d+3}{2}}\ell^{\Delta_\Sigma-\frac{3}{2}(d-1)}}{2^{\Delta_\Sigma+1}}\int ds(\frac{i\sqrt{s}}{2})^{\Delta_\Sigma-\frac{d+7}{2}}\epsilon^{\frac{3-d}{2}}K_{\frac{d-3}{2}}(i\ell\sqrt{s}\epsilon)\frac{iT(s,\theta)}{|\sin\theta|}\,, \tag{3.120}$$

where $\epsilon=\delta/\sqrt{s_{12}}$. We use the standard notation for scattering energy i.e., $s=\tilde{\gamma}$, and θ is the scattering angle $\cos\theta=1+2t/s$. We can see eq. (3.120) precisely give eq. (3.63) that is proposed in [21], provided with $i\epsilon=\xi$ and eq. (3.105) (where $m=0$). The same formula was also understood as bulk-point singularity in CFT [24], because integrating over $\tilde{\gamma}$ leads to divergence in $\delta=0$, and this is also the reason we keep $\delta\neq 0$ to regulate the answer. In terms of cross-ratio $(z,\bar{z})$, the singularity $\epsilon\to 0$ is actually $z-\bar{z}^{\circlearrowleft}\to 0$ where $\circlearrowleft$ represents the analytic continuation which is automatically done in our discussion.

3.3.4.2 Include massive particles

As we explain in the previous subsection, if at least one external particle is massive, β and γ pick their saddle-points up

$$\beta^*=i\,,\quad \gamma^*=\frac{\Delta_\Sigma}{2}\,. \tag{3.121}$$

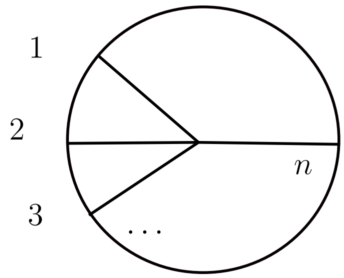

Figure 3.10: The contact Witten diagram. The dots represents other legs.

So the formula (3.113) simply becomes

$$\langle \mathcal{O}_1 \cdots \mathcal{O}_n \rangle = \frac{\mathcal{N} \ell^{\frac{n(1-d)}{2}+d+1}}{(2\pi i)^{\frac{n(n-3)}{2}}} \mathcal{F}(s_{ij}) T(s_{ij}) \,, \tag{3.122}$$

where $\mathcal{F}(s_{ij})$ is the determinant factor and the rest exponents from picking up saddle-points of β and γ

$$\mathcal{F} = (-1)^{\frac{1}{4}n(n+1)} (\frac{\ell^2}{2\Delta_\Sigma})^{\frac{1}{2}\Delta_\Sigma} (2\pi)^{\frac{1}{2}(n^2-3n-2)} \prod_i |p_i|^{\Delta_i} \mathrm{i}^{\Delta_\Sigma - n} e^{-\frac{1}{2}\Delta_\Sigma} \sqrt{\frac{(2\pi)^n}{\det(A_{ij})}} \Big|_{\beta=i} \,, \tag{3.123}$$

Let us explain this factor $\mathcal{F}(s_{ij})$ together with the normalization. Assume we consider the simplest contact interaction with no any derivatives

$$\mathcal{L}_{\text{int}} = \phi_1 \phi_2 \cdots \phi_n \,. \tag{3.124}$$

This contact interaction is illustrated using Witten diagram in Fig 3.10. In flat-space, this kind of contact interaction simply gives $T(s_{ij}) = 1$, which indicates that the factor $\mathcal{F}(s_{ij})$ is nothing more than contact Witten diagram at large AdS radius limit $\ell \to \infty$. This fact was verified for $n = 4$ identical particles in [3] and for non-identical particles in appendix A.4. Now we can see that the formula (3.122) is exactly the amplitudes conjecture of the flat-space limit in coordinate space [3]. Moreover, [3] shows that the contact Witten diagram can actually give rise to momentum conservation delta function, see also appendix A.4 for a more general case. Since the contact Witten diagram can be understood as delta function of momentum conservation, multiplying it with amplitudes will then be interpreted as S-matrix which equates CFT correlator.

3.3.5 From coordinate space to partial-waves

To consider partial-waves, we focus on four-point amplitudes. It is natural to start with the flat-space limit in the coordinate space and then expand CFT and amplitudes in terms of conformal blocks and partial-waves respectively. As consequence, a dictionary map between phase-shift and the OPE coefficients (together with anomalous dimensions) can be established. At tree-level, such a dictionary relates the partial-wave amplitudes to the anomalous-dimensions at leading order.

Represented by partial-waves, the massless scattering and massive scattering is sharply distinguished. The origin of this sharp difference results from the spectra of exchanged operators in four-point function of a CFT $\langle\mathcal{O}_1\mathcal{O}_2\mathcal{O}_2\mathcal{O}_1\rangle$, which can be approximately represented as the double-twist family [53]

$$[\mathcal{O}_1\mathcal{O}_2]_{n,J} = \mathcal{O}_1\partial^{2n}\partial_{\mu_1}\cdots\partial_{\mu_J}\mathcal{O}_2\,, \quad \Delta = \Delta_1+\Delta_2+J+2n+\gamma_{n,J}\,, \tag{3.125}$$

where $\gamma_{n,J}$ is the anomalous dimension. For external massless particles where $\Delta_1 \sim \Delta_2 \sim \mathcal{O}(1)$, the four-point function is dominated by massive exchanged particles $\Delta \sim 2n \to \infty$, effectively making n continuous. On the other hand, for massive $\mathcal{O}_1$ or $\mathcal{O}_2$, double-twist dimension Δ is already large, and thus we should include all integer n.

We will need the conformal block in a limit that the exchanged operator is heavy, i.e., large Δ limit [113]

$$G_{\Delta,J}(r,\theta)|_{\Delta\to\infty} = \frac{J!}{(d-2)_J}\frac{(4r)^{\Delta}C_J^{\frac{d}{2}-1}(\cos\theta)}{(1-r^2)^{\frac{d}{2}-1}\sqrt{(1+r^2)^2-4r^2\cos^2\theta}}\,. \tag{3.126}$$

Nonetheless, we should not take eq. (3.126) for granted. This conformal block eq. (3.126) assumes $\Delta_i \ll \Delta$ and thus is only applicable for massless scattering in principle. For massive scattering, we have additional large parameters $\Delta_i \sim \Delta$, which may modify eq. (3.126). Fortunately, as we will see in appendix A.5, only Δ_{12} can appear in the

Casimir equation eq. (A.63). Thus eq. (3.126) is still valid for identical masses. [3] considers identical particles and apply eq. (3.126) to study partial-wave/phase-shift formula. A worse situation is the scattering with non-identical massive particles, where a standard (r,θ) frame breaks down, thus we have to be careful about the conformal block eq. (3.126). In appendix A.5, we focus on non-identical operators and adopt a new conformal frame (see eq. (A.65)) which reduces to eq. (3.109) and (3.111) when $\Delta=\sqrt{s}\ell$. We solve the conformal block, and surprisingly, the expression eq. (3.126) is still valid, but with slightly modified normalization and (r,θ) defined differently!

The dictionary are nicely presented in the literature for both massless amplitudes and massive amplitudes, here we will derive them in a hopefully original way.

3.3.5.1 Massless phase-shift

For massless case, the conformal block eq. (3.126) can be further modified. Notice there is bulk-point singularity $\epsilon\to 0$ (according to eq. (3.105), we should then have $r=e^{-i\epsilon-i\pi}$), which could be served as UV cut-off of spectrum Δ. Thus a more physical limit is taking $\Delta\to\infty, r\to 1$ but keeping $\Delta\epsilon$ fixed. The conformal block with this limit (analytically continued to Lorentzian signature) is [24]

$$G_{\Delta,J}(e^{-i\epsilon-i\pi},\theta)=\frac{2^{\frac{1-d}{2}+2\Delta}J!e^{-i\pi\Delta}}{\sqrt{\pi}(d-2)_J}\sqrt{\Delta}(i\epsilon)^{\frac{3-d}{2}}K_{\frac{d-3}{2}}(i\Delta\epsilon)\frac{C_J^{\frac{d}{2}-1}(\cos\theta)}{|\sin\theta|}\,. \tag{3.127}$$

The four-point function can be expanded in terms of this conformal block, namely

$$\langle\mathcal{O}_1\cdots\mathcal{O}_4\rangle_c=4^{-(\Delta_1+\Delta_2)}\sum_{n,J}a_{n,J}G_{\Delta,J}(e^{-i\epsilon-i\pi},\theta)\,. \tag{3.128}$$

On the other hand, the amplitudes T can take the partial-wave expansion

$$T=\sum_J\frac{2^{d+1}(2J+d-2)\pi^{\frac{d-1}{2}}\Gamma(d-2)}{\Gamma(\frac{1}{2}(d-1))}\frac{1}{s^{\frac{d-3}{2}}}a_JC_J^{\frac{d}{2}-1}(\cos\theta)\,,\quad a_J=i(1-e^{2i\delta_J})\,, \tag{3.129}$$

where a_J is called the partial-wave amplitudes and δ_J is the scattering phase-shift. Comparing eq. (3.120) with the conformal block expansion eq. (3.128), it is not hard to find perfect match with the following dictionary, which is expected to be valid to any loop order and even nonperturbatively [106]

$$e^{-i\pi\gamma_{n,J}}\frac{c_{n,J}}{c^{(0)}_{n,J}}\Big|_{n\to\infty}=e^{2i\delta_J}\,,\quad 4n^2=\ell^2 s\,, \tag{3.130}$$

where $c^{(0)}_{n,J}$ is the OPE coefficients in MFT that can sum to disconnected contribution [53]

$$c^{(0)}_{n,J}=\frac{\sqrt{\pi}(d+2J-2)\Gamma(d+J-2)2^{-d+3}}{\Gamma\left(\frac{d}{2}-\frac{1}{2}\right)\Gamma(J+1)\Gamma(n+1)\Gamma\left(\frac{d}{2}+J+n\right)}\times$$
$$\frac{\left(-\frac{d}{2}+\Delta_1+1\right)_n\left(-\frac{d}{2}+\Delta_2+1\right)_n(\Delta_1)_{J+n}(\Delta_2)_{J+n}}{(-d+n+\Delta_1+\Delta_2+1)_n\,(J+2n+\Delta_1+\Delta_2-1)_J\left(-\frac{d}{2}+J+n+\Delta_1+\Delta_2\right)_n}\,. \tag{3.131}$$

At tree-level (i.e, $1/N^2$ order), it reduces to a more familiar formula $\gamma_{n,J}|_{n\to\infty}=-1/\pi a_J$ [24], which is verified to be valid even for gluons [2].

3.3.5.2 Massive phase-shift

We work with $n=4$ for eq. (3.122)

$$\langle\mathcal{O}_1\cdots\mathcal{O}_4\rangle_c=\mathcal{N}\frac{2^{\frac{3}{2}-4\bar{\Delta}_{12}}\ell^{1-d+\bar{\Delta}_{12}}\pi^{\frac{d}{2}+1}e^{-\bar{\Delta}_{12}+i\pi\bar{\Delta}_{12}}\bar{m}_{12}^{1-\bar{\Delta}_{12}}(s-m_{12}^2)^{\bar{\Delta}_{12}}(s-\bar{m}_{12}^2)^{\bar{\Delta}_{12}}}{\sqrt{(s-\bar{m}_{12}^2)(4m_1m_2-t)(s+t-m_{12}^2)}}\times$$
$$iT(s,t)\,. \tag{3.132}$$

Similar to massless scattering, we should then do conformal block and partial-wave expansion. The partial-wave expansion of amplitudes is rather straightforward, slightly generalizing eq. (3.129) to account for massive phase-space volume (see appendix

A.4)

$$T=\sum_J \frac{2^{d+1}(2J+d-2)\pi^{\frac{d-1}{2}}\Gamma(d-2)}{\Gamma(\frac{1}{2}(d-1))}\frac{s^{\frac{d-1}{2}}}{(s-m_{12}^2)^{\frac{d-2}{2}}(s-\bar{m}_{12}^2)^{\frac{d-2}{2}}}a_J C_J^{\frac{d}{2}-1}(\cos\theta)\,, \tag{3.133}$$

On the other hand, expanding the conformal correlator in terms of conformal block is a bit technically subtle. We use the conformal block eq. (A.70) we solve in appendix A.5. Carefully include all relevant factor, we have conformal block expansion

$$\langle\mathcal{O}_1\cdots\mathcal{O}_4\rangle=\frac{(s-m_{12}^2)^{\bar{\Delta}_{12}}(s+t-m_{12}^2)^{\Delta_{12}}}{4^{\bar{\Delta}_{12}}s^{\bar{\Delta}_{12}}(4m_1^2-t)^{\Delta_{12}}}\times$$
$$\sum_{\Delta,J}c_{\Delta,J}\Big(\frac{m_{12}^2(1+r_\Delta^2+2r_\Delta\eta_\Delta)+m^2(1+r_\Delta^2-2r_\Delta\eta_\Delta)+2m_{12}m(1-r_\Delta^2)}{(m^2-m_{12}^2(1+r_\Delta^2+2r_\Delta\eta_\Delta)^2)}\Big)^{\frac{\Delta_{12}}{2}}g_{\Delta,J}(r_\Delta,\eta_\Delta)\,, \tag{3.134}$$

where (r_Δ,η_Δ) is defined by $(w,\bar{w})$ in eq. (A.65). We emphasize here that (r_Δ,η_Δ) is not $(r,\eta=\cos\theta)$ defined via (s,t) in eq. (3.109). They only match when $\Delta=\sqrt{s}\ell$. More general, when Δ deviates from $\sqrt{s}\ell$, we find

$$\begin{aligned}
r_\Delta&=\frac{\bar{m}_{12}-\sqrt{s}}{\bar{m}_{12}+\sqrt{s}}-\frac{2m_{12}^2\bar{m}_{12}(\bar{m}_{12}-\sqrt{s})}{(\sqrt{s}+\bar{m}_{12})(\bar{m}_{12}^2(m_{12}^2-s)+st)}\delta+\cdots\,,\\
\eta_\Delta&=\frac{s(\bar{m}_{12}^2-s-2t)+m_{12}^2(s-\bar{m}_{12}^2)}{(m_{12}^2-s)(s-\bar{m}_{12}^2)}+\frac{4m_{12}^2\sqrt{s}t(m_{12}^2(s-\bar{m}_{12}^2)-s(-\bar{m}_{12}^2+s+t))}{(m_{12}^2-s)^2(s-\bar{m}_{12}^2)(s(t-\bar{m}_{12}^2)+m_{12}^2\bar{m}_{12}^2)}\delta+\cdots\,,
\end{aligned} \tag{3.135}$$

where $\delta=m-\sqrt{s}$. On the other hand, we can factorize MFT OPE $c^{(0)}_{\Delta,J}$ out, which exponentiates

$$\begin{aligned}
c^{(0)}_{\Delta,J}=&\frac{2^{d+2}\ell^{-\frac{d}{2}}(d+2J-2)\Gamma(d+J-2)}{\sqrt{\pi}\Gamma(\frac{d-1}{2})\Gamma(J+1)}m^{\frac{3d}{2}-2\Delta}(m-m_{12})^{\Delta-\Delta_{12}-\frac{d}{2}}(m+m_{12})^{\Delta+\Delta_{12}-\frac{d}{2}}\times\\
&(m-\bar{m}_{12})^{\bar{\Delta}_{12}-\Delta-\frac{d}{2}}(\bar{m}_{12}+m)^{\bar{\Delta}_{12}+\Delta-\frac{3d}{2}}(\bar{m}_{12}-m_{12})^{2\Delta_2+\frac{d}{2}}(\bar{m}_{12}+m_{12})^{\frac{d}{2}-2\Delta_1}\,.
\end{aligned} \tag{3.136}$$

We assume $c_{\Delta,J}/c^{(0)}_{\Delta,J}$ does not have further exponentially large factor, then we can use this MFT OPE and single out Δ dependence of (r_Δ, η_Δ) (i.e, use eq. (3.135)) to estimate the weighted sum of eq. (3.134). ultimately, we find an exponential factor

$$\mathcal{E}_\delta = \exp\Big[-\frac{\ell\delta^2 s\bar{m}_{12}\left(-\bar{m}_{12}^2+m_{12}^2+t\right)}{\left(\bar{m}_{12}-\sqrt{s}\right)\left(\bar{m}_{12}+\sqrt{s}\right)\left(s\left(\bar{m}_{12}^2-t\right)-m_{12}^2\bar{m}_{12}^2\right)}\Big]\,. \tag{3.137}$$

The appearance of this exponential factor extends the finding in [3] to non-identical particles. This exponential factor decays if $\Delta-\sqrt{s}\ell$ is large enough to go beyond $\mathcal{O}(\sqrt{\ell})$, which then effectively creates a spectra window together with additional factor that measures the width of the Gaussian distribution

$$\sum_{\Delta,J}(\cdots)\mathcal{E}_\delta \simeq \sum_J \frac{1}{N_J}\sum_{|\Delta-\sqrt{s}\ell|<\delta E}(\cdots)\times\Big(\frac{\pi\ell\left(\bar{m}_{12}-\sqrt{s}\right)\left(\bar{m}_{12}+\sqrt{s}\right)\left(s\left(\bar{m}_{12}^2-t\right)-m_{12}^2\bar{m}_{12}^2\right)}{s\bar{m}_{12}\left(-\bar{m}_{12}^2+m_{12}^2+t\right)}\Big)^{\frac{1}{2}}, \tag{3.138}$$

where $\delta E \preceq \mathcal{O}(\sqrt{\ell})$. Usually, include the exponential Gaussian factor, we could ignore the sum or integral and evaluate everything at the origin of Gaussian distribution multiplied by Gaussian width factor. However, we will see $(\cdots)$ contains phase factor $e^{-i\pi\Delta}$ which is then sensitive to finite change of Δ. Thus we keep the sum here but now the sum runs over a small window. $1/N_J$ appears to compensate for the remained sum and keep the normalization. The form of this window sum is exactly the one in [25]. Gather all factors, we find

$$\begin{aligned}\frac{\langle\mathcal{O}_1\cdots\mathcal{O}_4\rangle}{D_c} =& -i\sum_J\frac{1}{N_J}\sum_{|\Delta-\sqrt{s}\ell|<\delta E} e^{-i\pi(\Delta-\Delta_1-\Delta_2)}\frac{c_{\Delta,J}}{c^{(0)}_{\Delta,J}}\times\frac{2^{d+1}(2J+d-2)\pi^{\frac{d-1}{2}}\Gamma(d-2)}{\Gamma(\frac{1}{2}(d-1))}\times\\ &\frac{s^{\frac{d-1}{2}}}{(s-m_{12}^2)^{\frac{d-2}{2}}(s-\bar{m}_{12}^2)^{\frac{d-2}{2}}}C_J^{\frac{d}{2}-1}(\eta)\,,\end{aligned} \tag{3.139}$$

where

$$D_c = i\mathcal{N}\frac{2^{\frac{3}{2}-4\bar{\Delta}_{12}}\ell^{1-d+\bar{\Delta}_{12}}\pi^{\frac{d}{2}+1}e^{-\bar{\Delta}_{12}}\bar{m}_{12}^{1-\bar{\Delta}_{12}}(s-m_{12}^2)^{\bar{\Delta}_{12}}(s-\bar{m}_{12}^2)^{\bar{\Delta}_{12}}}{\sqrt{(s-\bar{m}_{12}^2)(4m_1m_2-t)(s+t-m_{12}^2)}}\,. \tag{3.140}$$

Use eq. (3.132) (subtract the MFT part) and compare to eq. (3.133), we conclude

$$e^{2i\delta_J} = \frac{1}{N_J} \sum_{|\Delta-\sqrt{s}\ell|<\delta E} e^{-i\pi(\Delta-\Delta_1-\Delta_2)} \frac{c_{\Delta,J}}{c^{(0)}_{\Delta,J}} . \tag{3.141}$$

For MFT, we can estimate N_J

$$N_J \simeq 2\delta E , \tag{3.142}$$

which is also consistent with what found in [3]. It is pointed out that there are some bound states below $\Delta = \Delta_1 + \Delta_2$, we refer [3] for more discussions.

3.4 Momentum-coordinate duality

The last section is devoted to discussions of variants stemming from the global scattering smearing. In addition to those flat-space limits discussed in the last section, we can also construct the flat-space amplitudes from momentum space of a CFT, as originally suggested by [26]. The origin of this momentum space prescription is Poincare AdS reconstruction. Naturally, we should ask, can we also establish connections between global scattering smearing and Poincare scattering smearing?

The answer is positive. Intuitively, when the AdS radius is large enough, the wave packets propagate freely in the bulk until they scatter through each other around a bulk region which is extremely local compared to the AdS radius. This region is where the flat-space S-matrix can be defined and we may call it the scattering region [114]. Physically, the scattering smearing kernel describes the bulk reconstruction of scattering region. The scattering region we are going to reconstruct must fall in one subregion A of AdS, then according to the subregion duality, this scattering region can be reconstructed from smearing over the subregion of boundary A_b spanned by A. For example, applying to one Poincare patch, we can reconstruct any scattering region inside the patch by the full M^d plane (which can be wick rotated to R^d), which is exactly what we find in eq. (3.45): reconstruct the scattering in terms of

$$M^d \xrightarrow{\text{wick rotation}} R^d \xrightarrow[\text{map}]{\text{conformal}} R\times S^{d-1} \xrightarrow{\text{wick rotation}} \text{Lorentzian } R\times S^{d-1}$$

Figure 3.11: The analytic operations taking CFT on M^d to CFT on Lorentzian $R\times S^{d-1}$.

the CFT correlator in the momentum space. Meanwhile, it is also possible to find another AdS subregion B which has overlap with A, and the overlap includes the same scattering region. If B's spanned boundary region B_b is different from A_b, then we can reconstruct the same S-matrix by two different CFT prescriptions. In a very robust way, since the S-matrix is the same one defined in the same scattering region, the two prescriptions of CFT correlators should be identified.

A bit trivial use of the idea suggested by subregion duality described above is to take A a certain Poincare patch and B the global AdS, as we study in this paper. Then we should be able to equate the global scattering smearing and Poincare scattering smearing, giving

$$\begin{aligned}&(\prod_i \sqrt{k_{id}}|\mathbf{k}_i|^{\Delta_i-\frac{d}{2}}e^{-i\tilde{\alpha}_{k_{id}}})\langle\mathcal{O}_1(\omega_1\ell,\mathbf{k}_1\ell)\cdots\mathcal{O}_n(\omega_n\ell,\mathbf{k}_n\ell)\rangle_L\\&=\int(\prod_i d\tau_i e^{i\omega_i\tau_i\ell}\ell^{-\frac{d-1}{2}}\xi_{\omega_i\Delta_i}|\vec{p}_i|^{1-\Delta_i}2^{\frac{d}{2}-1}\pi^{\frac{d-1}{2}})\langle\mathcal{O}_1(\tau_1,\widehat{p}_1)\cdots\mathcal{O}_n(\tau_n,\widehat{p}_n)\rangle\,,\end{aligned}\tag{3.143}$$

where we eliminate Gamma functions by assuming large Δ_i. For those finite Δ_i, the normalization depending on only Gamma functions can be easily restored. This equation (3.143) establishes a relation representing the Lorentzian CFT in the momentum space (with large momentum) by the CFT on Lorentzian $R\times S^{d-1}$. We call this relation the momentum-coordinate duality of a CFT. Such a duality is highly nontrivial, it connects two very different space of CFT, which can not be simply transformed via conformal map but via tricky operations as shown in Fig 3.11.

However, the momentum space in the Lorentzian signature is quite hard to keep track of, thus we may use a mild version of momentum-coordinate duality, starting with the middle of Fig 3.11 where the momentum space is already analytically continued to Euclidean space

$$\langle \mathcal{O}_1(p_1\ell)\cdots\mathcal{O}_n(p_n\ell)\rangle_E = \int \Big(\prod_i d\tau_i e^{i\omega_i\tau_i\ell}\ell^{-\frac{d-1}{2}}\frac{\xi_{\omega_i\Delta_i}|\vec{p}_i|^{1+\frac{d}{2}}}{\sqrt{\omega_i}}e^{i\tilde{\alpha}_{\omega_i}}2^{\frac{d}{2}-1}\pi^{\frac{d-1}{2}}\Big)\times \langle \mathcal{O}_1(\tau_1,\widehat{p}_1)\cdots\mathcal{O}_n(\tau_n,\widehat{p}_n)\rangle\,. \tag{3.144}$$

How is this momentum-coordinate duality possible? Note that the momentum of CFT is parametrically large, scaling as ℓ. This fact implies that the Fourier-transform can be approximately evaluated by some saddle-points. Let's play with single Fourier transform of one operator

$$\int d^dX e^{ip\cdot X\ell}\mathcal{O}_{\text{flat}}(X)\,. \tag{3.145}$$

To make contact with LHS of eq, (3.144), we make a conformal transformation, mapping $\mathcal{O}_{\text{flat}}$ to $\mathcal{O}_{\text{cyl}}$ (see [115] eq. (93) for this map)

$$\int d^dX e^{ip\cdot X\ell}\mathcal{O}_{\text{flat}}(X) \to \int d\tau d\Omega_{d-1}e^{-i\ell p e^{\tau}\Omega_p\cdot\Omega-(\Delta-d)\tau}\mathcal{O}_{\text{cyl}}(\tau,\widehat{n})\,, \tag{3.146}$$

where we have used

$$r=\sqrt{X^2}=e^{\tau}\,. \tag{3.147}$$

Then we just wick rotate $\tau\to i\tau$ and play with

$$\int d\tau d\Omega_{d-1}e^{i\ell p e^{i\tau}\Omega_p\cdot\Omega-i(\Delta-d)\tau}\mathcal{O}(\tau,\widehat{n})\,. \tag{3.148}$$

Since it is not possible for CFT correlators to develop exponentially growing factors of $\widehat{n}$, we can then approximate the integral of Ω_{d-1} by the saddle-points of $\widehat{n}$ in the Fourier factor. The saddle-points are precisely those directions along the momentum, i.e., $\widehat{n}=\widehat{p}$!

$$\int d\tau d\Omega_{d-1}e^{i\ell p e^{i\tau}\Omega_p\cdot\Omega-i(\Delta-d)\tau}\mathcal{O}(\tau,\widehat{n}) = \int d\tau\Big(\frac{2\pi}{p\ell}\Big)^{\frac{d-1}{2}}e^{i\ell p e^{-i\tau}-i(\Delta-\frac{1}{2})\tau}\mathcal{O}(\tau,\widehat{p})\,. \tag{3.149}$$

It comes close to the LHS of eq. (3.144), but we still have to figure out how Fourier factor depending on τ can be identical. Note the extremum of the remaining exponents in eq. (3.149) is not giving the correct saddle-points of τ, because CFT correlators develop further exponential growing terms involving τ. As we show in the last section 3.3, the global smearing kernel is not the end of the story, the τ integral can actually be dominated by saddle-points eq. (3.84). We can see, if we use eq. (3.149) rather than the global smearing kernel eq. (3.28), we only need to slightly change the first line of eq. (3.82)

$$-\sum_{i\neq k}\frac{\beta_i\beta_k}{m_\Sigma}\sin\tau_{ik}|p_i||p_k|+i(e^{-i\tau_i}p-m\tau_i)=0\,, \tag{3.150}$$

which gives rise to the exactly same saddle-points eq. (3.84)! Thus we can simply estimate $e^{-i\tau}$ around these saddle-points just for showing eq. (3.149) can be identified to global smearing,

$$e^{i\tau}\simeq e^{i\tau^*}(1+i(\tau-\tau^*))\,. \tag{3.151}$$

Picking up the linear τ term, it explicitly gives

$$\exp[i\ell p e^{i\tau^*}-i\Delta\tau^*]=e^{i\omega\tau}\,. \tag{3.152}$$

Other terms with τ^* simply gives

$$\xi_{\omega,\Delta}e^{i\tilde{\alpha}_\omega}\,, \tag{3.153}$$

both giving rise to ξ factor and cancelling $e^{-i\tilde{\alpha}_\omega}$. Till now we basically show

$$\int d^dXe^{ip\cdot X\ell}\mathcal{O}_{\text{flat}}(X)\sim\int d\tau e^{i\omega\tau}\mathcal{O}(\tau,\widehat{p})\,. \tag{3.154}$$

However, we have to note that using the described trick is not possible to exactly determine the correct normalization, because we partially use the saddle-points approximation, which completely ruin the information of normalization [3]. Nevertheless, as the form $e^{i\omega\tau}$ is established, we can easily normalize it as shown in Appendix A.2.

As summary, we use the notation of subregion duality to relate the global scattering smearing and Poincare scattering smearing, which indicates the momentum-coordinate duality. Although the examples of global AdS and Poincare AdS are a bit trivial, this notion of duality has its potential to be more general. The scattering region, as shown in [114] recently, must lie in the connected entanglement wedge of boundary subregion where CFT correlators are defined. We may find different entanglement wedges contain the same scattering region, and then it is possible to connect different CFT prescriptions by saddle-points approximation. We leave this idea for future work.

3.5 Fun with spinning flat-space limit

In this section, we aim to gain some insights about the flat-space limit for spinning operators/particles. We do not have a much rigorous way to present a convincing formula for flat-space limit of spinning operators, but it is quite natural to state that the saddle-points of embedding coordinate should not change even for spinning particles. A new building block for spinning operators is the embedding polarization Z, which is subject to null conditions

$$Z^2 = 0\,, \quad Z\cdot P = 0\,, \tag{3.155}$$

and the redundancy $Z \simeq Z + \#P$. Constrained by these conditions, we conjecture the following parameterization

$$P = -\frac{i}{|p|}(m,\omega,i\vec{p})\,, \quad Z = (\frac{\vec{p}\cdot\vec{\epsilon}}{\omega-m},\frac{\vec{p}\cdot\vec{\epsilon}}{\omega-m},i\vec{\epsilon})\,, \tag{3.156}$$

[3]One can convince himself about this fact by a simple example $\int dx e^{\ell a^3\log x-1/3\ell x^3}f(x)$ where $f(x)$ has no large exponential terms. If we directly evaluate it by saddle-point approach, we obtain $\sqrt{2\pi/(3\ell)}a^{a^3\ell-1/2}e^{-a^3\ell/3}f(a)$. However, if we first linearize $\log x$ around $x=a$, and then evaluate the integral using saddle-point, we find $\sqrt{\pi/\ell}a^{a^3\ell-1/2}e^{-a^3\ell/3}f(a)$, which is basically the same answer but losing a numerical factor of normalization $\sqrt{2/3}$.

where $\vec{\epsilon}$ represents the spatial polarization and is null $\vec{\epsilon}\cdot\vec{\epsilon}=0$. Since we have no way to fix appropriate overall factor for Z, we will not give ourselves a hard time on normalization throughout this section. Not exactly similar to P where $(\omega, i\vec{p})$ in P is the wick rotated momentum p, $(\vec{p}\cdot\vec{\epsilon}/(\omega-m), i\vec{\epsilon})$ in Z is not the wick rotated polarization ϵ except for massless case.

We will play with photon-photon-massive three-point function $\langle VV\mathcal{O}\rangle$ using eq. (3.156). We will verify that the flat-space limit indeed gives rise to correct three-point amplitudes in QFT.

In [2], the authors construct the helicity basis for $d=3$ CFT. The helicity basis resembles the helicity states in QFT and is found to diagonalize three-point pairing, shadow matrix, OPE matrix and parity-conserving anomalous dimensions of gluon scattering at tree level, where the partial-wave expansion is also found to satisfy bulk-point phase-shift formula eq. (3.130) compared to flat-space gluon amplitudes [2]. It is then of interest to ask: does three-point function in helicity basis already match with three-point amplitude?

The construction of helicity basis starts with working in the conformal frame $(0, x, \infty)$ and then Fourier-transform x to p, though the concept of helicity is naturally conformal invariant [2]. The trick is to use SO(2) which stablize p to label the helicity, separating the indices that are perpendicular or along p. The constructed structure is then automatically orthogonal with respect to contracting p. As discussed in [2], this trick is easily to extend to higher dimensions, where one organize the structures by SO$(d-1)$ subgroup that fixes p. One can perform the dimension reduction of SO(d) group to SO$(d-1)$, which lists perpendicular indices $J' < J$ for spin J operator. The following differential operator help single out the perpendicular indices

$$\mathcal{P}_{\epsilon}^{(k)} = \big(1 - \frac{2^k (p\cdot\epsilon)^k}{p^{2k}(d-2-k-2+2n)_k} p^{\mu}\mathcal{D}_{\mu}^{\epsilon}\big)\mathcal{P}_{\epsilon}^{(k-1)}\,, \quad \mathcal{P}_{\epsilon}^{(0)} = 1\,, \tag{3.157}$$

where the differential operator $\mathcal{D}_{\mu}^{\epsilon}$ is used to restore the indices from ϵ [116]

$$\mathcal{D}_{\mu}^{\epsilon} = (\frac{d}{2} - 1 + \epsilon\cdot\frac{\partial}{\partial\epsilon})\frac{\partial}{\partial\epsilon^{\mu}} - \frac{1}{2}\epsilon_{\mu}\frac{\partial^2}{\partial\epsilon\cdot\partial\epsilon}\,. \tag{3.158}$$

The parity-even three-point structures can then be constructed [4]

$$
\begin{aligned}
& T_{123}^{i_1,i_2,i_3}(p) \propto (p\cdot\epsilon_1)^{J_1-i_1}(p\cdot\epsilon_2)^{J_2-i_2}(p\cdot\epsilon_3)^{J_3-i_3}p^{\alpha}\times \\
& \mathcal{P}_{\epsilon_1}^{(i_1)}\mathcal{P}_{\epsilon_2}^{(i_2)}\mathcal{P}_{\epsilon_3}^{(i_3)}(\epsilon_1\cdot\epsilon_2)^{\frac{i_{123}}{2}}(\epsilon_1\cdot\epsilon_3)^{\frac{i_{132}}{2}}(\epsilon_2\cdot\epsilon_3)^{\frac{i_{231}}{2}}\,,
\end{aligned}
\tag{3.159}
$$

where $i_{abc} = i_a + i_b - i_c$ and $\alpha = \Delta_{123} - (J_1 - i_1) - (J_2 - i_2) - (J_3 - i_3)$ (we also denote $\Delta_{123} = \Delta_1 + \Delta_2 - \Delta_3$). By taking different integers from 0 to J_1, J_2 for i_1, i_2 respectively followed by taking i_3 among $|i_1 - i_2|, |i_1 - i_2| + 2, \cdots i_1 + i_2$, different structures that are orthogonal in p can thus be produced. The overall normalization is not relevant to our purpose. This construction follows the same spirit of construction of scattering amplitudes using center-of-mass frame, ensuring a counting map to flat-space [117].

We will be focusing on conserved spin-1 operator, which is dual to photon or more general gluon (the difference is the color structure encoded in OPE). There are two parity-even structures [2]

$$
\begin{aligned}
T_p = \Bigg\{ & \frac{[p^2(\epsilon_1\cdot\epsilon_3)-(p\cdot\epsilon_1)(p\cdot\epsilon_3)]\,[p^2(\epsilon_2\cdot\epsilon_3)-(p\cdot\epsilon_2)(p\cdot\epsilon_3)]}{(p\cdot\epsilon_3)^2} - \frac{p^2(\epsilon_1\cdot\epsilon_2)-(p\cdot\epsilon_1)(p\cdot\epsilon_2)}{d-1}\,, \\
& p^2(\epsilon_1\cdot\epsilon_2)-(p\cdot\epsilon_1)(p\cdot\epsilon_2)\Bigg\}(p\cdot\epsilon_3)^{J_3}p^{d-4-\Delta_3-J_3}\,.
\end{aligned}
\tag{3.160}
$$

We can Fourier-transform these structures back to coordinate space and rewrite in terms of embedding formalism

$$
T_x = M_V.B_V\,, \tag{3.161}
$$

[4]We constructed these structures with Simon Caron-Huot during the preparation of [2]. [2] only presents $d = 3$ case, where these structures reduce to parity-even helicity basis.

where B_V is the basis constructed in embedding space

$$B_V = \frac{1}{P_{12}^{\frac{1}{2}(2d-\Delta_3-J_3)} P_{13}^{\frac{1}{2}(\Delta_3+J_3)} P_{23}^{\frac{1}{2}(\Delta_3+J_3)}} \times \Big\{ -H_{12}(-V_3)^{J_3}\,, H_{31}H_{23}(-V_3)^{J_3-2}\,, V_1V_2(-V_3)^{J_3}\,, H_{31}V_2(-V_3)^{J_3-1}\,, H_{23}V_1(-V_3)^{J_3-1}\Big\}\,, \tag{3.162}$$

in which we follow [47] to define

$$H_{ij} = -2\left(P_i\cdot P_j Z_i\cdot Z_j - P_i\cdot Z_j P_j\cdot Z_i\right)\,, \quad V_i := V_{i,jk} = \frac{P_i\cdot P_k P_j\cdot Z_i - P_i\cdot P_j P_k\cdot Z_i}{P_j\cdot P_k}\,. \tag{3.163}$$

The 2×5 matrix M_V is given below

$$\begin{pmatrix} \frac{2n\beta}{1-d} & \frac{-\mathcal{J}_3+(d-1)(2-\tilde{\Delta}_3)^2}{d-1} & \frac{2n(4-2d(n+1)-4J_3)}{1-d} & \frac{2n(J_3-(d-1)(\tilde{\Delta}_3-2))}{1-d} & \frac{2n(J_3-(d-1)(\tilde{\Delta}_3-2))}{1-d} \\ 2n(d-\beta-1) & (1-J_3)J_3 & 2n(2J_3+\beta) & -2nJ_3 & -2nJ_3 \end{pmatrix}, \tag{3.164}$$

where we have defined $\mathcal{J}_3 = J_3(J_3+d-2)$, $\Delta_3 - J_3 = 2(d-2+n)$ and $\tilde{\Delta}_3 = d-\Delta_3$ to simplify the expression. We use our parameterization eq. (3.156) with center-of-mass frame

$$p_1 = (\omega, \vec{p})\,, \quad p_2 = (\omega, -\vec{p})\,, \quad p_3 = (-2\omega, 0)\,, \tag{3.165}$$

where we set $|p_3| = 0$ by scaling P_3. Since $\mathcal{O}_3$ is massive, we should scale it $\Delta_3 \sim m_3\ell$ and only keep the leading term that dominates at $\ell \to \infty$. In the end, by identifying $\epsilon = \vec{\epsilon}, p = |\vec{p}|$ we find

$$T_x \propto \Delta_3^2 T_p\,. \tag{3.166}$$

This is a spinning version of momentum-coordinate duality we discuss in the previous section!

They are also equal to three-point amplitudes in flat-space, where the corresponding vertex is [118] (for simplicity, we consider photon, while gluon follows similarly)

$$\left\{\partial_{\mu_1}\cdots\partial_{\mu_{J_3-2}}F_{\mu_{J_3-1}\nu}F_{\mu_{J_3}}{}^{\nu}\mathcal{O}^{\mu_1\cdots\mu_{J_3}}\,,\partial_{\mu_1}\cdots\partial_{\mu_{J_3}}(F_{\mu\nu}F^{\mu\nu})^2\mathcal{O}^{\mu_1\cdots\mu_{J_3}}\right\}. \quad (3.167)$$

By Feynman rule, we can easily read off the three-point amplitudes. We still adopt the center-of-mass frame eq. (3.165). After making orthogonal combination of these vertices, we indeed verify

$$T_{\text{amp}} \propto \int d^dx e^{ip\cdot x}\langle V(0)V(x)\mathcal{O}(\infty)\rangle \propto \langle V(0)V(x)\mathcal{O}(\infty)\rangle\,. \quad (3.168)$$

We verify that the structures eq. (4.7) are indeed corresponding to nicely orthogonal structures of amplitude, however, there is a puzzle. Using eq. (4.7), [2] find a messily non-diagonal shadow and OPE matrices except for $d = 3$ even for MFT, which is counterintuitive comparing to amplitude. The resolution is simple. We have to notice that the OPE matrix contains ratio of rational function of Δ where Δ is the conformal dimension of exchanged operator that is massive. To match with flat-space, we should really take $\Delta \to \infty$ and keep the leading term. The leading term is perfectly diagonal (the OPE matrix remains diagonal up to $\mathcal{O}(1/\Delta^2)$)

$$c^{\text{MFT}}(\Delta, J) = \frac{1}{2(d-2)^2(d-1)^3}\begin{pmatrix} 1 & 0 \\ 0 & \frac{(J-1)J}{(d-2)(d+J-2)(d+J-1)} \end{pmatrix}, \quad (3.169)$$

which readily generalizes $d = 3$ diagonal OPE matrix obtained in [2].

3.6 Conclusion

In this paper, we constructed the scattering smearing kernels for both global AdS (eq. (3.27)) and Poincare AdS (eq. (3.45)), which represent flat-space S-matrix in $d+1$ in terms of CFT correlator in d. We found that the scattering smearing kernel from Poincare AdS is a simple Fourier factor that brings the CFT correlator to momentum space. The scattering smearing kernel from global AdS is more nontrivial, and we found that it is served as the unified origin of other known frameworks of flat-space limit: Mellin space, coordinate space, and partial-waves.

We focused on global AdS and employed the Mellin representation of CFT correlators. We found that the scattering smearing kernel is dominated by specific configurations of CFT embedding coordinate, which is the coordinate parameterization conjectured in [3]. These kinematic saddle-points are valid regardless of mass, but we found that one more saddle-point regarding Mellin constraints is developed for massive scattering. According to this crucial observation, we found a Mellin formula that unifies massless formula and massive formula, see eq. (3.96). We used the unified Mellin formula to readily derive a unified formula describing the flat-space limit in coordinate space eq. (3.113), which reduces to the bulk-point limit [24] for massless scattering and also gives rise to both amplitude and S-matrix conjecture proposed in [3]. We readily derived the phase-shift formula for massless scattering by doing the partial-wave expansion. As the positions of CFT operators are restricted by kinematic saddle-points, we introduced a new conformal frame, which solves the conformal block at the heavy limit of both internal and external conformal dimensions. This conformal block was then used to derive a phase-shift formula for non-identical massive scattering, proving the proposal of [25].

The notion of subregion duality suggests that the Poincare scattering smearing kernel eq. (3.45) should be transformed to the global scattering smearing kernel eq. (3.45). We thus came up with a momentum-coordinate duality, which establishes a bridge for the large momentum limit of CFT correlator and smeared CFT correlator in the coordinate space eq. (3.143). By analyzing the saddle-points of Fourier-transform, we verified this duality and thus connected the flat-space limit in momentum space with other frameworks of flat-space limit. As this final gap was filled, the main result of this paper is to show that all existed frameworks of the flat-space limit of AdS/CFT are equivalent.

The final part of this paper is to play with the flat-space limit for spinning operators. We proposed a reasonable parameterization of embedding polarizations and then verified that the coordinate space and the momentum space of three-point function $\langle VV\mathcal{O}\rangle$ in the flat-space limit are indeed equivalent to each other, and they are equivalent to photon-photon-massive three-point amplitudes. We also quoted the MFT OPE matrix of conserved current four-point function, which becomes diagonal by taking the flat-space limit of intermediate operators $\Delta \to \infty$.

There are some interesting questions that we do not explore in this paper. Since OPE and anomalous dimensions in CFT can be identified to the phase-shift in QFT, it is then natural to ask, does taking the flat-space limit of Lorentzian inversion formula [43, 61] yield the Froissart-Gribov formula (see [119] for a review)? A related question is that does the flat-space limit of CFT dispersive sum rule [120, 89] give rise to dispersion relation in QFT? These questions are all relevant to analytic and unitary properties of AdS/CFT [121, 122, 123, 124] under the flat-space limit and the investigations of them are in active progress [33, 125]. Regarding the analytic analysis, the AdS impact parameter space [126] can serve as an important tool (e.g., probe the conformal Regge limit [127]), and its flat-space limit (see, e.g., [128]) could potentially cover large spin regime where $s \sim \Delta^2 - J^2$ [33]. These aspects could shed light on constraining AdS EFT (e.g., [77, 129]) by recently developed techniques of numerically obtaining EFT bounds [82, 130].

It is also of great importance to derive complete formulas of flat-space limit for spinning correlators, or at least do more examples at four-point level in terms of Mellin space, coordinate space or partial-wave expansion, see e.g., [131, 132] for recent nice trying. This could shed light on color-kinematic duality and double-copy relation (see [133, 134]) in CFT (see [135, 136, 137, 138] for insightful studies in momentum space of AdS/CFT).

Another interesting topic is to investigate the relation to celestial amplitude. Flat-space massless four-point amplitudes, as projected to celestial sphere, develop two lower-dimensional CFT structures with bulk-point delta function $\delta(z-\bar{z})$ [139], it is then interesting to clarify its relation to bulk-point limit, as was done in four dimensions [140].

Acknowledgements

We would like to thank for Simon Caron-Huot for valuable discussions and support. We would also like to thank for Balt C. van Rees, Anh-Khoi Trinh, Zahra Zahraee and Xiang Zhao for useful conversations. We are also grateful to referee's comments and suggestions. Work of Y.-Z.L. is supported in parts by the Fonds de Recherche du Québec - Nature et Technologies and by the Simons Collaboration on the Non-perturbative Bootstrap.

Chapter 4

Helicity basis for three-dimensional conformal field theory

4.0 Bridging section

Chronologically, the manuscript that this Chapter reproduces [2] was published previous to the manuscript that Chapter 3 reproduces [1]. We arranged the order of Chapters by following the logic “from scalar case to spinning case”: we focused on studying the flat-space limit of scalar correlators in Chapter 3, while in this Chapter, we explore the spinning correlators in details.

In the last Chapter, we studied the scalar amplitudes in AdS using the holographic reconstruction of scalar fields in terms of boundary operators. The reconstruction kernel in the flat-space limit is dominated by saddle points, which enables us to unify different formulas for extracting scalar S-matrix in flat-space from scalar conformal correlation functions. Those different frameworks we unify in the last Chapter have been established and studied well in the literature for scalars [21, 22, 23, 24, 3, 25, 26].

Nevertheless, explorations based on scalar scattering are not rich enough to answer whether local AdS scattering can reproduce and define scattering amplitudes and S-matrix in Minkowski spacetime. Massless particles with spin, such as gluon and graviton, play essential roles in the universe, and stringent self-consistency conditions constrain their perturbative S-matrix. Although the spinning amplitudes are more involved than scalar amplitudes due to the spinning tensor structures, the scattering of free particles is still trivial. One can easily diagonalize this S-matrix $S = 1$. However, previous to the manuscript that this Chapter reproduces [2], it was hard to verify that the flat-space limit of massless spinning amplitudes indeed reconstructs the S-matrix, even for the free scattering. The reason is that the OPE matrices of mean field theory were not diagonal in the previous basis of tensor structures [141]. We propose the helicity basis in $\mathrm{AdS}_4/\mathrm{CFT}_3$. This helicity basis naturally diagonalizes the OPE of mean field theory [2]. We also consider the tree-level scattering in AdS and explicitly verify that the description of flat-space limit in terms of the phase shift, i.e., (3.130) in the last Chapter, can be generalized to massless spinning particles.

Both manuscripts [1] (the last Chapter) and [2] (this Chapter) contribute to a better understanding of the flat-space limit of AdS scattering/conformal correlators. The last Chapter is devoted to profoundly understanding the origin and connections of the existing formulas of flat-space limit. In contrast, this Chapter provides nontrivial verifications of the flat-space limit for massless spinning scattering. It paves the way to generalize the last Chapter's analysis to spinning cases.

During the research project from which this manuscript was born, we came up with a general construction of orthogonal three-point structures in any dimension. Nevertheless, we only write the results of three dimensional CFT in this manuscript [2], where the orthogonal basis can be naturally and easily interpreted as the helicity basis. On the other hand, although the three-point structures are orthogonal in any dimensions, we did not find that it diagonalizes OPE matrix in dimensions higher than three. In (3.5) of the last manuscript, I found an opportunity to present the general dimensional basis and provide evidence that the basis diagonalizes the OPE matrix of mean field theory in the flat-space limit.

4.1 Introduction

It is an old proposition to use self-consistency conditions, such as unitarity, analyticity and crossing symmetry, to "bootstrap" physical observables like the S-matrix of Lorentz invariant quantum field theories. Nonperturbatively, this philosophy has been successfully applied in recent years to conformal field theories (CFT). This has allowed to nonperturbatively explore the space of conformal theories, and to extract precision spectra for a number of specific theories (for a review see [39]).

A surprising feature of the bootstrap is that a small number of correlators often suffice to obtain interesting constraints. Many studies therefore focus on four-point correlators of scalar operators. Spinning correlators are technically more complicated but much progress has been made and numerical studies involving them are now possible [142, 143, 144, 145, 146]. As nontrivial representations of rotation groups, spinning operators are bound to involve fancier structures. Three-point functions, for example, can be constructed using the embedding formalism [47, 147], and four-point conformal blocks, key ingredient to the bootstrap, may then be obtained by acting with corresponding spinning-up or weight-shifting operators on scalar seeds [147, 148]. This heavy machinery comes at a cost. This is especially visible in analytic work, which has so far specialized to limits such as free theories, the Regge limit, or conformal collider kinematics (see for example [79, 149, 141, 150, 151, 152, 153]).

There are several motivations to pursue analytic work with spinning correlators. A main one is the analogy with perturbative S-matrices, where massless spinning particles obey stringent self-consistency conditions. These include Weinberg's derivation of perturbative general relativity from soft limits [154], or to give just one more modern example, on-shell recursion relations for gluon amplitudes [155, 156]. For strongly coupled conformal theories with a holographic AdS dual that includes weakly coupled gravity, stress-tensor correlators are thus expected to strongly constrain not only gravity, but its coupling to matter. Indeed any CFT has a stress tensor, which, like gravity, couples to every degree of freedom.

A useful starting point for analytic approaches is good control of mean-field theory, around which one can start various approximations, be these in large spins, large N, small ϵ, or other quantities [41, 40, 54, 55, 56, 57, 42]. When the mentioned technology is applied to spinning correlators, the OPE data become matrices in the space of tensor structures. But even making seemingly natural choices, one finds dense, non-diagonal matrices already in mean field theory (MFT) [141]! It is difficult to bring oneself to study corrections to such a zeroth approximation.

A possible way forward is the fascinating observation that the number of spinning structures in CFT_d is identical to the number of structures for scattering amplitudes in QFT_{d+1} [117]. While physically natural from the viewpoint of the bulk-point or flat space limits of correlators, it is still unclear whether this counting extends to a useful map beyond that limit. Indeed, the non-diagonal nature of MFT correlators stands in sharp contrast with the QFT side, where diagonalizing trivial scattering $S = 1$ was never a big challenge! We should then ask: can one find a basis of CFT three-point structures in which MFT correlators are diagonal?

In this paper we address this question in the special case of CFT_3, exploiting the fact that in QFT_4 massless particles come with two helicity states $\pm$. We point out that the "helicity" of a conserved current is a meaningful (crossing-symmetric) concept also in CFT_3, which formally implies that a helicity basis of three-point structures will automatically diagonalize crossing symmetry. We will confirm this by computing explicit OPE data in MFT, as well as the first correction to CFT_3 current correlators dual to tree-level gluon scattering in AdS_4.

This paper is organized as follows. In section 4.2, we construct the helicity basis for three-point functions and explain that it diagonalizes a well-defined operator h. We also introduce the group-theoretic concepts to be used in later sections, including three-point pairings, shadow transforms, Euclidean and Lorentzian inversion formula. In section 4.3, we use both inversion formulas to independently obtain mean-field OPE data for conserved currents of various spins. In section 4.4, we apply our scheme to study $\mathrm{YM}_4/\mathrm{CFT}_3$, using the Lorentzian inversion formula to extract the analytic-in-spin part of the leading-order double-twist anomalous dimensions of currents. In section 4.5, we explicitly check that the anomalous dimensions of the double-twist states $[VV]_{n,J}$ at large-n agree with flat-space partial waves for tree-level gluon scattering.

This paper contains a number of technical appendices. In appendix B.1, we relate CFT_3 three-point functions conserved currents to the bulk YM_4 couplings, using the AdS embedding formalism. In appendix B.2, we explain how to simplify certain calculations by representing polarization vectors as spinors and give formulas for Fourier transforms. In appendix B.3, we review the series expansion of scalar conformal blocks. Moreover, we show how to compute OPE data for correlators that are powers of cross-ratios multiplied with Gegenbauer polynomials, which may have applications to other problems; we also record simplified expansions for certain scalar, currents and stress-tensors exchanges. Finally, flat-space gluon amplitudes, including Yang-Mills and higher-derivative couplings, are reviewed in appendix B.4.

4.2 Generalities

The structure of conformal correlators for spinning external operators is by now well understood. Here we aim to concisely summarize key results so as to state our new three-point structures as early as possible (eq. (4.10) below). We eschew the use of embedding space and cross-ratios. Rather, we use conformal symmetry to place local operators at standard locations such as $(0, x, \infty)$ as shown in figure 4.1, or $(0, x, y^{-1}, \infty)$ for four-points.

In this frame, three point functions for scalar operators are determined by dimensional analysis up to a normalization:

$$T_{123}(x) = \langle \mathcal{O}_1(0)\mathcal{O}_2(x)\mathcal{O}_3(\infty)\rangle = \frac{1}{|x|^{\Delta_1+\Delta_2-\Delta_3}}, \quad |x| \equiv \sqrt{x_\mu x^\mu}\,. \tag{4.1}$$

We define $\mathcal{O}_i(\infty)$ by taking the limit $x^{-1} \to 0$ in an inverted frame (with an inversion tensor inserted for spinning operators), so it behaves as an operator of dimension $-\Delta_i$ (see eq. (114) of [115]). We will often Fourier transform with respect to the second position x:

$$T_{123}(p) = \langle \mathcal{O}_1(0)\mathcal{O}_2(p)\mathcal{O}_3(\infty)\rangle = \int d^d x e^{-ip\cdot x}\langle \mathcal{O}_1(0)\mathcal{O}_2(x)\mathcal{O}_3(\infty)\rangle. \tag{4.2}$$

This was used in [141] to simplify calculations of shadow transforms and to compute conformal pairings, which all become simple algebraic operations.

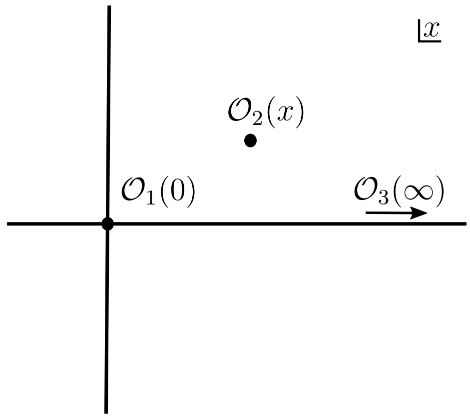

Figure 4.1: Conformal frame used for three-point functions: $\langle \mathcal{O}_1(0)\mathcal{O}_2(x)\mathcal{O}_3(\infty)\rangle$.

It is important to note that we do not Fourier transform all operators, as is sometimes considered in the literature, e.g. in [157]. The only Fourier integrals we will compute involve powers of a single variable as in (4.1) which are rather straightforward. Physically, singling out one operator is natural in conformal bootstrap applications, as we typically treat external and internal states asymmetrically. We think of the third operator as the exchanged one $\mathcal{O}$ in the conformal block decomposition of a four-point correlator, as shown in figure 4.2.

4.2.1 Three-point functions: helicity basis

Multiple index contractions generally exist between spinning operators, and three-point structures are correspondingly no longer unique. They are straightforward to classify in the above frame [158]. For pedagogical reasons, let us focus on the case where all operators are symmetric traceless tensors, $\mathcal{O}^{\mu_1\cdots\mu_J}$, where J is the spin of the operator. In $d = 3$, this covers all bosonic operators. We work in index-free notation [47] and dot into the J'th power of a null polarization vector ϵ^μ. Our two-point functions follow the standard normalization:

$$\langle \mathcal{O}(0)\mathcal{O}(\infty)\rangle = (\epsilon_1\cdot\epsilon_2)^J\,. \tag{4.3}$$

Any index contraction between the ϵ_i^μ and x^μ defines an allowed three-point function. For example, for two operators of spin-1 and a third of spin J_3 $\langle V_1 V_2 \mathcal{O}_3\rangle$, a basis

$$\langle \mathcal{O}_1\mathcal{O}_2\mathcal{O}_3\mathcal{O}_4\rangle \quad = \quad \Sigma_{\mathcal{O}}$$

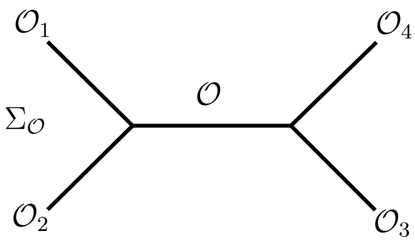

Figure 4.2: Four-point function factorized into three-point functions.

of five independent (parity-even) monomials is easily enumerated:

$$B_V = \left\{\epsilon_1{\cdot}\epsilon_2, \quad \frac{\epsilon_1{\cdot}x\ \epsilon_2{\cdot}x}{x^2}, \quad \frac{\epsilon_1{\cdot}x\ \epsilon_2{\cdot}\epsilon_3}{\epsilon_3{\cdot}x}, \quad \frac{\epsilon_1{\cdot}\epsilon_3\ \epsilon_2{\cdot}x}{\epsilon_3{\cdot}x}, \quad \frac{\epsilon_1{\cdot}\epsilon_3\ \epsilon_2{\cdot}\epsilon_3}{(\epsilon_3{\cdot}x)^2}x^2\right\} \times \frac{(\epsilon_3{\cdot}x)^{J_3}}{|x|^{\Delta_1+\Delta_2-\Delta_3+J_3}}\,. \tag{4.4}$$

Each monomial has homogeneity $(1,1,J_3)$ with respect to the three ϵ_i. It will be useful to treat structures analytically in the third spin J_3. The fact that $1/(\epsilon_3{\cdot}x)$ appears in the denominator implies that certain structures cease to exist at low spin. It will be possible to use a common labelling scheme for all values of J_3, but we will have to remember that certain structures do not contribute at low J_3.

Although our frame choice breaks permutation symmetry it is trivial to restore it. For example to exchange 1 and 2, we simply take translation by an amount $-x$ and substitute $x^\mu \mapsto -x^\mu$.[1] Less trivially, to interchange operators 1 and 3, we use the inversion $x^\mu \mapsto x^\mu/x^2 \equiv x^{-1}$, acting with the inversion tensor on ϵ_2:

$$T_{123}(\infty,x,0) = x^{-2\Delta_2}T_{123}(0,x^{-1},\infty)\Big|_{\epsilon_2^\mu\mapsto I^{\mu\nu}(x)\epsilon_2^\nu}, \qquad I^{\mu\nu}(x) = \delta^{\mu\nu} - 2\frac{x^\mu x^\nu}{x^2}. \tag{4.5}$$

There is no need to include inversions acting on ϵ_1, ϵ_3 because inversion is included in the definition of $\mathcal{O}(\infty)$. The structures in eq. (4.4) become

$$\left\{\epsilon_1{\cdot}\tilde\epsilon_2, \quad -\frac{\epsilon_1{\cdot}x\ \epsilon_2{\cdot}x}{x^2}, \quad \frac{\epsilon_1{\cdot}x\ \tilde\epsilon_2{\cdot}\epsilon_3}{\epsilon_3{\cdot}x}, \quad -\frac{\epsilon_1{\cdot}\epsilon_3\ \epsilon_2{\cdot}x}{\epsilon_3{\cdot}x}, \quad \frac{\epsilon_1{\cdot}\epsilon_3\ \tilde\epsilon_2{\cdot}\epsilon_3}{(\epsilon_3{\cdot}x)^2}x^2\right\} \times \frac{(\epsilon_3{\cdot}x)^{J_3}}{|x|^{\Delta_3+\Delta_2-\Delta_1+J_3}} \tag{4.6}$$

where $\tilde\epsilon_2^\mu = \epsilon_2^\mu - 2x^\mu\epsilon_2{\cdot}x/x^2$.

[1] This is really a substitution, not a symmetry transformation. It can be done whether or not the theory is parity symmetric.

Let us now improve this in steps. Instead of just "listing all monomials", a good idea is to use the SO(d−1) symmetry which preserve the point x. An SO(d) traceless symmetric tensor of rank J can be written as a direct sum of multiple SO(d−1) tensors, with rank $0 \leq J' \leq J$ indices, roughly, how many indices are perpendicular to x. Three-point structures are then in one-to-one correspondence with SO(d−1) singlets in the tensor products of the three representations from the three legs. Such a scheme was used for example in ref. [158]. While effective for generic operators, this is *not* the scheme we shall use, since we are interested in conserved currents. In x-space, conservation is a cumbersome differential constraint.

The next improvement is to use instead SO(d−1) tensors in *momentum* space, separating indices that are parallel or perpendicular to p in the frame in eq. (4.2). For conserved currents one simply has to drop all the structures that are not fully perpendicular to p. For example, for two conserved currents in d dimensions (which have scaling dimension $\Delta_1 = \Delta_2 = d - 1$) there are just two allowed structures, proportional to:

$$\begin{aligned}&\left\{\frac{[p^2(\epsilon_1{\cdot}\epsilon_3)-(p{\cdot}\epsilon_1)(p{\cdot}\epsilon_3)]\,[p^2(\epsilon_2{\cdot}\epsilon_3)-(p{\cdot}\epsilon_2)(p{\cdot}\epsilon_3)]}{(p\cdot\epsilon_3)^2}-\frac{p^2(\epsilon_1{\cdot}\epsilon_2)-(p{\cdot}\epsilon_1)(p{\cdot}\epsilon_2)}{d-1}\,,\right.\\ &\left.\quad p^2(\epsilon_1{\cdot}\epsilon_2)-(p{\cdot}\epsilon_1)(p{\cdot}\epsilon_2)\right\}\times(p\cdot\epsilon_3)^{J_3}|p|^{d-4-\Delta_3-J_3}\,.\end{aligned} \tag{4.7}$$

These two structures are transverse with respect to ϵ_1 and ϵ_2 and are respectively SO($d-1$) traceless symmetric tensors of rank 2 and 0 with respect to ϵ_3. The first structure is analytic for spin $J \geq 2$, and the second for $J \geq 0$. In this example "transverse" simply means invariant under $\epsilon_i \mapsto \epsilon_i + p_i$. For higher-rank conserved currents, the correct statement will involve an operator $\mathcal{D}$ designed to preserve the constraint $\epsilon_i^2 = 0$ [116]:

$$p^\mu \mathcal{D}^{\epsilon_1}_\mu T = p^\mu \mathcal{D}^{\epsilon_2}_\mu T = 0, \qquad \mathcal{D}^{\epsilon}_\mu \equiv \left(\frac{d}{2} - 1 + \epsilon\cdot\frac{\partial}{\partial\epsilon}\right)\frac{\partial}{\partial\epsilon^\mu} - \frac{\epsilon_\mu}{2}\frac{\partial}{\partial\epsilon}\cdot\frac{\partial}{\partial\epsilon}\,. \tag{4.8}$$

Such a scheme could be used to label three-point structures in any dimension d, including operators $\mathcal{O}_3$ in mixed representations of SO(d).[2] We now specialize to

[2] There are momentum-space constructions for spinning operators in the literature, where all

$d = 3$, where further simplifications occur.

In $d = 3$, SO(d−1) irreps (transverse to p) are one-dimensional and labelled by helicity $\pm J$. For two conserved currents of any spin there are thus only four structures. A projector onto the positive-helicity component of ϵ_2 can be written by combining parity-even and odd structures:

$$\epsilon_{2\mu}\Pi^{\mu\nu}_{\pm p}\epsilon_{3\nu} \equiv \frac{1}{2}\left(\epsilon_2{\cdot}\epsilon_3 - \frac{(p{\cdot}\epsilon_2)(p{\cdot}\epsilon_3)}{p^2} \pm \frac{i}{|p|}(\epsilon_2, p, \epsilon_3)\right). \tag{4.9}$$

Here $(a, b, c) = \epsilon_{\mu\nu\sigma}a^\mu b^\nu c^\sigma$ denotes contraction with $\epsilon_{123} = +1$ the antisymmetric tensor in Euclidean signature. The projector satisfies $\Pi^2_{\pm p} = \Pi_{\pm p}$ and $p{\cdot}\Pi_{\pm p} = 0$. For p along the z axis, it can be written as $\frac{1}{2}(1, i, 0)^\mu(1, -i, 0)^\nu$.

Given two conserved currents of spin J_1 and J_2 in $d = 3$, we thus define a complete basis of four possible three-point couplings, including a convenient factor, as:

$$\boxed{T^{\pm,\pm}_{123} \equiv \frac{(4\pi)^{\frac{3}{2}}(-i\sqrt{2})^{J_1+J_2+J_3}}{2^{\tau_1+\tau_2-\Delta_3}} \times (\epsilon_1\Pi_{\mp p}\epsilon_3)^{J_1}(\epsilon_2\Pi_{\pm p}\epsilon_3)^{J_2} \times (p\cdot\epsilon_3)^{J_3-J_1-J_2}|p|^{\beta_{12;3}-3}\,,} \tag{4.10}$$

where $\beta_{12;3} = (\Delta_1 + J_1) + (\Delta_2 + J_2) - (\Delta_3 + J_3)$ and $\tau_i = \Delta_i - J_i$ is the twist. The two superscripts represent the helicity of each operator. Note the reversal of the momentum in the first projector, since the first operator has momentum $-p$, so that helicity retains its physical interpretation as spin along momentum axis. The transversality condition (4.8) is readily verified for any J_i.

Eq. (4.10) defines the helicity basis we will use throughout. The opposite-helicity structures T^{+-}_{123} and T^{-+}_{123} are only allowed for local operators (polynomial in ϵ_3) when $J_3 \geq J_1 + J_2$. On the other hand, since SO(2) representations are one-dimensional, the projectors satisfy the identity:

$$(\epsilon_1\Pi_-\epsilon_3)(\epsilon_2\Pi_+\epsilon_3) = (\epsilon_1\Pi_-\epsilon_2)(\epsilon_3\Pi_-\epsilon_3) = -\frac{(p{\cdot}\epsilon_3)^2}{2p^2}(\epsilon_1\Pi_-\epsilon_2)\,, \tag{4.11}$$

three positions are Fourier transformed, see, e.g., [157, 159, 160, 137] and references therein, which enjoy potential applications to inflationary cosmology [161, 162].

which extends the range of same-helicity structures T_{123}^{++} and T_{123}^{--} to: $J_3 \geq |J_1 - J_2|$. These ranges coincide with the usual selection rules for the total angular momentum of two massless particles in flat four-dimensional space.

Although eq. (4.10) is primarily meant to be used for conserved currents, where $\Delta_i = 1 + J_i$ for $i = 1, 2$, we kept Δ_i free since the structures make sense for any Δ_i. In particular, we will use the same expressions below for shadow-transformed operators. For spin-0 states, we keep the same formula but drop superscripts.

Once the helicity basis is defined in momentum space, it is often necessary to transform it to coordinate space. The Fourier-transform of a power-law is straightforward

$$\int \frac{d^d p}{(2\pi)^d} e^{ip\cdot x} p^{2k} = \frac{4^k}{x^{2k+d}} \frac{\Gamma(\frac{d}{2}+k)}{\pi^{\frac{d}{2}}\Gamma(-k)}\,. \tag{4.12}$$

Our strategy is to perform Fourier-transform for pure power-laws at first, and then replace

$$p \cdot \epsilon \to -i\epsilon \cdot \partial\,. \tag{4.13}$$

Doing so, one finds that the parity-even and odd components produce disparate gamma-functions that don't nicely combine. Many calculations are thus simplified by switching to an Even/Odd basis of parity eigenstates. Each parity sector contains two elements, representing states with opposite or same helicity:

$$\begin{aligned}
\left\{T_{123}^{E,\text{opp}}, T_{123}^{E,\text{same}}\right\} &\equiv \frac{\Gamma\left(\frac{3-\tau_1-\tau_2+\Delta_3+J_3}{2}\right)}{\Gamma\left(\frac{\tau_1+\tau_2-\tau_3}{2}\right)} \times \left\{\frac{T_{123}^{+-}+T_{123}^{-+}}{\sqrt{2}}, \frac{T_{123}^{++}+T_{123}^{--}}{\sqrt{2}}\right\},\\
\left\{T_{123}^{O,\text{opp}}, T_{123}^{O,\text{same}}\right\} &\equiv \frac{\Gamma\left(\frac{2-\tau_1-\tau_2+\Delta_3+J_3}{2}\right)}{\Gamma\left(\frac{1+\tau_1+\tau_2-\tau_3}{2}\right)} \times \left\{\frac{T_{123}^{+-}-T_{123}^{-+}}{\sqrt{2}}, \frac{T_{123}^{++}-T_{123}^{--}}{\sqrt{2}}\right\},
\end{aligned} \tag{4.14}$$

where we introduced gamma-factor normalizations for future convenience. These ensure that the transform produces polynomials in Δ_3 and J_3 of the lowest possible degree, as the denominator cancels spurious double-twist poles from the Fourier transform.

Fourier transforms may now be straightforwardly computed, by expanding the even/odd structures into dot products of p with polarizations, up to a possible single odd factor $(p, \epsilon_i, \epsilon_j)$.

As a trivial example, in the scalar case $J_1 = J_2 = 0$, there is just a single structure

$$T^E_{00\mathcal{O}} = 2^{\frac{J_3}{2}} |x|^{\Delta_3 - J_3 - \Delta_1 - \Delta_2} (x{\cdot}\epsilon_3)^{J_3} \,. \tag{4.15}$$

As a more illustrative example, for two spin-1 currents $\langle V_1 V_2 \mathcal{O}\rangle$ the two even structures turn out to be proportional to eq. (4.7) (in the same order). As it should, the transform takes the form of a matrix acting on the basic structures B_V in eq. (4.4):

$$\begin{pmatrix} T^{E,\text{opp}}_{11\mathcal{O}} \\ T^{E,\text{same}}_{11\mathcal{O}} \end{pmatrix} = 2^{\frac{J_3+1}{2}} n \begin{pmatrix} 2(n{-}\tilde{J}_3) & 2(n{-}1) & (3\tilde{J}_3{-}4n{+}1) & (3\tilde{J}_3{-}4n{+}1) & \frac{\tilde{J}_3^2-(8n+1)\tilde{J}_3+8n^2}{2n} \\ 2(-n{-}J_3) & 2(n{-}1) & J_3 & J_3 & \frac{(J_3-1)J_3}{2n} \end{pmatrix} \cdot B_V \,, \tag{4.16}$$

where n is defined through $\tau_3 = \tau_1 + \tau_2 + 2n$, and $\tilde{J}$ denotes the "spin shadow": $\tilde{J} = -1 - J$ in $d = 3$ [62]. The parity-odd structures can be similarly represented in terms of four odd monomials:

$$B'_V = \left\{ \frac{(\epsilon_1, x, \epsilon_3)\epsilon_2{\cdot}x}{x^2}, \quad \frac{(\epsilon_1, x, \epsilon_3)\epsilon_2{\cdot}\epsilon_3}{x{\cdot}\epsilon_3}, \quad \frac{(\epsilon_2, x, \epsilon_3)\epsilon_1{\cdot}x}{x^2}, \quad \frac{(\epsilon_2, x, \epsilon_3)\epsilon_1{\cdot}\epsilon_3}{x{\cdot}\epsilon_3} \right\} \frac{(\epsilon_3{\cdot}x)^{J_3-1}}{|x|^{\Delta_1+\Delta_2-\Delta_3+J_3-1}} \,, \tag{4.17}$$

in which

$$\begin{pmatrix} T^{O,\text{opp}}_{11\mathcal{O}} \\ T^{O,\text{same}}_{11\mathcal{O}} \end{pmatrix} = 2^{\frac{J_3+1}{2}} \begin{pmatrix} (1{-}2n) & (1{+}J_3{+}2n) & (1{-}2n) & (1{+}J_3{+}2n) \\ (1{-}2n) & ({-}1{+}J_3{+}2n) & ({-}1{+}2n) & (1{-}J_3{-}2n) \end{pmatrix} \cdot B'_V \,. \tag{4.18}$$

Notice that so far n is simply a notation for the twist, but when n takes on (half-)integer values it will represent so-called double-twist operators. Parity-even double twists have integer n while parity-odd ones have half-integer n.

A technical complication when dealing with higher-rank tensors and odd structures is the presence of Gram determinant relations (antisymmetrizing any four vectors gives zero). In our calculations below, we circumvent this either by evaluating expressions on a symbolic three-dimensional parametrization, or by using the spinor formulation in appendix B.2.

The opposite-helicity structure in eq. (4.16) is physically allowed for $J_3 \geq 2$, but there is an important discrete exception: when $\mathcal{O}_3$ is a conserved current ($J_3 = 1$ and $\Delta_3 = 2$). Then the complicated polynomial in the fifth column vanishes, shielding the problematic denominator in eq. (4.4). The three structures: $T^{E,\text{opp}}, T^{E,\text{same}}, T^{O,\text{same}}$ then define valid (and independent) couplings between three currents. We verify in appendix B.1 that these map, *respectively*, to bulk Yang-Mills couplings $\text{Tr}F^2$, and to parity even/odd parts of $\text{Tr}F^3$!

4.2.2 Helicity is conformally invariant

The reader may worry that our definition of helicity structures in eq. (4.10) is tied to the specific frame $(0, x, \infty)$. However, it turns out to be independent of this! Here we construct a conformal integral transform, whose eigenvalue is helicity. Its existence will automatically imply that crossing is diagonal in the helicity basis.

It is intuitively clear from holography that helicity should be frame-independent, since momentum-space currents with definite helicity source AdS_4 gauge fields that are either self-dual or anti-self-dual near the boundary [161, 163]. Helicity structures for correlators of three higher-spin currents in momentum space, and their relation with bulk AdS couplings, were discussed in [164]. (For a spinor-helicity formalism in AdS_4, see also [165].) Since the self-dual decomposition is invariant under conformal isometries, we expect it to be independent of frame and agree between all channels.

In momentum space, the operation which measures helicity is simply

$$hJ^\mu(p) \equiv -i\frac{\epsilon^{\mu\nu\sigma}p_\sigma}{|p|}J^\nu(p)\,. \tag{4.19}$$

Fourier transforming this defines an integral transform:

$$hJ^\mu(x) = \int d^3y H^{\mu\nu}(x-y)J_\nu(y)\,, \qquad H^{\mu\nu}(x-y) \equiv \frac{\epsilon^{\mu\nu\sigma}}{2\pi^2}\frac{\partial}{\partial y^\sigma}\frac{1}{(x-y)^2}\,. \tag{4.20}$$

We now show that h commutes with conformal transformations. Normally, this would require the kernel H to transform like a two-point function between a current and its shadow, $\langle J^\mu(x)\tilde{J}^\nu(y)\rangle$. For a generic operator, this is impossible: conformal two-point functions between operators of different dimension must vanish! (This follows easily from scale invariance in the frame $(x,y)=(0,\infty)$.) The loophole here is that since $J^\nu(y)$ is conserved, the shadow $\tilde{J}^\nu$ is defined *modulo* a derivative: the kernel H only needs to be conformally invariant modulo a total derivative $\partial_y^\nu X^\mu(x,y)$.

Let's thus check invariance under inversion $x^\mu \mapsto x^\mu/x^2$. Applying the standard transformation laws, a short calculation gives:

$$\frac{\mathcal{I}^{\mu\mu'}(x)\mathcal{I}^{\nu\nu'}(y)}{x^4y^2}H^{\mu\nu}(x^{-1}-y^{-1}) = \frac{1}{\pi^2}\left[\frac{\epsilon^{\mu\nu\sigma}(y-x)_\sigma}{(x-y)^4}+\frac{\epsilon^{\mu\nu\sigma}x_\sigma}{(x-y)^2x^2}+2\frac{(x-y)^\nu\epsilon^{\mu\rho\sigma}y_\rho x_\sigma}{x^2(x-y)^4}\right] \tag{4.21}$$

We have used the Schouten identity to eliminate terms with x^μ or y^μ. With a bit of inspection, we find that the sum of H and its transform is indeed a total derivative:

$$H^{\mu\nu}(x-y)+\frac{\mathcal{I}^{\mu\mu'}(x)\mathcal{I}^{\nu\nu'}(y)}{x^4y^2}H^{\mu\nu}(x^{-1}-y^{-1}) = \frac{\partial}{\partial y^\nu}\frac{\epsilon^{\mu\rho\sigma}y_\rho x_\sigma}{\pi^2(x-y)^2}\,. \tag{4.22}$$

This shows formally that h is invariant under inversion (up to an overall sign change):

$$(hJ)^{-1} = -h(J^{-1}) \tag{4.23}$$

where $(J^{-1})^\mu(x) = \mathcal{I}^{\mu\mu'}J^{\mu'}(x^{-1})/x^4$ denotes the inversion map. The sign change was expected since h is parity-odd. One could equivalently say that h is invariant under the combination of inversion and parity.

To illustrate the action of h, let us briefly consider two-point functions. A special feature of $d=3$ CFTs is that *two* structures are allowed by conformal invariance [166]:

$$\langle J_\mu(x)J_\nu(0)\rangle = \left(\delta_{\mu\nu}\partial^2-\partial_\mu\partial_\nu\right)\frac{\tau}{32\pi^2x^2}+\frac{i\kappa}{2\pi}\epsilon_{\mu\nu\rho}\partial^\nu\delta^3(x)\,, \tag{4.24}$$

where the coefficient κ of the contact term is defined modulo an integer. It is easy to see (for example using momentum space expressions from ref. [166]) that acting with h on $J_\mu(x)$ yields the same with τ and $8\kappa/\pi$ interchanged. This confirms that h takes conformal two-point functions to conformal two-point functions. Of course, just like the shadow transform, hJ is generally not a local operator.

For higher-spin conserved currents, a similar transform can be defined

$$hT^{\mu_1\cdots\mu_J}(x) = \int d^3y\,(H^{\mu_1\nu_1}(x-y)T^{\nu_1\mu_2\cdots\mu_J}(y) + (J-1)\text{ permutations of }\mu_1) \tag{4.25}$$

Generally, $h^2 = J^2$, and one can easily verify that the structures in eq. (4.10) are eigenstates:

$$h_1 T_{123}^{\pm_1,\pm_2} = (\pm_1 J_1) T_{123}^{\pm_1,\pm_2} \qquad h_2 T_{123}^{\pm_1,\pm_2} = (\pm_2 J_2) T_{123}^{\pm_1,\pm_2}\,. \tag{4.26}$$

Although we did not construct a total derivative akin to eq. (4.22) in the higher-spin case, we believe h to be conformal as well, given the fact that all data computed in the next sections will turn out diagonal.

In Lorentzian signature, there is a subtlety: h depends on operator ordering through the branch choice $|p| \equiv \sqrt{p^2 \pm i0}$ in eq. (4.19). While eqs. (4.26) remain valid as long as the same branch is used for h and T, this means that taking discontinuities or commutators do not preserve h eigenstates; one can explicitly see in eqs. (4.16)-(4.18) that even and odd structures acquire different phases. This will be important below in our discussion of Lorentzian inversion.

4.2.3 Simple operations: three-point pairings and shadow map

Since h is a conformal operation, three-point structures with definite helicity will be orthogonal under all natural operations. Here we review two simple operations, which will form useful building blocks later.

The simplest may be the conformal pairing between three-point structures and shadow structures:

$$P_{123}^{a,b} = \left(T_{123}^{a}, T_{\tilde{1}\tilde{2}\tilde{3}}^{b}\right) \equiv \int \frac{d^dx_1 d^dx_2 d^dx_3}{\mathrm{vol}(\mathrm{SO}(d+1,1))} \langle \mathcal{O}_1\mathcal{O}_2\mathcal{O}_3\rangle^a \langle \tilde{\mathcal{O}}_1\tilde{\mathcal{O}}_2\tilde{\mathcal{O}}_3\rangle^b \tag{4.27}$$

$$= \frac{1}{2^d \mathrm{vol}(\mathrm{SO}(d-1))} \sum_{\epsilon_1,\epsilon_2,\epsilon_3} T_{123}^{a}(\epsilon_1,\epsilon_2,\epsilon_3)(1)\ T_{\tilde{1}\tilde{2}\tilde{3}}^{b}(\epsilon_1^*,\epsilon_2^*,\epsilon_3^*)(1)\,, \tag{4.28}$$

where we have used the symmetry to put $x = 1$. The denominator is the volume form of the "little group" that keeps the frame $(0, 1, \infty)$ fixed [141].

A good way to compute index contraction is to use the differential operator (4.8)

$$\sum_{\epsilon} f(\epsilon^*) g(\epsilon) = \frac{1}{J!(\frac{d-2}{2})_J} f(\mathcal{D}_\epsilon) g(\epsilon). \tag{4.29}$$

For example, for vector-vector-general $\langle V_1 V_2 \mathcal{O}\rangle$ case, the pairings between Even or Odd structures (4.16) and (4.18) is readily evaluated:

$$P_{11\mathcal{O}}^{E} = 16 P_s N_{11\mathcal{O}}^{E} \begin{pmatrix} \frac{(J_3+1)(J_3+2)}{(J_3-1)J_3} & 0 \\ 0 & 1 \end{pmatrix}, \qquad P_{11\mathcal{O}}^{O} = 16 P_s N_{11\mathcal{O}}^{O} \begin{pmatrix} \frac{(J_3+1)(J_3+2)}{(J_3-1)J_3} & 0 \\ 0 & 1 \end{pmatrix}, \tag{4.30}$$

where P_s is just the pairing of two scalars and one spinning operator [141][3]

$$P_s = \frac{1}{2^d \mathrm{vol}(\mathrm{SO}(d-1))} \frac{(d-2)_{J_3}}{\left(\frac{d-2}{2}\right)_{J_3}} \tag{4.31}$$

and for latter convenience we introduce the N factor, which is precisely the product of the gamma-functions in eq. (4.14) and its shadow:

$$N_{J_1 J_2 \mathcal{O}}^{E} = \left(\tfrac{\tau_1+\tau_2-\tau_3}{2}\right)_{J_1+J_2} \left(\tfrac{3+\beta_3-\beta_1-\beta_2}{2}\right)_{J_1+J_2},$$

$$N_{J_1 J_2 \mathcal{O}}^{O} = \left(\tfrac{1+\tau_1+\tau_2-\tau_3}{2}\right)_{J_1+J_2-1} \left(\tfrac{4+\beta_3-\beta_1-\beta_2}{2}\right)_{J_1+J_2-1}. \tag{4.32}$$

Many other examples can be straightforwardly worked out and it turns out that

[3]Our scalar structures are larger by a factor $2^{J_3/2}$ than those of [141]: $P_s^{\mathrm{here}} = 2^{J_3} P_s^{\mathrm{there}}$.

the three-point pairing is always orthogonal. In fact there is a rather mechanical explanation: the x-space pairing is also proportional to the momentum-space one [141][4]:

$$P_{123}^{a,b} = \frac{1/(2\pi)^d}{2^d \mathrm{vol}(\mathrm{SO})(d-1)} \sum_{\epsilon_1,\epsilon_2,\epsilon_3} T_{123}^a(\epsilon_1,\epsilon_2,\epsilon_3)(p)\ T_{\tilde{1}\tilde{1}\tilde{1}}^b(\epsilon_1^*,\epsilon_2^*,\epsilon_3^*)(-p)\,. \tag{4.34}$$

Due to this, the diagonal pairing would be rather trivially diagonal in any d, using the momentum space basis discussed above eq. (4.7). Without derivation, we thus quote the diagonal 4×4 matrix of pairings in the $d=3$ helicity basis (4.10):

$$P_{123}^{(h_1,h_2),(\bar{h}_1',\bar{h}_2')} = \delta_{h_1}^{h_1'}\delta_{h_2}^{h_2'} \times P_s \times 4^{|h_1|+|h_2|}(-1)^{|h_1-h_2|}\frac{(J_3+1)_{|h_1-h_2|}}{(-J_3)_{|h_1-h_2|}}\,. \tag{4.35}$$

Taking Even/Odd combinations (4.14) simply adds the $N^{E/O}$ factors, reproducing the $J_1=J_2=1$ example quoted in eq. (4.30). The fact that the pairing is diagonal (with $\bar{h}=-h$) is a first hint that the structures are well chosen.

A second natural and useful operation is the shadow transform

$$\mathbf{S}[\mathcal{O}_1(x)] \equiv \int d^dy \langle\tilde{\mathcal{O}}_1(x)\tilde{\mathcal{O}}_1(y)\rangle\mathcal{O}_1(y)\,, \tag{4.36}$$

which maps operators to their shadow operators nonlocally. Operating on three-point structures this generally produces a shadow matrix $S([\mathcal{O}_1]\mathcal{O}_2\mathcal{O}_3)^a{}_b$:

$$\langle\mathbf{S}[\mathcal{O}_1]\mathcal{O}_2\mathcal{O}_3\rangle^a = S([\mathcal{O}_1]\mathcal{O}_2\mathcal{O}_3)^a{}_b\langle\tilde{\mathcal{O}}_1\mathcal{O}_2\mathcal{O}_3\rangle^b\,. \tag{4.37}$$

The shadow transform for conserved currents in $d=3$ is simple: the two-point function in momentum space can be diagonalized by helicity, which is always maximal

[4]This can be proven formally by moving gauge-fixing factors in the frame $(0,x,\infty)$:

$$\int \frac{d^dx}{\mathrm{vol}(\mathrm{SO}(d)\times\mathrm{SO}(1,1))}T(x)\tilde{T}(x) = \int d^dx \int \frac{d^dp\ d^dp'\ e^{ix\cdot(p+p')}}{(2\pi)^{2d}\mathrm{vol}(\mathrm{SO}(d)\times\mathrm{SO}(1,1))}T(p)\tilde{T}(p')\,. \tag{4.33}$$

The x integral simply gives a delta-function setting $p'=-p$.

for conserved currents. Using $2^{\Delta-\tilde{\Delta}}\mathcal{A}_{j,j}\big|_{\Delta=J+1}$ from eq. (E.11) of [141], we get simply

$$S([\tilde{\mathcal{O}}_1]\mathcal{O}_2\mathcal{O}_3)^{(h_1',h_2')}{}_{(h_1,h_2)} = \delta_{h_1}^{h_1'}\delta_{h_2}^{h_2'}(-4)^{J_1}\pi^2 \times \mathcal{C}_{J_1}, \qquad \mathcal{C}_J \equiv \frac{1+\delta_{J,0}}{2(2J)!}\,. \tag{4.38}$$

This holds when acting on the shadow of a conserved current $\tilde{\mathcal{O}}_1$, or a scalar with the same twist $\Delta_1 = 1$. (We note that S is not invertible and $S[\mathcal{O}_1] = 0$ acting on a conserved current.) The transform in the Even/Odd basis is of course also diagonal, but displays additional scalar factors due to the gamma-functions in (4.14).

The shadow transform with respect to $\mathcal{O}_3$ will be technically more difficult to compute; we will find below (see (4.81)) that it is also diagonal.

4.2.4 Spinning conformal blocks

A more interesting and nontrivial object is the correlator of four operators. The Operator Product Expansion distills those in terms of a given theory's spectrum and OPE coefficients. Using conformal symmetry we can assume the four points are at $(0, x, y^{-1}, \infty)$ (where y^{-1} is the point y^μ/y^2). Factoring out a conventional prefactor to trivialize the $x \to 0$ and $y \to 0$ limits

$$\langle \mathcal{O}_1(0)\mathcal{O}_2(x)\mathcal{O}_3(y^{-1})\mathcal{O}_4(\infty)\rangle = \frac{|y|^{\Delta_3+\Delta_4}}{|x|^{\Delta_1+\Delta_2}}G(z,\bar{z}). \tag{4.39}$$

Our notation $\mathcal{O}_3(y^{-1})$ implies that we apply inversion tensors to the indices on the third (and fourth) operator. The complex variable z (which is complex conjugate to $\bar{z}$ in Euclidean signature) encodes the sizes and angles of the vectors x^μ and y^μ:

$$z\bar{z} = x^2y^2, \qquad z+\bar{z} = 2x\cdot y\ . \tag{4.40}$$

Inserting a complete basis of states between $\mathcal{O}_1, \mathcal{O}_2$ gives the operator product expansion

$$G(z,\bar{z}) = \sum_{\Delta,J,a,b} \lambda_{12\mathcal{O}a}\lambda_{43\mathcal{O}b}G^{a,b}_{\Delta,J}(z,\bar{z}) \tag{4.41}$$

where the sum runs over the spectrum of the theory, and the λ's are OPE coefficients. When the external operators have spin, there are generally multiple index contractions a, b to sum over representing the different three-point structures, each of which has an independent coefficient. The special functions $G^{a,b}_{\Delta,J}(z,\bar{z})$ are the so-called conformal blocks, which we normalize so they approach as $x \to 0$ a simple product of three-point structures (summing over the polarizations of the intermediate operator $\mathcal{O}$):

$$\lim_{x\to 0} G^{a,b}_{\Delta,J}(z,\bar{z}) = \frac{x^{\Delta_1+\Delta_2}}{y^{\Delta_3+\Delta_4}} \sum_{\epsilon_{\mathcal{O}}} T^a_{12\mathcal{O}}(x) T^b_{43\mathcal{O}}(y) \equiv \mathcal{P}^{a,b}_{\Delta,J}(x,y) \tag{4.42}$$

For example, for scalar external operators in our normalization (4.15) one finds

$$\mathcal{P}_{\Delta,J}(\widehat{x},\widehat{y}) = (|x||y|)^{\Delta} \frac{(d-2)_J}{\left(\frac{d-2}{2}\right)_J} \tilde{C}_J\left(\tfrac{x\cdot y}{|x||y|}\right) \to_{z\ll\bar{z}\ll 1} (z\bar{z})^{\Delta/2} (z/\bar{z})^{J/2} \tag{4.43}$$

where $\tilde{C}_j(\xi) = C_J(\xi)/C_J(1) = {}_2F_1(-J, J+d-2, \frac{d-1}{2}, \frac{1-\xi}{2})$ is a Gegenbauer normalized to unity at $\xi = 1$. In terms of cross-ratios, $\frac{x\cdot y}{|x||y|} = \frac{z+\bar{z}}{2\sqrt{z\bar{z}}}$.

The conformal block G contains an infinite tower of terms suppressed by powers of x (or $z, \bar{z}$), arising from exchange of descendants $\partial^k \mathcal{O}_\Delta$. Series expansions for these terms are available from refs [112, 167, 168], as well as an efficient Zamolodchikov recursion algorithm, see [169, 146]. In practice we will use the spinning up/spinning down method. We write the spinning block as a derivative of a scalar one,

$$G^{a,b}_{\Delta,J} = \mathbb{P}^a_{(\alpha)} \mathbb{P}^b_{(\beta)} \mathcal{D}^{(\alpha,\beta)}_{\uparrow} G^{(\alpha,\beta)}_{\Delta,J}\,. \tag{4.44}$$

Let us explain our notation here. The indices $\alpha, \beta, \cdots$ span the space of spinning-up operators (see eq. (4.91) below), so that the $\mathbb{P}^b_{(\beta)}$ are constant matrices, that depend only on Δ, J but not on spacetime coordinates; $\tilde{G}^{(\alpha,\beta)}$ is a scalar conformal blocks, where the superscripts denote the specific shift of conformal dimensions associated with the particular spinning-up operator (α, β). Explicit operators will be written in section 4.3.3 below; a simple recursion for scalar conformal blocks is reviewed in appendix B.3.1.

4.2.5 Euclidean inversion formula

The OPE sum runs over the spectrum of the theory, which we generally don't know exactly. For analytics it is often better to replace the sum by an integral, the "harmonic analysis":

$$G(z,\bar{z}) = \sum_{J,a,b} \frac{1}{2}\int_{d/2-i\infty}^{d/2+i\infty} \frac{d\Delta}{2\pi i} c_{a,b}(\Delta,J)\left(G^{a,b}_{\Delta,J}(z,\bar{z}) + \text{shadow}\right). \tag{4.45}$$

The "shadow term" is the same block with $\Delta \mapsto \tilde{\Delta} = d - \Delta$ and with a specific coefficient, see [170, 127]. This shadow term ensures that the parenthesis is Euclidean single-valued (i.e. does not have a branch cut) in the limits $x \to y^{-1}$ and $x \to \infty$. Explicitly, this term is

$$S(\mathcal{O}_1\mathcal{O}_2[\mathcal{O}])^a{}_c\ (S(\mathcal{O}_3\mathcal{O}_4[\tilde{\mathcal{O}}])^{-1})^b{}_d\ G^{c,d}_{\tilde{\Delta},J}\,. \tag{4.46}$$

To obtain the OPE (4.41) from the integral (4.45) one simply closes the contour to the right in the G term, and the formulas will match provided

$$-\operatorname*{Res}_{\Delta'\to\Delta} c_{a,b}(\Delta,J) = \lambda_{12\mathcal{O}a}\lambda_{43\mathcal{O}b}. \tag{4.47}$$

The function $c_{a,b}(\Delta,J)$ will be useful below since it simultaneously encodes the spectrum (through the location of its poles) and OPE coefficients (through the residues); this enables one to speak about OPE coefficients without having to first know the spectrum.

As single-valued eigenfunctions of a Casimir differential operator, the harmonic functions satisfy an orthogonality relation

$$\int \frac{d^dx_1\cdots d^dx_4}{\text{vol}(\text{SO}(d+1,1))}\langle 1234\rangle^{a,b}_{\Delta,J}\langle\tilde{1}\tilde{2}\tilde{3}\tilde{4}\rangle^{c,d}_{\tilde{\Delta},J} = (\mathcal{N}(\Delta,J)_{(a,b),(c,d)})^{-1}\ [2\pi\delta(\nu-\nu') + \text{shadow}], \tag{4.48}$$

where $\Delta = \frac{d}{2} + i\nu$ and the tildes denote shadow operators; tensor indices are meant to be contracted between each operator and its shadow. Note that we abbreviate ($G_{\Delta,J}+$ shadow) as $\langle 1234\rangle_{\Delta,J}$. The symmetry can be used to fix the points to $(0,x,1,\infty)$ so the integral is really just over x. The normalization $\mathcal{N}(\Delta,J)$ can be expressed in terms of the pairing $P^{(a,b)}$ of eq. (4.35), since the δ-function originates from the $x\to 0$ limit, where the blocks can be approximated by their limit (4.42). Explicitly, the normalization reads [141]

$$\mathcal{N}(\Delta,J)_{(a,b),(c,d)} = \mu(\Delta,J)\;(P^{a,c}_{12\mathcal{O}})^{-1}\;(P^{b',d'}_{34\tilde{\mathcal{O}}})^{-1}\;S(34[\tilde{\mathcal{O}}])^{b'}{}_{b}\;S(\tilde{3}\tilde{4}[\mathcal{O}])^{d'}{}_{d}\,, \quad (4.49)$$

where the “Plancherel measure” is

$$\mu(J,\Delta) = \frac{(d+2J-2)\Gamma(d+J-2)\Gamma(\Delta-1)\Gamma(d-\Delta-1)(\Delta+J-1)(d-\Delta+J-1)}{2^d\pi^d\mathrm{vol}(\mathrm{SO}(d))\Gamma(d-1)\Gamma(J+1)\Gamma(\frac{d}{2}-\Delta)\Gamma(\Delta-\frac{d}{2})}\,. \quad (4.50)$$

Evaluated in terms of cross-ratios, this gives an integral over the complex-z plane[5]

$$c_{a,b}(\Delta,J) = \frac{\mathcal{N}(\Delta,J)_{(a,b),(c,d)}}{2^{2d-1}\mathrm{vol}(\mathrm{SO}(d-2))}\int\frac{d^2z}{z^2\bar{z}^2}\left|\frac{z-\bar{z}}{z\bar{z}}\right|^{d-2}\left(\tilde{G}^{c,d}_{d-\Delta,J}(z,\bar{z})+\text{non-shadow}\right)G(z,\bar{z}) \quad (4.52)$$

where index contractions with $G(z,\bar{z})$ is again implied. To extract the spectrum using this formula one would have to know the exact correlator $G(z,\bar{z})$, which of course is impractical unless one already has solved the theory. The usefulness of this formula is that it provides analytic estimates for the OPE data in certain limits. Specifically, following [141] we will use this formula to extract OPE data in mean field theory in section 4.3.

[5]We used eq. (4.28) and the relation $\frac{\mathrm{vol}(\mathrm{SO}(d-1))}{\mathrm{vol}(\mathrm{SO}(d-2))}=\mathrm{vol}S_{d-2}$ to write, for any conformal function $(\cdots)$:

$$\int\frac{d^dx_1\cdots d^dx_4}{\mathrm{vol}(\mathrm{SO}(d+1,1))}\frac{(\cdots)}{x_{12}^{2d}x_{34}^{2d}} = \frac{1}{2^{2d-1}\mathrm{vol}(\mathrm{SO}(d-2))}\int\frac{d^2z}{z^2\bar{z}^2}\left|\frac{z-\bar{z}}{z\bar{z}}\right|^{d-2}(\cdots)\,. \quad (4.51)$$

4.2.6 Spinning Lorentzian inversion formula

An effective method to go beyond MFT is to analytically continue the Euclidean inversion formula to Lorentzian signature, which gives the Lorentzian inversion formula [43, 61, 62]. It expresses OPE data as a sum of so-called t- and u-channel double-discontinuities.

A practical advantage relevant for the present paper is that at tree-level in theories with a large-N expansion, the double-discontinuity is saturated by single-trace exchanges [106, 171], effectively giving AdS cutting rules (see also [121, 124]).

The formula was generalized to the spinning case in ref. [62]. The t-channel contribution is given as:

$$c^t_{a,b}(\Delta, J) = \mathcal{N}^L_{(a,b),(c,d)} \int_0^1 \frac{dzd\overline{z}}{z^2\overline{z}^2} \left| \frac{z-\overline{z}}{z\overline{z}} \right|^{d-2} \tilde{G}^{c,d}_{J+d-1,\Delta-d+1}(z,\bar{z}) \mathrm{dDisc}[G(z,\bar{z})] \,, \quad (4.53)$$

where the tilde denotes that the external operators are shadow operators, and the tensor indexes are contracted between $\tilde{G}$ and dDisc$[G]$. A key result of ref. [62] is an elegant way to calculate the normalization factor $\mathcal{N}^L$, which is generally a matrix, in terms of "light-transforms". The light-transform of a spinning operator is defined as

$$\mathbf{L}[\mathcal{O}](x,\epsilon) = \int_{-\infty}^{\infty} d\alpha(-\alpha)^{-\Delta-J} \mathcal{O}(x - \frac{\epsilon}{\alpha}, \epsilon) \,. \quad (4.54)$$

(Despite appearance, the integral has no branch point at $\alpha = 0$ due to the behavior of $\mathcal{O}$. We refer to [62] for further details on the precise branch choices, which we will ignore in this presentation.) When the light-transform acts on the third operator of a three-point function, it simply induces a Weyl reflection for that operator ($\Delta \mapsto 1-J, J \mapsto 1-\Delta$) with an overall light-transform matrix, i.e.

$$\langle \mathcal{O}_1\mathcal{O}_2\mathbf{L}[\mathcal{O}_{\Delta,J}]\rangle^a = L^a_b(\mathcal{O}_1\mathcal{O}_2[\mathcal{O}])\langle \mathcal{O}_1\mathcal{O}_2\mathcal{O}_{1-\Delta,1-J}\rangle^b \,. \quad (4.55)$$

We found that the integrand can be computed directly in our frame $(0, x, \infty)$, using a special conformal transformation along the direction ϵ_3 to keep $x_3 = \infty$ and move

x_2 instead. This reduces to a simple substitution:

$$x \mapsto x + \frac{x^2}{\alpha}\epsilon_3\,, \quad \epsilon_2 \mapsto \epsilon_2 + \left(x\cdot\epsilon_2 - \frac{x^2\epsilon_2\cdot\epsilon_3}{\alpha+2x\cdot\epsilon_3}\right)\frac{2\epsilon_3}{\alpha} - \frac{2\epsilon_2\cdot\epsilon_3}{\alpha+2x\cdot\epsilon_3}x \tag{4.56}$$

and we have to multiply three-point functions by $(1+2x{\cdot}\epsilon_3/\alpha)^{\Delta_1-\Delta_3}$. Using this rule, and integrating over α following ref. [62], we find that the light-transform matrix in the Even/Odd basis is actually independent of J_1 and J_2:

$$L^E(J_1J_2[\mathcal{O}_{\Delta,J}]) = L_s^{(0)}\begin{pmatrix}0 & 1\\ 1 & 0\end{pmatrix}\,, \quad L^O(J_1J_2[\mathcal{O}_{\Delta,J}]) = L_s^{(1)}\begin{pmatrix}0 & 1\\ 1 & 0\end{pmatrix}\,, \tag{4.57}$$

where $L_s^{(\Delta_{12})}$ denotes the scalar light transform [62]

$$L_s^{(\Delta_{12})} = -i\frac{2^{\frac{3-\beta}{2}}\pi\Gamma(\beta-1)}{\Gamma\left(\frac{\beta-\Delta_{12}}{2}\right)\Gamma\left(\frac{\beta+\Delta_{12}}{2}\right)}\,. \tag{4.58}$$

We note that the light transform is not diagonal. Attempting to transform from the Even/Odd basis to the helicity basis (via eq. (4.14)) would produce a matrix that is not only non-diagonal, but also dense. The reason the light transform does not commute with helicity is that its calculation requires taking a discontinuity, which does not commute with h, as found at the end of subsection 4.2.2. We will therefore work in the Even/Odd basis, where the simple form of eq. (4.57) will enable us to write the Lorentzian inversion formula very explicitly below.

The remaining ingredient is the inverse of a "Lorentzian" pairing between three-point structures [62], which reads in the $x=1$ gauge:

$$P^{a,b}_{12[\mathcal{O}],L} = \frac{(-2\epsilon_3\cdot 1)^{d-2}}{2^{2d-2}\mathrm{vol}(\mathrm{SO}(d-2))}\sum_{\epsilon_1,\epsilon_2} T^a_{123}(\epsilon_1,\epsilon_2,\epsilon_3)T^b_{\tilde{1}\tilde{2}3^{\mathbf{S}}}(\epsilon_1^*,\epsilon_2^*,\epsilon_3)(1)\,. \tag{4.59}$$

The tilde denotes the shadow, and the superscript $\mathbf{S}$ denotes the full shadow where both the scaling dimension and the spin are reflected ($\Delta \mapsto d{-}\Delta$, $J \mapsto 2{-}d{-}J$). Similarly to the Euclidean pairing discussed above, we find that it is nicely diagonal in the even/odd basis:

$$P^{E}_{J_1 J_2[\mathcal{O}_{\mathbf{L}}],L} = (-4)^{J_1+J_2} P_{s,L} N^{E}_{J_1 J_2 \mathcal{O}_{\mathbf{L}}} \times \mathbb{I}\,, \quad P^{O}_{J_1 J_2 \mathcal{O}_{\mathbf{L}},L} = -(-4)^{J_1+J_2} P_{s,L} N^{O}_{J_1 J_2 \mathcal{O}_{\mathbf{L}}} \times \mathbb{I}\,, \tag{4.60}$$

where the factor $N^{E/O}$ is defined in eq. (4.32) and the subscript $\mathbf{L}$ denotes Weyl reflection associated with the light-transform $(\Delta \mapsto 1-J,\ J \mapsto 1-\Delta)$. $P_{s,L}$ is simply the Lorentzian pairing of two scalars and one spinning operator [62]

$$P_{s,L} = \frac{(-1)^d 2^{1-\frac{3d}{2}}}{\mathrm{vol}(\mathrm{SO}(d-2))}\,. \tag{4.61}$$

The normalization $\mathcal{N}^{L}_{(a,b),(c,d)}$ in the Lorentzian inversion formula (4.53) is then given as

$$\mathcal{N}^{L}_{(a,b),(c,d)} = \frac{1}{2^{\Delta+J}(\Delta+J-1)} \widehat{L}_{a,c}(\mathcal{O}_1\mathcal{O}_2[\mathcal{O}_{J,\Delta}]) \widehat{L}_{b,d}(\mathcal{O}_3\mathcal{O}_4[\mathcal{O}_{J,\Delta}])\,, \tag{4.62}$$

where $\widehat{L}$ is a sort of inverse of the light transform with respect to the pairing:

$$\widehat{L}_{a,c}(\mathcal{O}_1\mathcal{O}_2[\mathcal{O}_{J,\Delta}]) L^{d}_{e}(\mathcal{O}_1\mathcal{O}_2[\mathcal{O}_{J,\Delta}]) P^{c,e}_{L}(\mathcal{O}_1\mathcal{O}_2[\mathcal{O}_{1-\Delta,1-J}]) = -i\delta^{d}_{a} P_{s,L}\,. \tag{4.63}$$

For scalars, it is straightforward to verify that the above expression reduces to

$$\mathcal{N}^{L}_{s} = \frac{1}{4}\kappa^{(\Delta_{12},\Delta_{34})}_{\beta}\,, \qquad \kappa^{(\Delta_{12},\Delta_{34})}_{\beta} = \frac{\Gamma(\frac{\beta-\Delta_{12}}{2})\Gamma(\frac{\beta+\Delta_{12}}{2})\Gamma(\frac{\beta-\Delta_{34}}{2})\Gamma(\frac{\beta+\Delta_{34}}{2})}{2\pi^2\Gamma(\beta-1)\Gamma(\beta)}\,. \tag{4.64}$$

More generally, we can write explicitly the normalization factor in the spinning Lorentzian inversion formula (4.53) in the Even/Odd basis:

$$\mathcal{N}^{L}_{(a,b),(c,d)} = \frac{1}{4} \frac{\kappa^{(\Delta_{12},\Delta_{34})}_{\beta}(-4)^{-\sum_{i=1}^{4} J_i}}{N^{E/O}_{J_1 J_2 \mathcal{O}_{\mathbf{L}}} N^{E/O}_{J_3 J_4 \mathcal{O}_{\mathbf{L}}}} \begin{pmatrix} 0 & 1 \\ 1 & 0 \end{pmatrix}_{a,c} \begin{pmatrix} 0 & 1 \\ 1 & 0 \end{pmatrix}_{b,d} \tag{4.65}$$

where a and c must have the same parity, as well as b and d. We set $\Delta_{12} = 0$ if a, b are even and $\Delta_{12} = 1$ if they are both odd, and similarly for Δ_{34}. (If operator 1 or 2 is a scalar, there is only one structure a and we drop the corresponding matrix.)

Performing (4.53) is a bit challenging because generally evaluating the spinning conformal blocks is a hard task. A nice idea, following ref. [148], is to "integrate-by-parts" the spin-up from eq. (4.44) acting on the block to get instead spinning-down operators acting on the correlator:

$$c^t_{a,b}(\Delta, J) = \mathcal{N}^L_{(a,b),(c,d)} \int \frac{dz d\bar{z}}{z^2\bar{z}^2} \left|\frac{z-\bar{z}}{z\bar{z}}\right|^{d-2} \tilde{G}^{(\alpha,\beta)}_{J+d-1,\Delta-d+1}(z,\bar{z}) \mathrm{dDisc}[\mathbb{P}^c_\alpha \mathbb{P}^d_\beta \mathcal{D}^{(\alpha,\beta)}_{\downarrow} G(z,\bar{z})]\,, \tag{4.66}$$

which will effectively reduce us to the scalar Lorentzian inversion formula. Eq. (4.97) below gives a concrete expression in a specific basis of spin-down operators.

4.3 OPE data for spinning Generalized Free Fields

4.3.1 From Euclidean inversion and shadow representation

Using the shadow transform, the OPE data in MFT can be efficiently evaluated by the Euclidean inversion formula [141]. It is especially effective for three-point functions in momentum-space. To use this, it is best to write the Euclidean inversion formula (4.52) in a covariant way

$$c_{a,b}(\Delta, J) = \widehat{\mathcal{N}}(\Delta, J)_{(a,b),(c,d)} \int \frac{d^dx_1 \cdots d^dx_4}{\mathrm{vol}(\mathrm{SO}(d+1),1)} \langle 1234 \rangle (\Psi^{\tilde{\Delta}_i}_{\tilde{\Delta},J})^{c,d}\,, \tag{4.67}$$

where the tildes denote shadow operators. The factor $\widehat{\mathcal{N}}$ is the same as $\mathcal{N}$ in eq. (4.49) but with the factor $S(\tilde{3}\tilde{4}[O])$ dropped (*ie.* replaced by identity). The harmonic function $\Psi^{\Delta_i}_{\Delta,J}$ is a combination of block and shadow, which, importantly, can be written as integral of two three-point functions (this is called the shadow representation):

$$(\Psi^{\Delta_i}_{\Delta,J})^{a,b} = S(34[\tilde{\mathcal{O}}])^b{}_c\, (G^{a,c}_{J,\Delta} + \text{shadow}) \tag{4.68}$$

$$= \int d^dx\, \langle 12\mathcal{O}(x)\rangle^a \langle \tilde{\mathcal{O}}(x)34\rangle^b\,. \tag{4.69}$$

We now consider a Mean Field Theory four-point function:

$$\langle 1234\rangle = \langle 12\rangle\langle 34\rangle + \langle 13\rangle\langle 24\rangle + \langle 14\rangle\langle 23\rangle\,. \tag{4.70}$$

We focus on the t-channel contribution $\langle 23\rangle\langle 14\rangle$ to illustrate the algorithm for computing the OPE data of MFT. The u-channel contributions $\langle 13\rangle\langle 24\rangle$ can be evaluated in the same way, while the s-channel $\langle 12\rangle\langle 34\rangle$ is trivial to evaluate: it contributes to the identity exchange. Considering the term $\langle 23\rangle\langle 14\rangle$, the integrals over x_3, x_4 in (4.67) boil down to the shadow-transform for $\tilde{3}$ and $\tilde{4}$, and the remaining integrals are all removed by the gauge-fixing, leaving a simple pairing [141]:

$$c^{t,\mathrm{MFT}}_{a,b}(\Delta, J) = \mu(\Delta, J)(P^{a,c}_{34\tilde{\mathcal{O}}})^{-1} S([\tilde{1}]\tilde{2}\tilde{\mathcal{O}})^{c}{}_{d} S(1[\tilde{2}]\tilde{\mathcal{O}})^{d}{}_{e} S(12[\tilde{\mathcal{O}}])^{e}{}_{b}\,. \tag{4.71}$$

This formula breaks the calculation of MFT coefficients into simple algebraic operations: three shadows and a pairing.

The pairing and first two shadows were presented earlier in subsection 4.2.3. Before we calculate the third shadow, let us revisit the shadow transform, defined in eq. (4.36). It can be computed algebraically as multiplication in momentum space:

$$\sum_{\epsilon_1'} K_{\tilde{1}\tilde{1}'}(p) T_{1'23}(p)^a = S([\mathcal{O}_1]\mathcal{O}_2\mathcal{O}_3)^a{}_b T_{\tilde{1}23}(p)^b\,, \tag{4.72}$$

where $K_{11'}$ is the Fourier transform of the two-point function of $\mathcal{O}_1$ [172]:

$$K_{11'}(p) = \sum_{k=0}^{J} \mathcal{K}_k(\Delta, J)(\epsilon_1\cdot p)^k (p\cdot\epsilon_1')^k (\epsilon_1\cdot\epsilon_1')^{J-k} |p|^{2\Delta-d-2k}\,,$$

$$\mathcal{K}_k(\Delta, J) = \frac{\pi^{d/2}\Gamma(J+1)2^{d-2\Delta+k}\Gamma\left(\frac{d}{2}+k-\Delta\right)\Gamma(J-k+\Delta-1)}{\Gamma(\Delta-1)\Gamma(k+1)\Gamma(J+\Delta)\Gamma(J-k+1)}\,. \tag{4.73}$$

Applying this map to the helicity structures normalized as in eq. (4.10), we find the simple result

$$K_{11'}(p)T^{\pm,\pm}_{\tilde{1}'2\mathcal{O}}(p) = \frac{\pi^{\frac{3}{2}}\Gamma(\frac{3}{2}-\Delta_1)}{(\Delta_1+J_1-1)\Gamma(\Delta_1-1)} \times T^{\pm,\pm}_{12\mathcal{O}}(p)\,, \tag{4.74}$$

which reproduces as $\Delta_1 \to J_1+1$ the formula for conserved current in eq. (4.38).

The third shadow transform is technically more difficult to evaluate since we defined our structures in a frame where $x_3=\infty$. The trick is to use the rule eq. (4.5) to interchange x_1 and x_3 in position space, then Fourier transform back to the momentum space, where we can apply eq. (4.72). These steps are somewhat lengthy (we found the Fourier transform (B.19) helpful), but thankfully the last step turns out to simply multiply each structure by an overall factor. This had to be the case since the shadow transform commutes with h_1 and h_2. Trying a few cases we observe a simple pattern:

$$S(12[\mathcal{O}])^{h_1,h_2}{}_{h_1',h_2'} = \delta^{h_1}_{h_1'}\delta^{h_2}_{h_2'}\,\frac{4^{2\Delta-3}\pi^{\frac{3}{2}}\Gamma(2+J-\Delta)\Gamma(\Delta-\frac{3}{2})}{\Gamma(\Delta-1)\Gamma(\Delta+J)} \times \frac{(2-\Delta)_{|h_1+h_2|}}{(\Delta-1)_{|h_1+h_2|}}\,. \tag{4.75}$$

Combining the shadows (4.74) and (4.75) with the pairing (4.35) thus gives MFT coefficients (4.71):

$$\begin{aligned} c^{t,\mathrm{MFT}}_{h_1,h_2,\bar{h}_3,\bar{h}_4}(\Delta,J) = \delta^{h_4}_{h_1}\delta^{h_3}_{h_2}\; 2^{5-4\Delta}\pi\frac{\Gamma(\Delta-1)}{\Gamma(\Delta-\frac{3}{2})}\frac{\Gamma(\Delta+J)}{\Gamma(J-\Delta+2)}\frac{\Gamma(J+\frac{3}{2})}{\Gamma(J+1)}\mathcal{C}_{J_1}\mathcal{C}_{J_2} \\ \times\frac{(-J)_{|h_1-h_2|}}{(J+1)_{|h_1-h_2|}}\frac{(\Delta-1)_{|h_1+h_2|}}{(2-\Delta)_{|h_1+h_2|}}\,, \end{aligned} \tag{4.76}$$

where the constant $\mathcal{C}_J$ is defined in eq. (4.38). The u-channel identity (if operators 1 and 3 are identical) gives the same result times $(-1)^J$ and with h_3 and h_4 swapped.

Eq. (4.76) can be used in the harmonic decomposition (4.45). Where are the poles and corresponding OPE data? To read off the local OPE data, we have to keep in mind that tensor structures in the helicity basis have poles at double-twist locations. To find OPE data from residues, it is best to convert to the Even/Odd basis defined in eq. (4.14), in which the position-space structures do not have poles. Performing the rotation, we get extra gamma-functions which nicely combine to give scalar MFT coefficients, times the same matrix in the even and odd cases:

$$c^{t,\mathrm{MFT,E/O}}(\Delta,J)=c^{\mathrm{E/O}}(\Delta,J)^{s}\begin{pmatrix}\frac{(-J)_{J_1+J_2}(\Delta-1)_{|J_1-J_2|}}{(J+1)_{J_1+J_2}(2-\Delta)_{|J_1-J_2|}} & 0\\ 0 & \frac{(-J)_{|J_1-J_2|}(\Delta-1)_{J_1+J_2}}{(J+1)_{|J_1-J_2|}(2-\Delta)_{J_1+J_2}}\end{pmatrix}\mathcal{C}_{J_1}\mathcal{C}_{J_2}\,, \tag{4.77}$$

where we normalized it by the OPE data for scalars of twist 1 or 2 in the even and odd cases, more precisely:

$$c^{\mathrm{E}}(\Delta,J)^{s}=c(1,1;\Delta,J)^{s}\,,\quad c^{\mathrm{O}}_{J}(\Delta)^{s}=\tfrac{1}{2}c(1,2;\Delta,J)^{s}\,. \tag{4.78}$$

The scalar MFT data $c(\Delta_1,\Delta_2;\Delta,J)^s$ can be found from earlier literature [53] and is recorded in eq. (B.31) (with $p=\Delta_1+\Delta_2,\ a=b=\frac{\Delta_2-\Delta_1}{2}$).

For future reference, let us summarize all the ingredients in the Even/Odd basis. The products of "easy" shadows, $S([\tilde{1}]\tilde{2}\tilde{\mathcal{O}})S(1[\tilde{2}]\tilde{\mathcal{O}})$, are given as

$$\mathbb{S}^{E}=\mathbb{S}^{E}_{s}N^{E}_{J_1J_2\tilde{\mathcal{O}}}(-4)^{J_1+J_2}\times\mathcal{C}_{J_1}\mathcal{C}_{J_2}\mathbb{I}\,,\quad \mathbb{S}^{O}=\tfrac{1}{2}\mathbb{S}^{O}_{s}N'_{J_1J_2\tilde{\mathcal{O}}}(-4)^{J_1+J_2+1}\times\mathcal{C}_{J_1}\mathcal{C}_{J_2}\mathbb{I}\,, \tag{4.79}$$

where $\mathbb{S}^{E/O}_{s}$ are just the scalar factor for $(\Delta_1,\Delta_2)=(1,1)$ and $(1,2)$ respectively [62]

$$\mathbb{S}^{E}=\frac{4\pi^4}{(1-\beta)(\tau-2)}\,,\quad \mathbb{S}^{O}=-2\pi^4\,. \tag{4.80}$$

The third shadow (4.75) yields

$$S^{E/O}(12[\mathcal{O}])=S_s(12[\mathcal{O}])\begin{pmatrix}\frac{(2-\Delta)_{|J_1-J_2|}}{(\Delta-1)_{|J_1-J_2|}} & 0\\ 0 & \frac{(2-\Delta)_{J_1+J_2}}{(\Delta-1)_{J_1+J_2}}\end{pmatrix}, \tag{4.81}$$

with the same matrix for both even and odd, and where S_s is just the shadow coefficients of scalars [173, 141]

$$S_s(12[\mathcal{O}]) = \frac{\pi^{d/2}\Gamma(\Delta-\frac{d}{2})\Gamma(J+\Delta-1)\Gamma\left(\frac{1}{2}(J+\tilde{\Delta}+\Delta_{12})\right)\Gamma\left(\frac{1}{2}(J+\tilde{\Delta}-\Delta_{12}\right)}{\Gamma(\Delta-1)\Gamma\left(\frac{1}{2}(J+\Delta+\Delta_{12})\right)\Gamma\left(\frac{1}{2}(J+\Delta-\Delta_{12})\right)\Gamma(J+\tilde{\Delta})} \tag{4.82}$$

with $\Delta_{12} = 0$ for parity-even and $\Delta_{12} = 1$ for parity-odd cases. Finally, the pairing (4.35):

$$P^{E/O}_{12\mathcal{O}} = \delta^{h_1'}_{h_1}\delta^{h_2'}_{h_2} \times P_s \times N^{E/O}_{12\mathcal{O}} 4^{|h_1|+|h_2|}(-1)^{|h_1-h_2|}\frac{(J_3+1)_{|h_1-h_2|}}{(-J_3)_{|h_1-h_2|}}\,. \tag{4.83}$$

Multiplying these ingredients again according to (4.71) gives eq. (4.77).

4.3.2 OPE data and remarks on the leading trajectory

Let us now describe the OPE data which stems from eq. (4.77). When computing the integral (4.45) as a sum of poles, one finds two sorts of terms: double-twist poles at $\Delta - J = 2 + 2n$ from the gamma-function in eq. (4.77), and spurious poles from the block, at $\Delta - J = 3, 4, \ldots$. The position of the latter is set by their kinematical origin as zero-norm descendants ("null states") of the exchanged primary.

We are in the unfortunate situation that the physical and spurious poles overlap. In principle, we should subtract the spurious poles using the results from ref. [169] for the poles of spinning 3d blocks. We pursue a simpler, heuristic method, to be justified in the next subsection. For scalar mean-field-theory with $\Delta_1 = \Delta_2 = 1$, the poles are simpler and have been discussed in ref. [43]. Using eq. (3.9) there, we find that the spurious poles effectively *double* the OPE coefficient. On the other hand, the leading trajectory $n = 0$ has no corresponding spurious pole and so does not double.

Such a relative factor $\frac{1}{2}$ was also found in the spinning case [141], and so our tentative guess is that the same happens in our basis and the spurious poles just double the non-leading trajectories, that is:

$$\begin{aligned}\lambda^E_{12\mathcal{O}}\lambda^E_{43\mathcal{O}}\big|_{n,J} &= -2\operatorname*{Res}_{\Delta=2+2n+J} c^{E,\mathrm{MFT}}(\Delta,J)\\ &= \frac{2\mathcal{C}_{J_1}\mathcal{C}_{J_2}}{2^{4n+2J}}\frac{(J+1)_{\frac12}(2n+J+\frac12)_{\frac12}}{(n+\frac12)_{\frac12}(n+J+1)_{\frac12}}M(2+2n+J,J) \quad (n=1,2,3,\ldots),\end{aligned} \tag{4.84a}$$

$$\begin{aligned}\lambda^O_{12\mathcal{O}}\lambda^O_{43\mathcal{O}}\big|_{n,J} &= -2\operatorname*{Res}_{\Delta=2+2n+J} c^{O,\mathrm{MFT}}(\Delta,J)\\ &= \frac{2\mathcal{C}_{J_1}\mathcal{C}_{J_2}}{2^{4n+2J}}\frac{(J+1)_{\frac12}(2n+J+\frac12)_{\frac12}}{(n+1)_{-\frac12}(n+J+\frac32)_{-\frac12}}M(2+2n+J,J) \quad \left(n=\tfrac12,\tfrac32,\tfrac52,\ldots\right),\end{aligned} \tag{4.84b}$$

where $M(\Delta,J)$ is the 2×2 matrix

$$M(\Delta,J) = \begin{pmatrix} \frac{(-J)_{J_1+J_2}(\Delta-1)_{|J_1-J_2|}}{(J+1)_{J_1+J_2}(2-\Delta)_{|J_1-J_2|}} & 0 \\ 0 & \frac{(-J)_{|J_1-J_2|}(\Delta-1)_{J_1+J_2}}{(J+1)_{|J_1-J_2|}(2-\Delta)_{J_1+J_2}} \end{pmatrix}. \tag{4.85}$$

Some comments are in order. We recall that the first structure (opposite-helicity) exists only for $J\geq J_1+J_2$. This is reflected in an overall zero from $(-J)_{J_1+J_2}$ in the first entry. Even below this range, the denominator always have fewer zeros than the numerator, so the vanishing is never ambiguous. The range of the J-sums is built-in!

The second structure (same-helicity) is more subtle. It generically exists only for $J\geq |J_1-J_2|$. But since $2-\Delta=-2n-J$, it may look like the second entry of the matrix M diverges for the lowest few trajectories. However, inspection of the structures $T^E_{12\mathcal{O}}$ reveals that these have corresponding zero for precisely those cases (a special case is visible in eq. (4.18) with $n=\frac12$, $J=1$). The conformal blocks thus have a double zero, which shields the singularity from the denominator. This means that mean-field-theory doesn't have operators at these places. For $n=0$, we will find below that there is a single leading trajectory.

The set of operators appearing in MFT can thus be characterized as:

- Opposite-helicity: One operator for each $n\geq 0$ and $J\geq J_1+J_2$

- Same-helicity: One operator for each $n \geq 1$ and $J \geq \max(|J_1 - J_2|, J_1 + J_2 - n)$

This spectrum is depicted in fig. 4.3. (The helicity of the $n = 0$ double-twists is really undefined.)

Let us discuss more the leading trajectory, $n = 0$. Since there are no spurious poles, one might think that we should take half the above formula. This is correct but misleading. The reason is that when $n = 0$ the same- and opposite- helicity structures become degenerate, as visible from eq. (4.16). Helicity is simply not defined for $n = 0$. One can verify that this happens whenever $\mathcal{O}_1, \mathcal{O}_2$ are spinning operators, of any spin. The resolution is to rotate to a new basis near $n = 0$:

$$\begin{pmatrix} T_{123}^{E,\text{reg}} \\ T_{123}^{E,\text{sing}} \end{pmatrix} = \begin{pmatrix} 1 & 0 \\ -\frac{(-J)_{J_1+J_2}(J+1)_{|J_1-J_2|}}{(J+1)_{J_1+J_2}(-J)_{|J_1-J_2|}}\frac{1}{n} & \frac{1}{n} \end{pmatrix} \begin{pmatrix} T_{123}^{E,\text{opp}} \\ T_{123}^{E,\text{same}} \end{pmatrix}. \tag{4.86}$$

As the two structures degenerate, both combinations are smooth around $n = 0$. Since the second structure $T_{123}^{E,\text{sing}}$ has a non-vanishing double-discontinuity (in fact it has poles $1/x_{12}^2$), its coefficient is guaranteed to vanish in MFT. The fact that the two structures become T^{reg} effectively doubles the *real* $n = 0$ coefficient. In the rotated basis $(T_{123}^{E,\text{reg}}, T_{123}^{E,\text{sing}})$, the leading-trajectory data is thus given by

$$\lambda_{12\mathcal{O}}^{E,\text{rotated}} \lambda_{43\mathcal{O}}^{E,\text{rotated}}\Big|_{0,J} = \frac{2\Gamma(J+1)^2}{\Gamma(2J+1)} \times \mathcal{C}_{J_1}\mathcal{C}_{J_2} \frac{(-J)_{J_1+J_2}(J+1)_{|J_1-J_2|}}{(J+1)_{J_1+J_2}(-J)_{|J_1-J_2|}} \begin{pmatrix} 1 & 0 \\ 0 & 0 \end{pmatrix}. \tag{4.87}$$

The above fully describes the OPE decomposition of t-channel exchange. To be fully explicit, let us write out the s-channel OPE decomposition of the full MFT correlator including identity in all three-channels, without any matrix, and including

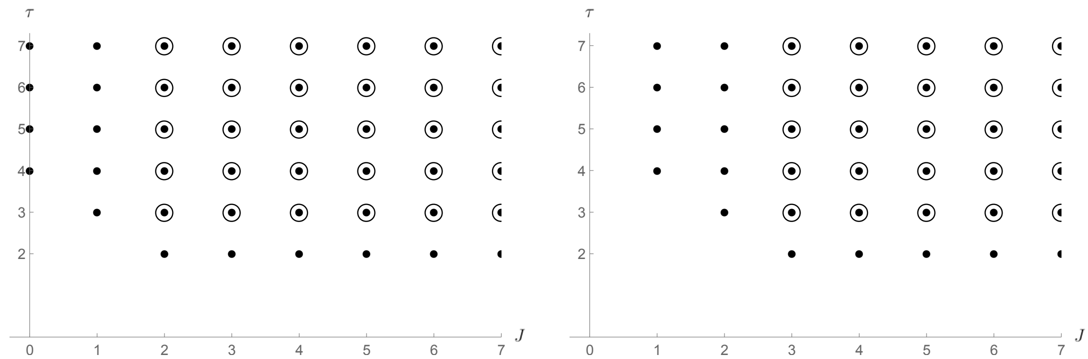

(a) two currents ($J_1 = J_2 = 1$) (b) one current and one stress tensor

Figure 4.3: Spectrum of double-twist operators of the form $[JJ]_{n,J}$ and $[JT]_{n,J}$. Double circles indicate multiplicity: there is a single trajectory for $n = 0$ and two for each $n \geq 1$.

color indices in the case we have several currents:

$$\begin{aligned}
\mathcal{G}^{abcd,\mathrm{MFT}} = \quad & \delta^{ab}\delta^{cd} + \\
& + \sum_{n\geq 0}\sum_{J\geq J_1+J_2} \lambda_{12\mathcal{O}}^{E,\mathrm{same}}\lambda_{43\mathcal{O}}^{E,\mathrm{same}}\Big|_{n,J}\left(\delta^{bc}\delta^{ad} + (-1)^J\delta^{ac}\delta^{bd}\right)\; G_{\Delta,J}^{E,\mathrm{same},\ E,\mathrm{same}} \\
& + \sum_{n\geq 1}\sum_{J\geq J_0(n)} \lambda_{12\mathcal{O}}^{E,\mathrm{opp}}\lambda_{43\mathcal{O}}^{E,\mathrm{opp}}\Big|_{n,J}\left(\delta^{bc}\delta^{ad} + (-1)^J\delta^{ac}\delta^{bd}\right)\; G_{\Delta,J}^{E,\mathrm{opp},\ E,\mathrm{opp}} \\
& + \sum_{n\geq \frac{1}{2}}\sum_{J\geq J_1+J_2} \lambda_{12\mathcal{O}}^{O,\mathrm{same}}\lambda_{43\mathcal{O}}^{O,\mathrm{same}}\Big|_{n,J}\left(\delta^{bc}\delta^{ad} + (-1)^J\delta^{ac}\delta^{bd}\right)\; G_{\Delta,J}^{O,\mathrm{same},\ O,\mathrm{same}} \\
& + \sum_{n\geq \frac{1}{2}}\sum_{J\geq J_0(n)} \lambda_{12\mathcal{O}}^{O,\mathrm{opp}}\lambda_{43\mathcal{O}}^{O,\mathrm{opp}}\Big|_{n,J}\left(\delta^{bc}\delta^{ad} - (-1)^J\delta^{ac}\delta^{bd}\right)\; G_{\Delta,J}^{O,\mathrm{opp},\ O,\mathrm{opp}}, \qquad (4.88)
\end{aligned}$$

where $J_0(n) = \max(|J_1 - J_2|, J_1 + J_2 - n)$ and the λ's refer to elements of (4.84a). The last two sums run over half-integer n.

Typically, one would further decompose the global symmetry indices into s-channel irreps, and symmetrical versus antisymmetrical combinations. The t and u channels contributions then effectively remove half the spins (the double-twist operators with the wrong symmetry), and otherwise effectively double the coefficient.

Let us cross-check the above MFT spectrum. MFT operators can be written as products of two operators and their derivatives: $\partial^\#\mathcal{O}_1\partial^\#\mathcal{O}_2$; the game is to enumerate linear combinations that are primaries. An equivalent exercise is to enumerate three-point structures of the form eq. (4.10) whose Fourier transform are polynomials in x. Although finding such explicit polynomials is somewhat cumbersome, it is straightforward to count them by making a generating function. We now summarize this exercise.

We make a generating function where a power $q^{\Delta}z^{J}$ represents an SO(3) multiplet of dimension Δ and spin J (that is, $2J+1$ states). Starting from a scalar operator ϕ of dimension Δ, we could characterize its descendants in terms of symmetric-traceless tensors, times Laplacian: $(\partial^{\mu_1}\cdots\partial^{\mu_J} - \text{traces})(\partial^2)^n\phi$, which contributes a term $q^{\Delta+2n+J}z^J$. Summing over n and J gives a generating function $\frac{q^\Delta}{(1-q^2)(1-zq)}$ which enumerates descendants of a scalar. Omitting steps, we find similar generating functions for the descendants of conserved currents and generic primaries:

$$Z_J^{\text{conserved}} = \frac{q^{J+1}z^J}{(1-q)(1-qz)}\,, \quad Z_{\Delta,J}^{\text{generic}} = q^\Delta \frac{z^J + q(1+z)\frac{q^J-z^J}{q-z}}{(1-q^2)(1-qz)}\,. \tag{4.89}$$

For conserved currents, the dimension-one generator responsible for $\frac{1}{1-q}$ is simply the curl $\vec{\nabla}\times\bullet$, that is, the numerator of eq. (4.25). To find the primaries that enter the OPE product of two conserved currents, we have to match the generating functions:

$$Z_{J_1}^{\text{conserved}} \times Z_{J_2}^{\text{conserved}} = \sum_{n,J} c_{n,J} Z_{2+n+J,J}^{\text{generic}} \tag{4.90}$$

where the c's are multiplicities of the various representations appearing. Putting in the multiplicities from fig. 4.3 and comparing the series for various values of J_1, J_2, we find perfect agreement.

4.3.3 From Lorentzian inversion formula

Beyond MFT, the Euclidean inversion formula is less efficient as double-twist operators contaminate the cross-channel OPE. We should thus seek another way to extract the relevant OPE data: using the Lorentzian inversion formula. As a warm-up, we demonstrate that we can reproduce the above OPE data from the Lorentzian inversion formula, using spinning-down technology. As we will explain, within this framework it is straightforward to disentangle physical and spurious poles, so this calculation will also confirm the decomposition (4.88). In this subsection, we restrict attention to parity-even four currents ("VVVV") as a concrete example.

In $d = 3$, all bosonic conformal blocks can be written as spin-ups of scalar conformal blocks. In embedding space, a convenient set of spinning-up differential operators is [147]

$$D_{ii}^{ij} = Z_i^A \left((X_i \cdot X_j) \frac{\partial}{\partial X_j^A} + (X_i \cdot Z_j) \frac{\partial}{\partial Z_j^A} - X_j^A (X_i \cdot \frac{\partial}{\partial X_j}) - Z_j^A (X_i \cdot \frac{\partial}{\partial Z_j}) \right) ,$$

$$\begin{aligned} D_{ij}^{ij} &= Z_i^A \left((X_i \cdot X_j) \frac{\partial}{\partial X_i^A} + X_j^A (Z_i \cdot \frac{\partial}{\partial Z_i}) - X_j^A (X_i \cdot \frac{\partial}{\partial X_i}) \right) , \\ D_{iO}^{ij} &= \epsilon_{ABCDE}\ Z_i^A X_i^B \frac{\partial}{\partial X_{iC}} \left(X_j^D \frac{\partial}{\partial X_{jE}} + Z_j^D \frac{\partial}{\partial Z_{jE}} \right) . \end{aligned} \tag{4.91}$$

D_{ii}^{ij} increases the spin and decreases the conformal dimension of ith operator by one unit simultaneously. On the other hand, D_{ij}^{ij} increases the spin of ith operator by one unit and decreases the conformal dimension of jth operator by one unit simultaneously, while the odd operator D_{iO} only changes the first spin but not the dimensions. Using these operators, (for example) our two parity-even three-point structures $\langle V_1 V_2 O \rangle$ can be constructed by acting on scalar three-point functions $\langle \mathcal{O}_1 \mathcal{O}_2 \mathcal{O} \rangle$ with five spin-up operators

$$\langle V_1 V_2 O \rangle^a = \mathbb{P}^a_{(\alpha)} \mathcal{D}_\uparrow^{(\alpha)} \langle \mathcal{O}_1 \mathcal{O}_2 \mathcal{O} \rangle^{(\alpha)} , \quad \mathcal{D}_\uparrow^{(\alpha)} = \left(D_{11}^{12} D_{22}^{21}, H_{12}, D_{12}^{12} D_{22}^{21}, D_{21}^{21} D_{11}^{12}, D_{12}^{12} D_{21}^{21} \right) , \tag{4.92}$$

where H_{12} is

$$H_{12} = 2\big((X_1 \cdot Z_2)(Z_1 \cdot X_2) - (X_1 \cdot X_2)(Z_1 \cdot Z_2) \big) . \tag{4.93}$$

As mentioned previously, it is important to note that the operators act on different three-point functions (α) as the dimensions Δ_1 and Δ_2 are shifted differently for different operators. For example, the first and the third structures are actually

$(D_{11}^{12}D_{22}^{21}, D_{12}^{12}D_{21}^{21})\langle\mathcal{O}_{\Delta_1+1}\mathcal{O}_{\Delta_2+1}\mathcal{O}_{\Delta,J}\rangle$, and the fourth structure is $D_{12}^{12}D_{22}^{21}\langle\mathcal{O}_{\Delta_1}\mathcal{O}_{\Delta_2+2}\mathcal{O}_{\Delta,J}\rangle$. Each of these can be written as a combination of the five basis monomials in eq. (4.4) and ultimately we are interested only in the linear combinations which produce the two conserved structures in our basis (4.16). We find that these combinations, when acting on the "funny block" $\tilde{G}^{(c,d)}_{J+d-1,\Delta-d+1}$, *with external shadow operators* are:

$$\mathbb{P}^a_\alpha = \begin{pmatrix} -\frac{\sqrt{2}(\beta+1)(4-\tau)}{(\Delta-3)(\Delta-2)} & \frac{(\beta+1)(\Delta-1)(4-\tau)}{\sqrt{2}(\Delta-3)} & \frac{\sqrt{2}(J+3)(\beta+1)(4-\tau)}{(J+1)(\Delta-3)(\Delta-2)} & \frac{\sqrt{2}(J+3)(\beta+1)(4-\tau)}{(J+1)(\Delta-3)(\Delta-2)} & \frac{\sqrt{2}(\Delta\tilde{\Delta}(J+5)-(J+1)^2(J+4))}{(J+1)(\Delta-3)(\Delta-2)} \\ \frac{\sqrt{2}(\beta+1)(4-\tau)}{(J+1)(J+2)} & -\frac{J(\beta+1)(4-\tau)}{\sqrt{2}(J+2)} & \frac{\sqrt{2}(\beta+1)(4-\tau)}{(J+1)(J+2)} & \frac{\sqrt{2}(\beta+1)(4-\tau)}{(J+1)(J+2)} & \frac{\sqrt{2}\big(\Delta\tilde{\Delta}-J(J+1)\big)}{(J+1)(J+2)} \end{pmatrix}, \tag{4.94}$$

where $\beta = \Delta + J$ and $\tau = \Delta - J$. (The coefficients are different if we want to get the currents instead of their shadows.)

After integrating by parts, the spinning-up operators $\mathcal{D}_\uparrow^{(\alpha)}$ become spinning-down operators, in our case $\mathcal{D}_\downarrow^{(\alpha)} = \left(\bar{D}_{22}^{21}\bar{D}_{11}^{12}, \bar{D}_{H_{12}}, \bar{D}_{22}^{21}\bar{D}_{12}^{12}, \bar{D}_{11}^{12}\bar{D}_{21}^{21}, \bar{D}_{21}^{21}\bar{D}_{12}^{12}\right)$. The spinning-down operators can be constructed from weight-shifting operators in [148], and we find convenient to define them so they are adjoints to the above. This is readily done using the operator $\mathcal{D}_Z$ from eq. (4.8)[6]:

$$\begin{aligned}
\bar{D}_{ii}^{ij} &= -\mathcal{D}_{Z_i}^A\left((X_i\cdot X_j)\frac{\partial}{\partial X_j^A} + (X_i\cdot Z_j)\frac{\partial}{\partial Z_j^A} - X_j^A(X_i\cdot\frac{\partial}{\partial X_j}) - Z_j^A(X_i\cdot\frac{\partial}{\partial Z_j})\right)\,, \\
\bar{D}_{ij}^{ij} &= -\mathcal{D}_{Z_i}^A\left((X_i\cdot X_j)\frac{\partial}{\partial X_i^A} - X_{jA}\left(d-1+(X_i\cdot\frac{\partial}{\partial X_i}) + (Z_i\cdot\frac{\partial}{\partial Z_i})\right)\right)\,, \\
\bar{D}_{H_{ij}} &= 2\big((X_i\cdot\mathcal{D}_{Z_j})(\mathcal{D}_{Z_i}\cdot X_j) - (X_i\cdot X_j)(\mathcal{D}_{Z_i}\cdot\mathcal{D}_{Z_j})\big)\,, \\
\bar{D}_{iO}^{ij} &= -\epsilon_{ABCDE}\,\mathcal{D}_{Z_i}^A X_i^B\frac{\partial}{\partial X_{iC}}\left(X_j^D\frac{\partial}{\partial X_{jE}} + Z_j^D\frac{\partial}{\partial Z_{jE}}\right)\,.
\end{aligned} \tag{4.95}$$

These are adjoint to the D's up to a spin-dependent factor which can be traced to eq. (4.29), namely:

$$\left(D_{11}^{12}T_{J_1J_2\ldots}, T_{J_1+1,J_2\ldots}\right) = \frac{1}{(J_1+\frac{d-2}{2})(J_1+1)}\left(T_{J_1J_2\ldots}, \bar{D}_{11}^{12}T_{J_1+1,J_2\ldots}\right)\,. \tag{4.96}$$

[6]While $\mathcal{D}_Z$ now acts on an embedding-space 5-vector Z, the dimension-dependent factor $\frac{d-2}{2}$ remains the *same* as in eq. (4.8). See ref. [47].

This identity makes it trivial to integrate-by-parts.[7] For $\bar{D}_{H_{ij}}$ there is an extra $\frac{1}{(J_2+\frac{d-2}{2})(J_2+1)}$ since both spins change. Boundary terms cannot arise in the above pairing, because the integration variables are ultimately all gauge-fixed to a point.

Interestingly, we find that $\bar{D}_{ij}^{ij}$ vanishes identically on conserved currents, so the last three spin-down operators in our list vanish identically, reducing us to a two-dimensional basis. It would be interesting to understand these simplifications from the perspective of the bispinor formalism for $\mathrm{AdS}_4/\mathrm{CFT}_3$ [174].

To find the spinned-down Lorentzian inversion formula, we now have two options. The first, as described so far, is to insert the matrix in eq. (4.94) inside eq. (4.65) and integrate-by-parts. Since the last three spin-down operators vanish, we can write eq. (4.66) in terms of two-by-two matrices. Generally, we have[8]

$$c^t_{a,b}(\Delta, J) = \sum_{\alpha,\beta} \frac{\kappa^{(\alpha,\beta)}_{\Delta+J}}{4} \int \frac{dz d\bar{z}}{z^2 \bar{z}^2} \left| \frac{z-\bar{z}}{z\bar{z}} \right|^{d-2} \tilde{G}^{(\alpha,\beta)}_{J+d-1,\Delta-d+1}(z,\bar{z}) \mathrm{dDisc}[\widehat{\mathbb{P}}_{a,\alpha} \widehat{\mathbb{P}}_{b,\beta} \mathcal{D}^{(\alpha,\beta)}_{\downarrow} G(z,\bar{z})] \,, \tag{4.97}$$

where, from eq. (4.65),

$$\widehat{\mathbb{P}}_{a,\alpha} = \frac{(-4)^{J_1+J_2}}{J_1! J_2! (\frac{1}{2})_{J_1} (\frac{1}{2})_{J_2}} \frac{1}{N^{E/O}_{J_1 J_2 \mathcal{O}_{\mathbf{L}}}} \begin{pmatrix} 0 & 1 \\ 1 & 0 \end{pmatrix}_{ac} \mathbb{P}^c_{\alpha} \,. \tag{4.98}$$

Explicitly, for $J_1 = J_2 = 1$, the parity-even matrix evaluates to:

$$\widehat{\mathbb{P}}^E_{a,\alpha} = \frac{2\sqrt{2}}{(\beta-1)(\tau-2)} \times \begin{pmatrix} \frac{-2}{(J+1)(J+2)} & \frac{J}{(J+2)} \\ \frac{2}{(\Delta-3)(\Delta-2)} & -\frac{(\Delta-1)}{(\Delta-3)} \end{pmatrix} \,, \tag{4.99}$$

where only $\Delta_{12} = 0$ appears in κ and the block. For odd structures, in the spin-down

[7]For the odd operators, we only verified that D_{iO} is the adjoint of $\bar{D}_{iO}$ when acting on scalar operators, sufficient for our purposes.

[8]There are no possible boundary terms because the potential limits $z, \bar{z} = 0, 1$ are not really "boundaries". The limit $z \to 0$ is regulated, on the Euclidean and Regge sheets, by the fact that Δ is continuous and $J > J_*$, respectively. Furthermore, as discussed in [43], the integral over dDisc near $z \to 1$ is defined most precisely as a boundary-free "keyhole" type contour integral.

basis $\mathcal{D}^{O}_{\downarrow} = (\bar{D}^{12}_{1O}\bar{D}^{21}_{22}, \bar{D}^{21}_{2O}\bar{D}^{12}_{11})$,

$$\widehat{\mathbb{P}}^{O}_{a,\alpha} = \frac{-\sqrt{2}}{(J+1)(\Delta-2)} \times \begin{pmatrix} \frac{1}{(J+2)(\Delta-1)} & \frac{-1}{(J+2)(\Delta-1)} \\ \frac{1}{J(\Delta-3)} & \frac{1}{J(\Delta-3)} \end{pmatrix} . \tag{4.100}$$

These matrices tell us how to convert the scalar inversion of the spinned-down correlators (given below in eq. (4.102)) to OPE data in opposite/same-helicity structures.

There is a simple check: acting with the spin-down operators $\widehat{\mathbb{P}}_{a,\alpha}\mathcal{D}^{\alpha}_{\downarrow}$ on the three-point spinning structure $T^{b}_{11\mathcal{O}}$, we must get δ^{b}_{a} times a canonically normalized scalar three-point structure $T_{00\mathcal{O}}$. In fact this gives a second method to directly find the matrix $\widehat{\mathbb{P}}_{a,\alpha}$, by-passing the spinning Lorentzian inversion formula. We find precise agreement between the two methods. (The second one being admittedly more straightforward.)

These operators can be applied to any correlator. We now consider t-channel identity exchange:

$$G = \frac{H_{23}H_{14}}{(-2X_2\cdot X_3)^{\Delta_2+1}(-2X_1\cdot X_4)^{\Delta_1+1}} , \tag{4.101}$$

which gives for example the even spinned-down correlator $\mathcal{D}_{\downarrow}G$

$$\begin{aligned}
\mathcal{D}^{(1,1)}_{\downarrow}G &= -\frac{3}{2}y(\bar{y}+1)(24y^4+3y^3(5-4\bar{y})+3y^2(\bar{y}(4\bar{y}+3)+1)-y(\bar{y}+1)(3\bar{y}(4\bar{y}+3)+1)\\
&\quad +3(\bar{y}+1)^2(\bar{y}(8\bar{y}+7)+1)) ,\\
\mathcal{D}^{(2,2)}_{\downarrow}G &= -y(\bar{y}+1)\left(y^2-y(\bar{y}+1)+(\bar{y}+1)^2\right) ,\\
\mathcal{D}^{(1,2)}_{\downarrow}G &= \mathcal{D}^{(2,1)}_{\downarrow}G = -\frac{1}{2}y(\bar{y}+1)\left(9y^3+y^2(1-5\bar{y})+y(\bar{y}+1)(5\bar{y}+1)-3(\bar{y}+1)^2(3\bar{y}+1)\right) ,
\end{aligned} \tag{4.102}$$

where we reparameterized the cross-ratios by ($z=\frac{y}{1+y}, \bar{z}=\frac{1}{1+\bar{y}}$).

Inserting in eq. (4.99) it remains to do the scalar inversion integrals of eqs. (4.102). A good strategy is to expand in $y\to 0$ to work out the integral over z twist-by-twist. This also requires the lightcone expansion $z\to 0$ for $\tilde{G}_{J+d-1,\Delta-d+1}(z,\bar{z})$ in the inversion formula (4.66), which can be done by noting (see, eq. (A.24) in [43])

$$\frac{\kappa(\beta)}{\kappa(\beta+2p)}(1-z)^{a+b}(1-\frac{z}{\bar{z}})^{d-2}G_{J+d-1,\Delta-d+1}\big|_{q,p} \sim B_{q,p}\, z^{\frac{J-\Delta}{2}+n+d-1}k_{\beta+2m}(\bar{z})\,, \tag{4.103}$$

where $B_{q,p}$ can be recursively solved by the quadratic Casimir equation [43]. Moreover, we can take use of the following integral formula to do the integral over $\bar{z}$ [43]

$$I_{\hat{\tau}}(\beta) = \int_0^1 \frac{d\bar{z}}{\bar{z}^2}(1-\bar{z})^{a+b}\kappa_\beta^{a,b}k_\beta^{a,b}(\bar{z})\,\mathrm{dDisc}[(\frac{1-\bar{z}}{\bar{z}})^{\frac{\hat{\tau}}{2}-b}(\bar{z})^{-b}]$$

$$= \frac{\Gamma(\frac{\beta}{2}-a)\Gamma(\frac{\beta}{2}+b)\Gamma(\frac{\beta}{2}-\frac{\hat{\tau}}{2})}{\Gamma(-\frac{\hat{\tau}}{2}-a)\Gamma(-\frac{\hat{\tau}}{2}+b)\Gamma(\beta-1)\Gamma(\frac{\beta}{2}+\frac{\hat{\tau}}{2}+1)}\,. \tag{4.104}$$

With this strategy we can calculate the result analytically for any $n>0$, and find a simple common formula given below.

The case $n=0$ is subtle as we discussed previously in subsection 4.3.2: the structures become degenerate. In fact the whole matrix (4.99) blows up as $\tau \to 2$. The solution, as above, is to apply a further rotation to the basis in eq. (4.86). In the $(T_{123}^{E,\mathrm{reg}},\ T_{123}^{E,\mathrm{sing}})$ basis, the matrix (4.99) becomes:

$$\widehat{\mathbb{P}}_{a,\alpha}^{E,\mathrm{rotated}} = \sqrt{2}\begin{pmatrix} -\frac{2J-1}{(J-1)J(J+1)(J+2)(2J+1)} & \frac{J}{(J-1)(J+1)(J+2)(2J+1)} \\ \frac{1}{2(J-1)J(2J+1)} & -\frac{J+1}{4(J-1)(2J+1)} \end{pmatrix}, \tag{4.105}$$

which is now nicely finite. The same rotation will also work in the computation of anomalous dimensions in the next section.

For MFT correlators discussed here where $\mathcal{D}_\downarrow G$ is actually a finite sum of powers of cross-ratios times Gegenbauer polynomials, a more compact and comprehensive trick is available to extract the OPE data, see appendix B.3.2. Our result, for $n \geq 1$, the coefficients of even (opposite/same) helicity structures are then:

$$\lambda^{E}_{12\mathcal{O}}\lambda^{E}_{43\mathcal{O}}\big|_{n,J} = \frac{(J+1)_{\frac{1}{2}}(2n+J+\frac{1}{2})_{\frac{1}{2}}}{2^{4n+2J+3}(n+\frac{1}{2})_{\frac{1}{2}}(n+J+1)_{\frac{1}{2}}}\begin{pmatrix} \frac{J(J-1)}{(J+2)(J+1)} & 0 \\ 0 & \frac{(2n+J+1)(2n+J+2)}{(2n+J)(2n+J-1)} \end{pmatrix}, \tag{4.106}$$

which is precisely eq. (4.84a) with $J_1 = J_2 = 1$. For the leading trajectory, in the rotated basis we find

$$\lambda^{E,\text{rotated}}_{12\mathcal{O}}\lambda^{E,\text{rotated}}_{43\mathcal{O}}\big|_{0,J} = \frac{2\Gamma(J+1)^2}{\Gamma(2J+1)} \times \frac{J(J-1)}{16(J+2)(J+1)}\begin{pmatrix} 1 & 0 \\ 0 & 0 \end{pmatrix}, \tag{4.107}$$

which again agrees with eq. (4.87) with $J_1 = J_2 = 1$. This confirms that spurious poles simply double the $n > 0$ trajectories.

4.4 Application to AdS$_4$/CFT$_3$

The simplicity and diagonal nature of the mean field OPE encourages us to look at the leading corrections. In this section, we study CFT$_3$ current correlators that are dual to bulk YM$_4$ gluon amplitudes at tree-level. The Lorentzian inversion formula will give us the corresponding anomalous dimensions in terms t- and u- channel exchanges of conserved currents.

These correlation functions have been previously discussed in momentum space. Results are remarkably tractable thanks to the fact that YM$_4$ is conformally invariant (at tree-level) and AdS$_4$ is conformally flat [161, 163, 135, 136, 175, 176]. Our goal is to obtain the corresponding OPE anomalous dimension, which we will then compare with the flat space limit in the next section. The flat space limit of AdS/CFT [16, 18, 21] ($R_{\text{AdS}} \to \infty$) has not been much studied for spinning operators (with a notable exception [26]) and we feel it is important to clarify it. Similarly to the scalar case, one may expect (massless) amplitudes to be encoded in the $z \to \bar{z}^{\circlearrowleft}$ "bulk-point" limit [23, 24], or equivalently the large-twist limit of OPE data. This will be confirmed in the next section.

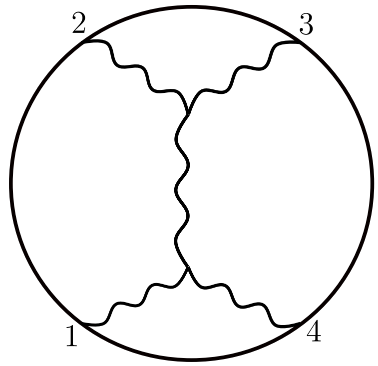

Figure 4.4: Witten diagram for $\langle VVVV\rangle$ with on-shell t-channel gluon exchange. Two even and one odd coupling can be used in each vertex; u-channel is similar with 1 and 2 swapped.

4.4.1 Setup for current correlators

Our strategy is to use spin-up/spin-down operators to reduce the calculation to scalar Lorentzian inversion formulas. The spin-down operators were described and validated in section 4.3.3, acting on identity exchange in the t- and u-channel. The exchanged operator is now a current, as shown in fig. 4.4. (Double-trace exchanges do not contribute to tree-level accuracy, thanks to the double-discontinuity.)

From the CFT perspective, each current exchange involves two parity-even and one odd coupling, described below eq. (4.108), which maps one-to-one with bulk on-shell three-gluon couplings. These can be obtained from a bulk Lagrangian including higher-derivative corrections:

$$\mathcal{L} = -\frac{1}{4g_{\rm YM}^2}F^a_{\mu\nu}F^{\mu\nu a} + \frac{\theta}{32\pi^2}F^a_{\mu\nu}\tilde{F}^{\mu\nu a} - \frac{f^{abc}}{3g_{\rm YM}^3}\left(g_{\rm H}\,F_\mu{}^{\nu a}F_\nu{}^{\rho b}F_\rho{}^{\mu c} + g'_{\rm H}\,\tilde{F}_\mu{}^{\nu a}\tilde{F}_\nu{}^{\rho b}\tilde{F}_\rho{}^{\mu c}\right) + \cdots\,, \tag{4.108}$$

where $\tilde{F}_{\mu\nu} = \frac{1}{2}\epsilon_{\mu\nu\sigma\rho}F^{\sigma\rho}$. We show that in appendix B.1 that the couplings satisfy:

$$\lambda^{(\rm e1)}_{VVV} = \frac{g_{\rm YM}}{16\sqrt{2}}, \qquad \lambda^{(\rm e2)}_{VVV} = \frac{g_{\rm H}}{8\sqrt{2}}, \qquad \lambda^{(\rm o2)}_{VVV} = \frac{g'_{\rm H}}{4\sqrt{2}\pi} \tag{4.109}$$

where the structures refer to the even/odd basis in eq. (4.14). (We recall that the first structure is the "opposite helicity" one which generically exists for spin $J \geq 2$.)

Having stated this dictionary, in this section we shall present results in terms of the CFT couplings $\lambda^{(i)}_{VVV}$.

We consider only the parity-even couplings. There are then four ways to dress the the graph in fig. 4.4:

$$\begin{aligned}
&G_{11}\,, \quad \text{Yang-Mills vertex to Yang-Mills vertex}\,,\\
&G_{22}\,, \quad \text{higher-derivative vertex to higher-derivative vertex}\,,\\
&G_{12}\,, \quad \text{Yang-Mills vertex to higher-derivative vertex}\,,\\
&G_{21}\,, \quad \text{higher-derivative vertex to Yang-Mills vertex}\,.
\end{aligned} \tag{4.110}$$

In each case the t-channel block can be written as the spin-up of a scalar block, so after spinning down $\mathcal{D}^{(c,d)}_{\downarrow}G(z,\bar{z})$ in eq. (4.66) gives a 8th order differential equation acting on scalar blocks. The cross-channel scalar blocks themselves are not known in closed form; in appendix B.3.3 we provide the series expansion of the $\log z$ term to any order in z, which is sufficient to calculate anomalous dimensions exactly, in terms of $(y = z/(1-z)), \bar{y} = (1-\bar{z})/\bar{z})$, i.e., eq. (B.38). For example, at the leading order in the lightcone expansion $y \to 0$, we find

$$\mathcal{D}_{\downarrow}G_{11} = \frac{\log y}{\pi}\begin{pmatrix} -\frac{9y(\bar{y}+1)\left(\bar{y}^3+27\bar{y}^2+675\bar{y}+1225\right)}{32\bar{y}^{9/2}} & \frac{3y\left(3\bar{y}^3-29\bar{y}^2-123\bar{y}-75\right)}{4\bar{y}^{7/2}} \\ \frac{3y\left(3\bar{y}^3-29\bar{y}^2-123\bar{y}-75\right)}{4\bar{y}^{7/2}} & -\frac{2y\left(9\bar{y}^2+26\bar{y}+9\right)}{\bar{y}^{5/2}} \end{pmatrix} + \mathcal{O}(y^2)\,, \tag{4.111}$$

where we parameterize $y = z/(1-z), \bar{y} = (1-\bar{z})/\bar{z}$. At the leading order, $\mathcal{D}_{\downarrow}G_{22}$ has the same expression as $\mathcal{D}_{\downarrow}G_{11}$, but differs at the second and higher orders. Up to the leading order, $\mathcal{D}_{\downarrow}G_{12} = \mathcal{D}_{\downarrow}G_{21}$ is

$$\mathcal{D}_{\downarrow}G_{12} = \frac{3\log y}{\pi}\begin{pmatrix} -\frac{3y(\bar{y}+5)\left(\bar{y}^3-9\bar{y}^2+171\bar{y}+245\right)}{32\bar{y}^{9/2}} & \frac{3y\left(\bar{y}^3+\bar{y}^2-9\bar{y}-25\right)}{4\bar{y}^{7/2}} \\ \frac{3y\left(\bar{y}^3+\bar{y}^2-9\bar{y}-25\right)}{4\bar{y}^{7/2}} & -\frac{2y\left(3\bar{y}^2-2\bar{y}+3\right)}{\bar{y}^{5/2}} \end{pmatrix} + \mathcal{O}(y^2)\,. \tag{4.112}$$

The above expansions eq. (4.111) and eq. (4.112) would then be used *in principle* to obtain the leading-twist anomalous dimensions by simply integrating over $\bar{y}$ using the formula (4.104). As discussed in subsection 4.3.2, the leading-twist analysis is a bit subtle due to a degeneracy in three-point structures, and is discussed below. As the rotation in eq. (4.86) removes all divergences, the anomalous dimension can be computed using just the logarithmic term in eq. (4.111). Nontrivially, we find a result proportional to the leading order matrix $\begin{pmatrix} 1 & 0 \\ 0 & 0 \end{pmatrix}$, as required by the fact that there is a single leading-twist family (the number of operators can't change under small perturbations). The anomalous dimension is then[9]

$$\gamma^E_{11}\Big|_{n=0} = -\Big(\tfrac{\beta^4-4\beta^3+28\beta^2-48\beta+32}{(\beta-4)(\beta-2)(\beta-1)\beta(\beta+2)}\big((\lambda^{\text{e1}}_{VVV})^2+(\lambda^{\text{e2}}_{VVV})^2\big)+\tfrac{2}{1-\beta}\lambda^{\text{e1}}_{VVV}\lambda^{\text{e2}}_{VVV}\Big)(T+(-1)^J U)\,. \tag{4.113}$$

At subleading twists, the calculation uses analogous expressions together with the s-channel expansion (4.103) and (4.104).

4.4.2 Anomalous dimensions: Yang-Mills case

This yields the anomalous dimensions as analytic functions of β for fixed $n \geq 1$. Including the $\widehat{\mathbb{P}}$ matrix in eq. (4.99), we obtain $\langle c\gamma\rangle_{J,\Delta}$, which we then divide by the generalized free OPE data (4.77) (with $J_1 = J_2 = 1$), to arrive at anomalous dimensions. It is important to include both t- and u-channel identity in the denominator, which effectively doubles it as discussed below (4.88). In the pure Yang-Mills case we find:

$$\gamma^E_{11} = \tfrac{128(\lambda^{(\text{e1})}_{VVV})^2}{\pi^2}\big(T+(-1)^J U\big)\,\text{diag}\begin{pmatrix} \psi_{\frac{\beta}{2}-n-2} - \psi_{\frac{\beta}{2}+n} - \frac{4}{(\beta-2n)(\beta-2n+2)} + \frac{4}{-2n+\beta-2} \\ \psi_{\frac{\beta}{2}-n} - \psi_{\frac{\beta}{2}+n+2} + \frac{4}{(\beta+2n-4)(\beta+2n-2)} + \frac{4}{2n+\beta} \end{pmatrix}, \tag{4.114}$$

[9]Since the second structure $T^{E,\text{sing}}_{11\mathcal{O}}$ has a nonvanishing discontinuity, its $\sim(\lambda^{(\text{e1})}_{VVV})^2$ OPE coefficient will be required to predict the one-loop dDisc, in addition to the given anomalous dimension.

where diag represents the diagonal matrix, and we have factored out T- and U-channel color structures

$$T = f^{bce} f^{ade}, \qquad U = f^{ace} f^{bde} \,. \tag{4.115}$$

These should be viewed as operators acting on the initial pair, for example both have the eigenvalue $T, U \mapsto C_A$ when acting on a color-singlet state δ^{ab}.

Eq. (4.114) (for $n \geq 1$) gives the CFT_3 analog of the four-point Parke-Taylor amplitude. We note that to all orders in the $1/\beta$, the two entries are related by the reciprocity relation $\beta \mapsto 2-\beta$, which could have been anticipated from the off-diagonal nature of the light transform in eq. (4.57). The fact that it is diagonal will match with the vanishing of non-helicity-conserving flat space amplitudes at tree-level.

The Yang-Mills self-interaction also gives diagonal anomalous dimension the odd double-twists (which have half-integer n):

$$\gamma^O_{11} = \frac{128(\lambda^{(\mathrm{e1})}_{VVV})^2}{\pi^2} \mathrm{diag} \begin{pmatrix} \left(\psi_{\frac{\beta}{2}-n} - \psi_{\frac{\beta}{2}+n} - \frac{8}{(\beta-2n-2)(\beta-2n)}\right)\left(T - (-1)^J U\right) \\ \left(\psi_{\frac{\beta}{2}-n} - \psi_{\frac{\beta}{2}+n} + \frac{8}{(\beta+2n-2)(\beta+2n)}\right)\left(T + (-1)^J U\right) \end{pmatrix} . \tag{4.116}$$

4.4.3 Higher-derivative corrections

Let us now record the pure higher-derivative corrections, which involve purely algebraic expressions:

$$\gamma^E_{22} = \frac{128(\lambda^{(\mathrm{e2})}_{VVV})^2}{\pi^2} \mathrm{diag} \begin{pmatrix} \frac{(n(\beta-1)+2)\left(4n^2+8(\beta-1)n+(\beta-2)\beta+4\right)}{(2n-\beta-2)(2n-\beta)(2n-\beta+2)(2n-\beta+4)} \left(-T - (-1)^J U\right) \\ \frac{(n(\beta-1)-2)\left(4(n+1)^2+\beta^2-2(4n+1)\beta\right)}{(2n+\beta-4)(2n+\beta-2)(2n+\beta)(2n+\beta+2)} \left(-T - (-1)^J U\right) \end{pmatrix} , \tag{4.117}$$

$$\gamma^O_{22} = \frac{128(\lambda^{(\mathrm{e2})}_{VVV})^2}{\pi^2} \mathrm{diag} \begin{pmatrix} \frac{(n(\beta-1)+2)\left(4n^2+8(\beta-1)n+(\beta-2)\beta+4\right)}{(2n-\beta-2)(2n-\beta)(2n-\beta+2)(2n-\beta+4)} \left(T - (-1)^J U\right) \\ \frac{(n(\beta-1)-2)\left(4(n+1)^2+\beta^2-2(4n+1)\beta\right)}{(2n+\beta-4)(2n+\beta-2)(2n+\beta)(2n+\beta+2)} \left(T + (-1)^J U\right) \end{pmatrix} . \tag{4.118}$$

The even and odd matrices are identical up to some signs, and again reciprocity $\beta \mapsto 2-\beta$ swaps the trajectories up to a minus sign.

The G_{12} contributions (one Yang-Mills and one higher-derivative vertex) violate helicity conservation and give purely off-diagonal anomalous dimensions. Since the

Lorentzian inversion formula gives us $\langle c\gamma\rangle_{J,\Delta}$, we divide the off-diagonal terms by the geometric mean of MFT coefficients to define a symmetrical anomalous dimension matrix $\gamma_{12}^{\text{even}} = \gamma_{21}^{\text{even}}$:

$$\gamma_{12}^{E} = \frac{128\lambda_{VVV}^{(\text{e1})}\lambda_{VVV}^{(\text{e2})}}{\pi^2}\frac{-4n(\beta-1)\sqrt{(\beta-2n)(\beta-2n+2)}(\beta(\beta-2)+4n^2-4)(T+(-1)^J U)}{(\beta-2n+2)(\beta-2n)\sqrt{(\beta-2n-4)(\beta-2n-2)(\beta+2n-4)(\beta+2n-2)(\beta+2n)(\beta+2n+2)}}\begin{pmatrix} 0 & 1 \\ 1 & 0 \end{pmatrix}. \tag{4.119}$$

The odd γ_{12} is the same and γ_{21} is also identical up to an overall minus sign (such that the sum vanishes: $\gamma_{12}^{O} + \gamma_{21}^{O} = 0$, which will be in agreement with symmetries of the scattering amplitude).

We end this section by giving the large-n limit of above anomalous dimensions, which will be compared in the next section with flat-space 2-to-2 gluon scattering amplitudes:

$$\begin{aligned}
\gamma_{11}^{E}|_{n\to\infty} &= \frac{128(\lambda_{VVV}^{(\text{e1})})^2}{\pi^2}(T+(-1)^J U)\text{diag}\begin{pmatrix} \psi_{J-1} - \log(2n) + \frac{2}{J} - \frac{1}{(J+1)(J+2)} \\ \psi_{J+1} - \log(2n) \end{pmatrix}, \\
\gamma_{11}^{O}|_{n\to\infty} &= \frac{128(\lambda_{VVV}^{(\text{e1})})^2}{\pi^2}\begin{pmatrix} \big(\psi_{J+1} - \log(2n) - \frac{2}{J(J+1)}\big)(T-(-1)^J U) \\ \big(\psi_{J+1} - \log(2n)\big)(T+(-1)^J U) \end{pmatrix}, \\
\gamma_{22}^{E/O}|_{n\to\infty} &= \frac{128(\lambda_{VVV}^{(\text{e2})})^2}{\pi^2}\begin{pmatrix} \frac{12n^4(\mp T+(-1)^J U)}{(J-1)J(J+1)(J+2)} & 0 \\ 0 & 0 \end{pmatrix}, \\
\gamma_{12}^{E/O}|_{n\to\infty} &= \frac{128\lambda_{VVV}^{(\text{e1})}\lambda_{VVV}^{(\text{e2})}}{\pi^2}\frac{-n^2(T+(-1)^J U)}{\sqrt{(J-1)J(J+1)(J+2)}}\begin{pmatrix} 0 & 1 \\ 1 & 0 \end{pmatrix}, \\
\gamma_{21}^{E/O}|_{n\to\infty} &= \frac{128\lambda_{VVV}^{(\text{e1})}\lambda_{VVV}^{(\text{e2})}}{\pi^2}\frac{\mp n^2(T+(-1)^J U)}{\sqrt{(J-1)J(J+1)(J+2)}}\begin{pmatrix} 0 & 1 \\ 1 & 0 \end{pmatrix}.
\end{aligned} \tag{4.120}$$

We note that each higher-derivative correction $\lambda_{VVV}^{(e2)}$ comes accompanied with a power of $n^2 \sim s$, as expected from bulk dimensional analysis. Furthermore, we see that the difference between even- and odd- same-helicity anomalous dimensions vanishes at

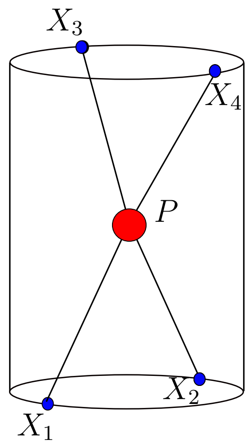

Figure 4.5: Bulk-point kinematics in Lorentzian cylinder of AdS. X_1 and X_2 are at Lorentzian time $-\pi/2$, X_3 and X_4 are at Lorentzian time $\pi/2$, where particles are focused on the bulk-point P.

large-n:

$$\gamma_{11}^{E,\text{same}} - \gamma_{11}^{O,\text{same}} = \frac{128(\lambda_{VVV}^{(\text{e1})})^2}{\pi^2} \frac{6(T+(-1)^J U)}{(\frac{\beta}{2}+n-2)_4} \sim \frac{1}{n^4}\,. \tag{4.121}$$

This indicates that the same-helicity amplitude $\mathcal{M}_{++++}$ vanishes in the flat-space limit (as expected). However, we find it remarkable that it is *not* identically zero in AdS space. This suggests that, in a more precise treatment where the flat-space limit is defined as $R \to \infty$ as opposed to $s \to \infty$, a distributional term near $s = 0$ may survive; such terms could potentially give a new perspective on four-dimensional unitarity and the rational one-loop amplitude $\mathcal{M}^{(1)}_{++++}$. We leave this to future work.

4.5 Large-n limit from gluon scattering amplitudes

There is a close relation between the anomalous dimensions at large dimension in a CFT_d and the scattering amplitude of a dual QFT_{d+1} in the flat space limit of AdS. This can be seen for example by considering kinematic configurations which focus particles — such as the analytically continued $z \to \bar{z}$ "bulk-point" limit, see for example [16, 18, 21, 22, 23, 24][10]. For massless external particles (dual to our currents), since the past and future states are connected by time π on the cylinder, the scattering phase is related to CFT anomalous dimensions by the simple dictionnary

$$\gamma_{n,J}\big|_{n\to\infty} \to -\frac{1}{\pi} a_J\,, \quad sR^2 = 4n^2\,, \tag{4.122}$$

where a_J is the partial-wave amplitudes with angular momentum J, s is the Mandelstam invariant of the bulk scattering process, and R is the AdS radius. We often take $R = 1$ below for simplicity and take $s \neq 0$, so the limit is equivalent to $n \to \infty$. (In general the amplitude maps to a weighted average of anomalous dimensions. A one-loop example is provided in [106].) We expect this relation to work for spinning operators as well, for suitably defined partial waves.

4.5.1 Partial waves in massless QFT$_4$

Two-particle scattering states in QFT$_4$ can be organized according to their SO(3) spin in the rest frame of their total momentum, $P = p_1 + p_2$. Since rotations commute with helicity, we can choose a basis of states with definite helicity. For definiteness, we focus here on the case of two massless spin 1 particles.

We use the spinor-helicity formalism where each null momentum is factorized into a product of spinors, $\not{p}_i = |i]\langle i|$, see [178]. Under little-group rotations of spinors $|i]$ and $|i\rangle$ by opposite phases, a state of helicity h transforms like $|i]^{2h}$. We treat two-particle states like a massive particle of momentum P and spin J, which in index-free notation is a polynomial $\sim |\epsilon\rangle^{2J}$ in a left-handed spinor $|\epsilon\rangle$. (There is no need to use right-handed spinors, since P can be used to convert one into the other, see [179].) Lorentz and little-group symmetries then uniquely fix the matrix elements of

[10]This kinematic configuration is, however, modified if external particles are massive [25, 93, 3, 177].

two-particle states $\Psi^J_{\pm}$:

$$\begin{aligned}
\langle 2^-1^-|\Psi^J_{--}\rangle &= \frac{\langle\epsilon 1\rangle^J\langle\epsilon 2\rangle^J}{\langle 12\rangle^{J-1}[12]}\,, \qquad & \langle 2^+1^-|\Psi^J_{-+}\rangle &= \frac{\langle\epsilon 1\rangle^{J+2}\langle\epsilon 2\rangle^{J-2}}{\langle 12\rangle^J}\,, \\
\langle 2^+1^+|\Psi^J_{++}\rangle &= \frac{\langle\epsilon 1\rangle^J\langle\epsilon 2\rangle^J}{\langle 12\rangle^{J+1}/[12]}\,, \qquad & \langle 2^-1^+|\Psi^J_{+-}\rangle &= \frac{\langle\epsilon 1\rangle^{J-2}\langle\epsilon 2\rangle^{J+2}}{\langle 12\rangle^J}\,.
\end{aligned} \tag{4.123}$$

More precisely, symmetries fix the states up to a power of $s = -P^2$, which we chose so that all states have the same dimension. We further define the state $|\Psi^J_{h_1h_2}\rangle$ to be orthogonal to gluons of other helicity.

In the above kinematic factors we treat the two particles as distinguishable. These are related to actual gluon states by adding color labels and accounting for Bose symmetry: fully decorated states can be defined as

$$\langle 3^{h_3c}4^{h_4d}|\Psi^{J,ab}_{h_1h_2}\rangle = \delta^{ad}\delta^{bc}\delta^{h_4}_{h_1}\delta^{h_3}_{h_2}\langle 3^{h_3}4^{h_4}|\Psi^J_{h_1h_2}\rangle + \delta^{ac}\delta^{bd}\delta^{h_3}_{h_1}\delta^{h_4}_{h_2}\langle 3^{h_3}4^{h_4}|\Psi^J_{h_1h_2}\rangle\,. \tag{4.124}$$

Since interactions can change helicities, the action of the S-matrix on these states takes the form of a 4×4 matrix:

$$\mathcal{S}|\Psi^J_{h_1a,h_2b}\rangle = \sum_{h_3,h_4,c,d} S^J_{h_1a,h_2b}{}^{h_4d,h_3c}|\Psi^J_{h_3c,h_4d}\rangle + \text{multi-particles}\,. \tag{4.125}$$

As is customary, we subtract the identity part: $\mathcal{S} = 1 + i\mathcal{A}$, where $\mathcal{A}$ is the scattering amplitude. In the $2\to 2$ sector, $S^J_{12}{}^{43} = \frac{1}{2}(\delta^4_1\delta^3_2 + \delta^3_1\delta^4_2) + ia^J_{12}{}^{43}$, where we use collective indices in $\delta^4_1 = \delta^{h_4}_{h_1}\delta^d_a$. The partial wave a is then simply the amplitude in the $|\Psi\rangle$ basis:

$$a^J = \mathcal{A}\otimes|\Psi^J\rangle\,, \tag{4.126}$$

which can be computed as a phase-space integral. To be fully explicit with indices (see also eq. (2.16) of [180]):

$$\begin{aligned} a^{J}_{h_1 a,h_2 b}{}^{h_4 d,h_3 c} &= \frac{1}{2}\sum_{h_1',h_2',a',b'}\int \frac{d\Omega}{64\pi^2}\frac{\langle 3^{h_3 c}4^{h_4 d}|\mathcal{A}|1^{a'}_{h_1'}2^{b'}_{h_2'}\rangle\langle 1^{h_1' a'}2^{h_2' b'}|\Psi^J_{h_1 a,h_2 b}\rangle}{\langle 3^{h_3}4^{h_4}|\Psi^J_{h_3,h_4}\rangle} \\ &= \frac{1}{16\pi}\int\frac{d\Omega}{4\pi}\langle 3^{h_3 c}4^{h_4 d}|\mathcal{A}|1^a_{h_1}2^b_{h_2}\rangle\frac{\langle 1^{h_1}2^{h_2}|\Psi^J_{h_1,h_2}\rangle}{\langle 3^{h_3}4^{h_4}|\Psi^J_{h_3,h_4}\rangle}\,. \end{aligned} \tag{4.127}$$

The second form will be particularly useful for calculations. Notice that the two terms in eq. (4.124) simply canceled the symmetry factor $\frac{1}{2}$. In this integral, p_3 and p_4 are held fixed and $d\Omega$ represents the solid angle of $\vec{p_1}$ in the rest frame of P.

The angular integral can be conveniently parametrized in terms of spinors via [181]

$$|1\rangle = \cos\theta|4\rangle - \sin\theta e^{i\phi}|3\rangle\,, \quad |2\rangle = \sin\theta e^{-i\phi}|4\rangle + \cos\theta|3\rangle\,, \tag{4.128}$$

with analogous expressions for the conjugate spinors $|1]$ and $|2]$ with the phase reversed $\phi \mapsto -\phi$. In the rest frame of P, the variables θ and ϕ represent physically (half) the azimuthal and polar angle with respect to p_1. The measure is then

$$\int\frac{d\Omega}{4\pi} = \int_0^{2\pi}\frac{d\phi}{2\pi}\int_0^{\frac{\pi}{2}}\sin(2\theta)d\theta\,. \tag{4.129}$$

It is important to note that both the numerator and denominator in eq. (4.127) depend on $|\epsilon\rangle$, p_3 and p_4, in addition to the integration variables θ,ϕ. However, since the result of the integral is determined by symmetry, the ratio *after* doing the integral is guaranteed to be a pure number independent of these variables.

This method allows us to define partial waves without having to worry about the normalization of the states. The idea is that the eigenvalues of the matrix $S^{J\ 43}_{12}$ map to weighted averages of CFT anomalous dimensions $e^{-i\pi\gamma}$. To leading order in perturbation theory, this relation gives simply, as quoted:

$$\gamma^{J\ 43}_{12} \approx -\frac{1}{\pi}a^{J\ 43}_{12}. \tag{4.130}$$

Surprisingly, the exact same relation has an interpretation purely in the context of QFT: the phase of the S-matrix acting on form factors of local operators gives the dilatation operator of the QFT: $\mathcal{S}\mathcal{F}^* = e^{-i\pi D}\mathcal{F}^*$ [180]. This was used there to compute anomalous dimensions of local operators of a QFT$_4$, as labelled by their two-particle form factors. (For example, the infrared-safe combination $\gamma^{0}_{++}{}^{++} - \gamma^{2}_{+-}{}^{+-}$ acting on a color-singlet state computes the QCD β-function.) Here $\gamma^{J}_{12}{}^{43}$ instead gives holographically a CFT$_3$ anomalous dimension $\gamma(n)$ where $4n^2 = sR^2$ is large. It is amusing that anomalous dimensions in the bulk QFT$_{d+1}$ and boundary CFT$_d$ are computed by literally the same formula.

4.5.2 Anomalous dimensions in Yang-Mills theory

On-shell amplitudes in YM$_4$ are recorded in appendix B.4. We use these on-shell amplitudes together with eq. (4.127) to extract the corresponding partial-wave amplitudes, from which we will find perfect agreement with CFT eq. (4.120).

We begin with the pure Yang-Mills theory, then add higher-derivative corrections.

4.5.2.1 Pure Yang-Mills

Using Yang-Mills amplitudes eq. (B.45), we can readily evaluate (4.127). For example, we obtain

$$\begin{aligned}(a^{\mathrm{YM}^2})_{-+}{}^{-+} = \tfrac{g_{\mathrm{YM}}^2}{8\pi\langle\epsilon 3\rangle^{J-2}\langle\epsilon 4\rangle^{J+2}} \int_0^{2\pi} d\phi \int_0^{\frac{\pi}{2}} d\theta (\langle\epsilon 4\rangle\cos\theta - \langle\epsilon 3\rangle \sin\theta e^{i\phi})^{J+2} \times \\ (\langle\epsilon 3\rangle\cos\theta + \langle\epsilon 4\rangle\sin\theta e^{-i\phi})^{J-2}\cos^4\theta \times (T\cot\theta + U\tan\theta)\,,\end{aligned}$$

$$\begin{aligned}(a^{\mathrm{YM}^2})_{-+}{}^{+-} = \tfrac{g_{\mathrm{YM}}^2}{8\pi\langle\epsilon 3\rangle^{J-2}\langle\epsilon 4\rangle^{J+2}} \int_0^{2\pi} d\phi \int_0^{\frac{\pi}{2}} d\theta e^{4i\phi} (\langle\epsilon 4\rangle\cos\theta - \langle\epsilon 3\rangle \sin\theta e^{i\phi})^{J-2} \times \\ (\langle\epsilon 3\rangle\cos\theta + \langle\epsilon 4\rangle\sin\theta e^{-i\phi})^{J+2}\sin^4\theta \times (T\cot\theta + U\tan\theta)\,, \qquad (4.131)\end{aligned}$$

and $(a^{\mathrm{YM}^2})_{+-}{}^{-+} = (a^{\mathrm{YM}^2})_{-+}{}^{+-}$ when the integral is evaluated. Same-helicity partial-wave amplitudes give

$$(a^{\mathrm{YM}^2})_{--}{}^{--} = (a^{\mathrm{YM}^2})_{++}{}^{++} = \frac{g_{\mathrm{YM}}^2}{8\pi\langle\epsilon 3\rangle^J\langle\epsilon 4\rangle^J}\int_0^{2\pi} d\phi \int_0^{\frac{\pi}{2}} d\theta(\langle\epsilon 4\rangle\cos\theta - \langle\epsilon 3\rangle\sin\theta e^{i\phi})^J \times$$
$$(\langle\epsilon 3\rangle\cos\theta + \langle\epsilon 4\rangle\sin\theta e^{-i\phi})^J \times \big(T\cot\theta + U\tan\theta\big)\,, \tag{4.132}$$

and other helicity-violation terms identically vanish, e.g., $a_{-+}{}^{--} = a_{--}{}^{-+} = 0$. It is worth noting that above integrals fail to converge due to IR divergence. In the context of computing UV anomalous dimensions in QFT, these could be subtracted using that the stress-tensor is protected [180]. However, in our context these reflect physical divergences of bulk anomalous dimensions as $R_{\mathrm{AdS}} \to \infty$. We thus regularize the above equations by introducing a small-angle cut-off $\epsilon < \theta < \frac{\pi}{2} - \epsilon$ which we will then compare with the bulk cutoff $n \to \infty$. The azimuthal integral can be readily evaluated, which gives

$$\begin{aligned}
(a^{\mathrm{YM}^2})_{-+}{}^{-+} &= -\tfrac{g_{\mathrm{YM}}^2}{4\pi}\big(\gamma_{\mathrm{E}} + \log\epsilon + \psi_{J-1} + \tfrac{2}{j} - \tfrac{1}{(j+2)(j+3)} + \tfrac{3}{(j-1)_4}\big)T + \tfrac{3g_{\mathrm{YM}}^2}{4\pi(J-1)_4}(-1)^J U\,,\\
(a^{\mathrm{YM}^2})_{-+}{}^{+-} &= -\tfrac{g_{\mathrm{YM}}^2}{4\pi}\big(\gamma_{\mathrm{E}} + \log\epsilon + \psi_{J-1} + \tfrac{2}{j} - \tfrac{1}{(j+2)(j+3)} + \tfrac{3}{(j-1)_4}\big)(-1)^J U + \tfrac{3g_{\mathrm{YM}}^2}{2\pi(J-1)_4}T\,,\\
(a^{\mathrm{YM}^2})_{--}{}^{--} &= (a^{\mathrm{YM}^2})_{++}{}^{++} = -\frac{g_{\mathrm{YM}}^2}{4\pi}\big(\gamma_{\mathrm{E}} + \log\epsilon + \psi_{J+1}\big)\big(T + (-1)^J U\big)\,.
\end{aligned} \tag{4.133}$$

As a simple check, acting on color-singlet states $(T, U \mapsto C_A)$ and taking large spin, we reproduce the famous logarithmic scaling of gauge theories, $\gamma = \frac{-a}{\pi} \to +\frac{g_{\mathrm{YM}}^2}{2\pi^2}\log J$.

To compare with anomalous dimensions evaluated in CFT, we should rotate to parity basis

$$\begin{aligned}
(a^{\mathrm{YM}^2})^E &= \frac{1}{2}\mathrm{diag}\begin{pmatrix} (a^{\mathrm{YM}^2})_{-+}{}^{-+} + (a^{\mathrm{YM}^2})_{-+}{}^{+-} + (+\leftrightarrow -) \\ (a^{\mathrm{YM}^2})_{--}{}^{--} + (a^{\mathrm{YM}^2})_{++}{}^{++} \end{pmatrix}\,,\\
(a^{\mathrm{YM}^2})^O &= \frac{1}{2}\mathrm{diag}\begin{pmatrix} (a^{\mathrm{YM}^2})_{-+}{}^{-+} - (a^{\mathrm{YM}^2})_{-+}{}^{+-} + (+\leftrightarrow -) \\ (a^{\mathrm{YM}^2})_{--}{}^{--} + (a^{\mathrm{YM}^2})_{++}{}^{++} \end{pmatrix}\,,
\end{aligned} \tag{4.134}$$

where $(+\leftrightarrow-)$ denotes flipping all helicity. Imposing following simple identification

$$\epsilon = \frac{e^{-\gamma_{\rm E}}}{2n}\,, \tag{4.135}$$

and using $\lambda^{(\rm e1)}_{VVV} = g_{\rm YM}/(16\sqrt{2})$ from eq. (4.109), we then find a perfect match with the CFT anomalous dimension in eq. (4.120):

$$\gamma^{E/O}_{11}|_{n\to\infty} = -\frac{1}{\pi}(a^{\rm YM^2})^{E/O}\,. \tag{4.136}$$

4.5.2.2 Higher-derivative corrections

Let us start with the pure higher-derivative interaction (e.g. at both vertices). Using the amplitudes recorded in eq. (B.46), we can immediately conclude that $(a^{\rm H^2})_{--}{}^{--} = (a^{\rm H^2})_{++}{}^{++} = 0$, because $\mathcal{M}^{\rm H^2}_{1_-2_-3_+4_+}$ only have s-channel pole and thus is evaluated to be identically zero, which nicely agrees with predictions from CFT. On the other hand, $(a^{\rm H^2})_{-+}{}^{-+}$ and $(a^{\rm H^2})_{-+}{}^{+-}$ contributes with T and U factors separately, giving

$$\begin{aligned}
(a^{\rm H^2})_{-+}{}^{-+} = &\tfrac{g^2_{\rm H}}{32\pi\langle\epsilon3\rangle^{J-2}\langle\epsilon4\rangle^{J+2}}\int_0^{2\pi}d\phi\int_0^{\frac{\pi}{2}}d\theta(\langle\epsilon4\rangle\cos\theta-\langle\epsilon3\rangle\sin\theta e^{i\phi})^{J+2}\times\\
&(\langle\epsilon3\rangle\cos\theta+\langle\epsilon4\rangle\sin\theta e^{-i\phi})^{J-2}(\cos\theta)^3\sin\theta(\cos(2\theta)-3)\times U\,,\\
(a^{\rm H^2})_{-+}{}^{+-} = &\tfrac{g^2_{\rm H}}{32\pi\langle\epsilon3\rangle^{J-2}\langle\epsilon4\rangle^{J+2}}\int_0^{2\pi}d\phi\int_0^{\frac{\pi}{2}}d\theta e^{4i\phi}(\langle\epsilon4\rangle\cos\theta-\langle\epsilon3\rangle\sin\theta e^{i\phi})^{J-2}\times\\
&(\langle\epsilon3\rangle\cos\theta+\langle\epsilon4\rangle\sin\theta e^{-i\phi})^{J+2}(\sin\theta)^3\cos\theta(\cos(2\theta)+3)\times T\,.
\end{aligned}\tag{4.137}$$

We can readily evaluate the integrals and find

$$(a^{\rm H^2})_{-+}{}^{-+} = \frac{3g^2_{\rm H}s^2}{4\pi^2(J-1)_4}(-1)^J U\,,\quad (a^{\rm H^2})_{-+}{}^{+-} = \frac{3g^2_{\rm H}s^2}{4\pi^2(J-1)_4}T\,, \tag{4.138}$$

and simultaneously flipping helicity $+\leftrightarrow-$ gives the same answer. Rotating to the Even/Odd parity basis readily gives

$$(a^{\rm H^2})^{E/O} = \frac{3g^2_{\rm H}s^2}{4\pi^2(J-1)_4}\begin{pmatrix}\left(\mp T+(-1)^J U\right) & 0\\ 0 & 0\end{pmatrix}\,. \tag{4.139}$$

Using $\lambda^{\mathrm{e}2}_{VVV} = g_H/(8\sqrt{2})$ from eq. (4.109) and $s = 4n^2$ from eq. (4.122), we achieve a perfect agreement with CFT anomalous dimensions from eq. (4.120).

$$\gamma^{E/O}_{22}|_{n\to\infty} = -\frac{1}{\pi}(a^{\mathrm{H}^2})^{E/O} \,. \tag{4.140}$$

The contact ambiguity that has the same scaling dimension as the a_H^2 interaction (see eq. (B.46)) affects the $J = 2$ OPE data, making the preceding partial wave valid only for $J > 2$. We believe that all other results are valid for $J > 1$ (with similar comments applying to the Lorentzian inversion formula results from the preceding section).

Finally, let us look at the product of Yang-Mills and higher-derivative couplings. Here, there are two kinds of amplitudes, for example $\mathcal{M}_{--+-}$ and $\mathcal{M}_{-+++}$, which is not symmetric and thus give slightly different partial-wave amplitudes that form a non-symmetric and anti-diagonal matrix; eigenvalues of the resulting matrix should agree with CFT eigenvalues from eq. (4.120) (that is, we only compare up to similarity transformation).

For example, we find some of $(a^{\mathrm{mix}}) = a\Big|_{g_{\mathrm{YM}}g_{\mathrm{H}}}$ for $\mathcal{M}_{--+-}$ type mixing reads

$$\begin{aligned}
(a^{\mathrm{mix}})_{-+}{}^{--} &= -\tfrac{g_{\mathrm{YM}}g_{\mathrm{H}}s}{8\pi\langle\epsilon 3\rangle^{J}\langle\epsilon 4\rangle^{J}}\int_0^{2\pi} d\phi\int_0^{\frac{\pi}{2}} d\theta e^{-2i\phi}(\langle\epsilon 4\rangle\cos\theta - \langle\epsilon 3\rangle\sin\theta e^{i\phi})^{J+2}\times \\
&\quad(\langle\epsilon 3\rangle\cos\theta + \langle\epsilon 4\rangle\sin\theta e^{-i\phi})^{J-2}\sin(2\theta)\times(T\cot\theta + U\tan\theta)\,, \\
(a^{\mathrm{mix}})_{--}{}^{+-} &= -\tfrac{g_{\mathrm{YM}}g_{\mathrm{H}}s}{8\pi\langle\epsilon 3\rangle^{J-2}\langle\epsilon 4\rangle^{J+2}}\int_0^{2\pi} d\phi\int_0^{\frac{\pi}{2}} d\theta e^{2i\phi}(\langle\epsilon 4\rangle\cos\theta - \langle\epsilon 3\rangle\sin\theta e^{i\phi})^{J}\times \\
&\quad(\langle\epsilon 3\rangle\cos\theta + \langle\epsilon 4\rangle\sin\theta e^{-i\phi})^{J}\sin^2\theta\cos^2\theta\times(T\cot\theta + U\tan\theta)\,.
\end{aligned} \tag{4.141}$$

$(a^{\mathrm{mix}})_{-+}{}^{++}$ gives the same as $(a^{\mathrm{mix}})_{-+}{}^{--}$, and $(a^{\mathrm{mix}})_{--}{}^{-+}$ is similar to $(a^{\mathrm{mix}})_{--}{}^{+-}$ but flipping $e^{2i\phi} \to e^{-2i\phi}$. Though the integrand looks a bit different when we flipping

$+ \leftrightarrow -$, we find they give the same result

$$
\begin{aligned}
(a^{\text{mix}})_{-+}{}^{--} = (a^{\text{mix}})_{-+}{}^{++} &= -\frac{g_{\text{YM}} g_{\text{H}} s}{8\pi J(J-1)} \big(T + (-1)^J U\big) \,, \\
(a^{\text{mix}})_{--}{}^{-+} = (a^{\text{mix}})_{--}{}^{+-} &= -\frac{g_{\text{YM}} g_{\text{H}} s}{8\pi (J+1)(J+2)} \big(T + (-1)^J U\big) \,,
\end{aligned}
\tag{4.142}
$$

and the same for flipping $\pm \to \mp$. Now we can rotate to the parity basis. To compare with CFT calculation where we record γ_{12} and γ_{21} separately, we should be careful about clarifying a^{mix}_{12} and a^{mix}_{21}: γ_{12} corresponds to a^{mix} with different helicity in (h_2, h_3) , and γ_{21} corresponds to a^{mix} with same helicity in (h_2, h_3). We find

$$
\begin{aligned}
(a^{\text{mix}}_{12})^{E/O} &= \frac{1}{2} \begin{pmatrix} 0 & (a^{\text{mix}})_{-+}{}^{--} + (a^{\text{mix}})_{+-}{}^{++} \\ (a^{\text{mix}})_{--}{}^{+-} + (a^{\text{mix}})_{++}{}^{-+} & 0 \end{pmatrix} , \\
(a^{\text{mix}}_{21})^{E/O} &= \pm\frac{1}{2} \begin{pmatrix} 0 & (a^{\text{mix}})_{-+}{}^{++} + (a^{\text{mix}})_{+-}{}^{--} \\ (a^{\text{mix}})_{--}{}^{-+} + (a^{\text{mix}})_{++}{}^{+-} & 0 \end{pmatrix} .
\end{aligned}
\tag{4.143}
$$

The signs work out so that, when we add the contributions from the two vertices, the parity-even part doubles and the odd part cancels out ($a^O_{12} + a^O_{21} = 0$), as found in the preceding section. Using the dictionary $\lambda^{\text{e2}}_{VVV} = g_H/(8\sqrt{2})$ and $\lambda^{\text{e2}}_{VVV} = g_H/(16\sqrt{2})$ from eq. (4.109) and $s = 4n^2$, we find that the eigenvalues of a^{mix} precisely coincide with γ_{12} and γ_{21} in eq. (4.120) up to $-1/\pi$, i.e.,

$$
\gamma^{E/O}\big|_{n\to\infty} \sim -\frac{1}{\pi} (a^{\text{mix}})^{E/O} \,,
\tag{4.144}
$$

and $\sim$ denotes the equivalence up to similarity transformation.

4.6 Conclusion

In this paper, we introduced a helicity basis for conformal blocks of conserved currents of any spins in three-dimensional CFTs. We observed that the concept of helicity is conformally invariant (see subsection 4.2.2) and can be defined without reference to any particular formalism such as momentum space. This ensures that the helicity basis plays nicely with crossing symmetry. We found evidence of this in the OPE decomposition of mean-field correlators, which turns out nicely diagonal (see eq. (4.76), and we further computed the CFT_3 OPE data dual to tree-level gluon scattering of Yang-Mills theory in AdS_4, including higher-derivative corrections.

The YM_4 calculation was done using the spinning Lorentzian inversion formula (see eq. (4.114), (4.116) and following), which gives the OPE data for sufficiently large spin $J > J_*$, where we expect $J_* = 1$ without including higher-derivative corrections and $J_* = 2$ with them. The anomalous dimensions follow a simple diagonal / off-diagonal pattern and precisely match, in the large-twist limit, with the partial waves in the flat space limit of the bulk theory, shown in eq. (4.120). We found a simple one-to-one dictionary between on-shell three-point interactions in bulk AdS_4 and three-point helicity structures (see eq. (B.14)).

We expect that a calculation of the $6j$ symbol (also known as crossing kernel) in the helicity basis could thus greatly help bootstrap calculations involving conserved currents and stress tensors in 3d CFTs. We expect the $6j$ symbols to be diagonal in helicity basis. It is also worth exploring if the helicity basis could also help numerical work by diagonalizing certain steps.

In higher spacetime dimensions, whether a basis exists which would diagonalize mean-field correlators remains an open question. Better understanding the flat-space limit of massless-massless-massive three-point functions could shed light on this question.

In perturbation theory, our findings pave the way for a study of loop corrections in YM_4 with a four-dimensional treatment of infrared effects. Compared with flat space, AdS physics comes with a built-in infrared regulator, and an interesting fact is that leading double-twist states (the $n = 0$ trajectory) do not have a definite helicity (see eq. (4.87)). The notion that zero-energy gluons do not have helicity resonates with findings from the asymptotic symmetry context (see for example [182]), and it would be interesting to make this connection closer. Eq. (4.121) suggests that the tree-level amplitude for four same-helicity gluons is not identically zero even in flat space, but retains a sort of distributional component around zero energy, which could be important for unitarity calculations in flat space.

Nonperturbatively, we expect the helicity basis to be particularly convenient for uncovering the implications of crossing symmetry on stress tensor correlators in CFT_3 and the dual gravitational physics.

Acknowledgement

We would like to thank for Nikhil Anand for useful conversations and initial collaboration on AdS calculations, and Petr Kravchuk for discussions. Work of S.C.-H. is supported by the National Science and Engineering Council of Canada, the Canada Research Chair program, the Fonds de Recherche du Québec - Nature et Technologies, the Simons Collaboration on the Nonperturbative Bootstrap, and the Sloan Foundation. Work of Y.-Z.L. is supported in parts by the Fonds de Recherche du Québec - Nature et Technologies.

Chapter 5

Graviton partial waves and causality in higher dimensions

5.0 Bridging section

In the last two manuscripts (Chapter 3 and 4), we discuss the flat-space limit of AdS scattering amplitudes. The precise definition of the flat-space limit is to take the AdS radius large compared to any other length scales such as the impact parameter b, the string length ℓ_s, and the Planck length $\ell_{\rm pl}$. The precise hierarchy is $R_{\rm AdS} \gg b > \ell_s \gg \ell_{\rm pl}$. For massless particles, such limit is also phrased as the bulk point limit because it ensures particles almost shot into a single point in the AdS bulk.

In Chapter 3, we show that all existing frameworks for achieving the flat-space limit can be related to each other. The origin of those formulas is the holographic reconstruction of wave packets in the AdS bulk in terms of conformal operators on the boundary. However, our starting point is the low-energy perturbative constructions of the smearing kernel. We know nothing about any UV and non-perturbative aspects of this formalism.

A similar situation happens in Chapter 4. We have to restrict our explorations of four-point gluon amplitudes to the perturbative AdS EFT regime. The reason is that we do not know any details of the underlying UV theory.

Although we do not assume any underlying UV theory, the Wilson coefficients of low-energy EFT encode some information about the UV theory. One can build the dispersion relations of amplitudes to relate the EFTs and UV theories. One can make use of the dispersion relations to carve out the allowed space of Wilson coefficients by only assuming the causality and the unitarity in the UV, see, e.g.,[77, 80, 81, 82, 83, 84, 85, 86, 87, 88] in flat space. The compatibility between AdS and flat-space for the allowed space of Wilson coefficients is the first step to making sense of defining the UV S-matrix from AdS in the flat-space limit. [33] proves this compatibility for scalar correlators. The authors of [33] show that the constraints of flat-space Wilson coefficients can be uplifted to AdS space up to small errors under the Regge limit $R_{\text{AdS}} \sim b \gg \ell_s \gg \ell_{\text{pl}}$. This finding suggests that scalar EFTs in AdS can define scalar EFTs in the flat-space at the large AdS radius by predicting the correct Wilson coefficients and vice versa.

In this manuscript, we study the constraints of Wilson coefficients for gravitational S-matrix. Although there is no definitive proof of uplifting spinning EFTs, we uplift our rigorous bounds to give central charge bounds of holographic CFT$_4$, see (5.30). In the future, if any researchers successfully establish the dispersion relations for stress-tensor correlation functions, they can use that dispersion relation to precisely bound the central charge ratios. Our uplifted bound will then provide a comparison. Therefore, our findings pave the way to understanding how stress-tensor correlation functions can predict gravitational S-matrix and vice versa.

In summary, we directly deal with the perturbative relations between AdS amplitudes and flat-space S-matrices in the last two Chapters, which is the efforts to answer **Q1** in the introduction. On the other hand, this Chapter provides the necessary ingredients for the future to bridge AdS amplitudes and S-matrices as gravitational EFTs controlled by an unknown UV origin, paving the way to understanding **Q2** in the introduction.

5.1 Introduction

Relativity and quantum mechanics lie at the heart of particle physics. Notions such as relativistic causality ("signals cannot move faster than light") naturally lead to the concepts of waves, fields, and particles as force carriers [8]. Gravity challenges this unification; for example the precise meaning of causality in a fluctuating spacetime remains unclear. In this Letter we study a situation where causality can be unambiguously stated, and is in principle experimentally testable.

Our setup is $2 \to 2$ scattering between initially well-separated objects in a flat Minkowski-like region of spacetime. A notion of causality is inherited from the flat background, and encoded in the mathematically precise axioms of scattering (S-matrix) theory. It can be used to constrain gravity itself. Consider higher-derivative corrections to Einstein's gravity at long distances:

$$S = \int \tfrac{d^D x\sqrt{-g}}{16\pi G}\left(R + \tfrac{\alpha_2}{4}C^2 + \tfrac{\alpha_4}{12}C^3 + \tfrac{\alpha_4'}{6}C'^3 + \dots\right), \tag{5.1}$$

where C^2, C^3, C'^3 are higher-curvature terms defined below. Weinberg famously argued that any theory of a massless spin-two boson must reduce to GR at long distances [183]. This was significantly extended in [77], who argued that the parameters α_i must be parametrically suppressed by the mass M of new higher-spin states. In parallel, S-matrix dispersion relations have been used to constrain signs and sizes of certain corrections [81, 80, 184].

Recently, by combining these methods we showed how to bound dimensionless ratios of the form $|\alpha_i M^i|$ in any scenario where $M \ll M_{\rm pl}$, such that corrections are larger than Planck-suppressed. However, these bounds featured the infrared logarithms that are well known to plague massless S-matrices in four dimensions.

In this Letter we present rigorous bounds in higher-dimensional gravity, where infrared issues are absent. We overcome significant technical hurdles regarding the partial wave decompositions of higher-dimensional amplitudes. The resulting bounds have interesting applications to holographic conformal field theories.

5.2 Four-point gravity amplitudes

5.2.1 Four-point S-matrices and local module

We treat the graviton as a massless particle of spin 2. The amplitude for $2 \to 2$ graviton scattering depends on the energy-momentum p_j^μ and polarization ε_j^μ of each. It can be written generally as a sum over Lorentz-invariant polynomials times scalar functions:

$$\mathcal{M} = \sum_{(i)} \mathrm{Poly}^{(i)}(\{p_j, \varepsilon_j\}) \times \mathcal{M}^{(i)}(s,t)\,. \tag{5.2}$$

We use conventions in which all momenta are outgoing and Mandelstam invariants, satisfying $s+t+u=0$, are

$$s = -(p_1+p_2)^2, \quad t = -(p_2+p_3)^2, \quad u = -(p_1+p_3)^2. \tag{5.3}$$

In kinematics where p_1, p_2 are incoming, s and $-t$ are respectively the squares of the center-of-mass energy and momentum transfer.

The allowed polynomials in (5.2) are restricted by the fact that graviton polarizations are transverse traceless and subject to gauge redundancies [178]:

$$p_j{\cdot}p_j = p_j{\cdot}\varepsilon_j = \varepsilon_j{\cdot}\varepsilon_j = 0, \quad \varepsilon_j \simeq \varepsilon_j + \# p_j\,. \tag{5.4}$$

Depending on the choice of spanning polynomials, the functions $\mathcal{M}^{(i)}(s,t)$ may develop spurious singularities which would complicate their use. As explained in [185], there exist special generators of the "local module" such that any amplitude that is polynomial in polarizations and momenta leads to $\mathcal{M}^{(i)}$'s that are polynomial in s and t. These can be simply presented using gauge- and Lorentz- invariant building blocks:

$$\begin{aligned} &H_{12} = F^{\mu}_{1\nu} F^{\nu}_{2\mu}\,, && H_{123} = F^{\mu}_{1\nu} F^{\nu}_{2\sigma} F^{\sigma}_{3\mu}\,, \\ &H_{1234} = F^{\mu}_{1\nu} F^{\nu}_{2\sigma} F^{\sigma}_{3\rho} F^{\rho}_{4\mu}\,, && V_1 = p_{4\mu} F^{\mu}_{1\nu} p_2^{\nu}\,, \end{aligned} \tag{5.5}$$

where $F^{\mu}_{i\nu} = p_i^{\mu}\varepsilon_{i\nu} - \varepsilon_i^{\mu} p_{i\nu}$ is proportional to the field strength. We define H's with other indices by permutation, and V_i by cyclic permutations.

In this notation, any S-matrix involving four photons (thus homogeneous of degree 1 in each of the vectors ε_j^{μ}) can be written as a sum of seven terms, involving three basic functions [185]:

$$\begin{aligned} \mathcal{M}_{4\gamma} = &\Big[H_{14}H_{23}\mathcal{M}^{(1)}_{4\gamma}(s,u) + X_{1243}\mathcal{M}^{(2)}_{4\gamma}(s,u) + \text{cyclic}\Big] \\ &+ S\mathcal{M}^{(3)}_{4\gamma}(s,t). \end{aligned} \tag{5.6}$$

Here, we introduced the shorthands X and S:

$$\begin{aligned} X_{1234} &= H_{1234} - \tfrac{1}{4}H_{12}H_{34} - \tfrac{1}{4}H_{13}H_{24} - \tfrac{1}{4}H_{14}H_{23}\,, \\ S &= V_1 H_{234} + V_2 H_{341} + V_3 H_{412} + V_4 H_{123}\,. \end{aligned} \tag{5.7}$$

Thanks to Bose symmetry, all basic functions $\mathcal{M}^{(i)}_{4\gamma}(a,b)$ are symmetrical in their two arguments, while the third one is further invariant under all permutations of s,t,u, since S is fully permutation symmetric. The combination X enjoys improved Regge behavior (discussed below).

The general four-graviton amplitude $\mathcal{M}$ can now be written using all products of the photon structures, supplemented by the element $\mathcal{G}$ equal to the determinant of all dot products between $(p_1, p_2, p_3, \varepsilon_1, \varepsilon_2, \varepsilon_3, \varepsilon_4)$. The resulting 29 generators organize under permutations as two singlets, seven cyclic triplets, and one sextuplet [185]:

$$\begin{aligned}
\text{singlets}:\ & \mathcal{G}\mathcal{M}^{(1)}(s,u),\ \ S^2\mathcal{M}^{(10)}(s,u),\\
\text{triplets}:\ & H_{14}^2H_{23}^2\mathcal{M}^{(2)}(s,u), H_{12}H_{13}H_{24}H_{34}\mathcal{M}^{(3)}(s,u),\\
& H_{14}H_{23}(X_{1243}-X_{1234}-X_{1324})\mathcal{M}^{(4)}(s,u), X_{1243}^2\mathcal{M}^{(6)}(s,u),\ \ X_{1234}X_{1324}\mathcal{M}^{(7)}(s,u),\\
& H_{14}H_{23}S\mathcal{M}^{(8)}(s,u),\ \ X_{1243}S\mathcal{M}^{(9)}(s,u),\\
\text{sextuplet}:\ & H_{12}H_{34}X_{1243}\mathcal{M}^{(5)}(s,u).
\end{aligned} \tag{5.8}$$

These constitute a basis in generic spacetime dimension ($D \geq 8$); lower dimensions are reviewed in appendix C.1.

5.2.2 Regge limit and dispersive sum rules

At low energies, the effect of quartic self-interactions in the effective theory (5.1) is to add polynomials in Mandelstam invariants to the amplitudes $\mathcal{M}^{(i)}$: this is a defining property of the local module [1]. We would like to use the assumption that graviton scattering remains sensible at all energies to constrain the size of these interactions.

Our axioms are best stated using smeared amplitudes:

$$\mathcal{M}_\Psi(s) \equiv \int_0^M dp\Psi(p)\mathcal{M}(s,-p^2). \tag{5.9}$$

As argued in [130, 33, 5, 186], for suitable wavefunctions Ψ, causality is interpreted as analyticity for s large in the upper-half plane, while unitarity further implies boundedness along any complex direction:

$$|\mathcal{M}_\Psi(s)|\big|_{s\to\infty} \leq s \times \text{constant}\,. \tag{5.10}$$

The essential conditions on $\Psi(p)$ are: finite support in p (required for analyticity of $\mathcal{M}_\Psi$), and normalizability at large impact parameters (ensuring boundedness).

[1] We omit terms with Riemann scalar and Ricci tensors from the action, since they are proportional to Einstein's equation of motion hence removable order-by-order in the low-energy expansion. The structure which multiplies C^2 in (5.1) is thus equivalent to the Gauss-Bonnet coupling.

H_{12}	H_{13}	H_{14}	X_{1234}	X_{1324}	X_{1243}	$X_{1234}{-}X_{1324}$	S	$\mathcal{G}$
s^1	s^1	s^0	s^2	s^2	s^1	s^1	s^2	s^2

Table 5.1: Behavior in the fixed-t Regge limit of polarization structures, omitting some simple permutations, i.e. $H_{34}{\sim}H_{12}$.

The bound (5.10) is assumed for polarizations that do not grow with energy. The behavior of the scalar functions $\mathcal{M}^{(i)}$ can be deduced from the Regge scaling of the polarization structures they multiply; leading growth rates are recorded in table 5.1. An important observation is that the leading terms are not all linearly independent, for example while both $X_{1234}, X_{1324} \sim s^2$, their difference grows more slowly. The coefficients of these structures inherit the opposite behavior. For example, the (smeared) photon amplitudes $\mathcal{M}^{(2)}_{4\gamma}(s,t) \pm \mathcal{M}^{(2)}_{4\gamma}(u,t)$ are bounded by constants times s^{-1} and s^0, respectively.

We say that a dispersive sum rule has Regge spin k if it converges assuming that $\mathcal{M}/s^k \to 0$; our axioms above state that sum rules with $k > 1$ converge. As can be seen from (5.8) and table 5.1, $\mathcal{M} \sim s^k$ implies $\mathcal{M}^{(3)} \sim s^{k-4}$, ensuring convergence of the following integral at fixed $t = -p^2$ (with $u = p^2 - s$):

$$B^{[1]}_k(p^2) = \oint_\infty \frac{ds}{4\pi i}\left[\frac{(s-u)\mathcal{M}^{(3)}(s,u)}{(-su)^{\frac{k-2}{2}}}\right] \equiv 0 \quad (k \geq 2 \text{ even}). \tag{5.11}$$

This identity yields a Kramers-Kronig type relation between scattering at low and high energies, by a standard contour deformation argument. Namely, one finds a low-energy contribution at the scale $M \ll M_{\rm pl}$ which is EFT-computable by assumption, plus a discontinuity at high energies $s \geq M^2$ (see [5] for more detail). See appendix C.4 for the low-energy amplitudes.

A salient feature of graviton scattering is that many sum rules, like $B^{[1]}_2$ above, have no denominator: only the poles of $\mathcal{M}$ contribute at low energies. Acting on the low-energy amplitude (see (C.40)), it yields:

$$8\pi G\left[\frac{1}{2p^2} + \frac{\alpha_2^2{-}2\alpha_4}{16}p^2\right] = \int_{M^2}^\infty \frac{ds}{\pi}(s-u)\text{Im}\mathcal{M}^{(3)}(s,u)\,. \tag{5.12}$$

The dependence on p is exact up to EFT-computable contributions from other light poles (such as light Kaluza-Klein modes), which we account for in our analysis below, and Planck-suppressed loop corrections, which we neglect since $M \ll M_{\rm pl}$. Thus (5.12) constitutes an infinite number of sum rules involving two EFT parameters α_i. This "superconvergence" phenomenon is related to the graviton's spin and gauge invariance, which led to the energy growth of structures in (5.8). For other sum rules we construct improved combinations $B_k^{\rm imp}(p^2)$ which are designed to probe finite sets of EFT couplings. Our complete set of sum rules is detailed in appendix C.1.1.

5.3 Construction of partial waves

Our assumptions about the right-hand-side of (5.12) and similar relations are minimal: Lorentz symmetry and unitarity with respect to the asymptotic states. The intermediate states that can appear in a scattering process in $D = d + 1$ dimensions form representations ρ under SO(d) rotations in the center-of-mass frame. Thus, the S-matrix can be written as a sum over projectors onto each representation. As far as the $2 \to 2$ S-matrix is concerned, unitarity is simply the statement that $|S_\rho| \leq 1$ for the coefficient of each projector.

The main technical complication in $D > 4$ is that many intermediate representations can appear. Furthermore, multiple index contractions can exist for a given representation. Listing them is equivalent to enumerating on-shell three-point vertices between two massless and one massive particle. We introduce here an efficient method to construct structures and projectors in arbitrary D.

5.3.1 Partial wave expansion

Concretely, the partial wave expansion for a $2 \to 2$ graviton scattering amplitude takes the form

$$\mathcal{M} = s^{\frac{4-D}{2}} \sum_\rho n_\rho^{(D)} \sum_{ij} (a_\rho(s))_{ji}\, \pi_\rho^{ij}, \tag{5.13}$$

where ρ runs over finite-dimensional irreps of SO(d), and the normalization $n_\rho^{(D)}$ is in (C.28). For completeness, a derivation of this formula is presented in appendix C.3.

The partial waves π_ρ^{ij} are functions of polarizations and momenta that transform in the representation ρ under the little group SO(d) preserving $P^\mu = p_1^\mu + p_2^\mu$. We build them by gluing vertices $v^{i,a}(n, e_1, e_2)$, where a is an SO(d)-index for ρ, i labels linearly-independent vertices, and

$$n^\mu \equiv \frac{p_2^\mu - p_1^\mu}{\sqrt{(p_1 - p_2)^2}}, \quad e_i^\mu \equiv \varepsilon_i^\mu - p_i^\mu \frac{\varepsilon_i \cdot P}{p_i \cdot P} \tag{5.14}$$

are natural vectors orthogonal to P. Note that $n^2 = 1$, and the e_i are gauge-invariant, null, and orthogonal to n:

$$n \cdot e_i = e_i^2 = 0\,. \tag{5.15}$$

In the center of mass frame, n and e_i are simply the orientation and polarizations of incoming particles. Defining an outgoing orientation similarly, $n'^\mu \propto (p_4 - p_3)^\mu$, partial waves are defined by summing over intermediate indices:

$$\pi_\rho^{ij} \equiv \left(\overline{v^i}, v^j\right) \equiv \overline{v^{i,a}}(n', e_3, e_4) g_{ab} v^{j,b}(n, e_1, e_2), \tag{5.16}$$

where g_{ab} is an SO(d)-invariant metric on ρ, and $\overline{f}$ denotes Schwarz reflection $\overline{f}(x) = (f(x^*))^*$.

Unitarity of S implies that the matrix $S_\rho(s) \equiv 1 + i a_\rho(s)$ satisfies $|S_\rho(s)| \leq 1$, which implies $0 \leq \operatorname{Im} a_\rho \leq 2$ (where an inequality of matrices is interpreted as positive-semidefiniteness of the difference). We illustrate these concepts in some examples in appendix C.3.

5.3.2 Review of orthogonal representations

A finite-dimensional irrep of SO(d) is specified by a highest weight $\rho = (m_1, \ldots, m_n)$, where $n = \lfloor d/2 \rfloor$, see e.g. [187, 188]. The m's are integers for bosonic representations and half-integers for fermionic representations, satisfying

$$m_1 \geq \cdots \geq m_{n-1} \geq |m_n|. \tag{5.17}$$

For tensor representations, $|m_i|$ are the row lengths of the Young diagram for ρ. Note that m_n must be positive in odd-d, but can be negative in even-d — the sign of m_n indicates the chirality of the representation. We omit vanishing m's from the end of the list, for instance denoting a spin-J traceless symmetric tensor by (J).

To manipulate tensors, we represent them as index-free polynomials in polarization vectors $w_1, \ldots, w_n \in \mathbb{C}^d$, one for each row. The traceless and symmetry properties of a given irrep are captured by taking these to be orthogonal and defined modulo gauge redundancies [189]:

$$w_i^2 = w_i{\cdot}w_j = 0, \quad w_j \sim w_j + \# w_i \;\; \text{for } j > i. \tag{5.18}$$

The latter means that allowed functions of w must be annihilated by $w_1{\cdot}\partial_{w_2}$, etc.. Three-point vertices are then simply $\mathrm{SO}(d)$-invariant polynomials $v^i(w_1, \ldots, w_n; n, e_1, e_2)$ where the w's play the same role for a massive particle that the ε's play for gravitons.

Polynomials satisfying the gauge condition can be easily constructed by inscribing vectors in the boxes of a Young tableau, where each column represents an antisymmetrized product with w's. For example, given vectors $a^\mu, \ldots, e^\mu \in \mathbb{C}^d$, we can define a tensor in the $(3,2)$ representation via

$$\begin{array}{|c|c|c|}\hline a & c & e \\ \hline b & d \\ \cline{1-2}\end{array} \equiv [w_1{\cdot}a \; w_2{\cdot}b - (a{\leftrightarrow}b)]\; [w_1{\cdot}c \; w_2{\cdot}d - (c{\leftrightarrow}d)]\; w_1{\cdot}e\,. \tag{5.19}$$

Any tableau defines a valid tensor. Tableaux are not unique, since we can permute columns. Also, antisymmetrizing all the boxes in one column with another box (of not higher height) yields a vanishing polynomial, e.g.:

$$\begin{array}{|c|c|}\hline a & c \\ \hline b \\ \cline{1-1}\end{array} + \begin{array}{|c|c|}\hline b & a \\ \hline c \\ \cline{1-1}\end{array} + \begin{array}{|c|c|}\hline c & b \\ \hline a \\ \cline{1-1}\end{array} = 0\,. \tag{5.20}$$

$\ytableaushort{{\bullet}{\bullet}}\ (e_1\cdot e_2)^2$ $\ytableaushort{{e_1}{e_2}{\bullet}{\bullet}}\ e_1\cdot e_2$ $\ytableaushort{{e_1}{e_1}{e_2}{e_2}{\bullet}{\bullet}}$	$\ytableaushort{{e_1}n{\bullet}{\bullet},{e_2}}\ e_1\cdot e_2$ $\ytableaushort{{e_1}{e_1}{e_2}n{\bullet}{\bullet},{e_2}}$	$(1+S)\ \ytableaushort{{e_1}{e_2}n{\bullet}{\bullet},n}\ e_1\cdot e_2$ $(1+S)\ \ytableaushort{{e_1}{e_2}{e_1}{e_2}n{\bullet}{\bullet},n}$	$\ytableaushort{{e_1}{\bullet}{\bullet},{e_2},n}\ e_1\cdot e_2$ $\ytableaushort{{e_1}{e_1}{e_2}{\bullet}{\bullet},{e_2},n}$	$\ytableaushort{{e_1}{e_1}{\bullet}{\bullet},{e_2}{e_2}}$ $\ytableaushort{{e_1}{e_2}{\bullet}{\bullet},nn}\ e_1\cdot e_2$ $\ytableaushort{{e_1}{e_2}{e_1}{e_2}{\bullet}{\bullet},nn}$	$\ytableaushort{{e_1}{e_1}{e_2}{\bullet}{\bullet},{e_2}nn,n}$ $\ytableaushort{{e_1}{e_1}{e_2}{e_2}{\bullet}{\bullet},nnnn}$
$(1+S)\ \ytableaushort{{e_1}{e_1}{e_2}{\bullet}{\bullet},{e_2}n}$	$\ytableaushort{{e_1}{e_1}{e_2}n{\bullet}{\bullet},{e_2}nn}$	$(1+S)\ \ytableaushort{{e_1}{e_1}{e_2}{e_2}n{\bullet}{\bullet},nnn}$	$\ytableaushort{{e_1}{e_1}n{\bullet}{\bullet},{e_2}{e_2},n}$	$(1+S)\ \ytableaushort{{e_1}{e_1}{e_2}n{\bullet}{\bullet},{e_2}n,n}$	$\ytableaushort{{e_1}{e_1}{\bullet}{\bullet},{e_2}{e_2},nn}$

Table 5.2: The 20 graviton-graviton-massive couplings in generic dimension ($D \geq 8$). Cells collect structures that can be in the same representation. $\ytableaushort{{\bullet}{\bullet}}$ stands for an arbitrary (possibly zero) even number of n boxes; S flips n and swaps e_1 and e_2.

5.3.3 Vertices with two massless and one heavy state

With this technology, we can straightforwardly write all three-point vertices between two gravitons and an arbitrary massive state. Here we focus on generic dimensions $D \geq 8$, relegating special cases in lower dimensions to appendix C.2. All we can write are the dot product $e_1\cdot e_2$ and Young tableaux in which each box contains either n, e_1 or e_2. Evidently, no tableau can have more than three rows, by antisymmetry.

As a warm-up, consider two non-identical massless scalars. Two-particle states form traceless symmetric tensors of rank J, i.e. single-row tableaux. The only possible SO(d)-invariant vertex involving n is then

$$(n\cdot w_1)^J = \ytableaushort{n{\cdots}n} \quad (J \text{ boxes}). \tag{5.21}$$

Denoting by $\ytableaushort{{\bullet}}$ an arbitrary (possibly zero) number of boxes containing n, the most general coupling between two scalars and a heavy particle is thus simply $\ytableaushort{{\bullet}}$.

Moving on to two spin-1 particles, one must add one power of each of e_1, e_2. These can appear either as $e_1\cdot e_2$ or inside a tableau, giving the exhaustive list:

$$\ytableaushort{{\bullet}}\, e_1\cdot e_2\,,\quad \ytableaushort{{e_1}{e_2}{\bullet}}\,,\quad \ytableaushort{{e_1}{\bullet},{e_2}}\,,\quad \ytableaushort{{e_1}{e_2}{\bullet},n}\,,\quad \ytableaushort{{e_1}{\bullet},{e_2},n}\,,\quad \ytableaushort{{e_1}{e_2}{\bullet},nn}\,. \tag{5.22}$$

A potential tableau $\ytableaushort{{e_2}{e_1}{\bullet},n}$ was removed since it is redundant thanks to (5.20). Thus, there are six possible vertices. If the two particles are identical, e.g. photons, we get additional restrictions on the parity in n — for example the number of boxes in the first two structures must be even.

The analogous basis of couplings for gravitons in generic dimension $D \geq 8$ are shown in table 5.2. This basis agrees with [118]. Changes in lower dimensions are listed in appendix C.2.

5.3.4 Gluing vertices using weight-shifting operators

To glue vertices into partial waves we need to sum over intermediate spin states. This can be achieved efficiently using weight-shifting operators [148]. A general weight-shifting operator $\mathcal{D}^a$ is an SO(d)-covariant differential operator that carries an index a for some finite-dimensional representation of SO(d), such that acting on a tensor in the representation ρ it gives a tensor in the representation with shifted weights $\rho + \delta$. We will be particularly interested in the operator $\mathcal{D}^{(h)\mu}$ that removes one box at height h from a Young diagram with height h:

$$\mathcal{D}^{(h)\mu} : \rho = (m_1, \ldots, m_h) \to (m_1, \ldots, m_h - 1) \equiv \rho'. \tag{5.23}$$

Conceptually, $\mathcal{D}^{(h)\mu}$ is a Clebsch-Gordon coefficient for $\rho' \subset \square \otimes \rho$: this ensures its existence and uniqueness up to normalization. Explicitly, $\mathcal{D}^{(h)\mu}$ is given by [2]

$$\mathcal{D}^{(h)\mu_0} = \left(\delta^{\mu_0}_{\mu_1} - \frac{w_1^{\mu_0}}{N_1^{(h)}}\frac{\partial}{\partial w_1^{\mu_1}}\right)\left(\delta^{\mu_1}_{\mu_2} - \frac{w_2^{\mu_1}}{N_2^{(h)}}\frac{\partial}{\partial w_2^{\mu_2}}\right)\cdots\left(\delta^{\mu_{h-1}}_{\mu_h} - \frac{w_h^{\mu_{h-1}}}{N_h^{(h)}-1}\frac{\partial}{\partial w_h^{\mu_h}}\right)\frac{\partial}{\partial w_{h\mu_h}}, \tag{5.24}$$

where $N_i^{(h)} = d - 1 + m_i + m_h - i - h$. Notice the shift by 1 in the last parenthesis: $1/(N_h^{(h)} - 1)$. The $h = 1$ case of (5.24) is the familiar Todorov/Thomas operator that acts on traceless symmetric tensors [116].

For the definition (5.24) to be consistent, the following properties must hold:

- $\mathcal{D}^{(h)\mu}$ preserves the gauge constraints: for all $i < j$, $w_i \cdot \partial_{w_j} \mathcal{D}^{(h)\mu} X = 0$ if X

[2]This weight-shifting operator was written in a different formalism in [141]. To our knowledge, the expression (5.24) in embedding coordinates w_i for general h is new.

satisfies the same.

- $\mathcal{D}^{(h)\mu}$ sends traces to traces. By "traces" we mean index contractions in strictly gauge-invariant polynomials (*not* just products $w_2{\cdot}w_3$) — for example, the following expression where μ denotes a unit-vector in the μ direction:

$$\sum_{\mu=1}^{d} \begin{array}{|c|c|}\hline a & c \\ \hline b & \mu \\ \hline \mu & \multicolumn{1}{c}{} \\ \cline{1-1}\end{array} \,. \tag{5.25}$$

These properties are nontrivial and determine $\mathcal{D}^{(h)\mu}$ up to an overall constant, which can be fixed by considering traces on height-h columns. For example, consider adjacent gauge transformations $w_i{\cdot}\partial_{w_{i+1}}$. Commuting across the i'th and $(i+1)$'th parentheses one finds an unwanted term proportional to $(N_i^{(h)} - m_i) - (N_{i+1}^{(h)} - m_{i+1} + 1)$, whose vanishing recursively determines all N's in terms of $N_h^{(h)}$ as stated below (5.24).

Effectively, $\mathcal{D}^{(h)}$ recovers indices from index-free polynomials and enables one to evaluate the pairing (5.16) recursively in terms of simpler pairings, for example

$$\left(\begin{array}{|c|c|}\hline a & \ \\ \hline b & \ \\ \hline c & \multicolumn{1}{c}{} \\ \cline{1-1}\end{array} \cdots , \begin{array}{|c|c|}\hline \ & \ \\ \hline \ & \ \\ \hline \ & \multicolumn{1}{c}{} \\ \cline{1-1}\end{array} \cdots \right) = \frac{1}{m_3} \left(\begin{array}{|c|c|}\hline a & \ \\ \hline b & \ \\ \hline \end{array} \cdots , c{\cdot}\mathcal{D}^{(3)} \left[\begin{array}{|c|c|}\hline \ & \ \\ \hline \ & \ \\ \hline \ & \multicolumn{1}{c}{} \\ \cline{1-1}\end{array} \cdots \right] \right)$$
$$+\, 2 \text{ cyclic rotations of } a, b, c. \tag{5.26}$$

Such a formula holds for any choice of a column of maximal height h on the left factor, giving $1/m_h$ times a sum with alternating sign over the boxes it contains, see (C.42). In practice, since $\mathcal{D}^{(h)}$ sends tableaux to tableaux, it can be elegantly implemented as a combinatorial operation, as discussed in appendix C.6.

By repeatedly applying (5.26) and its generalization (C.42), any pairing can be reduced to a pairing between single-row tableaux of length $m_1 = J$:

$$\left(\begin{array}{|c|c|c|c|c|c|}\hline a & b & c & n & \cdots & n \\ \hline \end{array} \,,\ \begin{array}{|c|c|c|c|c|c|}\hline e & f & g & n' & \cdots & n' \\ \hline \end{array} \right) . \tag{5.27}$$

This can be computed by taking derivatives with respect to n and n' of the scalar partial wave (see also [190]):

$$(\,\boxed{n|\cdots|n}\,,\ \boxed{n'|\cdots|n'}\,) = (n^{\mu_1}\cdots n^{\mu_J} - \text{traces})(n'_{\mu_1}\cdots n'_{\mu_J}) = \frac{(d-2)_J}{2^J(\frac{d-2}{2})_J}\mathcal{P}_J\,(n{\cdot}n')\,, \tag{5.28}$$

where $\mathcal{P}_J(x)$ is a Gegenbauer polynomial (see (C.32)) and $(a)_n$ is the Pochhammer symbol. Thus, (5.26) and (5.28) allow us to glue the vertices from table 5.2 into partial wave expressions which hold for arbitrary $J{=}m_1$, involving derivatives of $\mathcal{P}_J(x)$ times dot products between graviton polarizations e_j and directions n, n'. This procedure can be straightforwardly and efficiently automated on a computer.

To limit the size of final expressions, we use the Gegenbauer equation $(x^2 - 1)\partial_x^2\mathcal{P}_J(x) + \ldots = 0$ to remove any monomial of the form $x^a\mathcal{P}_J^{(b)}(x)$ with $a, b \geq 2$. We then insert a set of linearly independent polarizations to project onto the generators (5.8) of the local module and extract $\mathcal{M}^{(i)}$'s that are polynomials in x. Finally, we use the Gram-Schmidt method to find orthonormal combinations of vertices according to (C.33). As a consistency check on our results, we verified that our partial waves are eigenvectors of the SO(d) quadratic Casimir.

5.4 Results and interpretation

Dispersive sum rules like (5.12) express low-energy EFT parameters as sums of high-energy partial waves, times unknown positive couplings. The "bootstrap" game consists in finding linear combinations such that all unknowns contribute with the same sign. Such combinations yield rigorous inequalities that EFT parameters must satisfy if a causal and unitary UV completion exists.

To obtain optimal inequalities in a gravitational setting, we follow the numerical search strategy of [130, 5]. Because of the graviton pole, it is not legitimate to expand around the forward limit; rather our trial basis consists of the improved sum rules $B_k^{\text{imp}}(p^2)$ integrated against wavepackets $\psi_i(p)$ with $|p| \leq M$. We ask for a positive action on every state of mass $m \geq M$ and arbitrary SO(d) irrep, as well as on light exchanges of spin $J \leq 2$ and any mass. Full details of our implementation are given

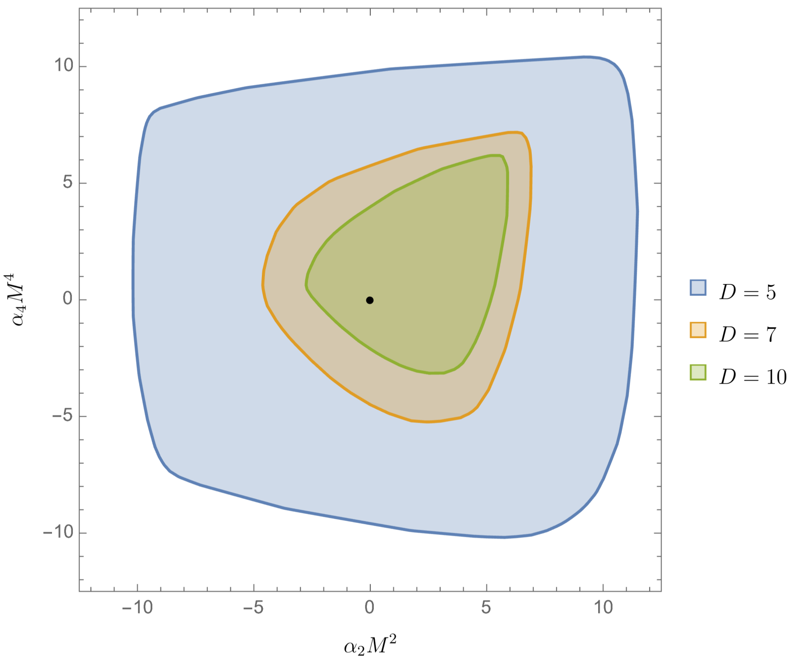

Figure 5.1: Allowed region for couplings α_2 and α_4 in $D = 5$, 7 and 10 spacetime dimensions, in units of the mass M of higher-spin states.

in appendix C.5.

Figure 5.1 displays our main result: the allowed region for the dimensionless parameters $(\alpha_2 M^2, \alpha_4 M^4)$ which control the leading corrections to the action (5.1), in terms of the mass M of higher-spin states. For the purposes of illustration, we show the results for $D = 5, 7, 10$; other dimensions D lead to qualitatively similar plots. The parameters are defined more precisely in (C.37), and enter the on-shell three-graviton vertex (C.39). It would be interesting to compare these bounds with the explicit values of Wilson coefficients in “theory islands" arising from known UV completions [191].

The M-scaling of the bounds is significant: it implies that higher-derivative corrections can never parametrically compete with the Einstein-Hilbert term, within the regime of validity of a gravitational EFT. As soon as corrections become significant, new particles must be around the corner. Since we assume $M \ll M_{\rm pl}$, graviton scattering is still weak at the cutoff. In gravity, unlike in other low-energy theories, the leading (Einstein-Hilbert) interactions cannot be tuned to zero without setting all other interactions to zero.

What happens at the scale M? Since we allowed for exchanges of arbitrary light states of low spins, M is associated with the mass of $J \geq 3$ states. The importance of higher-spin states was anticipated in [77]. In general, higher-spin states must come in towers that include all spins [84]. For instance, M could signal the beginning of a tower of higher-spin particles (as in weakly coupled string theory), that each couple to two gravitons with strength $\sim M^2\sqrt{G}$. Alternatively, M could be the energy at which loops representing a large number $N \sim M^{2-D}/G$ of two-particle states that couple with weaker strength $M^{\frac{D+2}{2}}G$ to two gravitons, become non-negligible [192] [3]. Either way, graviton scattering must be profoundly modified at the scale M and above, while remaining weak.

Our flat-space bounds have implications in curved spacetimes. As explained in [33], since the scattering processes under consideration take place in a region of small size $\sim 1/M$, flat-space dispersive bounds uplift in AdS to rigorous bounds on holographic CFTs, up to corrections suppressed by $1/(MR_{\text{AdS}}) = 1/\Delta_{\text{gap}}$.

Focusing on $D = 5$ (the $\text{AdS}_5/\text{CFT}_4$ correspondence), stress-tensor two- and three-point functions are characterized by three parameters, including the central charges a and c that enter the conformal anomaly [193]. Their relation to higher-derivative couplings is particularly simple when the EFT action is expressed in terms of Weyl tensors, so that renormalization of the AdS radius is avoided. Using the field redefinition invariant formulas from [194] we find:

$$a = \pi^2 \frac{R_{\text{AdS}}^3}{8\pi G}, \qquad \frac{c-a}{a} = \frac{2\alpha_2}{R_{\text{AdS}}^2}\,. \tag{5.29}$$

Fig. 5.1 thus implies a sharp central charge bound:

$$\left|\frac{c-a}{c}\right| \leq \frac{23}{\Delta_{\text{gap}}^2} + \mathcal{O}(1/\Delta_{\text{gap}}^4) \quad (\text{AdS}_5/\text{CFT}_4), \tag{5.30}$$

which could potentially be improved at the $\sim 5\%$ level. In holographic theories, this

[3] In a Kaluza-Klein reduction from a higher dimension, M can coincide with the higher-dimensional Planck mass. Even though gravity becomes strongly interacting at that scale, the scattering between D-dimensional gravitons remains weak, consistent with our bounds, since their wavefunctions are dilute in the extra dimensions.

result is stronger than the conformal collider bound $\frac{1}{3} \leq \frac{a}{c} \leq \frac{31}{18}$ [195] and establishes the parametric scaling anticipated in [18, 77, 79]. We stress that since $\Delta_{\rm gap}$ is the dimension of the lightest higher-spin (non double-trace) operator, the bound holds even in the presence of light Kaluza-Klein modes (as in $\mathrm{AdS}_5 \times \mathrm{S}_5$) and is generally independent of the geometry of the internal manifold. The sign of $(a-c)$ is significant [196]; our results do not exclude either sign.

The leading contact interaction in $D \geq 7$ is the 6-derivative "third Lovelock term", which is related to α_4' in (5.1). Our bounds for this coefficient depend only weakly on its sign and on α_2, α_4, and yield the absolute limits in e.g. $D = 7, 10$:

$$|\alpha_4' M^4| \leq 56 \ (D = 7), \quad |\alpha_4' M^4| \leq 25 \ (D = 10). \tag{5.31}$$

In analogy with scalar EFTs [83, 82, 86, 84, 197, 198] and four-dimensional gravitons and photons [199, 5, 200, 85], we expect this method to yield two-sided bounds on all higher-derivative interactions that can be probed by four-graviton scattering, and on many derivative couplings involving matter fields.

Acknowledgments

We thank Cyuan-Han Chang, Clifford Cheung, Yanky Landau, Petr Kravchuk, and Sasha Zhiboedov for discussions. DSD, SCH and YZL are supported by the Simons Foundation through the Simons Collaboration on the Nonperturbative Bootstrap. DSD is also supported by a DOE Early Career Award under grant no. DE-SC0019085. SCH is also supported by the Canada Research Chair program and the Sloan Foundation. JPM is supported by the DOE under grant no. DE-SC0011632. The computations presented here were conducted in the Resnick High Performance Computing Center, a facility supported by Resnick Sustainability Institute at the California Institute of Technology. This research was enabled in part by support provided by Calcul Québec and Compute Canada (Narval and Graham clusters).

Chapter 6

Flat-space structure of gluon and graviton in AdS

6.0 Bridging section

In Chapter 3, we focus on the flat-space limit of AdS scattering amplitudes for external scalars. The scalar amplitudes are well-studied in the AdS using different representations. In Chapter 3, we aimed to find a universal representation that allows us to unify the flat-space limit in those various representations. The spinning amplitudes in AdS, corresponding to the spinning correlation functions in CFT, are important but less explored because of the complexity arising from the tensor structures. In Chapter 4, we pave the way for studying spinning correlators in $\mathrm{AdS}_4/\mathrm{CFT}_3$ by proposing the helicity basis that naturally diagonalizes the OPE data up to the tree-level scattering in the AdS bulk. Using our results, we explicitly verify that the flat-space limit of gluon amplitudes in AdS indeed agrees with the flat-space gluon amplitudes, including the higher derivative corrections.

Although technically hard to prove, the validity of the flat-space limit is intuitively natural, as depicted in Fig 1.2. In this picture, the impact parameter b of the scattering follows the hierarchy $R_{\mathrm{AdS}} \gg b > \ell_s \gg \ell_{\mathrm{pl}}$. This drives the interest to ask whether it is possible to simply predict AdS scattering beyond the local region $R_{\mathrm{AdS}} \gg b$ from the flat-space scattering data. The answer to this question is positive:

slightly beyond the local region as $R_{\text{AdS}} \sim b$, [33] shows that the healthy values of Wilson coefficients in the flat-space low-energy EFTs can be extended to AdS. Using this argument, we studied gravitational EFT in $D \geq 5$ in Chapter 5 and uplifted our rigorous bounds on the low-lying Wilson coefficients to predict the allowed space of the central charges' ratio in holographic CFTs.

Recent developments show that the tree-level flat-space amplitudes of scalars can even predict the full scalar AdS amplitudes (that can happen way beyond the local region). This is realized by the differential representation [21, 22, 23, 24, 26, 25, 3, 93, 93, 1], which can uplift flat-space amplitudes by replacing kinematic variables by conformal generators. In this Chapter, as the duplication of [6], we will generalize the differential representation to three and four-point gluon and graviton amplitudes in AdS, arising from Yang-Mills theory and Einstein gravity. Our results provide possibility to uplift the gluon and graviton amplitudes from flat-space to AdS by using the weight-shifting operators with reordering. The uplift makes the differential double copy relation [201, 202, 203] at the three-point level straightforward. For four-point Yang-Mills amplitudes, we managed to uplift the Bern-Carrasco-Johansson (BCJ) relation [134], which can be useful for proving the differential doubly copy at the four-point level in the future.

In summary, Chapter 3 and 4 are making progress in answering **Q1** that we asked in the introduction by restricting to the picture Fig 1.2. In contrast, the last Chapter 5 and this Chapter intend to answer **Q2** that we asked in the introduction, aiming to gain a deeper understanding of Fig 1.3.

6.1 Introduction

Scattering theory plays an essential role in understanding the fundamental principles of particles. For past decades, there has been huge progress in scattering theory in flat-space, which not only successfully predicts and explains many exciting discoveries made by collider [8], but also remarkably reveals hidden structures linked to the entity of local quantum field theories, such as Bern-Carrasco-Johansson (BCJ) relations [134] and the double copy structures [201, 202, 203].

However, our universe is not flat. Although our universe is generally curved, the local scattering of particles in a small regime compared to the curvature can still be approximated by flat-space physics, as verified by scattering experiments. It is then natural and crucial to ask, do those beautiful structures of scattering remain for curved spacetime? How good can the locally flat scattering experiments say about curved spacetime? A natural starting point to answer these questions would be studying other maximally symmetric spacetimes, such as Anti de-Sitter (AdS) and de-Sitter (dS) space.

AdS scattering is studied extensively due to its correspondence with conformal field theories (CFT) [9]. The unitary AdS physics can be explored by using unitary large-N CFT [1] that is highly constrained by conformal symmetry and crossing symmetry (see [12, 13] for quick reviews). As expected, the appropriate limit of conformal correlators and conformal data corresponds to the flat-space limit of local AdS scattering, giving back the flat-space scattering data (see, e.g., [21, 22, 23, 24, 26, 25, 3, 93, 93, 1] and references therein) [2]. However, previously it is usually not expected to reconstruct full AdS amplitudes/CFT correlators from flat-space. In this sense, the flat-space limit of AdS/CFT is crucially different from "flat holography" [90]. Recent progress was made in [29, 30, 31, 7, 32, 206, 207], which surprisingly found the differential representation of scalar (A)dS amplitudes by writing (A)dS amplitudes as conformal generators acting on scalar contact Witten diagrams. This differential representation not only makes flat-space limit manifest but also allows one to uplift the flat-space amplitudes to (A)dS in a universal way.

In this paper, we aim to progress toward extending the differential representation to spinning correlators by focusing on massless gluon and graviton in AdS from Yang-Mills (YM) theory and Einstein gravity. Massless spinning particles in flat-space are constrained by stringent consistency conditions and encode hidden structures such

[1]For dS, although it turns out its essential structures are similar to AdS and analytic continuation exists to go from one to another [204], the unitarity of dS scattering is not a standard concept from CFT perspective [205].

[2]However, there exist exemptions for special analytic regimes that are not well-understood yet, see [3] for recent explorations.

as double copy [201, 202, 203]. We report the differential representation for YM and graviton amplitudes in AdS. We show we can uplift gluon and graviton amplitudes in AdS from flat-space up to a finite number of additional contact structures. We argue and expect that the additional contact structures can be bootstrapped by requiring the conservation of conserved currents and stress-tensors. The same arguments also apply to hidden structures like BCJ relations and the double copy, which are now in a differential format. Although we start our exploration in AdS, our results should be readily translated to dS [208].

The rest of this paper is organized as follows. In section 6.2, we introduce our differential operators for representing spinning correlators and comment on power counting principles in CFT. In section 6.3, we construct the differential representation for three-point and four-point YM amplitudes and graviton amplitudes; we show that the double copy is straightforward for three-point amplitudes. In section 6.4, we propose another differential representation for YM amplitudes, which allows us to uplift flat-space BCJ numerators and prove the differential BCJ relations. We summarize and point out future directions in section 6.5. We record detailed ingredients in our derivations in appendix D.2 and D.3.

Note: During the preparation of this work, [209] appeared, which has partial overlap with the idea of using weight-shifting operators and the discussions on three-point double copy in section 6.2 and subsection 6.3.1.

6.2 Building blocks for differential representation

This section introduces our notations and building blocks for differentially representing conserved current and stress-tensor correlators.

For scalars, it is easy to find the differential representation for any contact diagrams up to any points by using the coset construction [32]. The spirit is that the contracted bulk derivatives can be replaced by the contractions of conformal generators, as guaranteed by the conformal symmetry. For spinning objects, the tensor structures appear, which can either contract among themselves or with bulk derivatives. From the perspective of CFTs, the spinning indices shall be captured by the spin-up weight-shifting operator [148] (written in terms of embedding formalism [47])

$$\mathcal{D}_{\mu}^{0+} = (J+\Delta)Z_{\mu} + X_{\mu} Z\cdot\partial_X\,, \tag{6.1}$$

where X, Z are coordinates and polarizations in the embedding space of CFTs, they obey $X^2 = Z^2 = X\cdot Z \equiv 0$. Δ and J are the scaling dimension and spin of the operators it acts on, On the other hand, we speculate and show that bulk derivatives can be replaced by dimension-up weight-shifting operator $\mathcal{D}^{+0}$ (that raises the scaling dimensions [148]) modulo bulk coordinates

$$\begin{aligned}\mathcal{D}_{\mu}^{+0} &= c_1\partial_{X^{\mu}} + c_2 X_{\mu}\partial_X^2 + c_3 Z_{\mu}\partial_Z\cdot\partial_X + c_4 Z\cdot\partial_X\partial_{Z^{\mu}}\\ &\quad + c_5 X_{\mu} Z\cdot\partial_X\partial_Z\cdot\partial_X + c_6 Z_{\mu} Z\cdot\partial_X\partial_Z^2\\ &\quad + c_7 X_{\mu}(Z\cdot\partial_X)^2\partial_Z^2\,,\end{aligned} \tag{6.2}$$

where the coefficients can be found in [148]. An intuitive way to convince ourselves that the dimension-up weight-shifting operator plays a role like momentum in flat-space is that the flat-space momentum is $i\partial/\partial x$ which also increases the "scaling dimensions". In this paper, we find that it is instructive to define the following differential operators proportional to weight-shifting operators with state-dependent normalizations

$$\begin{aligned}\mathcal{E} &= -\frac{\big(X\cdot\partial_X + Z\cdot\partial_Z\big)}{X\cdot\partial_X\big(X\cdot\partial_X+1\big)}\mathcal{D}_{\mu}^{0+}\,,\\ \mathcal{P} &= \frac{2}{(X\cdot\partial_X+1)(d+X\cdot\partial_X-2)(d+2X\cdot\partial_X-2)}\mathcal{D}_{\mu}^{+0}\,,\end{aligned} \tag{6.3}$$

where $-X\cdot\partial_X$ gives Δ when it acts on operators with scaling dimension Δ, and $Z\cdot\partial_Z$ gives J when it acts on spin-J operators.

Before ending this section, we want to comment, in general, on how (6.3) can serve as fundamental ingredients for large- N CFT with natural power counting rules. We will show that YM and graviton amplitudes can be uplifted from flat-space to AdS by using (6.3). In addition to these examples, we claim that using (6.3) can uplift flat-space amplitudes of effective field theories (EFT) to AdS as general large-N conformal correlators, where Wilson coefficients depend on details of the conformal theory. The reason is that we find bulk derivatives can be replaced by $\mathcal{P}$ module additional terms with fewer numbers of $\mathcal{P}$. This claim implies that CFT correlators at large-N limit enjoy the same power counting rules as EFTs in flat-space, which also makes manifest of the counting maps between conformal correlators and flat-space amplitudes [117]. Remarkably, in this way, different OPE structures can be easily distinguished. For example, three-point functions of conserved currents in generic CFT have two parity-even structures corresponding to F^2 and F^3 in AdS bulk, respectively. There was no obvious way to construct three-point structures precisely corresponding to them using embedding formalism or spin-up operators [47]. This is the main reason that spinning bootstrap is so hard to perform since the OPE matrix might be messy in an inappropriate basis [141]. The helicity basis provides a clean way to organize the OPE matrix in CFT$_3$ [2]. However, simply staring at them is still challenging to distinguish between the two structures. Now (6.3) makes the distinction manifest as for flat-space amplitudes! In this way, the differential representation in terms of (6.3) with power counting rules encoded could be useful for a clean spinning bootstrap even beyond holographic CFTs in the future. We elaborate on the discussions here in appendix D.1.

6.3 Construction of the differential representation

We consider the following action for Yang-Mills theory and Einstein gravity

$$S=\int d^{d+1}x\sqrt{g}\Big(\frac{1}{16\pi G}(R-2\Lambda)-\frac{1}{4g_{\rm YM}^2}F^a_{\mu\nu}F^{a\mu\nu}\Big)\,, \tag{6.4}$$

where $\Lambda=-(d-1)(d-2)/(2R_{\rm AdS}^2)$. In this paper, we usually set $R_{\rm AdS}=1$ unless we emphasize it. Our goal is to compute the four-point function for conserved currents and stress-tensors in holographic CFT that is effectively described by (6.4). These "amplitudes" can be computed by using the holographic dictionary [10, 11]

$$\mathcal{M} := \langle \mathcal{O}_1 \cdots \mathcal{O}_n \rangle = \Big(\prod_i \frac{\delta}{\delta \mathcal{J}_i^{(0)}}\Big) \big\langle e^{-S_{\rm bulk}} \big\rangle_{\rm bulk} \,, \tag{6.5}$$

where $\mathcal{J}_i^{(0)}$ denotes the source as the non-normalizable mode of bulk fields, and we keep the spinning indices implicit. The variations produce the bulk-to-boundary propagators, and the remaining fields are Wick contracted by the bulk expectation value.

6.3.1 Warm-up: three-point amplitudes

6.3.1.1 Yang-Mills

We start by looking into three-point functions as a warm-up. For YM theory, it is rather straightforward to evaluate the three-point function

$$\mathcal{M}_{3,\rm YM} = g_{\rm YM} \int D^{d+1}Y \, f^{abc} V^{\mu,ab}_{g,12}(Y) \delta_3 A^c_\mu \,, \tag{6.6}$$

where we are using the embedding AdS coordinate Y [210] and the shorthand notation $D^{d+1}Y := d^{d+2}Y \, \delta(Y^2+1)$. For latter convenience, we explicitly write the three-point vertex function $V^{\nu,ab}_{ij}$

$$\begin{aligned} V^{\nu,ab}_{g,12} &= \big(\nabla_\mu \delta_1 A^{\nu a} \delta_2 A^{\mu b} - \delta_1 A^{\mu a} \nabla_\mu \delta_2 A^{\nu b}\big) \\ &+ \frac{1}{2}\big(\delta_1 A^{\mu a} \nabla^\nu \delta_2 A^b_\mu - \nabla^\nu \delta_1 A^a_\mu \delta_2 A^{\mu b}\big) \,, \end{aligned} \tag{6.7}$$

where $\delta_i A$ denotes the bulk-to-boundary propagator (in terms of the embedding space formalism [210])

$$\delta_i A^{\mu a} = \mathcal{C}_{d-1,1} \frac{2\big(X_i^\mu \, Y\cdot Z_i - Z_i^\mu \, Y \cdot X_i\big)}{\big(-2X_i\cdot Y\big)^d} \,. \tag{6.8}$$

We use the standard normalization

$$\mathcal{C}_{\Delta,J} = \frac{\pi^{-\frac{d}{2}}\Gamma(\Delta)(\Delta+J-1)}{2(\Delta-1)\Gamma\left(-\frac{d}{2}+\Delta+1\right)} \,. \tag{6.9}$$

Usually, it is also instructive to introduce the bulk embedding polarizations W to contract the bulk indices, where $W^2 = W \cdot Y \equiv 0$. Appropriate differential operators can recover the bulk indices [210]. It is easy to explicitly evaluate three-point functions like (6.7). Nevertheless, in this paper, we aim to provide a differential representation that rewrites (6.7) in terms of differential operators acting on scalar seeds with zero derivatives. As we claim in the last section, the bulk-to-boundary propagators shall be represented by weight-shifting operators modulo bulk coordinates. In our conventions, we find

$$\begin{aligned} \delta_i A_\mu &= \mathcal{E}_{i,\mu}\delta_i\phi_{d-1}\,, \\ \nabla_\mu \delta_i A_\nu &= \frac{d-1}{2}\Big(\mathcal{E}_{i,\nu}\mathcal{P}_{i,\mu}\delta_i\phi_{d-2} - Y_{(\mu}\mathcal{E}_{i,\nu)}\delta_i\phi_{d-1}\Big)\,, \end{aligned} \tag{6.10}$$

where $\delta\phi_\Delta$ denotes the bulk-to-boundary propagator of scalar ϕ whose corresponding operator has scaling dimension Δ. Aside of the second part of the second line in (6.10), we have already observed flat-space structure by identifying $\mathcal{E} \to \epsilon$, $\mathcal{P} \to p$, and the transverse property also remains

$$\mathcal{E}_i \cdot \mathcal{P}_i \, \delta_i\phi_{d-2} = 0\,. \tag{6.11}$$

The overall coefficient $(d-1)/2$ seems to ruin the precise flat-space structure, but we claim this is the normalization factor that can be absorbed into the plane wave in the flat-space limit. For $\mathrm{AdS}_4/\mathrm{CFT}_3$, this normalization is precisely unit. We can then readily show (6.7) can be rewritten by

$$\begin{aligned} \mathcal{M}_{3,\mathrm{YM}} = &-\frac{d-1}{2} g_{\mathrm{YM}}\mathcal{T}_{\mathcal{O}}\Big((\mathcal{E}_2\cdot\mathcal{E}_3)(\mathcal{E}_1\cdot\mathcal{P}_2)W_{d-1,d-2,d-1} \\ &-\big(1\leftrightarrow 2\big) + \big(2\to 1, 1\to 3\big)\Big) f^{123}\,, \end{aligned} \tag{6.12}$$

where W_{Δ_i} refers to the scalar contact Witten diagram with no derivatives, and $i \leftrightarrow j$ also permutes the corresponding legs for the contact Witten diagram. $\mathcal{T}_{\mathcal{O}}$ means the operator ordering, which always place $\mathcal{E}$ on the left hand side of $\mathcal{P}$ for the same point. For simplicity in this letter, we define the amplitudes by pure differential forms with contact seeds slipped off $\widehat{\mathcal{M}}$. It is easy to recover the contact seeds and go from $\widehat{\mathcal{M}}$ to $\mathcal{M}$ by power counting $\mathcal{P}$. By dividing appropriate normalization, (6.12) is a trivial uplift from flat-space by taking $\epsilon \to \mathcal{E}$, $p \to \mathcal{P}$ followed by operator reordering. It is also straightforward to uplift another three-point vertex corresponding to the cubic term F^3, see appendix D.1.

6.3.1.2 Graviton

For graviton three-point amplitude, we find (see also [163])

$$\mathcal{M}_{3,\text{grav}} = 4\sqrt{8\pi G}\int D^{d+1}Y V^{\mu\nu}_{h,12}(Y)\delta_3 h_{\mu\nu}\,, \tag{6.13}$$

where the vertex function $V^{\mu\nu}_{h,12}$ is lengthy and we leave its explicit expression to appendix D.2. Similarly, $\delta_i h_{\mu\nu}$ is the bulk-to-boundary propagator for graviton, given by (we dot it into bulk embedding polarizations to keep it light)

$$\delta_i h_{\mu\nu} W^\mu W^\nu = \mathcal{C}_{d,2}\frac{4\left(W\cdot X_i\, Y\cdot Z_i - W\cdot Z_i\, X_i\cdot Y\right)^2}{(-2X_i\cdot Y)^{d+2}}\,. \tag{6.14}$$

As we promise, we find

$$\begin{aligned}
\delta_i h_{\mu\nu} &= \mathcal{E}_{i,\mu}\mathcal{E}_{i,\nu}\delta_i\phi_d\,,\\
\nabla_\mu\delta_i h_{\nu\rho} &= \mathcal{E}_{i,\nu}\mathcal{E}_{i,\rho}\mathcal{P}_{i\mu}\delta_i\phi_{d-1} + \mathcal{O}(Y)\,,\\
\nabla_\mu\nabla_\nu\delta_i h_{\rho\sigma} &= \mathcal{E}_{i,\rho}\mathcal{E}_{i,\sigma}\mathcal{P}_{i\mu}\mathcal{P}_{i\nu}\delta_i\phi_{d-2} + \mathcal{O}(Y,g)\,,
\end{aligned} \tag{6.15}$$

where we drop out the lengthy terms depending on bulk coordinates and metric Y_μ and $g_{\mu\nu}$. We record the complete expressions in appendix D.3. As contracted, these terms $\mathcal{O}(Y,g)$ can either be annihilated or give rise to contact terms with fewer derivatives. For the three-point function, they are completely canceled, and we arrive at a precisely flat-space uplift

$$\widehat{\mathcal{M}}_{3,\text{grav}} = \mathcal{T}_{\mathcal{O}}\left(\mathcal{M}^{\text{flat}}_{3,\text{grav}}\Big|_{\epsilon\to\mathcal{E},p\to\mathcal{P}}\right). \tag{6.16}$$

6.3.1.3 The differential double copy

Using differential operators (6.3), three-point amplitudes have the same structure as in flat-space up to universal reordering. Therefore, the double copy structure at the three-point level should be straightforward. To show this, we find that although $\mathcal{P}$ itself is not conserved as the momentum, effective conservation emerges at the level of three-point amplitudes for both YM and graviton, e.g., three-point amplitudes are invariant under the following replacement

$$\mathcal{E}_3 \cdot \mathcal{P}_2 \to -\mathcal{E}_3 \cdot \mathcal{P}_1\,, \quad \mathcal{P}_1 \cdot \mathcal{P}_2 \to 0\,. \tag{6.17}$$

Keeping these identities in mind, three-point amplitudes in AdS then make not much difference from flat-space, and the differential double copy is valid

$$\widehat{\mathcal{M}}_{3,\text{grav}} = \frac{4}{(d-1)^2}\frac{8\sqrt{8\pi G}}{g^2_{\text{YM}}}\mathcal{T}_{\mathcal{O}}\left[(\widehat{\mathcal{M}}_{3,\text{YM}})^2\right]. \tag{6.18}$$

6.3.2 Four-point amplitudes

6.3.2.1 Yang-Mills

Let us start by considering only the s-channel exchange diagram in YM theory

$$\begin{aligned}\mathcal{M}^{(s)}_{4\text{ex,YM}} =& g^2_{\text{YM}}\int D^{d+1}Y_1 D^{d+1}Y_2\, f^{abc}f^{deg}\times \\ & V^{\mu,ab}_{g,12}(Y_1)\left\langle A^c_\mu(Y_1)A^g_\nu(Y_2)\right\rangle_{\text{bulk}} V^{\nu,de}_{g,34}(Y_2)\,,\end{aligned} \tag{6.19}$$

where the expectation value of the remaining bulk fields gives rise to the bulk-to-bulk propagator

$$\langle A_\mu(Y_1) A_\nu(Y_2)\rangle := \Pi_{g,\mu\nu}(Y_1, Y_2)\,, \tag{6.20}$$

which satisfies the following equation in the transverse gauge

$$\nabla^2_{Y_1} \Pi_{g,\mu\nu}(Y_1, Y_2) = -\delta_{\mu\nu}\, \delta(Y_1 - Y_2)\,. \tag{6.21}$$

The trick to finding the differential representation is eliminating the bulk-to-bulk propagator by the conformal Casimir operator minus its eigenvalue for the propagating field. This procedure produces effective contact diagrams that include only the bulk-to-boundary propagators. Indeed, we find

$$\mathcal{D}_{12}^{d-1,1} V_{12}^{\mu,ab} = \nabla^2_{Y_1} V_{12}^{\mu,ab}\,, \tag{6.22}$$

where

$$\mathcal{D}_{12}^{\Delta,J} = \mathcal{C}_{12} - \big(\Delta(\Delta-d) + J(J+d-2)\big)\,, \tag{6.23}$$

The conformal Casimir $\mathcal{C}_{12}$ is

$$\mathcal{C}_{12} = -\frac{1}{2}(L_1 + L_2)^2\,, \quad L_i^{\mu\nu} = X_i^{[\mu} \partial_{X_i}^{\nu]} + Z_i^{[\mu} \partial_{Z_i}^{\nu]}\,. \tag{6.24}$$

By integration-by-parts, we can move this bulk Laplacian to act on the bulk-to-bulk propagator and (6.21) then reduces it to effective contact interactions (note $\mathcal{D}_{12}^{d-1,1} \equiv \mathcal{C}_{12}$)

$$\mathcal{C}_{12} \mathcal{M}^{(s)}_{\text{4ex,YM}} = -g^2_{\text{YM}} \int D^{d+1}Y\, f^{abe} f^{cde} V_{12}^{ab}(Y) \cdot V_{34}^{cd}(Y)\,, \tag{6.25}$$

We can then represent these effective contact terms using (6.10). In addition to the exchanged diagram, the YM theory also provides a four-point contact diagram A^4.

This contact diagram can be trivially uplifted from flat-space using (6.10). Combining with permutations to include all channels, we obtain

$$\widehat{\mathcal{M}}_{4,\text{YM}} = \frac{(d-1)^2}{4}\mathcal{T}_{\mathcal{O}}\Big(\widehat{\mathcal{M}}_{4,\text{YM}}\Big|_{\epsilon\to\mathcal{E},p\to\mathcal{P},1/s_{ij}\to 1/(2\mathcal{D}_{ij}^{d-1,1})}\Big)\,, \tag{6.26}$$

where we follow [7, 32] to define the operator $1/\mathcal{D}_{ij}$ satisfying $1/\mathcal{D}_{ij}\,\mathcal{D}_{ij}\equiv 1$, and now the operator ordering $\mathcal{T}_{\mathcal{O}}$ always keeps $1/\mathcal{D}_{ij}$ on the most left.

6.3.2.2 Graviton

We follow the same logic for evaluating graviton amplitudes

$$\begin{aligned}\mathcal{M}^{(s)}_{4\text{ex,grav}} =& 16\times 8\pi G\int D^{d+1}Y_1 D^{d+1}Y_2\times\\ &V^{\mu\nu}_{h,12}(Y_1)\big\langle h_{\mu\nu}(Y_1)h_{\rho\sigma}(Y_2)\big\rangle_{\text{bulk}}V^{\rho\sigma}_{h,34}(Y_2)\,.\end{aligned} \tag{6.27}$$

To correctly deal with the graviton, we must be careful about the trace part of the graviton and the vertex. We adopt the de-Donder gauge for bulk-to-bulk propagating gravitons and a meticulous analysis shows [7, 211] (see also appendix D.4 for more details)

$$\begin{aligned}\mathcal{D}^{d,2}_{12}\mathcal{M}^{(s)}_{4\text{ex,grav}} =& 16\times 8\pi G\int D^{d+1}Y\times\\ &V^{\mu\nu}_{h,12}(Y)P_{\mu\nu,\rho\sigma}V^{\rho\sigma}_{h,34}(Y)\,,\end{aligned} \tag{6.28}$$

where $P_{\mu\nu,\rho\sigma}$ is the projector precisely the same as the flat-space propagator

$$P_{\mu\nu,\rho\sigma} = -\frac{1}{2}\Big(g_{\mu\rho}g_{\nu\sigma} + g_{\mu\sigma}g_{\rho\sigma} - \frac{2}{d-1}g_{\mu\nu}g_{\rho\sigma}\Big)\,. \tag{6.29}$$

The resulting contact terms can then be represented by using (6.15) (precisely one is (D.13)). To have well-defined amplitudes, we should also include four graviton contact contributions from the Einstein-Hilbert action ((D.12) in appendix D.2). These contributions can again be rewritten using (6.15). We can use many identities to eliminate all Y dependences (see appendix D.3). This procedure represents the graviton amplitude in terms of differential operators $\mathcal{E}$ and $\mathcal{P}$. We find that we can write down the resulting differential amplitude by uplifting the flat-space graviton amplitude plus an extra contact contribution coming from the cosmological constant term in the action $S_\Lambda \propto \int d^{d+1}x\sqrt{-g}\Lambda$

$$\begin{aligned}\widehat{\mathcal{M}}_{4,\text{grav}} =&\mathcal{T}_{\mathcal{O}}\Big(\widehat{\mathcal{M}}_{4,\text{grav}}\Big|_{\epsilon\to\mathcal{E},p\to\mathcal{P},1/s_{ij}\to 1/(2\mathcal{D}^{d,2}_{ij})}\Big)\\ &+\frac{1}{R^2_{\text{AdS}}}\widehat{\mathcal{M}}^{\text{AdS}}_{4,\text{grav}}\,. \end{aligned} \tag{6.30}$$

We explicitly write down $1/R^2_{\text{AdS}}$ to emphasize that this term is solely contributed by the AdS term S_Λ and is vanishing in the flat-space limit. This extra term is

$$\begin{aligned}\widehat{\mathcal{M}}^{\text{AdS}}_{4,\text{grav}} =& 4\pi G d\Big(\big((\mathcal{E}_1\cdot\mathcal{E}_2)^2(\mathcal{E}_3\cdot\mathcal{E}_4)^2\\ &-4\mathcal{E}_1\cdot\mathcal{E}_2\,\mathcal{E}_2\cdot\mathcal{E}_3\,\mathcal{E}_3\cdot\mathcal{E}_4\,\mathcal{E}_4\cdot\mathcal{E}_1\big)+\text{perm}\Big)\,. \end{aligned} \tag{6.31}$$

Under the gauge transformation $h_{\mu\nu}\to h_{\mu\nu}+\nabla_{(\mu}\xi_{\nu)}$, the action cannot be gauge invariant without S_Λ. For this reason, the term $\widehat{\mathcal{M}}^{\text{AdS}}_{4,\text{grav}}$ in the amplitude has to exist as the consequence of the gauge invariance in the AdS bulk (which is the conservation of stress-tensors on the CFT side). This provides an idea to “bootstrap” stress-tensor correlators from flat-space amplitudes. To obtain the stress-tensor correlator, we can directly uplift the flat-space amplitudes and then append the enumerated crossing symmetric structures with fewer numbers of $\mathcal{P}$. The coefficients of those appended structures should be fixed by requiring the conservation of stress-tensors.

6.3.3 Comment on gauge invariance and conservation

Before we end this section, we would like to discuss and comment on the relation between bulk gauge invariance and boundary conservation law using our uplift operators (6.3).

From the bulk perspective, the action is invariant under the gauge transformation

$$A_\mu \to A_\mu + \nabla_\mu \chi\,, \quad h_{\mu\nu} \to h_{\mu\nu} + \nabla_{(\mu}\xi_{\nu)}\,, \tag{6.32}$$

where χ is arbitrary scalar and ξ vector. According to our statement that bulk derivatives can be replaced by $\mathcal{P}$ modulo bulk coordinates, we expect this gauge invariance, as in flat-space, to be represented by the invariance of boundary correlator under

$$\mathcal{E}_\mu \to \mathcal{E}_\mu + \#\mathcal{P}_\mu\,. \tag{6.33}$$

In other words, if we replace $\mathcal{E}$ by $\mathcal{P}$ (without changing the scaling dimension of the building scalar contact), the correlator should be completely vanishing

$$\mathcal{M}\Big|_{\mathcal{E}_i\to\mathcal{P}_i} = 0\,. \tag{6.34}$$

This statement reminds us of the conservation of conserved current and stress-tensor, as promised by AdS/CFT correspondence [9, 10, 11]. To show this, we should first recover the boundary tensor indices by using

$$\mathcal{D}_Z^\mu = \frac{d-2}{2}\partial_Z^\mu + Z\cdot\partial_Z\partial_Z^\mu - \frac{1}{2}Z^\mu\partial_Z^2\,, \tag{6.35}$$

then we contract one index with a boundary derivative. For the same point, we can show

$$\begin{aligned}
&\partial_X\cdot\mathcal{D}_Z\,\mathcal{E}_\mu = -\frac{2}{d}\mathcal{P}_\mu\,,\\
&\partial_X\cdot\mathcal{D}_Z\,\mathcal{E}_\mu\mathcal{E}_\nu = -\frac{2d}{(d+2)(d-1)(d-2)}\mathcal{P}_\mu\mathcal{E}_\nu\,,
\end{aligned} \tag{6.36}$$

where the first line is the identity for conserved currents and the second line for stress-tensors [3]. These identities confirm that the conservation is equivalent to (6.34) and

[3]These identities can trivially pass the strange operator $1/\mathcal{D}_{ij}$, because the Ward identity always allows us to change (ij) legs to other legs that $\partial_X\cdot\mathcal{D}_Z$ does not act.

is consistent with the expectation from bulk gauge invariance. We then claim we can even uplift the flat-space gauge invariance condition!

However, it is hard to impose or verify the conservation condition (6.34) for differential representation. Because there are several difficulties arise after we do the replacement $\mathcal{E} \to \mathcal{P}$. Firstly, the ordering of differential operators is no longer in the operator ordering, which makes the organization messy. Secondly, it is not trivial to move differential operators to remove the poles $1/\mathcal{D}_{ij}$. In the end, we do not find conservation of $\mathcal{P}$ analogous to flat-space [4]. We leave these problems to be resolved in the future works.

6.4 Differential BCJ relation for YM amplitudes

6.4.1 Differential representation using conformal generators

We have already found a differential representation for YM amplitudes in terms of the weight-shifting operators. However, for the four-point case, we need the simple analogy of the momentum conservation in flat-space in terms of $\mathcal{P}$. On the other hand, the conformal generators enjoy the analogy of "momentum conservation" because of conformal symmetry

$$\sum_{i=1}^{n} L_i^{\mu\nu} f(X_i) \equiv 0 \,, \tag{6.37}$$

where $f(X_i)$ is any conformal invariant function. To manifest hidden structures of YM amplitude, we propose replacing $\mathcal{P}$ with the conformal generators. Although it is not obvious, we indeed find such a replacement

$$\mathcal{E}_i \cdot P_j \mathcal{E}_k \cdot P_l \to 2\mathcal{E}_i^{\mu}\mathcal{E}_k^{\nu} L_{j\mu}{}^{\rho} L_{l\rho\nu} \,, \quad P_i \cdot P_j \to -\frac{1}{2} L_i \cdot L_j \,, \tag{6.38}$$

[4] Since the replacement $\mathcal{E} \to \mathcal{P}$ makes even YM amplitude not linear in $\mathcal{P}$, the simple representation using conformal generator proposed in sec 6.4 does not work.

simultaneously the scalar contact seeds are now uniform $W_{d-1,d-1,d-1,d-1}$. We now arrive at an differential representation that enjoys the "momentum conservation" (that we can replace L_4 by $-L_1 - L_2 - L_3$) and the transversity

$$\mathcal{E}_i^\mu \mathcal{E}_k^\nu L_{i\mu}{}^\rho L_{l\rho\nu} = 0 \,, \quad \mathcal{E}_i^\mu \mathcal{E}_k^\nu L_{j\mu}{}^\rho L_{k\rho\nu} = 0 \,. \tag{6.39}$$

6.4.2 Establishing the differential BCJ

Similar to the flat-space, it is instructive to study the color-ordered amplitudes. We can easily extract the color-ordered amplitudes by recalling

$$\begin{aligned} f^{12e} f^{34e} = &\operatorname{Tr}\big(T^1 T^2 T^3 T^4\big) - \operatorname{Tr}\big(T^1 T^2 T^4 T^3\big) \\ &- \operatorname{Tr}\big(T^1 T^3 T^4 T^2\big) + \operatorname{Tr}\big(T^1 T^4 T^3 T^2\big) \,. \end{aligned} \tag{6.40}$$

The colour-ordered amplitude $\mathcal{M}[i_1, i_2, i_3, i_4]$ is the coefficient of $\operatorname{Tr}\big(T^{i_1} T^{i_2} T^{i_3} T^{i_4}\big)$.

Let us take $\mathcal{M}[1234]$ as an example. We find, similar to the flat-space, we can write the color-slipped amplitude as

$$\widehat{\mathcal{M}}[1234] = \frac{1}{\mathcal{D}_{12}^{d-1,1}} \mathcal{N}_s - \frac{1}{\mathcal{D}_{23}^{d-1,1}} \mathcal{N}_t \,. \tag{6.41}$$

As in flat-space, the differential numerator $\mathcal{N}$ is also ambiguous. For example, shifting $\mathcal{N}_s$ by $\mathcal{N}_s \to \mathcal{N}_s + \text{const} \times \mathcal{D}_{12}^{d-1,1}$ and similarly for $\mathcal{N}_t$ doesn't change the amplitudes. It is not hard to find such numerators satisfying the following permutation properties

$$\mathcal{N}_s\big|_{2\leftrightarrow 4} = -\mathcal{N}_t \,, \quad \mathcal{N}_s\big|_{2\to 4, 3\to 2, 4\to 3} = \mathcal{N}_t \,, \tag{6.42}$$

which could be obtained by uplifting flat-space numerators

$$\mathcal{N}_s = \mathcal{T}_{\mathcal{O}}\Big(n_s^{\text{flat}}\Big|_{\epsilon\to\mathcal{E}, p\to\mathcal{P}} \Big) \,, \tag{6.43}$$

followed by replacement (6.38). Nevertheless, even though we uplift the flat BCJ numerators that satisfy the kinematic Jacobi relation [134]

$$n_s + n_t + n_u = 0\,, \tag{6.44}$$

it still does not guarantee that the differential numerators satisfy these kinematic Jacobi relations. The culprit is the ordering of differential operators; more specifically, terms like $f(\mathcal{E})L_i \cdot L_j$ do not manifestly cancel the denominator $\mathcal{D}^{d-1,1}$. To resolve this problem, we should move $L_i \cdot L_j$ to the most left. We can easily do this by noting

$$\begin{aligned}\mathcal{E}_{i_1}\cdot\mathcal{E}_{i_2}\,\mathcal{E}_{i_3}\cdot\mathcal{E}_{i_4}\,L_{i_1}\cdot L_{i_3} &= \mathcal{D}^{d-1,1}_{i_1 i_3}\mathcal{E}_{i_1}\cdot\mathcal{E}_{i_2}\,\mathcal{E}_{i_3}\cdot\mathcal{E}_{i_4}\\ &- 2\big(\mathcal{E}_{i_2}\cdot\mathcal{E}_{i_4}\,\mathcal{E}_{i_1}\cdot\mathcal{E}_{i_3} - \mathcal{E}_{i_2}\cdot\mathcal{E}_{i_3}\,\mathcal{E}_{i_1}\cdot\mathcal{E}_{i_4}\big)\,.\end{aligned} \tag{6.45}$$

It turns out that additional terms such as the second line above would generally cancel out in the final expression, and we then trivially move $L_i \cdot L_j$ to the most left as $\mathcal{D}^{d-1,1}_{ij}$. After this operation, we can then use the Ward identity to rewrite $L_4 = -L_1 - L_2 - L_3$ followed by the transversity (6.39) to eliminate unwanted terms. We also have to show

$$\big(\mathcal{D}^{d-1,1}_{12} + \mathcal{D}^{d-1,1}_{13} + \mathcal{D}^{d-1,1}_{23}\big) f_{1,d-1}(X_i) = 0\,, \tag{6.46}$$

where $f_{1,d-1}$ is any conformal invariant function with spin weights $J = 1$ and scaling weights $\Delta = d-1$. This statement is equivalent to $L_i^2 f_{1,d-1} = 0$, which can be easily proved by acting L_i^2 on shadow representation [170, 141] of any such function $f_{1,d-1}$

$$\begin{aligned}f_{1,d-1} =& \sum_J \int d\Delta I(\Delta, J)\times\\ &\int D^d X_5 \langle V_1 V_2 \mathcal{O}_{\Delta,J}(X_5)\rangle\langle\tilde{\mathcal{O}}_{d-\Delta,J}(X_5) V_3 V_4\rangle\,.\end{aligned} \tag{6.47}$$

Taking all of these into account, we can then prove the differential kinematic Jacobi identity

$$\mathcal{N}_s + \mathcal{N}_t + \mathcal{N}_u = 0\,. \tag{6.48}$$

Following the same operations described above, we can readily prove the differential BCJ relation

$$\mathcal{D}_{12}^{d-1,1}\widehat{\mathcal{M}}[1234] - \mathcal{D}_{13}^{d-1,1}\widehat{\mathcal{M}}[1324] = 0\,. \tag{6.49}$$

6.4.3 Comment on four-point double copy

The uplift of the BCJ numerators (6.48) strongly suggests that there should be a differential double copy relation up to contact terms suppressed by the AdS radius, namely,

$$\widehat{\mathcal{M}}_{4,\mathrm{grav}} \propto \mathcal{T}_{\mathcal{O}}\Big(\frac{1}{\mathcal{D}_{12}^{d,2}}\mathcal{N}_s^2 + \frac{1}{\mathcal{D}_{23}^{d,2}}\mathcal{N}_t^2 + \frac{1}{\mathcal{D}_{24}^{d,2}}\mathcal{N}_u^2\Big) + \widehat{\mathcal{M}}_{\mathrm{ct}}\,. \tag{6.50}$$

However, it is hard to find the remaining term $\widehat{\mathcal{M}}_{\mathrm{ct}}$ and prove this proposal. The most important reason is that the momentum conservation is built into the double copy relation, but we do not manage to find a clean way to replace $\mathcal{P}$ in (6.30) by L. There are large redundancies to rewrite (6.30) in terms of conformal generators. It is thus difficult to locate a nice minimum basis that allows us to prove (6.50) by figuring out what is $\widehat{\mathcal{M}}_{\mathrm{ct}}$. Another way to explore (6.50) might be generalizing the algorithm in [211] that translates the differential representation to final amplitudes in the Mellin space. The resulting Mellin amplitudes [107, 22] may help explicitly verify the relation and fill in the missing corner $\widehat{\mathcal{M}}_{\mathrm{ct}}$. We can also hope to completely determine $\widehat{\mathcal{M}}_{\mathrm{ct}}$ by enumerating all possible contact structures and requiring the conservation of stress-tensors in the stress-tensor correlator $\widehat{\mathcal{M}}_{4,\mathrm{grav}}$. We leave this interesting question for future studies.

6.5 Summary

We proposed the differential representation for tree-level gluon and graviton scattering from YM and Einstein gravity in AdS. The essential differential operators are proportional to dimension-up and spin-up weight-shifting operators. They provide a natural scheme for organizing (A)dS amplitudes and large-N conformal correlators by counting the number of $\mathcal{P}$, where the hierarchy of different structures is made manifest, as we explain in appendix D.1. Using these differential operators, three-point and four-point amplitudes in AdS are straightforwardly uplifted from flat-space cousins. For three-point amplitudes, such an uplift makes the double copy relation straightforward. At the four-point level, we find a different differential representation for YM amplitudes by using spin-up weight-shifting operators and the conformal generators, for which differential BCJ numerators can be uplifted from flat-space ones, building differential BCJ relations. The differential BCJ numerators follow the kinematic Jacobi identity. We could then argue that the double copy structure for the four-point function should be valid up to the remaining contact terms. It would be interesting to make connections between our findings and the similar structures in momentum space [135, 136, 209, 212, 212, 213, 214] or Mellin space [101, 215, 216] (by generalizing to supersymmetric theories [30]). These connections, as analytically continued to the dS space [204, 217], could improve the understanding of cosmological correlators by following the lines of, e.g., [218, 219, 220, 221, 222, 162].

This paper is the first step toward revealing the hidden structures of spinning correlators. Most importantly, our surprising findings rely on more or less guessing work. It is thus crucial to develop a more systematic way for uplifting by using (6.3), and relevant operators, similar to the scalar case [29, 32]. Besides, the ordering of differential operators and non-conservation of operators $\mathcal{P}$ prevent one from proving or imposing the conservation for current and stress-tensor operators. One possible way to resolve this problem is to carefully think about algebra that (6.3) may form together with other differential operators (such as emergent $\mathrm{SO}(5,5)$ algebra for bispinor representation of $\mathrm{AdS}_4/\mathrm{CFT}_3$ [174]). Besides, the uplift from flat-space convinces us there should also exist the Parke-Taylor formula, and we believe the bispinor formalism [174] would be the correct tool. As these challenges are overcome, we believe the four-point double copy in AdS can be precisely established.

It would also be interesting to understand why this differential representation manifests the flat-space limit by detailed investigation of the Inönü-Wigner contraction of the conformal group, and its representations [223]. This exploration can help understand many aspects of S-matrix as the flat-space limit of conformal correlators, following the lines of [3, 27, 33, 224, 225].

Ultimately, we want to emphasize that the differential representation might help bootstrap holographic CFTs beyond the scope of the Lorentzian inversion formula [43, 61, 62]. The Lorentzian inversion formula does not work well for spin-zero trajectories, while the differential representation precisely captures the contact terms with complete OPE data built into the numerators.

Acknowledgments

We thank Simon Caron-Huot, Julio Parra-Martinez, Jiajie Mei, Joao Penedones and David Simmons-Duffin for discussions. We thank Yi Wang for the hospitality during my visit to HKUST Jockey Club Institute for Advanced Study. YZL is supported by the Simons Foundation through the Simons Collaboration on the Nonperturbative Bootstrap.

Chapter 7

Discussions of all findings

In Chapter 3, we briefly review the different frameworks that have been proposed for describing the flat-space limit of AdS/CFT. The existing approaches extract the flat-space S-matrix from conformal correlation functions using a variety of representations, including momentum space, Mellin space, coordinate space, and partial wave expansions. In particular, these formulas for describing the massless and massive amplitudes differ even in the same representation. It is thus essential to understand these differences.

Our goal in Chapter 3 is to unify these different frameworks and show how they all arise from the AdS/CFT correspondence. We do this by building the holographic reconstruction kernels at the perturbative level and exploring their behaviours in the flat-space limit. Our findings show that the holographic reconstruction kernel is the key to reconstructing the flat-space amplitudes in the limit of the large AdS radius.

In the momentum space representation, we find that the origin of the flat-space limit is the smearing kernel in Poincare AdS. On the other hand, the other formulas for the flat-space limit arise from the smearing kernel in the global AdS. In Mellin space, our results lead us to propose a Mellin formula that unifies the massless and massive flat-space limits, which can then be transformed into coordinate space and partial wave expansions. Furthermore, we show that in the limit of the large AdS radius, it is possible to transform the formula in the momentum space representation into the smearing kernel in the global AdS. This finding connects all of the existing perturbative frameworks and provides a comprehensive understanding of the flat-space limit in AdS/CFT.

The smearing integrals are multi-dimensional, and we resort to a rough saddle point analysis for convenience. The idea behind this method is to identify the saddle points, expand the smearing kernel in their vicinity, and then simplify the integration process by performing Gaussian integrals. This technique, however, has its limitations and might not take into account all the details. In particular, this method bypasses the AdS Landau singularity that was reported in the study conducted by [3]. The subtlety arises when one tries to deform the integral contours of the Mellin amplitudes to reach the saddle points. To do this, one needs to move along the path of deepest descent, but during this process, the contour could pass through the poles of the Mellin amplitudes, leading to additional contributions. In some cases, these additional contributions can be significant and dominate the final result. As a result, the flat-space limit might not be valid for certain regimes of the kinematic variables.

The breakdown of the flat-space limit remains puzzling to me because, from the point of view of the Lagrangian, the flat-space limit should always be valid. In order to resolve the puzzle, it would be essential to understand the underlying mechanisms for the breakdown of the flat-space limit using the smearing formula (3.27), where a more rigorous saddle points analysis should come in. Typically, our approach in Chapter 3 builds the flat-space limit of amplitudes by studying the flat-space limit of the holographic reconstruction, which involves smearing the correlation functions, as described in equation (3.27). This is different from the approach used in [3], where the authors directly study the correlation functions. The additional integrals in our formula (3.27) offer a new possibility to understand the breakdown of the flat-space limit. Is it possible that a rigorous saddle points analysis of these additional integrals can pick up contributions that suppress or even cancel the AdS Landau diagrams? This is an important project to explore in the future.

Another interesting topic relevant to the AdS Landau diagrams is how to understand the analyticity of the S-matrix from the analyticity of AdS amplitudes by taking the flat-space limit. For example, the consistency between the dispersive sum rules between holographic CFTs and flat-space S-matrix for massless particles was shown in [33]. This is the primary tool we use to uplift the bounds of flat-space gravitational EFT to holographic CFTs in Chapter 5. A similar logics applies to massive particles, where the authors of [27] show that the S-matrix reduced from AdS amplitudes indeed obeys the dispersion relation, unitarity conditions, and the Froissart-Martin bound. For example, they show that the Lorentzian inversion formula for obtaining the anomalous dimensions [43] gives rise to the Froissart-Gribov formula for extracting the phase shift [226], where the contribution of the AdS Landau diagrams is also present. This provides a profound understanding of the phase-shift formula (3.141) (that we proved in Chapter 3) from the point of view of the analyticity. As we emphasize, the authors of [27] directly studied the correlation functions. Thus, it is essential to see how the smearing procedure (3.27) in our findings can be consistent with the results of [27]. Our results of the mixed conformal block in the limit of both large Δ_i and Δ (e.g., (A.70) also pave the way for generalizing the analysis of [27] to the mixed correlators.

The exploration of the flat-space limit has been a topic of great interest in the field of AdS/CFT correspondence, which also drives the interest to study whether the flat-space amplitudes can be uplifted to AdS ones the flat-space limit can be made manifest. Aside from the issues relevant to the AdS Landau diagrams where special kinematic regimes come in, researchers have found that AdS amplitudes and the corresponding CFT correlators admit nontrivial representations that make the structures of flat-space amplitudes manifest. These recent developments can be found in several papers, including [29, 30, 31, 7, 32, 206, 207]. These nontrivial representations they found for scalar AdS amplitudes are phrased as the differential representation, which can be obtained by writing AdS amplitudes as conformal generators acting on scalar contact Witten diagrams. A trivial example is the 2-to-2 scalar amplitudes from ϕ^3 theory in AdS

$$W_{\phi^3} = \frac{1}{\mathcal{C}_{12} - \Delta(\Delta - d)} W_{\mathrm{ct}}\,, \tag{7.1}$$

where $W_{\rm ct}$ is the contact Witten diagram of ϕ^4 theory, and $\mathcal{C}_{12}$ is the quadratic conformal Casimir operator. One can obviously see that this formula looks the same as the flat-space ϕ^3 amplitudes by replacing the Mandelstam variable s with the quadratic Casimir operator and rewriting the mass in terms of the scaling dimension. The same principle applies to even more complicated theories where the exchange of gluons and gravitons are included, and the general dictionary is to relate the conformal generator in holographic CFTs and the momentum in flat-space QFT

$$p_i^\mu p_{j\mu} \leftrightarrow L_i^{\mu\nu} L_{j\mu\nu}\,, \tag{7.2}$$

where $L_i^{\mu\nu}$ refers to the conformal generator for the ith point. This has been rigorously established as a general statement for theories that do not contain higher derivative terms [7, 32]. Therefore, the differential representation not only highlights the flat-space limit, but it also provides a universal method for uplifting flat-space amplitudes to AdS, as shown in Fig 1.3. The results of these studies have opened up new avenues of research in the field and have the potential to deepen our understanding of the relationship between AdS amplitudes and flat-space amplitudes. The results of these studies have provided a new framework for understanding and analyzing AdS amplitudes and CFT correlators, and have paved the way for further developments in this area. For instance, in one of the projects that I am currently working on, we demonstrate how the differential representation approach can effectively simplify the calculation of six-point Witten diagrams with gluon exchange, which has proven to be a challenging task in the past.

In Chapter 4, we study the spinning correlation functions in holographic CFTs. The spinning operators have obtained much attention in recent years due to their potential to shed light on more stringent constraints on conformal field theories. The spinning correlators admit multiple tensor structures that are compatible with the conformal symmetry. One particularly interesting example of spinning conformal correlators is the conserved currents in three dimensions. In particular, we have shown that the helicity of these conserved currents commute with conformal transformations, and this has been used to construct three-point structures that diagonalize the helicity. This is a significant finding, because it allows us to gain more complete understandings of the OPE data for conserved currents.

Our results highlight the importance and utility of the helicity basis in understanding the correlation functions of conserved currents and stress tensor in holographic theories. The diagonal OPE data in this basis makes it easier to further extract meaningful information from these correlators, and the Lorentzian inversion formula provides a powerful tool for obtaining results for anomalous dimensions. Moreover, the comparison between the anomalous dimensions obtained using the Lorentzian inversion formula and the corresponding flat-space gluon scattering amplitudes provides valuable insights into the flat-space limit of spinning correlators. The perfect agreement achieved by taking the flat-space limit proves the validity of our results and the power of the helicity basis used in our calculations.

We emphasize that the helicity basis will be extremely helpful even beyond the holographic theories because it constructs excellent three-point structures regardless of the specific details of dynamical theories. The diagonal nature of the MFT OPE also has wide-ranging applications and makes it possible to understand conserved currents and the stress tensor beyond just the scope of the holographic theories. We expect it can simplify and clean up the set-up of numerical conformal bootstrap involving conserved currents and stress tensor [144].

In order to better understand the relationship between the three-point Witten diagrams and the bulk three-point vertices $\nabla_\mu A_\nu A^\mu A^\nu$ and $\mathrm{Tr}F^3$, we explicitly computed the former, and we were able to identify them with the corresponding helicity basis. This identification has provided us with a dictionary that relates three-point OPEs and bulk coupling constants. This detail has also allowed us to precisely verify the validity of the bulk point limit in our analysis. However, it is still somewhat puzzling that there is no obvious way to identify the helicity basis with the bulk three-point gluon vertices simply by staring at them. In the case of flat-space, one could easily count the number of momenta in three-point amplitudes to distinguish between their origins from these two vertices. This principle is what is phrased as the power counting procedure in the construction of EFTs. Therefore, it becomes essential to investigate whether there is a differential representation for gluon and graviton amplitudes in AdS that can uplift the flat-space amplitudes with the power counting rule made manifest, as we did in Chapter 6.

In Chapter 5, we focus on flat-space gravitational scattering and present a significant result regarding the gravitational EFTs as the corrections to Einstein's General Relativity at low energies. Through rigorous analysis, the Chapter 5 shows that any graviton S-matrix that obey the minimal assumptions of causality and unitarity cannot differ greatly from Einstein gravity. Moreover, we provide sharp and rigorous constraints on the size of low-lying possible corrections to Einstein gravity in terms of the mass M of novel higher-spin states in spacetime dimensions $D \geq 5$, in which the S-matrix does not suffer from the infrared divergence. The key ingredients that enable us to achieve this is the full set of $\mathrm{SO}(D-1)$ partial waves, and we show the computation toward them can be performed with efficiency through Young tableau manipulations. Besides, we also construct all dispersion relations relevant to graviton scattering, which is general and applicable even when loop effects are included, as long as the Regge boundedness assumption is satisfied for the smeared version of amplitudes. We then derive new sharp bounds on the central charges of holographic conformal theories in four dimensions by uplifting the flat-space bounds to AdS in five dimensions, see (5.30).

However, one issue that we have already realized in Chapter 5 is that our existing bounds are not guaranteed to be optimal. This is due to the complexity of finding positive functionals, which is a significant challenge. Technically speaking, the current searching algorithm that we are using (follow the routes of [130] and [5]) is not able to fully cover the space of the UV spectrum in the impact parameter space, especially for the asymptotes in the large spin limit when $J \to \infty$. This would probably require a more sophisticated algorithm for finding the positive-definite functionals. By doing this in the future, we can hope to achieve optimal bounds for gravitational EFTs in higher dimensions and more accurately predict the central charge bounds in holographic CFTs.

On the other hand, if we think of the gravitational EFT as the theory obtained by integrating out the massive modes circling the loops in gravity-matter systems [199, 227], our rigorous bounds can imply the specious bounds of matter fields, namely the number of matter particles cannot be too large. Otherwise, the causality and the unitarity will be violated. Because for this type of model, the Wilson coefficients g are scaled by the large number of species $g \sim GN$, and our bounds $g < \#G/M^{\text{dim}+D-2}$ then suggest

$$N < \# \frac{M^{2-D}}{G} \,. \tag{7.3}$$

In my ongoing project with Simon Caron-Huot, we are trying to make this statement sharp by studying the Einstein gravity coupled to massless $\mathcal{O}(N)$ scalar, fermion and vector models where $G \to 0$ but $GNs^{\frac{D-2}{2}}$ kept fixed. By including all loop ingredients, we can then utilize the dispersive sum rules we obtained in Chapter 5 to search for the allowed space of the number of species. This species bound (7.3) can also be uplifted to AdS/CFT, as then it constrains the number of primary operators in the holographic CFTs in d-dimension

$$N < \# \frac{C_T}{\Delta_{\text{gap}}^{d-1}} \,. \tag{7.4}$$

In Chapter 5, we use the analysis in [33] as the basis for our derivation of (5.30). We must, however, acknowledge that the adoption of this approach is not entirely rigorous. This is due to the fact that the authors of [33] focused their analysis solely on scalar correlators, which suggests that flat-space bounds on scalar EFTs can be uplifted to AdS up to small errors. Thus, our result serves as a prediction of the precise bound on central charges in holographic conformal field theory (CFT) in four dimensions. We recognize that a more rigorous method of verification is still necessary to confirm the validity of our central charge bound. This is where and why the dispersion relations of spinning correlators should be constructed.

The task of building spinning dispersive sum rules is difficult, primarily due to the intricate tensor structures present in spinning conformal correlators. These tensor structures can be particularly problematic as they may interfere with the analytic structures of correlation functions, for example see [228]. A similar situation arises in flat-space, where the construction of dispersion relations can become more challenging when an inappropriate basis of spinning amplitudes leads to spurious poles. Nevertheless, it is not hard to overcome this issue in flat-space by constructing the local modules from four-point contact vertices in the Lagrangian and using them as the basis of tensor structures. This procedure was described in [185] in details and we directly use it in Chapter 5. Despite the challenges of constructing the spinning dispersive sum rules for CFTs, we can still hope to make progress by exploring possible approaches towards constructing the local modules in CFTs in the future. One potential strategy to address this question is to consider the use of differential operators (6.3). By using these operators to uplift the flat-space local modules, we can explore the analytic structures of spinning correlators under the resulting basis. Such an approach might prove to be a crucial step towards building spinning dispersive sum rules in CFTs.

In Chapter 6, we report the differential representation of three-point and four-point amplitudes for Yang-Mills fields and Einstein gravity in AdS at tree-level. As we briefly reviewed in the previous discussions, it turns out that it is straightforward to find the differential representation for any contact diagrams of scalar amplitudes up to any points using the coset construction. The proof was shown in [32]. For spinning objects, the tensor structures mess things up. However, we surprisingly found the differential operators (6.3) that can realize the differential representation for gluon and graviton amplitudes. These differential operators provide the nontrivial generalization of the scalar differential representation to massless spinning amplitudes. As a result, we can show that the gluon and graviton amplitudes in AdS exhibit the flat-space structures by using those differential operators (6.3) with reordering. This allows us to uplift the corresponding amplitudes in flat-space to AdS directly. Such differential representation makes the differential double copy relation at the three-point level straightforward, as shown in (6.18). We also observe a different differential representation for four-point Yang-Mills amplitudes, embracing the conformal generators. This representation establishes the differential BCJ relation, which can be helpful for proving the differential doubly copy at the four-point level in the future, as we proposed in (6.50).

It is worth noting that the differential operators (6.3) we found in Chapter 6 are complementary to our findings in Chapter 4. This is because (6.3) encodes natural power counting rules for conserved currents and stress tensors in large-N CFTs. As we show in Chapter 6, any bulk derivatives can be replaced by $\mathcal{P}$ up to other terms with fewer numbers of $\mathcal{P}$. Therefore, it is evident that (6.3) can uplift EFTs from flat-space to AdS. This observation is powerful. Because it implies that CFT correlators at large-N limit share the same power counting rules as EFTs in flat-space. As we emphasized in Chapter 6, this manifests the agreements of the number of structures between conformal correlators and flat-space amplitudes [117]. Remarkably, our methods allow us to easily tell how different AdS vertices, i.e., $\nabla_\mu A_\nu A^\mu A^\nu$ and $\mathrm{Tr}F^3$ in the AdS bulk, give rise to different OPE structures. Because what we need to do is to start with flat-space three-point amplitudes and make the following replacement

$$p_{i\mu} \to \mathcal{P}_{i\mu}\,, \quad \epsilon_{i\mu} \to \mathcal{E}_{i\mu}\,. \tag{7.5}$$

We expect that this principle also applies to graviton three-point structures and four-point amplitudes in gluon and gravitational EFTs. The power counting rule would be the same as in flat-space using (7.5). In this way, the differential representation in terms of (6.3) with power counting rules encoded could be beneficial for a clean spinning bootstrap in the future.

During the project [2] which Chapter 4 reproduces, we were unable to find a diagonal MFT OPE in higher dimensions using the basis that we proposed (see (3.159)). We did find, however, that the higher dimensional MFT OPE is diagonal only in the flat-space limit, where the third operator is heavily massive with a fixed ratio of Δ/R_{AdS}. This finding was demonstrated in the last section of Chapter 3. The basis (3.159) may not be the most suitable for finding the diagonal MFT OPE matrix in higher dimensions. However, the three-point structures that were uplifted from flat-space using (6.3) may prove to be different from the basis (3.159) and could allow for the discovery of a diagonal MFT OPE matrix in higher dimensions without taking any limits. Thus, we suggest that pursuing this direction could be an important future project.

In order to gain a deeper understanding of the differential representation and its relation to the flat-space limit, it is crucial to investigate the Inönü-Wigner contraction of the conformal group and its irreducible representations. That is, a group theoretical understanding of Fig 1.3. The simplest such example is the generators of the underlying symmetry group. The Poincare generators of the flat-space $\mathbb{R}^{d+1}$ can be obtained by the Inönü-Wigner contraction of the conformal generators

$$p_a = \lim_{R_{\text{AdS}}\to\infty} \frac{1}{R_{\text{AdS}}} J_{-1a}\,, \quad s_{ab} = J_{ab}\,, \tag{7.6}$$

where the space indices a are indices of $\mathbb{R}^{d+1}$, going from 0 to d (to be consistent with the convention in (2.6) and (2.7)). p_a and s_{ab} denote the translation and the rotation in $\mathbb{R}^{d+1}$, respectively. Similarly, the Inönü-Wigner contraction of the quadratic conformal Casimir gives rise to the momentum squared in the flat-space

$$p^2 = \lim_{R_{\text{AdS}}\to\infty} \frac{1}{R_{\text{AdS}}^2} \mathcal{C}_{12}\,. \tag{7.7}$$

This provides a group theoretical understanding of the scalar differential representation. However, in order to understand the spinning amplitudes, we will have to deal with the Inönü-Wigner contraction for different irreducible representations. This investigation can provide valuable insights into many analytic aspects of the S-matrix, particularly as it relates to the flat-space limit of conformal correlators [3, 27, 33, 224, 225]. It is also worth noting that the differential representation may be particularly helpful when it comes to bootstrapping holographic CFTs beyond the Lorentzian inversion formula. While the Lorentzian inversion formula has proven to be an effective tool for many purposes, it does not always work well when it comes to low-spin trajectories. This is where the differential representation can be especially useful, as it is able to capture contact terms with complete OPE data built into the numerators. By using the differential representation to better understand the low-spin and twist zero trajectory of Yang-Mills scattering, we may be able to gain new insights into the loop corrections of Yang-Mills in AdS.

Another physical implication of our results in Chapter 6 is that they provide insights on Cosmological correlators as they are analytically continued to dS space. It was noted very early days that Euclidean AdS correlators could be analytically continued to the dS wave-function coefficients that compute the spectrum of Cosmological correlators [208]. This drives booming the recent developments that aim to more efficiently and powerfully understand and compute the Cosmological correlators using the techniques from CFT and AdS, see [218] for a comprehensive review. Our results provide the differential representation of graviton three and four-point amplitudes, which could, as Fourier transformed to the momentum space, help solve the bispectrum and trispectrum of graviton spectator in the slow roll inflationary scenario. Besides, our differential representation realizes a direct uplift from flat-space. This could shed light on understanding the general structures of Cosmological correlators: flat-space amplitudes enhanced with total energy singularity [161].

Chapter 8

Conclusion

In this thesis, we have investigated aspects of the flat-space structures of AdS/CFT in-depth. We have partially answered the following four essential questions regarding the flat-space structures in AdS/CFT.

1. Why are there seemingly different frameworks for taking the flat-space limit that all work nicely?

2. Does spinning correlation functions in holographic CFT define the correct spinning S-matrix in flat-space?

3. What constraints on holographic CFTs can be imposed by flat-space physics?

4. Can we uplift the flat-space gluon and graviton amplitudes to AdS?

In Chapter 3, we start with both global AdS and Poincare AdS and then construct the scattering smearing kernels to define the flat-space S-matrix by CFT correlators. We show that the smearing kernel in global AdS served as a common origin of flat-space limit in terms of Mellin space, coordinate space, and partial waves. On the other hand, the smearing kernel in Poincare AdS performs the Fourier transform of CFT correlators and thus leads to the flat-space limit in the momentum space. We also observe that the saddle points of Fourier-transform further connect Poincare smearing and global smearing, indicating that all existing frameworks of the flat-space limit of AdS/CFT are equivalent. In the end, we briefly analyze the flat-space limit of spinning operators more covered by Chapter 4.

In Chapter 4, we construct a helicity basis for conformal correlators of conserved operators in three-dimensional CFTs. We show that the concept of helicity is conformally invariant. Using this basis, we provide a diagonal representation of conformal data. Using the helicity basis, we compute the OPE of mean-field correlators. We further extract the CFT_3 OPE data contributed by tree-level gluon scattering AdS_4, which turns out to be diagonal. Our results at the bulk-point limit achieve perfect agreement with flat-space gluon scattering phase shift, including higher derivative corrections.

In Chapter 5, we build the dispersion relations of (flat-space) graviton scattering in high dimensions representing the low-energy EFT in terms of UV partial waves with positive coefficients. By constructing graviton partial waves, we utilize the dispersion relations to sharply constrain the Wilson coefficients that control the leading corrections of Einstein-Hilbert action. We uplift our results to AdS and thus provide numerical bound on central charges in terms of Δ_{gap}.

In Chapter 6, we develop the differential operators built from the weight-shifting operators. These differential operators enable us to find the differential representation of gluon and graviton amplitudes in AdS. The differential representation demonstrates the flat-space structure, which can be obtained by uplifting the flat-space amplitudes. We show that the three-point doubly copy can be made manifest using our differential representation. On the other hand, we prove the differential BCJ relation for four-point YM amplitudes. This motivates us to propose the four-point differential doubly copy relation yet to be explored and proved.

In Chapter 7, we provide detailed discussions of all our findings in the manuscripts that Chapter 3, 4, 5 and 6 base on. We point out valuable and intriguing outlooks for possible future directions.

Appendix A

Appendices for Chapter 2

A.1 Momentum space for Euclidean CFT

In subsection 3.2.2, we construct the scattering smearing kernel from Poincare AdS, which Fourier transform Lorentzian CFT correlators, giving rise to the flat-space limit in the momentum space eq. (3.45). However, Lorentzian CFTs admit more subtle analytic structures (see [62] for fun), making it not easy to perform Fourier transform. It is better to represent S-matrix in terms of Euclidean CFT, where the Fourier transform is much straightforward. This is the flat-space limit proposed in [26]. In this appendix, we demonstrate how, in a direct way, to rewrite eq. (3.45) in terms of Euclidean CFT, which, as the massless condition is turned on, reduces to [26].

Of course we should wick rotate Lorentzian CFT to Euclidean CFT, i.e., $T \to iT$. Correspondingly, we have $E \to iE$ where E now is spatial momentum rather than energy. However, this procedure causes some troubles for modes expansion eq. (3.30), as we discussed there. A simple resolution is to wick rotates $z \to iz$, and consequently the Bessel function of the first kind J_ν remains valid as mode functions. Importantly, we should also retain the spacetime in the flat-space limit eq. (3.45) as a Minkowski space. We can formally do this by taking $\ell \to i\ell$ and $x_d \to ix_d$. To be more clear, we do wick rotations as follows

$$T \to iT\,, \quad z \to iz\,, \quad \ell \to i\ell\,, \quad x_d \to ix_d\,, \quad t \to -t\,, \quad x_{i<d} \to ix_{i<d}\,. \tag{A.1}$$

It is easy to see that after doing these analytic continuations, AdS becomes dS and the flat-space limit remains as Minkowski. It is then readily to find the remanning parts of analyzing the flat-space limit still follow subsection 3.2.2, but with the momentum continued correspondingly

$$\omega \to \omega\,, \quad k_{i<d} \to -ik_{i<d}\,, \quad k_d \to ik_d = i\sqrt{|\mathbf{k}|^2 + m^2}\,, \tag{A.2}$$

where $|\mathbf{k}| = \sqrt{\omega^2 + k_{i<d}^2}$. Now it is easy to see that ω is no longer the energy but one component of spatial momentum, and the additional momentum coming from bulk k_d is the actual energy as the proposal in [26]. We may stick to the usual notation calling energy ω, then the scattering smearing kernel eq. (3.45) basically remains the same but replacing $k_d \to i\omega$ since k_d now is energy

$$S = \int \Big(\prod_i d^d x_i 2^{1-\frac{d}{2}+\Delta_i} \ell^{-\Delta_i} \sqrt{\frac{\Gamma(1+\Delta_i - \frac{d}{2})}{\Gamma(\frac{d}{2} - \Delta_i)}} \frac{\omega^{\frac{1}{2}}}{|p_i|^{\Delta_i - \frac{d}{2}}} e^{-i\tilde{\alpha}_\omega} e^{ip_i \cdot x_i} \Big) \langle \mathcal{O}_1 \cdots \mathcal{O}_n \rangle_{\mathrm{E}}\,, . \tag{A.3}$$

A.2 Normalizing scattering smearing kernel

The scattering smearing kernels we construct in section 3.2 are already normalized. We show in subsection 3.2.3 that using HKLL formula and LSZ can somehow determine the scattering smearing kernels up to normalization. Here we demonstrate we can fix the normalization by requiring the canonical condition

$$S_{12} = \langle p_1 | p_2 \rangle = (2\pi)^d 2\omega \delta^{(d)}(p_1 - p_2)\,. \tag{A.4}$$

A.2.1 Global smearing

For global smearing, we start with a smearing kernel with momentum dependence unknown for S_{12}

$$S_{12} = \int dt_1 dt_2 e^{i(\omega_2 t_2 - \omega_1 t_1)} A_g(p_1) A_g(p_2) \langle \mathcal{O}_1(\tau_1, \widehat{p}_1) \mathcal{O}_2(\tau_2, \widehat{p}_2) \rangle \,, \tag{A.5}$$

where $A_g(p)$ is the yet-to-be-determined normalization. We use the following representation of two-point function, basically constructed from quantization eq. (3.19)

$$\langle \mathcal{O}_1(\tau_1, \widehat{p}_1) \mathcal{O}_2(\tau_2, \widehat{p}_2) \rangle = \frac{\mathcal{C}_\Delta}{2^\Delta (\cos \tau_{12} - \widehat{p}_1 \cdot \widehat{p}_2)^\Delta} = \sum_{n,J} (N^{\mathcal{O}}_{\Delta,n,J})^2 e^{iE_{n,J}(\tau_1 - \tau_2)} Y_{Jm_i}(\widehat{p}_1) Y_{Jm_i}(\widehat{p}_2) \,. \tag{A.6}$$

As we show in subsection 3.2.1, taking $\ell \to \infty$ yields

$$\langle \mathcal{O}_1(\tau_1, \widehat{p}_1) \mathcal{O}_2(\tau_2, \widehat{p}_2) \rangle = \int d\omega \frac{2^{d-2\Delta-1} \ell^{2\Delta-d+1} p^{2\Delta-d}}{\xi^2_{\omega\Delta} \Gamma(\Delta + 1 - \frac{d}{2})^2} e^{i\omega(t_1 - t_2)} \delta^{(d-1)}(\widehat{p}_1 - \widehat{p}_2) \,. \tag{A.7}$$

Plugging into eq. (A.5), we can perform the integral of $t_{1,2}$ to have $(2\pi)^2 \delta(\omega - \omega_1) \delta(\omega - \omega_2)$. Then we can integrate out ω, leaving only one delta function $\delta(\omega_1 - \omega_2)$. We have

$$\begin{aligned} S_{12} &= \frac{2^{d-2\Delta+1} \ell^{2\Delta-d+1} p_1^{2\Delta-d} \pi^2}{\xi^2_{\omega_1\Delta} \Gamma(\Delta + 1 - \frac{d}{2})^2} A_g(p_1)^2 \delta(\omega_1 - \omega_2) \delta^{(d-1)}(\widehat{p}_1 - \widehat{p}_2) \,, \\ &= \frac{2^{d-2\Delta+1} \ell^{2\Delta-d+1} p_1^{2(\Delta-1)} \pi^2}{\xi^2_{\omega_1\Delta} \Gamma(\Delta + 1 - \frac{d}{2})^2} A_g(p_1)^2 \omega_1 \delta^{(d)}(p_1 - p_2) \,, \end{aligned} \tag{A.8}$$

where we have used the on-shell condition to rewrite the delta functions

$$\delta(\omega_1 - \omega_2) \delta^{(d-1)}(\widehat{p}_1 - \widehat{p}_2) = \omega_1 p_1^{d-1} \delta^{(d)}(p_1 - p_2) \,. \tag{A.9}$$

Equating to eq. (A.4), we obtain correctly

$$A_g(p) = 2^\Delta \ell^{\frac{d-1}{2} - \Delta} p^{1-\Delta} \pi^{\frac{d-2}{2}} \xi_{\omega\Delta} \Gamma(\Delta + 1 - \frac{d}{2}) \,. \tag{A.10}$$

A.2.2 Poincare smearing

Similarly, we consider S_{12} with normalization factor A_p to be fixed

$$S_{12} = \int d^d x_1 d^d x_2 e^{i(p_1\cdot x_1 - p_2\cdot x_2)} A_p(p_1) A_p(p_2) \langle \mathcal{O}_1(T_1, Y_1) \mathcal{O}_2(T_2, Y_2) \rangle \,, \tag{A.11}$$

where

$$\langle \mathcal{O}_1(T_1, Y_1) \mathcal{O}_2(T_2, Y_2) \rangle = \frac{\mathcal{C}_\Delta}{|-(T_1 - T_2)^2 + (Y_1 - Y_2)^2|^\Delta} \,. \tag{A.12}$$

It is more convenient to work with Euclidean CFT, and we can also work with variables x_{12} and x_2

$$S_{12} = \int d^d x_{12} d^d x_2 e^{ip_1\cdot x_{12} + ip_{12}\cdot x_2} A_p(p_1) A_p(p_2) \frac{\mathcal{C}_\Delta \ell^{2\Delta}}{x_{12}^{2\Delta}} \,. \tag{A.13}$$

The integral of x_{12} performs the Fourier transform for $p_1^{(d)}$, and the integral of x_2 simply gives delta function $(2\pi)^d \delta(p_1 - p_2)$

$$S_{12} = 2^{d-2\Delta-1} p_1^{2\Delta-d} \frac{\Gamma(\frac{d}{2} - \Delta)}{\Gamma(1 + \Delta - \frac{d}{2})} \ell^{2\Delta} \times A_p(p_1)^2 (2\pi)^d \delta^{(d)}(p_1 - p_2) \,. \tag{A.14}$$

Compare with eq. (A.4), and then analytically continue back to Lorentzian signature, we find

$$A_p(p) = 2^{1-\frac{d}{2}+\Delta} \ell^{-\Delta} \sqrt{\frac{\Gamma(1 + \Delta - \frac{d}{2})}{\Gamma(\frac{d}{2} - \Delta)}} \frac{k_d^{\frac{1}{2}}}{|\mathbf{k}|^{\Delta - \frac{d}{2}}} \,. \tag{A.15}$$

A.3 Derivation of formulas in Mellin space

We break our derivation of Mellin space formula into two steps. First, we approximate four-point function in terms of Mellin amplitudes at saddle-points of δ_{ij} and then we recall scattering kernel and perform integration over time around its saddle-point for massless case and massive case separately.

A.3.1 Limit of Mellin representation and massive formula

Start with Mellin representation of four-point functions eq. (3.70), we scale $\delta_{ij} = \ell^2 \sigma_{ij}$ and exponentiate all integrands as we describe in subsection 3.3.2, include the explicit prefactor we have

$$\begin{aligned}\langle \mathcal{O}_1 \cdots \mathcal{O}_n \rangle = \frac{\mathcal{N}}{(2\pi i)^{\frac{n(n-3)}{2}}} \int \prod_{i=1}^{n} \frac{d\beta_i}{2\pi} [d\sigma_{ij}] \ell^{n(n-1)+\Delta_\Sigma} \prod_{i=1}^{n} \frac{\mathrm{i}}{\beta_i} (\frac{2\pi}{\ell^2})^{\frac{n(n-1)}{4}} \times \\ \frac{\prod_{i=1}^{n} |p_i|^{\Delta_i}}{(2\Delta_\Sigma)^{\frac{1}{2}\Delta_\Sigma}} \prod_{i<j} (\sigma_{ij}^*)^{-\frac{1}{2}} \exp[\cdots] \,,\end{aligned} \tag{A.16}$$

where the exponent is exactly eq. (3.77). To be general, we expand the exponent around saddle-points as recorded in eq. (3.93), which works for both massless and massive situation. In general, β is not determined unless further saddle-points are dominated as for massive particles. We may take a gauge choice that sets $\beta_1 = \beta$ to keep track of β, which introduces additional integration

$$\int \frac{d\delta\beta_0}{2\pi} \exp[i\delta\beta_0 \delta\beta_1] \,. \tag{A.17}$$

We can make further simplification by following [23] to redefine ϵ_{ij}

$$u_{ij} = \epsilon_{ij} - \frac{2n}{n-2} q \cdot (p_i + p_j) - \delta s_{ij} \,, \tag{A.18}$$

and we obtain

$$\begin{aligned}&\langle \mathcal{O}_1 \cdots \mathcal{O}_n \rangle = \frac{\mathcal{N}}{(2\pi i)^{\frac{n(n-3)}{2}}} \times \\ &\int d\beta \prod_{a=0}^{n} \frac{\delta\beta_a}{2\pi} [du_{ij}] (\frac{\ell^2 \beta^2}{2\Delta_\Sigma})^{\frac{n(n-1)}{2}} (\frac{i}{\beta})^n (\frac{2\pi}{\ell^2})^{\frac{n(n-1)}{4}} \prod_{i<j} (\sigma_{ij}^*)^{-\frac{1}{2}} (\frac{\ell^2\beta^2}{2\Delta_\Sigma})^{\frac{1}{2}\Delta_\Sigma} \prod_{i} |p_i|^{\Delta_i} \exp[\cdots] \,,\end{aligned} \tag{A.19}$$

where the exponent here is

$$\exp\Big[i\delta\beta_0\delta\beta_1 - \frac{\ell^2\beta}{2\Delta_\Sigma}\sum_{i<j}\big((\delta\beta_i+\delta\beta_j)(s'_{ij}-(m_i+m_j)^2)+\beta\delta s_{ij}\big) - \frac{\ell^2 n^2\beta^2}{2\Delta_\Sigma}q^2$$
$$+\frac{\ell^2\beta}{\Delta_\Sigma}\sum_{i<j}\big(\frac{\beta u_{ij}^2}{4(s'_{ij}-(m_i+m_j)^2)} - \frac{(\delta\beta_i+\delta\beta_j)}{2}(u_{ij}+2n\frac{q\cdot(p_i+p_j)}{n-2}+\delta s_{ij})\big)$$
$$+\frac{\ell^2}{4\Delta_\Sigma}\sum_{i<j}\big((s'_{ij}-(m_i+m_j)^2)(\delta\beta_i+\delta\beta_j)^2\big) + \frac{1}{\beta}\sum_i \Delta_i\delta\beta_i(1-\frac{\delta\beta_i}{2\beta}) + \frac{1}{2}\beta^2\Delta_\Sigma\Big]\,. \tag{A.20}$$

Integrating out u_{ij} gives an overall factor

$$(2\pi)^{\frac{n(n-1)}{4}}\big(\prod_{i<j}(s'_{ij}-(m_i+m_j)^2)\big)^{\frac{1}{2}}\big(-\frac{2\Delta_\Sigma}{\ell^2\beta^2}\big)^{\frac{n(n-1)}{4}}\,, \tag{A.21}$$

accompanied with an exponent

$$\exp\big[-\frac{\ell^2}{4\Delta_\Sigma}\sum_{i<j}(s'_{ij}-(m_i+m_j)^2)(\delta\beta_i+\delta\beta_j)^2\big]\,. \tag{A.22}$$

We should then integrate out $\delta\beta_i$. The exponent relevant to $\delta\beta_a$ can be concisely written in terms of matrices

$$\exp[-\frac{1}{2}\delta\beta.A_\beta.\delta\beta^{\mathrm{T}} + B_\beta.\delta\beta^{\mathrm{T}}]\,,\quad \delta\beta=(\delta\beta_0,\cdots,\delta\beta_n)\,, \tag{A.23}$$

where

$$(A_\beta)_{0i}=(A_\beta)_{i0}=-\mathrm{i}\,\delta_{i1}\,,\quad (A_\beta)_{ij}=\frac{1}{\beta^2}\Delta_i\delta_{ij}+\frac{\ell^2}{2\Delta_\Sigma}(s'_{ij}-(m_i+m_j)^2)\,,$$
$$(B_\beta)_0=0\,,\quad (B_\beta)_i=\frac{\Delta_i}{\beta}-\frac{\ell^2\beta}{2\Delta_\Sigma}\sum_{j\neq i}(s'_{ij}-(m_i+m_j)^2+\delta s_{ij}+\frac{2n}{n-2}q\cdot(p_i+p_j))\,. \tag{A.24}$$

Integrating out $\delta\beta_a$ thus simply gives

$$\sqrt{\frac{(2\pi)^{n+1}}{\det A_\beta}}\,\exp[\frac{1}{2}\sum_{i,j}(A_\beta^{-1})_{ij}(B_\beta)_i(B_\beta)_j]\,. \tag{A.25}$$

$\det A$ is difficult to be evaluated for general n, nevertheless we can find its pattern follows

$$\det A_\beta = \frac{\ell^{2(n-1)}\det'(s_{ij}-(m_i+m_j)^2)}{(2\Delta_\Sigma)^{n-1}} + \frac{\prod_{i=2}^n \Delta_i}{\beta^{2(n-1)}} \\ + \sum_{m=2}^{n-2}(-1)^{m+1}\sum_{\{i_m\}\neq 1}\Big(\prod_{i=2,i\neq\{i_m\}}^{n}\Delta_i\Big)\Big(\prod_{(k,l)>1,(k,l)\neq\{\bar{i_m}\}}^{n}(s_{kl}-(m_k+m_l)^2)\Big)\frac{\ell^{2m}}{4\beta^{2(n-1-m)}}\,, \tag{A.26}$$

where $\det'$ denotes the determinant with discarding the first raw and column. We should explain more on the notation. $\{i_m\}$ denotes a length m list of numbers and $\{\bar{i_m}\}$ denotes the complementary of $\{i_m\}$ through $i>1$. For massless case, all the followed terms are subdominate compare to the first term, thus the expression reduces to

$$\det A_\beta \simeq \frac{\ell^{2(n-1)}\det'(s_{ij})}{(2\Delta_\Sigma)^{n-1}}\,. \tag{A.27}$$

Including all pieces, we obtain

$$\langle\mathcal{O}_1\cdots\mathcal{O}_n\rangle = \frac{\mathcal{N}}{(2\pi i)^{\frac{n(n-3)}{2}}}\int d\beta\,\mathcal{D}(s_{ij},\beta)e^{S(q,\delta s_{ij},\beta)}M\Big(\delta_{ij}=\frac{\ell^2\beta^2}{2\Delta_\Sigma}\big(s_{ij}-(m_i+m_j)^2\big)\Big)\,, \tag{A.28}$$

where

$$\mathcal{D}(s_{ij},\beta) = (-1)^{\frac{1}{4}n(n+1)}(\frac{\ell^2}{2\Delta_\Sigma})^{\frac{1}{2}\Delta_\Sigma}(2\pi)^{\frac{1}{2}(n^2-3n-2)}\beta^{\Delta_\Sigma-n}\prod_i |p_i|^{\Delta_i}\sqrt{\frac{(2\pi)^{n+1}}{\det A_\beta}}\,,$$
$$S(q,\delta s_{ij},\beta) = -\frac{\ell^2\beta^2}{2\Delta_\Sigma}\sum_{i<j}\delta s_{ij} - \frac{\ell^2\beta^2 n^2}{2\Delta_\Sigma}q^2 + \frac{1}{2}\sum_{i,j}(A_\beta^{-1})_{ij}(B_\beta)_i(B_\beta)_j + \frac{1}{2}\beta^2\Delta_\Sigma\,. \tag{A.29}$$

The second step is then integrating time and q. Generally evaluating this two integrals analytically is technically difficult, fortunately we can discuss massive case and massless case separately, which can largely simplify the problem. For formula involving massive external particles, the situation is much more trivial and it is actually not necessary to really do the derivation. In this case, eq. (A.28) can be further simplified by assigning $\beta = i$ to integrands and dropping integral of β. Performing integral over τ_i and q, we simply obtain a formula that equates flat-space amplitudes to Mellin amplitudes with $\delta_{ij} = -\ell^2\beta^2/(2\Delta_\Sigma)\big(s_{ij}-(m_i+m_j)^2$ up to an overall normalization, namely

$$T(s_{ij}) \propto M\Big(\delta_{ij} = -\frac{\ell^2}{2\Delta_\Sigma}\big(s_{ij}-(m_i+m_j)^2\big)\Big)\,. \tag{A.30}$$

The proportional factor is universal, since it is originated from universal kinematic factor KI in eq. (3.69) and universal factor $\mathcal{D}(s_{ij},i)e^{S(q,\delta s_{ij},i)}$ in eq. (A.28). Thus we can determine the proportional factor by simply considering a contact example eq. (3.124). Both flat-space amplitude and Mellin amplitude of such contact interaction are simply coupling constant, thus the proportional factor of above formula is simply 1!

A.3.2 Derivation of massless formula

When all external particles are massless, the derivation becomes highly nontrivial. The expected form of the formula is

$$T(s_{ij}) \sim \int d\beta f(\beta) M\Big(\delta_{ij} = \frac{\ell^2\beta^2}{2\Delta_\Sigma}\big(s_{ij}-(m_i+m_j)^2\big)\Big)\,, \tag{A.31}$$

however, the existence of integral over β makes it impossible to simply determine the proportional function $f(\beta)$ by contact interaction, unless we know $f(\beta)$. A nice derivation is available in [23], and we review their derivation here but with a different gauge.

Let's first describe how our gauge choice can be transformed to the one used in [23]. The gauge choice in [23] is $\epsilon_{12} = 0$ rather than $\beta_1 = \beta$ we use. To transform the gauge to $\epsilon_{12} = 0$, we only need to redefine β by $\beta \to \beta - \delta\beta_1$ with a specific $\delta\beta_1$ rendering $\epsilon_{12} = 0$

$$\delta\beta_1 \simeq \frac{\beta\epsilon_{12}}{2s_{12}} \,. \tag{A.32}$$

Then we have

$$\exp[i\delta\beta_0\delta\beta_1] \to \exp[i\delta\beta_0\frac{\epsilon_{12}\beta}{2s'_{12}}] \,. \tag{A.33}$$

We can then change some variables by

$$\frac{\beta\ell^2}{2\Delta_\Sigma}\delta\beta_i = i\lambda_i \,, \quad \frac{\delta\beta_0\beta}{2s'_{12}} = \lambda_0 \,, \tag{A.34}$$

which provide the following prefactors

$$(-\frac{2i\Delta_\Sigma}{\beta\ell^2})^n\frac{2s'_{12}}{\beta} \,. \tag{A.35}$$

Then trivially changing the variable β by $\beta = i\sqrt{\Delta_\Sigma/(2\alpha)}$ (which will also be used with our gauge anyway) makes the integrand become

$$\prod_{i=1} d\delta\tau_i d\alpha \prod_{a=0} \lambda_a [d\epsilon_{ij}] (-\frac{\ell^2}{4\alpha})^{\frac{n(n-3)}{2}} (-\frac{s'_{12}}{\alpha}) (\frac{2\pi}{\ell^2})^{\frac{n(n-1)}{4}} \prod_{i<j} (\sigma^*_{ij})^{-\frac{1}{2}} (-\frac{\ell^2}{4\alpha})^{\frac{1}{2}\Delta_\Sigma} \prod_i \omega_i^{\Delta_i} \,, \tag{A.36}$$

where the exponent is exactly eq. (107) in [23] by simply noting $\ell\big|_{\text{here}} = R\big|_{\text{there}}$ and $\delta\tau_{ij}\big|_{\text{here}} = t_{ij}/R\big|_{\text{there}}$. It is also easy to check that the prefactors also match with [23].

With our gauge, we now should start with eq. (A.28) and integrate both $\delta\tau_i$ and q over. The massless limit simplifies the exponent in eq. (A.28)

$$\frac{1}{2}\sum_{i,j}(A_\beta^{-1})_{ij}(B_\beta)_i(B_\beta)_j = 2n^2(\frac{\ell^2\beta}{2\Delta_\Sigma})^2\sum_{i,j}(q\cdot p_i)(q\cdot p_i)(A_\beta^{-1})_{ij} - \frac{1}{2}\sum_{l,m}(A_\tau^1)_{lm}\delta\tau_l\delta\tau_m\,, \tag{A.37}$$

where

$$\begin{aligned}(A_\tau^1)_{lm} = -4\big(\frac{\ell^2\beta}{2\Delta_\Sigma}\big)^2 n\Big(\sum_i q\cdot p_i\big((A_\beta^{-1})_{il}+(A_\beta^{-1})_{im}\big)\omega_m\omega_l(1-\delta_{lm})\\ -\sum_i\sum_{k\neq m} q\cdot p_i\big((A_\beta^{-1})_{im}+(A_\beta^{-1})_{ik}\big)\omega_k\omega_m\delta_{lm}\Big)\,.\end{aligned} \tag{A.38}$$

Now let us first take a look at $\delta\tau_i$. We follow [23] to introduce an exponent $\exp[-\sum_i \frac{\delta\tau_i^2}{2T^2}]$ with cut-off $T\to\infty$, which benefits the derivation. Then we can write the time relevant exponent as

$$\exp[-\frac{1}{2}\delta\tau.A_\tau.\delta\tau^{\mathrm{T}}]\,,\quad \delta\tau = (\delta\tau_1,\cdots,\delta\tau_n)\,. \tag{A.39}$$

The linear term is suppressed by large AdS radius ℓ and the matrix A_τ can be organized as

$$(A_\tau)_{lm} = (A_\tau^0)_{lm} + (A_\tau^q)_{lm}\,,\quad (A_\tau^q)_{lm} = (A_\tau^1)_{lm} + (A_\tau^2)_{lm}\,,\quad (A_\tau^0)_{lm} = \frac{1}{T^2}\delta_{lm} + \frac{\beta^2\ell^2}{\Delta_\Sigma}\omega_l\omega_m\,, \tag{A.40}$$

where

$$A_\tau^2 = -\frac{\beta^2\ell^2}{\Delta_\Sigma}nq_0\omega_l\delta_{lm}\,,\quad A_\tau^3 = \frac{\beta^2\ell^2}{\Delta_\Sigma}\omega_l\omega_m\,. \tag{A.41}$$

The inverse of A_τ can be evaluated as [23]

$$((A_\tau^0)^{-1})_{lm} = T^2\delta_{lm} + \omega_l\omega_m(-\frac{T^2}{\sum \omega_i^2} + \frac{\Delta_\Sigma}{\beta^2\ell^2(\sum_i \omega_i^2)^2}) + \mathcal{O}(T^{-2}) \,,$$
$$(A_\tau)^{-1} = (A_\tau^0))^{-1}(1 - A_\tau^q(A_\tau^0)^{-1} + (A_\tau^q(A_\tau^0)^{-1})^2) \,. \tag{A.42}$$

Then performing the integral over $\delta\tau_i$, the following prefactor is obtained

$$\text{pref}_\tau = (\frac{\Delta_\Sigma}{\sum \omega_k^2\beta^2})^{\frac{1}{2}} \frac{T^{n-1}(2\pi)^{\frac{n}{2}}}{\ell} \,, \tag{A.43}$$

which comes with the following exponent

$$\exp[-\frac{1}{2}\sum_{ij}(A^{-1})_{ij}\omega_i\omega_j\ell^2] \,. \tag{A.44}$$

The remaining exponent is recorded below

$$\exp[-\frac{1}{2}\frac{\Delta_\Sigma}{\beta^2} + Q(q_\mu)] \,, \tag{A.45}$$

where $Q(q_\mu)$ can be organized as

$$Q(q) = -\frac{\ell^2 n^2\beta^2}{2\Delta_\Sigma}q^2 + 2n^2(\frac{\ell^2\beta}{2\Delta_\Sigma})^2\sum_{i,j}(q\cdot p_i)(q\cdot p_i)(A_\beta^{-1})_{ij}$$
$$-\frac{1}{2}(\frac{\Delta_\Sigma T}{\sum \omega_k^2\ell})^2\sum_{kl}(\delta_{kl} - \frac{\omega_k\omega_l}{\sum \omega_i^2})\tilde{A}_k^q\tilde{A}_l^q \,, \tag{A.46}$$

where

$$\tilde{A}_m^q = \sum \omega_i A_{im}^q = 4(\frac{\ell^2}{2\Delta_\Sigma})^2 n\sum_{i,k} q\cdot p_i\big((A_\beta^{-1})_{im} + (A_\beta^{-1})_{ik}\big)\omega_k\omega_m(\omega_m - \omega_k) - \frac{\ell^2}{\Delta_\Sigma}nq_0\omega_k^2 \,. \tag{A.47}$$

Finally we are in the right position to integrate over q to get

$$\sqrt{\frac{(2\pi)^{d+1}}{\det Q_{qq}}} \,, \quad Q_{qq} = -\frac{\partial}{\partial q^\mu}\frac{\partial}{\partial q^\nu}Q \,, \tag{A.48}$$

where explicitly we obtain

$$\begin{aligned}Q_{qq} = &\frac{\ell^2 n^2 \beta^2}{\Delta_\Sigma}\delta_{\mu\nu} - 2n^2\left(\frac{\ell^2\beta}{2\Delta_\Sigma}\right)^2\sum_{i,j}(p_i^\mu p_j^\nu + p_j^\mu p_i^\nu)(q\cdot p_i)(A_\beta^{-1})_{ij} \\ &+ \frac{1}{2}\left(\frac{\Delta_\Sigma T}{\sum\omega_k^2\ell}\right)^2\sum_{kl}\left(\delta_{kl} - \frac{\omega_k\omega_l}{\sum\omega_i^2}\right)\left(\frac{\partial}{\partial q^\mu}\tilde{A}_k^q\frac{\partial}{\partial q^\nu}\tilde{A}_l^q + \frac{\partial}{\partial q^\nu}\tilde{A}_k^q\frac{\partial}{\partial q^\mu}\tilde{A}_l^q\right).\end{aligned} \tag{A.49}$$

It is not hard to find that the second and the third term in Q_{qq} is only rank-$(n-1)$ up to $\mathcal{O}(q)$, thus by taking $T\to\infty$, the whole determinant of Q_{qq} can be evaluated by multiplying the rank-$(n-1)$ determinant of the last term with the rank-$(d-n+2)$ determinant of the first term [23]. Using this trick, we can pull out β and T, which is crucial for determining $f(\beta)$. Pulling out T cancels T^{n-1} in pref$_\tau$, leaving the final answer independent of cut-off T. On the other hand, it contributes $\beta^{-(d-n+2)}$. Together with eq. (A.28) (also note eq. (A.45)), one can readily find the β (or α) dependence $f(\beta)\sim\beta^{\Delta_\Sigma-d}$

$$d\beta\beta^{\Delta_\Sigma-d}e^{-\frac{1}{2}\frac{\Delta_\Sigma}{\beta^2}} \sim d\alpha\alpha^{\frac{d-\Delta_\Sigma}{2}}e^\alpha\,. \tag{A.50}$$

The remaining part is technically difficult to evaluate, but nevertheless it is not necessary to evaluate it. The form of $f(\beta)$ in (A.31) is now fixed, and the remaining factor serves simply as normalization factor and should be determined by contact interaction.

A.4 $n=4$ Contact Witten diagram

We consider Witten diagram given by contact interaction

$$\mathcal{L} = \phi_1^2\phi_2^2\,. \tag{A.51}$$

The AdS amplitude is simply

$$A = \int d^{d+2}X\prod_{i=1}^4 G_{b\partial}(X,P_i)\,, \tag{A.52}$$

where $G_{b\partial}$ is the bulk-to-boundary propagator

$$G_{b\partial}(X,P_i)=\frac{\mathcal{C}_{\Delta_i}}{\ell^{\frac{d-1}{2}}(-2P_i\cdot X/\ell)^{\Delta_i}}\,. \tag{A.53}$$

The contact Witten diagram can be represented by D-function [229]

$$A=\ell^{3-d}\mathcal{C}^2_{\Delta_1}\mathcal{C}^2_{\Delta_2}D_{\Delta_1\Delta_2\Delta_2\Delta_1}(P_i)\,, \tag{A.54}$$

where

$$D_{\Delta_1\Delta_2\Delta_2\Delta_1}(P_i)=\frac{1}{\ell\Gamma(\Delta_1)^2\Gamma(\Delta_2)^2}\int_0^\infty(\prod_i dt_i t_i^{\Delta_i-1})\int dX e^{-2\sum_{i=1}^4 t_i\frac{P_i\cdot X}{\ell}}\,. \tag{A.55}$$

Integrate out the bulk coordinate X, one found a simple representation of this Witten diagram [22]

$$A=\ell^{3-d}\pi^{\frac{d}{2}}\Gamma(\frac{\Delta_\Sigma-d}{2})\prod_{i=1}^4\frac{\mathcal{C}_{\Delta_i}}{\Gamma(\Delta_i)}\int_0^\infty(\prod_{i=1}^4 dt_i t_i^{\Delta_i-1})e^{-\sum_{i<j}t_it_jP_{ij}}\,. \tag{A.56}$$

This representation can be straightforwardly transformed into Mellin amplitudes. We start with this representation, it is then not surprise it gives rise to the same answer as Mellin space provides. We find saddle-points of t_i are

$$\begin{aligned}
t_1&=-\frac{i\sqrt{\ell}(m+m_{12})(m+\bar{m}_{12})}{4\sqrt{\bar{m}_{12}}m}\,,\quad t_2=-\frac{i\sqrt{\ell}(m-m_{12})(m+\bar{m}_{12})}{4\sqrt{\bar{m}_{12}}m}\,,\\
t_3&=\frac{i\sqrt{\ell}(m+m_{12})(m-\bar{m}_{12})}{4\sqrt{\bar{m}_{12}}m}\,,\quad t_2=\frac{i\sqrt{\ell}(m-m_{12})(m-\bar{m}_{12})}{4\sqrt{\bar{m}_{12}}m}\,.
\end{aligned} \tag{A.57}$$

Picking up these saddle-points and including all reasonable normalization, we find it indeed gives rise to D_c in eq. (3.140) for $s=m^2$.

We can also follow the routine of [3] to verify that the contact Witten diagram is equivalent to momentum conservation delta function. To show this, we evaluate

$$\int\frac{d|p_3|}{2\omega_3}\frac{d^dp_4}{2\omega_4}|p_3|^{d-1}A\,. \tag{A.58}$$

In flat-space, this evaluates the phase-space volume

$$\int \frac{d|p_3|}{2\omega_3}\frac{d^d p_4}{2\omega_4}|p_3|^{d-1}\delta^{(d+1)}(p_1+p_2+p_3+p_4) = \frac{(s-m_{12}^2)^{\frac{d-2}{2}}(s-\bar{m}_{12}^2)^{\frac{d-2}{2}}}{2^d s^{\frac{d-1}{2}}}\,, \quad \text{(A.59)}$$

which is the factor appear in partial-wave expansion of amplitudes eq. (3.133). To show the match, we still use saddle-points of P_i eq. (3.101) but setting p_3, p_4 off-shell in frame eq. (3.107)

$$p_1 = (\omega_1, p\widehat{n})\,, \quad p_2 = (\omega_2, -p\widehat{n})\,, \quad p_3 = (-|\omega_3|, |p_3|\widehat{n}')\,, \quad p_4 = (-|\omega_4|, -|p_4|\widehat{n}'')\,, \quad \text{(A.60)}$$

where $|\omega_i| = \sqrt{m_i^2+|p_i|^2}$. Then we find the saddle-points of eq. (A.58) are eq. (A.57) together with

$$|p_3| = |p_4| = p\,, \quad \widehat{n}'' = \widehat{n}'\,. \quad \text{(A.61)}$$

Include all relevant factors, it is equivalent to momentum conservation delta function.

A.5 Conformal blocks with large Δ and $\Delta_{1,2}$

A.5.1 From Casimir equation

We consider four-point function expanded in terms of conformal block

$$\langle \mathcal{O}_1 \cdots \mathcal{O}_4 \rangle = \frac{1}{(P_{12}P_{34})^{\frac{\Delta_1+\Delta_2}{2}}}\left(\frac{P_{24}}{P_{14}}\right)^{\frac{\Delta_{12}}{2}}\left(\frac{P_{14}}{P_{13}}\right)^{\frac{\Delta_{21}}{2}}\sum_{\Delta,J} c_{\Delta,J} G_{\Delta,J}(z,\bar{z})\,. \quad \text{(A.62)}$$

Acting with Casimir operator yields the Casimir equation [230]

$$\mathcal{D} G_{\Delta,J} = (\Delta(\Delta-d)+J(J+d-2))G_{\Delta,J}\,, \quad \text{(A.63)}$$

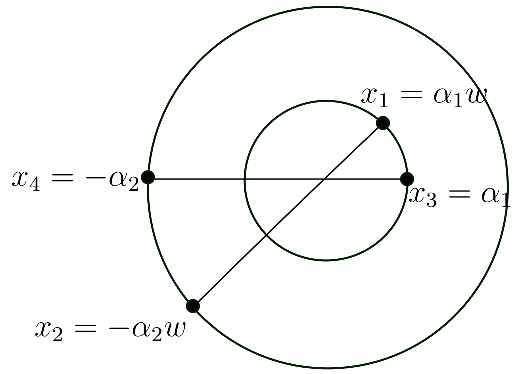

Figure A.1: A convenient conformal frame for solving conformal block at $\Delta, \Delta_i \to \infty$. Non-identical operators subject to flat-space saddle-points can also have access to above conformal frame. In general, $\alpha_1 \neq \alpha_2$.

where

$$\mathcal{D} = \mathcal{D}_z + \mathcal{D}_{\bar{z}} + 2(d-2)\frac{z\bar{z}}{z-\bar{z}}((1-z)\partial_z - (1-\bar{z})\partial_{\bar{z}})\,,$$
$$\mathcal{D}_z = 2(z^2(1-z)\partial_z^2 - (1+a+b)z^2\partial_z - abz)\,. \tag{A.64}$$

$(z, \bar{z})$ is the usual cross-ratios, and note $a = b = \Delta_{21}/2$. For $\Delta_1 = \Delta_2$ or $\Delta_i \ll \Delta$, the Casimir equation simplifies and easily gives eq. (3.126). For $\Delta_1 \neq \Delta_2$, the term with Δ_{12} is very important. Inspired by eq. (3.109) and (3.111), we now adopt the following conformal frame

$$z = \frac{4m^2 w}{(m^2 - m_{12}^2)(1+w)^2}\,, \quad \bar{z} = \frac{4m^2 \bar{w}}{(m^2 - m_{12}^2)(1+\bar{w})^2}\,, \tag{A.65}$$

where $w = re^{i\theta}$, which is depicted in Fig A.1. For $m_{12} = 0$, the parameterization eq. (A.65) reduces to the usual radial frame [112]. The Casimir equation eq. (A.63) now reads

$$\mathcal{A}G(r,\eta) + \mathcal{B}_1\partial_r G(r,\eta) + \mathcal{B}_2\partial_\eta G(r,\eta) + \mathcal{C}_1\partial_r^2 G(r,\eta) + \mathcal{C}_2\partial_\eta^2 G(r,\eta) + \mathcal{C}_3\partial_r\partial_\eta G(r,\eta) = 0\,, \tag{A.66}$$

where

$$
\begin{aligned}
&\mathcal{A} = (r^2-1)(r^2-2\eta r+1)^3((d-2)J(m_{12}-m)(m+m_{12})(r^2+2\eta r+1)^2 \\
&+\Delta(-d(m_{12}-m)(m+m_{12})(r^2+2\eta r+1)^2-m^3\ell(r^2+2\eta r+1)^2 \\
&+m_{12}^2\Delta(r^4+(4\eta^2-6)r^2+1))+J^2(m_{12}-m)(m+m_{12})(r^2+2\eta r+1)^2)\,, \\
\\
&\mathcal{B}_1 = -r(r^2+2\eta r+1)(-m^2(r^2-2\eta r+1)^2(d(r^2+1)(r^4+(2-4\eta^2)r^2+1) \\
&+r^2(r^4+4\eta^2(r^2+3)-7r^2-9)-1)+m_{12}^2(r^2+2\eta r+1)(d(r^4-2\eta(r^2+1)r \\
&-6r^2+1)(r^2-2\eta r+1)^2+r(2\eta+r(r^6+18r^4+8\eta^3(r^2+3)r-16r^2-4\eta^2(5r^4 \\
&-4r^2+7)-2\eta(r^4+r^2+15)r+30))-1)+8\eta m^2m_{12}r(r^2-1)^2\ell(r^2-2\eta r+1)^2)\,, \\
\\
&\mathcal{B}_2 = (1-r^2)(r^2+2\eta r+1)(\eta(-m^2)(r^2-2\eta r+1)^2(dr^4-4(d+1)\eta^2r^2+2dr^2 \\
&+d-r^4+6r^2-1)+m_{12}^2(r^2+2\eta r+1)(-8(d+1)\eta^4r^3+4(3d+1)\eta^3r^2(r^2+1) \\
&+2\eta^2r((5-3d)r^4+2(d-3)r^2-3d+5)+\eta(r^2+1)((d-1)r^4-2(7d+1)r^2+d-1) \\
&+4r((d-2)r^4+2(d+2)r^2+d-2))-8(\eta^2-1)m^2m_{12}r(r^2+1)\ell(r^2-2\eta r+1)^2)\,, \\
\\
&\mathcal{C}_1 = -r^2(r^2-1)(r^2-2\eta r+1)(r^2+2\eta r+1)^2(m_{12}^2(r^4+(4\eta^2-6)r^2+1) \\
&-m^2(r^2-2\eta r+1)^2)\,, \\
\\
&\mathcal{C}_2 = (\eta^2-1)(1-r^2)(r^2-2\eta r+1)(r^2+2\eta r+1)^2(m_{12}^2(r^4+(4\eta^2-6)r^2+1) \\
&-m^2(r^2-2\eta r+1)^2)\,, \\
\\
&\mathcal{C}_3 = 8\left(\eta^2-1\right)m_{12}^2r^2\left(r^2-1\right)^2\left(r^2-2\eta r+1\right)\left(r^2+2\eta r+1\right)^2\,.
\end{aligned}
\tag{A.67}
$$

We denote $\eta = \cos\theta$. The expression looks horrible, but we find it is especially useful to define

$$g_{\Delta,J}(z,\bar{z}) = \left(\frac{P_{24}}{P_{14}}\right)^{\frac{\Delta_{12}}{2}} \left(\frac{P_{14}}{P_{13}}\right)^{\frac{\Delta_{21}}{2}} G_{\Delta,J}(z,\bar{z})\,. \tag{A.68}$$

Then the leading order of Casimir equation is trivially satisfied by scaling $r^{\Delta} f(r,\eta)$ and the sub-leading order of the equation reads

$$r(d((r^2+1)^2 - 4\eta^2 r^2) + 4(\eta^2-1)(r^2+1))f + (r^2-1)(r^4 + (2-4\eta^2)r^2 + 1)\partial_r f = 0\,. \tag{A.69}$$

Finally, we end up with a simple solution (include reasonable normalization)

$$g_{\Delta,J}(r,\theta)|_{\Delta,\Delta_i\to\infty} = \frac{J!N_\Delta}{(d-2)_J} \frac{(4r)^{\Delta} C_J^{\frac{d}{2}-1}(\cos\theta)}{(1-r^2)^{\frac{d}{2}-1}\sqrt{(1+r^2)^2 - 4r^2\cos^2\theta}}\,, \tag{A.70}$$

where

$$N_\Delta = \frac{\Delta^{2\Delta}}{(\Delta-\Delta_{12})^{\Delta-\Delta_{12}}(\Delta+\Delta_{12})^{\Delta+\Delta_{12}}}\,. \tag{A.71}$$

The expression looks the same as eq. (3.126) up to additional normalization factor, but the definition of (r,θ) is no longer the same, besides, $g_{\Delta,J}$ is defined by including appropriate prefactors. It is also worth noting that here (r,θ) depend on Δ, so when we sum over conformal blocks, we should be careful about addressing conformal block itself. To avoid confusion, we may denote (r_Δ,θ_Δ) in the main text. In the next subsection, we verify our solution by working specifically in $d = 2, 4$.

A.5.2 Explicit check in $d = 2, 4$

In $d = 2, 4$, the conformal block can be exactly solved [230, 231]

$$d = 2\,, \qquad G_{\Delta,J} = k^{a,b}_{\Delta+J}(z)k^{a,b}_{\Delta-J}(\bar{z}) + k^{a,b}_{\Delta+J}(\bar{z})k^{a,b}_{\Delta-J}(z)\,,$$

$$d = 4\,, \qquad G_{\Delta,J} = \frac{z\bar{z}}{z-\bar{z}}\left(k^{a,b}_{\Delta+J}(z)k^{a,b}_{\Delta-J-2}(\bar{z}) - k^{a,b}_{\Delta+J}(\bar{z})k^{a,b}_{\Delta-J-2}(z)\right)\,, \quad \text{(A.72)}$$

where

$$k^{a,b}_{\beta}(z) = z^{\frac{\beta}{2}}\,{}_2F_1(a+\frac{\beta}{2}, b+\frac{\beta}{2}, \beta, z) \tag{A.73}$$

We can find $k^{a,a}_{\beta}(z)|_{\beta,a\to\infty}$ by using the Barnes representation

$${}_2F_1(a,b,c,z) = \frac{\Gamma(c)}{\Gamma(a)\Gamma(b)}\int_{-i\infty}^{i\infty}\frac{ds}{2\pi i}\frac{\Gamma(a+s)\Gamma(b+s)\Gamma(-s)}{\Gamma(c+s)}(-z)^s\,. \tag{A.74}$$

We deform the contour to right and find there is a saddle-point of s

$$s^* = \frac{w\beta(\beta+2a)}{(1-w)\beta - 2a(1+w)}\,. \tag{A.75}$$

Then by performing the integral dominated by this saddle-point, we obtain

$$\begin{aligned} k^{a,a}_{\beta} = {} & \frac{\beta^\beta}{\sqrt{1-w}}(a+\frac{\beta}{2})^{-2a-\beta}(w+1)^{2a-\frac{1}{2}}w^{\beta/2}(\beta-2a)^{\frac{\beta(\beta-2a)}{2a(w+1)+\beta(w-1)}}(2a+\beta)^{\frac{\beta w(2a+\beta)}{2a(w+1)+\beta(w-1)}}\times \\ & (\beta^2-4a^2)^{\frac{(w+1)(4a^2-\beta^2)}{2a(w+1)+\beta(w-1)}-\frac{\beta(2a(w-1)+\beta(w+1))}{2\beta(1-w)-4a(w+1)}}(2\beta(1-w)-4a(w+1))^{-2a} \end{aligned} \tag{A.76}$$

This expression looks tough, but it turns out those transcendental factors exactly give rise to the wanted prefactor. Plug eq. (A.76) in eq. (A.72) and absorb the prefactors, we find

$$\begin{aligned} d = 2\,, \qquad & g_{\Delta,J} = N_\Delta \frac{(4r)^\Delta}{\sqrt{1+r^2-2r^2\cos(2\theta)}} \times 2\cos(J\theta)\,, \\ d = 4\,, \qquad & g_{\Delta,J} = N_\Delta \frac{(4r)^\Delta}{(1-r^2)\sqrt{1+r^2-2r^2\cos(2\theta)}} \times \frac{\sin((J+1)\theta)}{\sin\theta}\,, \end{aligned} \tag{A.77}$$

which precisely match with the general result eq. (A.70).

Appendix B

Appendices for Chapter 3

B.1 $\langle VVV \rangle$ from Witten-diagram

In this appendix, we start from AdS Lagrangian in $d = 3$ to derive $\langle VVV \rangle$ three-point functions. From helicity basis we constructed in the main text, it follows that $\langle VVV \rangle$ has three independent structures, and it is expected the first structure corresponds to the Yang-Mills vertex and the higher-derivative coupling in AdS is captured by the second two (the odd and even "same-helicity" ones, which are analytic in spin for $J \geq 0$). Our starting point is the following Lagrangian for Yang-Mills in AdS (omitting gravity):

$$\mathcal{L} = -\frac{1}{4g_{\rm YM}^2} F^a_{\mu\nu} F^{\mu\nu a} + \frac{\theta}{32\pi^2} F^a_{\mu\nu} \tilde{F}^{\mu\nu a} - \frac{f^{abc}}{3g_{\rm YM}^3} \left(g_{\rm H}\, F_\mu{}^{\nu a} F_\nu{}^{\rho b} F_\rho{}^{\mu c} + g'_{\rm H}\, \tilde{F}_\mu{}^{\nu a} \tilde{F}_\nu{}^{\rho b} \tilde{F}_\rho{}^{\mu c} \right) + \cdots \,, \tag{B.1}$$

where a, b, c are $\mathrm{SU}(N)$ group indices, f^{abc} is the structure constant, $\tilde{F}_{\mu\nu} = \frac{1}{2}\epsilon_{\mu\nu\sigma\rho}F^{\sigma\rho}$ and $\cdots$ is other terms that are not relevant to our purpose. After rescaling the fields by the coupling to make A canonically normalized, it follows that we have two three-point gluon vertices

$$\begin{aligned} &\text{Yang-Mills:} && -\, g_{\rm YM}\, f^{abc} \partial_\mu A^a_\nu A^{\mu b} A^{\nu c} \,, \\ &\text{Higher-derivative:} && -\, \frac{g_{\rm H}}{3} f^{abc}\, F_\mu{}^{\nu a} F_\nu{}^{\rho b} F_\rho{}^{\mu c} + \text{odd part} \,, \end{aligned} \tag{B.2}$$

where only the linearized part of $F_{\mu\nu}$ will contribute in the second case.

It is most convenient to work with the AdS embedding formalism [210] where the bulk-to-boundary propagator with conformal dimension Δ and spin J is [210]

$$\Pi_{\Delta,J}(Y,W;X,Z)=\mathcal{C}(\Delta,J)\frac{\big((-2X\cdot Y)(W\cdot Z)+2(W\cdot X)(Z\cdot Y)\big)^J}{(-2X\cdot Y)^{\Delta+J}}\,, \tag{B.3}$$

where X and Z are embedding coordinate and auxiliary polarization respectively for boundary CFT, similarly Y and W are $(d+2)$-dimensional embedding coordinate and polarization for the bulk AdS_{d+1}, which are constrained by

$$X^2=X\cdot Z=Z^2=0\,,\quad Y^2=-1\,,\quad Y\cdot W=W^2=0\,, \tag{B.4}$$

and have the further redundancy $Z\simeq Z+\alpha X$. The normalization factor reads

$$\mathcal{C}(\Delta,J)=\frac{(J+\Delta-1)\Gamma(\Delta)}{2\pi^{\frac{d}{2}}(\Delta-1)\Gamma(\Delta+1-\frac{d}{2})}\,. \tag{B.5}$$

Derivatives in AdS can be evaluated using the bulk covariant derivative operator [210]

$$\nabla_A=\frac{\partial}{\partial Y^A}+Y_A(Y\cdot\frac{\partial}{\partial Y})+W_A(Y\cdot\frac{\partial}{\partial W})\,. \tag{B.6}$$

which commutes with the constraints. It is also convenient to introduce the differential operator K_A [210]

$$K_A^W=\left(\frac{\partial}{\partial W^A}+Y_A(Y\cdot\frac{\partial}{\partial W})\right)\left(\frac{d-3}{2}+W\cdot\frac{\partial}{\partial W}\right)-\frac{1}{2}W_A\left(\frac{\partial^2}{\partial W\cdot\partial W}+(Y\cdot\frac{\partial}{\partial W})^2\right)\,, \tag{B.7}$$

which helps do index contractions in AdS:

$$\sum_W f(W^*)g(W)=\frac{1}{J!(\frac{d-1}{2})_J}f(K^W)g(W)\,. \tag{B.8}$$

With these ingredients, we are ready to compute $\langle VVV\rangle$ by performing the following integrals over (Euclidean) AdS $Y^2 = -1$:

$$
\begin{aligned}
\langle V(X_1)V(X_2)V(X_3)\rangle^{\mathrm{YM}} &= -g_{\mathrm{YM}} f^{abc}\, \mathcal{C}^{\frac{3}{2}}_{d-1,1} \int_{\mathrm{EAdS}} dY \sum_{W_1,W_2} (W_1^* \cdot \nabla\Pi_{d-1,J}(Y,W_2^*;X_1,Z_1)) \\
&\qquad \times \Pi_{d-1,J}(Y,W_1;X_2,Z_2)\Pi_{d-1,J}(Y,W_2;X_3,Z_3) + (5 \text{ permutations}) \\
\langle V(X_1)V(X_2)V(X_3)\rangle^{\mathrm{H}} &= -2g_{\mathrm{H}} f^{abc}\, \mathcal{C}^{\frac{3}{2}}_{d-1,1} \int_{\mathrm{EAdS}} dY \sum_{W_1,W_2,W_3} \\
&\times \left(W_1^* \cdot \nabla\Pi_{d-1,1}(Y,W_2;X_1,Z_1) - W_2 \cdot \nabla\Pi_{d-1,1}(Y,W_1^*;X_1,Z_1)\right) \\
&\times \left(W_2^* \cdot \nabla\Pi_{d-1,1}(Y,W_3;X_2,Z_2) - W_3 \cdot \nabla\Pi_{d-1,1}(Y,W_2^*;X_2,Z_2)\right) \\
&\times \left(W_3^* \cdot \nabla\Pi_{d-1,1}(Y,W_1;X_3,Z_3) - W_1 \cdot \nabla\Pi_{d-1,1}(Y,W_3^*;X_3,Z_3)\right),
\end{aligned}
\tag{B.9}
$$

where the factor $\mathcal{C}^{\frac{3}{2}}_{d-1,1}$ ensures our VV two-point function follows the CFT normalization. The integrals can be done in elementary ways, for example using Feynman/Schwinger parameters. We obtain (in $d = 3$):

$$
\begin{aligned}
\langle VVV\rangle^{\mathrm{YM}} &= \frac{3g_{\mathrm{YM}}}{16\sqrt{2}} f^{abc} \frac{H_{23}V_1 + H_{13}V_2 + H_{12}V_3 + V_1V_2V_3}{(-2X_1\cdot X_2)^{\frac{3}{2}}(-2X_1\cdot X_3)^{\frac{3}{2}}(-2X_2\cdot X_3)^{\frac{3}{2}}}\,, \\
\langle VVV\rangle^{\mathrm{H}} &= \frac{-g_{\mathrm{H}}}{8\sqrt{2}} f^{abc} \frac{H_{23}V_1 + H_{13}V_2 + H_{12}V_3 + 5V_1V_2V_3}{(-2X_1\cdot X_2)^{\frac{3}{2}}(-2X_1\cdot X_3)^{\frac{3}{2}}(-2X_2\cdot X_3)^{\frac{3}{2}}}\,,
\end{aligned}
\tag{B.10}
$$

where H_{ij} follows the definition in eq. (D.3) and V_i is defined by (see [47] for more details)

$$
V_i := V_{i,jk} = \frac{(X_i\cdot X_k)(Z_i\cdot X_j) - (X_i\cdot X_j)(Z_i\cdot X_k)}{X_j\cdot X_k}\,. \tag{B.11}
$$

To project onto the conformal frame $(0, x, \infty)$, we parameterize X_i, Z_i (in embedding lightcone coordinates) as

$$
\begin{aligned}
&X_1 = (1,0,0)\,, \quad Z_1 = (0,0,\epsilon_1)\,, \quad X_2 = (1,x^2,x)\,, \quad Z_2 = (0, 2\epsilon_2\cdot x, \epsilon_2)\,, \\
&X_3 = (0,1,0)\,, \quad Z_3 = (0,0,\epsilon_3)\,.
\end{aligned}
\tag{B.12}
$$

We thus end up with

$$\begin{aligned}\langle VVV\rangle^{\rm YM} &= \frac{3g_{\rm YM}f^{abc}}{16\sqrt{2}|x|^3}\left[(x\cdot\epsilon_1)(\epsilon_2\cdot\epsilon_3)+(x\cdot\epsilon_2)(\epsilon_1\cdot\epsilon_3)-(x\cdot\epsilon_3)(\epsilon_1\cdot\epsilon_2)+\frac{(x\cdot\epsilon_1)(x\cdot\epsilon_2)(x\cdot\epsilon_3)}{x^2}\right],\\ \langle VVV\rangle^{\rm H} &= \frac{-g_{\rm H}f^{abc}}{8\sqrt{2}|x|^3}\left[(x\cdot\epsilon_1)(\epsilon_2\cdot\epsilon_3)+(x\cdot\epsilon_2)(\epsilon_1\cdot\epsilon_3)-(x\cdot\epsilon_3)(\epsilon_1\cdot\epsilon_2)-3\frac{(x\cdot\epsilon_1)(x\cdot\epsilon_2)(x\cdot\epsilon_3)}{x^2}\right].\end{aligned} \tag{B.13}$$

Comparing the above results with $M_V B_V$ (see eq. (4.4) and eq. (4.16)) for conserved currents, the agreement can be easily observed and the OPE coefficients can be readily read off

$$\lambda^{(\rm e1)}_{VVV} = \frac{g_{\rm YM}}{16\sqrt{2}}\,, \qquad \lambda^{(\rm e2)}_{VVV} = \frac{g_{\rm H}}{8\sqrt{2}}\,, \qquad \lambda^{(\rm o2)}_{VVV} = \frac{g'_{\rm H}}{4\sqrt{2}\pi}\,, \tag{B.14}$$

where we strip off color factors by defining $\langle VVV\rangle$ three-point functions as

$$\langle VVV\rangle^a = f^{abc}\times\lambda^a_{VVV}T^a_{111}\,, \tag{B.15}$$

in which a runs through structures in eq. (4.14).

B.2 Simplifying Fourier transforms using spinors

We find that much of the calculations can be streamlined analytically by representing the polarization vectors as a product of two spinors (see also [141]).

Given a two-component spinor $|\epsilon\rangle$, we define $\langle\epsilon| \equiv |\epsilon\rangle^T\cdot i\sigma_2$, and parametrize the null polarizations as

$$\epsilon_i^\mu \equiv \frac{1}{2}\langle\epsilon_i|\sigma^\mu|\epsilon_i\rangle \tag{B.16}$$

where σ^μ, $\mu = 1, 2, 3$, are Pauli matrices. This vector is automatically null. Other useful identities include:

$$\langle a|\sigma^\mu|b\rangle\langle c|\sigma_\mu|d\rangle = -\langle ac\rangle\langle bd\rangle - \langle ad\rangle\langle bc\rangle, \quad (\epsilon_1, p, \epsilon_3) = \frac{i}{2}\langle\epsilon_1\epsilon_3\rangle\langle\epsilon_1|p|\epsilon_3\rangle\,. \tag{B.17}$$

The three-point helicity structures in eq. (4.10) are very simple in terms of spinors:

$$\begin{aligned} T_{123}^{\pm,\pm}(p) = {} & \frac{(4\pi)^{\frac{3}{2}}}{2^{\tau_1+\tau_2-\Delta_3}}\left(\frac{-i\langle\epsilon_3|p|\epsilon_3\rangle}{\sqrt{2}}\right)^{J_3-J_1-J_2} \langle\epsilon_1\epsilon_3\rangle^{2J_1}\langle\epsilon_2\epsilon_3\rangle^{2J_2}|p|^{\beta_{12;3}-3} \\ & \times\left(\frac{1-\xi_{1,p,3}}{2}\right)^{2J_1}\left(\frac{1+\xi_{2,p,3}}{2}\right)^{2J_2} \end{aligned} \tag{B.18}$$

where $\xi_{i,p,3} \equiv \frac{\langle\epsilon_i|p|\epsilon_3\rangle}{|p|\langle\epsilon_i\epsilon_3\rangle}$ is a measure of spin along the p axis.

When we go to Fourier space using eq. (4.12) and its derivatives, we find remarkable simplifications thanks to the fact that the vector ϵ_3 is orthogonal to all other vectors multiplying p. In fact the Fourier-transform involves only similar-looking objects and we were able to Fourier-transform the generic term analytically:

$$\begin{aligned} \int & \frac{d^3p}{(2\pi)^3}e^{ip\cdot x}p^{2k}\left(-i\langle\epsilon_3|p|\epsilon_3\rangle\right)^J(\xi_{1,p,3})^a(\xi_{2,p,3})^b \\ & = \frac{2^{2k+J}}{\pi^{\frac{3}{2}}}\frac{\langle\epsilon_3|x|\epsilon_3\rangle^J}{x^{2k+2J+3}} \times \sum_{a',b'} f^{a,b}_{a',b'}\frac{\Gamma\left(\frac{a'+b'+3}{2}+k+J\right)}{\Gamma\left(\frac{a+b}{2}-k\right)}(\xi_{1,x,3})^{a'}(\xi_{2,x,3})^{b'} \end{aligned} \tag{B.19}$$

where the sum runs over $a' \le a$, $b' \le b$ such that $(a+b-a'-b')$ is even, and f is the following combinatorial factor

$$f^{a,b}_{a',b'} = \frac{(2i)^{a'+b'}}{2^{a+b}}\frac{a!}{a'(a-a')!}\frac{b!}{b'!(b-b')!}\frac{(a+b-a'-b')!}{\left(\frac{a+b-a'-b'}{2}\right)!}\,. \tag{B.20}$$

Using the integral (B.19) it is straightforward to convert the structures in eq. (B.18) back and forth between momentum and coordinate space. The other operations also have simple forms:

- Conformal inversion: this takes $(\infty, x, 0) \mapsto (0, x^\mu/x^2, \infty)$ and $|\epsilon_2\rangle \mapsto i\frac{x|\epsilon_2\rangle}{|x|}$. The net effect is simply: $\xi_{2,x} \mapsto 1/\xi_{2,x}$ and $\langle\epsilon_2\epsilon_3\rangle \mapsto i\langle\epsilon_2\epsilon_3\rangle\xi_{2,x}$.

- Shadow transform: two-point functions in position and Fourier space are simply:

$$\begin{aligned}\langle\mathcal{O}_1(0)\mathcal{O}_2(x)\rangle &= \frac{\langle 1|x|2\rangle^{2J}}{(-2)^J|x|^{\Delta+J}},\\ \langle\mathcal{O}_1(0)\mathcal{O}_2(p)\rangle &= \frac{(4\pi)^{\frac{3}{2}}\Gamma(\frac{3}{2}-\Delta)(\frac{1}{2})_J}{(-2)^J 4^\Delta\Gamma(\Delta+J)}|p|^{\Delta-\frac{3}{2}}\langle\epsilon_1\epsilon_2\rangle^{2J} \ \times {}_2F_1\big(-J,\tfrac{3}{2}-\Delta,\tfrac{1}{2},\xi^2_{1,p,2}\big)\,.\end{aligned} \tag{B.21}$$

- Index contractions: the sum over a basis of spin-J states (4.29) becomes:

$$\sum_\epsilon f(\epsilon^*)g(\epsilon) = \frac{(-2)^J}{(2J)!}f(\partial_\epsilon)g(\epsilon)\,. \tag{B.22}$$

B.3 More on conformal blocks

B.3.1 Series expansion of conformal blocks

Here we review how to obtain a series expansion for conformal blocks using the conformal Casimir operator, following the work of ref. [112] for scalar blocks. The same recursion will come in handy for doing certain inversion integrals in the next subsection. The conformal symmetry generators act on a spinning primary $\mathcal{O}(x,\epsilon)$ of dimension Δ as

$$\begin{aligned} D &= x^\mu\partial_{x\mu}+\Delta, & J^{\mu\nu} &= x^\mu\partial_x^\nu - x^\nu\partial_x^\mu + \epsilon^\mu\partial_\epsilon^\nu - \epsilon^\nu\partial_\epsilon^\mu,\\ P^\mu &= \partial_x^\mu, & K^\mu &= x^2\partial_x^\mu - 2x^\mu D + 2(x\cdot\epsilon\partial_\epsilon^\mu - \epsilon^\mu x\cdot\partial_\epsilon),\end{aligned} \tag{B.23}$$

where D, J, P and K generate respectively dilations, rotations, translations and special conformal transformations. The Casimir operator is then $\mathcal{C}_2 = D^2 - \frac{1}{2}J_{\mu\nu}J^{\mu\nu} + \frac{1}{2}\{P_\mu, K^\mu\}$, which has eigenvalue $\mathcal{C}_{\Delta,J} = \Delta(\Delta-d)+J(J+d-2)$ if $\mathcal{O}$ is a rank-J tensor.

Four-point conformal blocks are (by definition) eigenfunctions of the Casimir acting on the pair of operators $1, 2$:

$$\mathcal{C} = D_{12}^2 - \frac{1}{2} J_{12}^{\mu\nu} (J_{12})_{\mu\nu} + \frac{1}{2} \{P_{12}^{\mu}, (K_{12})_{\mu}\} \tag{B.24}$$

where the subscripts denote the fields on which the generators act: $D_{12} \equiv D_1 + D_2$ etc. This form of the Casimir operator however can't be used for the correlator in the frame $0, x, y^{-1}, \infty$. The problem is that P_{12} does not preserve the condition $x_1 = 0$. Fortunately, there is a simple solution: we can use conformal invariance of the four-point correlator to rewrite $P_{12} \mapsto -P_{34}$. Accounting for a commutator, the Casimir is

$$\mathcal{C} = \left[D_{12}(D_{12} - d) - \frac{1}{2} J_{12}^{\mu\nu} (J_{12})_{\mu\nu} \right] + K_x^{\mu} K_{y\mu} \equiv \mathcal{C}^{(0)} + \mathcal{C}^{(1)}. \tag{B.25}$$

Notice that $\mathcal{C}^{(0)}$ is homogenous in x, while $\mathcal{C}^{(1)}$ increases the weight in x and y by one unit. Furthermore, the former is diagonalized by the three-point structures $\mathcal{P}^{ab}_{\Delta,J}$ in eq. (4.43). This suggests writing the block as an infinite series in $\mathcal{P}^{ab}_{\Delta,J}$:

$$G_{J,\Delta}^{(a,b)}(z, \bar{z}) = \sum_{m=0}^{\infty} \sum_{k=-m}^{m} A_{m,k}^{(aa')(bb')} \mathcal{P}^{a,b}_{\Delta+m, J+k}(\hat{x}, \hat{y}) \,, \tag{B.26}$$

such that the Casimir (B.25) gives a recursion relation for the coefficients A. For example, for scalar operators, applying the Casimir to the Gegenbauer polynomials (4.43) gives

$$\mathcal{C}^{(0)} \mathcal{P}^{a,b}_{\Delta,J} = \mathcal{C}_{\Delta,J} \mathcal{P}^{a,b}_{\Delta,J}, \qquad \mathcal{C}^{(1)} \mathcal{P}^{a,b}_{\Delta,J} = \gamma^{a,b,-}_{\Delta,J} \mathcal{P}^{a,b}_{\Delta+1,J-1} + \gamma^{a,b,+}_{\Delta,J} \mathcal{P}^{a,b}_{\Delta+1,J+1}, \tag{B.27}$$

with

$$\begin{aligned} \gamma^{a,b,+}_{\Delta,J} &= (\Delta + J + 2a)(\Delta + J + 2b) \,, \\ \gamma^{a,b,-}_{\Delta,J} &= \frac{J(d + J - 3)(-2a + d - \Delta + J - 2)(-2b + d - \Delta + J - 2)}{(d + 2J - 4)(d + 2J - 2)} \,, \end{aligned} \tag{B.28}$$

from which one deduces the recursion [112]

$$\left(\mathcal{C}_{\Delta,J}-\mathcal{C}_{\Delta+m,J+k}\right)A_{m,k}=\gamma^{-}_{\Delta+m-1,J+k-1}A_{m-1,k+1}+\gamma^{+}_{\Delta+m-1,J+k+1}A_{m-1,k-1}. \tag{B.29}$$

Note a,b in $\gamma^{a,b,\pm}_{\Delta,J}$ is not representing the structure index, they are simply $a=1/2(\Delta_2-\Delta_1), b=1/2(\Delta_3-\Delta_4)$. These coefficients eq. (B.28) will also play important role when we are dealing with MFT, see appendix B.3.2.

This method allows to extend this result straightforwardly to spinning operators [188]. We can use eq. (4.42) to construct $\mathcal{P}^{a,b}_{\Delta,J}$ from three-point functions, and in general $\mathcal{P}^{a,b}_{\Delta,J}$ can be organized as Gegenbaur polynomials and their derivatives, which is consistent with group theoretical analysis for projectors [189].

B.3.2 Inverting powers of cross-ratios times Gegenbauers

In this appendix, we present a more compact approach to deal with the spinning MFT. To be more precise, there is a surprisingly concise and powerful trick that can be used perform Lorentzian inversion formula for a scalar MFT correlator extended with Gegenbauer polynomial, namely

$$\mathcal{G}=\frac{u^{\frac{p}{2}}}{v^{\frac{p}{2}+a}}\tilde{C}_{J'}\left(\xi'\right), \tag{B.30}$$

where $u=z\bar{z}$, $v=(1-z)(1-\bar{z})$ and $\xi'=(1-u-v)/(2\sqrt{uv})$. The punchline is that we find a recursion relation for OPE data associated with above correlator, see eq. (B.33). This formula enjoys more general applications, since as just shown, conformal blocks admit series expansion of precisely this form (after interchanging operators 3 and 4 operators). This was used in [232] to estimate Lorentzian inversion integrals at large dimensions in the $3d$-Ising model. In this paper, we apply the formula to $\mathcal{G}=\mathcal{D}_{\downarrow}G$ for spinning MFT, which is a finite sum of terms (B.30).

The starting point of the recursion is the scalar case, $J'=0$. The relevant OPE data can be found in literatures, at least for equal external operators $a=b$, e.g., [53, 60]. There is a trivial modification that also works for independent a, b, p:

$$c^{a,b}_{0,p,J}(\Delta) = \frac{\Gamma\left(\frac{d-p}{2}-a\right)\Gamma\left(\frac{d-p}{2}+b\right)}{2\Gamma\left(\frac{p}{2}+a\right)\Gamma\left(\frac{p}{2}-b\right)} \frac{\Gamma\left(\frac{\Delta+J}{2}+a\right)\Gamma\left(\frac{\Delta+J}{2}-b\right)}{\Gamma\left(\frac{d-\Delta+J}{2}-a\right)\Gamma\left(\frac{d-\Delta+J}{2}+b\right)}$$
$$\times \frac{\Gamma(\Delta-1)\Gamma\left(J+\frac{d}{2}\right)\Gamma(d-\Delta+J)}{\Gamma(J+1)\Gamma\left(\Delta-\frac{d}{2}\right)\Gamma(\Delta-1+J)} \frac{\Gamma\left(\frac{p-\Delta+J}{2}\right)\Gamma\left(\frac{p-d+\Delta+J}{2}\right)}{\Gamma\left(\frac{-p+d+\Delta+J}{2}\right)\Gamma\left(\frac{-p+2d-\Delta+J}{2}\right)}. \qquad \text{(B.31)}$$

This was tested by checking that the obtained OPE coefficients (obtained from the residues at $\Delta = p+J+2m$) reproduce the series expansion of the bracket in eq. (B.30) with $J' = 0$ to high order. To proceed on generalizing above OPE data to those with $J' \neq 0$, we shall slightly modify $\mathcal{P}_{\Delta,J}$ in (B.26) by interchanging operator 3 and 4, for which eq. (B.27) becomes

$$\begin{aligned}
\mathcal{C}^{(0)} \frac{u^{\frac{p}{2}}}{v^{\frac{p}{2}+a}} \tilde{C}_{J'}\left(\xi'\right) &= \mathcal{C}_{p,J'} \frac{u^{\frac{p}{2}}}{v^{\frac{p}{2}+a}} \tilde{C}_{J'}\left(\xi'\right), \\
\mathcal{C}^{(1)} \frac{u^{\frac{p}{2}}}{v^{\frac{p}{2}+a}} \tilde{C}_{J'}\left(\xi'\right) &= \frac{u^{\frac{p+1}{2}}}{v^{\frac{p+1}{2}+a}} \left(\gamma^{a,-b,-}_{p,J'} \tilde{C}_{J'-1}\left(\xi'\right) + \gamma^{a,-b,+}_{p,J'} \tilde{C}_{J'+1}\left(\xi'\right)\right),
\end{aligned} \qquad \text{(B.32)}$$

with $\gamma^{a,b,\pm}_{\Delta,J}$ already given in eq. (B.28). Since we can integrate-by-parts the Casimir operator in the inversion integral, by eliminating $\tilde{C}_{J'+1}$ from this equation, we get a recursion relation in t-channel spin J':

$$\gamma^{a,-b,+}_{p-1,J'-1}\ c^{a,b}_{J',p,J}(\Delta) = \left(\mathcal{C}_{\Delta,J} - \mathcal{C}_{p-1,J'-1}\right) c^{a,b}_{J'-1,p-1,J}(\Delta) - \gamma^{a,-b,-}_{p-1,J'-1}\ c^{a,b}_{J'-2,p,J}(\Delta)\,. \qquad \text{(B.33)}$$

Let's end by explaining how do we extract OPE data in spinning MFT by using above formula. We first decompose $\mathcal{D}_{\downarrow}G$, e.g., eq. (4.102) into a finite sum of (B.30), next we obtain OPE data for each term by using eq. (B.33) and in the end we can sum them over to get a final answer.

B.3.3 Cross-channel expansion of blocks

In this appendix, we expand (scalar) conformal blocks as $\bar{z} \to 1$ as an exact function of z. To accomplish the computations of the anomalous dimensions in the main-text, we would need t-channel conformal blocks with scalar-exchange, conserved-current-exchange and stress-tensor-exchange. In particular, since we are only concerned about the anomalous dimensions, the logarithmic part of t-channel conformal blocks are enough for our purpose. Our formulae can be deduced from geodesic Witten-diagram [233] by doing a bit of guesswork as described in [234], and is consistent with the most general t-channel conformal blocks in terms of (u, v) rather than $(y, \bar{y})$ provided recently in [235, 236] (see also [237]). Throughout this appendix, we use the variables:

$$y = \frac{z}{1-z}, \qquad \bar{y} = \frac{1-\bar{z}}{\bar{z}}\,. \tag{B.34}$$

In the main text, we use these conformal blocks in the t-channel dDisc, where we take $z \mapsto 1-\bar{z}$ (using y variables, it is $y \to \bar{y}$).

- Scalar exchange

  For scalar-exchange, we can provide a more general t-channel conformal blocks, beyond only picking up logarithmic part. The explicit series is given by

$$\begin{aligned} G_{0,\Delta}(z,\bar{z}) = y^{\frac{\Delta}{2}}(1+y)^b(1+\bar{y})^a \sum_k \Big(& \frac{(-1)^k \bar{y}^{k+\frac{a+b}{2}}\Gamma(\Delta)\Gamma(-a-b-k)\big(a+\frac{\Delta}{2}\big)_k}{k!\Gamma(-b+\frac{\Delta}{2})\Gamma(-a-k+\frac{\Delta}{2})} s_{a,b,k}(y) \\ & + (a \to -a, b \to -b)\Big) \end{aligned} \tag{B.35}$$

  where

$$s_{a,b,k}(y) = {}_3F_2\Big(\tfrac{\Delta-2a}{2}, \tfrac{2b+\Delta}{2}, \tfrac{-2a-d+\Delta-2k+2}{2}; \tfrac{-d+2\Delta+2}{2}, \tfrac{-2a+\Delta-2k}{2}, -y\Big)\,. \tag{B.36}$$

  In practice, what we use in the main text is the logarithmic part $\log \bar{y}$ of above series from setting $a = b = 0$. Note the first line of eq. (B.35) does not have $\log \bar{y}$, and the second line gives us

$$G_{0,\Delta}(z,\bar{z}) = -\sum_k \frac{\Gamma(\Delta)\Gamma(k-\frac{\Delta}{2}+1)y^{\frac{\Delta}{2}}}{\Gamma(\frac{\Delta}{2})^2\Gamma(k+1)^2\Gamma(-k-\frac{\Delta}{2}+1)} \bar{y}^k \log \bar{y}\, s_{0,0,k}(y)\,. \tag{B.37}$$

- Conserved-current exchange

  The $\log \bar{y}$ part of t-channel conformal block with conserved-current-exchange is exhibited as follows:

$$G_{1,d-1}(z,\bar{z}) = \sum_k \mathcal{N}_k^{(1)} \frac{\bar{y}^k\, y^{\frac{d-2}{2}} \log \bar{y}}{y+1} \big(v_{\frac{d-2}{2},k,1} - \frac{2(d-2)ky}{(d-2k)(d-2+2k)} v_{\frac{d}{2},k,0} \big) \,, \tag{B.38}$$

  where

$$\mathcal{N}_k^{(1)} = -\frac{2^{d-1}\Gamma\left(\frac{d+1}{2}\right)\Gamma\left(\frac{d}{2}+k\right)}{\sqrt{\pi}(k!)^2\Gamma\left(\frac{d}{2}\right)\Gamma\left(\frac{d}{2}-k\right)} \,, \quad v_{p,k,m} = {}_2F_1(p,-k+m,p+1-k,-y) \,. \tag{B.39}$$

- Stress-tensor exchange

  The $\log \bar{y}$ part of t-channel conformal block with stress-tensor-exchange was also obtained in [234], it is given by

$$\begin{aligned} G_{2,d}(z,\bar{z}) = \sum_k \mathcal{N}_k^{(2)} \frac{\bar{y}^k\, y^{\frac{d-2}{2}} \log \bar{y}}{y+1} \big((d-2)(3d(y+1) + 2(ky+k-2y-1)) g_{\frac{d}{2},k}(y) \\ - 2\big(2d^2(y+1) + d(k(4y+3) - 6y - 5) + 2(k-1)(ky+k-2y-1)\big) g_{\frac{d-2}{2},k}(y) \big) \,, \end{aligned} \tag{B.40}$$

  where

$$\begin{aligned} \mathcal{N}_k^{(2)} &= \frac{2^{d+1}\Gamma\left(\frac{d+3}{2}\right)\Gamma\left(\frac{d}{2}+k+1\right)}{\sqrt{\pi}(d+2k-2)(d+2k)\Gamma\left(\frac{d}{2}+1\right)\Gamma(k+1)^2\Gamma\left(\frac{d}{2}-k+1\right)} \,, \\ g_{p,k}(y) &= {}_2F_1\big(p,-k,\tfrac{1}{2}(d+2-2k),-y\big) \,. \end{aligned} \tag{B.41}$$

B.4 Four-dimensional gluon amplitudes in flat space

Here we record the bulk YM_4 tree-level gluon amplitudes corresponding to the Lagrangian in eq. (B.1) used in the main text. We start with the three-point ones, from which the four-point amplitudes are then determined by factorization (see [178], whose conventions we follow, for a pedagogical introduction), up to contact interactions with the mass dimension of g_H^2. The form of on-shell three-point amplitudes are fixed by Lorentz and little-group symmetries, up to coupling-dependent prefactors, which we find to be

$$\mathcal{M}^{\rm YM}_{1_-2_-3_+} = i\sqrt{2} f^{abc} g_{\rm YM} \frac{\langle 12\rangle^3}{\langle 23\rangle\langle 31\rangle}\,, \quad \mathcal{M}^{\rm H}_{1_-2_-3_-} = i\sqrt{2} f^{abc}(g_{\rm H} - i g'_{\rm H})\langle 12\rangle\langle 23\rangle\langle 31\rangle\,. \tag{B.42}$$

For $\mathcal{M}^{\rm YM}_{1_+2_+3_-}$ and $\mathcal{M}^{\rm H}_{1_+2_+3_+}$, we simply replace angle-bracket by square-bracket and reverse the odd coupling $g_{\rm H'}$. Tree-level four-point amplitudes can be cut into a product of on-shell three-point amplitudes

$$\mathcal{M}_{1234}\Big|_{p_I^2\to 0} = \frac{\mathcal{M}_{12I}\mathcal{M}_{I34}}{p_I^2}\,. \tag{B.43}$$

We can use this factorization property to construct four-point amplitudes.

Let's first consider the pure Yang-Mills case. One might try to directly use (B.43) for all channels and sum them over, however, this overcounts the pole structures, since the s-channel residue has poles in t or u channel. The standard strategy (see [179]) is to make an ansatz which correctly counts helicity weight and number of derivatives without violating locality

$$\mathcal{M}_{1_-2_-3_+4_+} = \langle 12\rangle^2[34]^2\left(\frac{A}{st} + \frac{B}{su} + \frac{C}{tu}\right)\,. \tag{B.44}$$

By demanding the factorization (B.43), one can readily obtain the Parke-Taylor form

$$\mathcal{M}^{\rm YM^2} = 2g_{\rm YM}^2\langle ij\rangle^4\Big(\frac{T}{\langle 12\rangle\langle 23\rangle\langle 34\rangle\langle 41\rangle} + \frac{U}{\langle 12\rangle\langle 24\rangle\langle 43\rangle\langle 31\rangle}\Big)\,, \tag{B.45}$$

where i, j are gluons that have negative helicity, $T = f^{bce}f^{ade}$ is the t-channel color factor previously defined in eq. (4.115), and U is the same with a and b swapped.

Note that the first term above actually contains s and t-channel poles, and the second term contains s and u poles.

For pure higher-derivative coupling, the nonvanishing amplitudes again all have two gluons of each helicity: $\mathcal{M}^{\mathrm{H}^2}_{1_-2_-3_+4_+}$, $\mathcal{M}^{\mathrm{H}^2}_{1_-2_+3_+4_-}$ and $\mathcal{M}^{\mathrm{H}^2}_{1_-2_+3_-4_+}$ that arise from s-channel, t-channel and u-channel respectively. Using the factorization (B.43) and Bose symmetry, we obtain:

$$\mathcal{M}^{\mathrm{H}^2}_{1_-2_+3_+4_-} = 2(g_{\mathrm{H}}^2 + g_{\mathrm{H}}'^2)\langle 14\rangle^2[23]^2 T\, \frac{u-s}{2t} + c\langle 14\rangle^2[23]^2\,, \tag{B.46}$$

and permutations thereof. The contact ambiguity c depends on higher-derivative terms in the Lagrangian but doesn't contribute to the analysis in the main text as it has finite support in spin. (The tree-level all-$+$ amplitude, also a pure contact term but controlled by a different constant, similarly does not contribute.)

Finally, the mixed $g_{\mathrm{YM}}g_{\mathrm{H}}$ amplitudes (including the higher-derivative correction on both vertices) are quite similar to pure Yang-Mills amplitudes. For example, for $\mathcal{M}^{\mathrm{mix}}_{1_-2_+3_+4_+}$ we consider an ansatz suggested by its helicity scaling and derivative order: $\langle 12\rangle\langle 14\rangle[23][34][24]^2$ times two-channel poles like $1/(st)$. We then obtain:

$$\begin{aligned}
\mathcal{M}^{\mathrm{YM-H}}_{1_-2_-3_-4_+} &= 2g_{\mathrm{YM}}(g_{\mathrm{H}} - ig_{\mathrm{H}}')T\frac{\langle 12\rangle\langle 23\rangle\langle 13\rangle^2}{\langle 34\rangle\langle 41\rangle} + (1\leftrightarrow 2)\,,\\
\mathcal{M}^{\mathrm{YM-H}}_{1_-2_+3_+4_+} &= 2g_{\mathrm{YM}}(g_{\mathrm{H}} + ig_{\mathrm{H}}')T\frac{[23][34][24]^2}{[12][41]} + (3\leftrightarrow 4)\,,
\end{aligned} \tag{B.47}$$

and permutations thereof.

Appendix C

Appendices for Chapter 4

C.1 Local module and sum rules in various dimensions

C.1.1 Sum rules in $D \geq 8$

In $D \geq 8$, there are 19 independent sum rules with even spin $k \geq 2$ that can be constructed from applying dispersion relations to coefficients of the local basis with independent Regge limits (5.8):

$$B_k(p^2) = \oint_\infty \frac{ds}{4\pi i} \Big\{ \tfrac{(s-u)\mathcal{M}^{(3,10)}(s,u)}{(-su)^{\frac{k-2}{2}}}, \tfrac{(s-u)\mathcal{M}^{(2,5,8,9)+}(s,t)}{(-su)^{\frac{k-2}{2}}}, \tfrac{(s-u)(\mathcal{M}^{(6)+}(s,t)+\mathcal{M}^{(7)}(s,u))}{(-su)^{\frac{k-2}{2}}}, \tfrac{\mathcal{M}^{(4,6,9)-}(s,t)}{(-su)^{\frac{k-2}{2}}}, \tfrac{\mathcal{M}^{(5)-}(s,u)}{(-su)^{\frac{k-2}{2}}}, \tfrac{(s-u)\mathcal{M}^{(1,6,7,8)}(s,u)}{(-su)^{\frac{k}{2}}}, \tfrac{(s-u)\mathcal{M}^{(3)+}(s,t)}{(-su)^{\frac{k}{2}}}, \tfrac{(s-u)(\mathcal{M}^{(5)+}(t,s)-2\mathcal{M}^{(4)}(s,u))}{(-su)^{\frac{k}{2}}}, \tfrac{\mathcal{M}^{(5)-}(t,u)}{(-su)^{\frac{k}{2}}}, \tfrac{(s-u)\mathcal{M}^{(2)}(s,u)}{(-su)^{\frac{k+2}{2}}} \Big\} = 0 \,, \tag{C.1}$$

where $\mathcal{M}^{\pm} \equiv \mathcal{M} \pm (s \leftrightarrow u)$ and $t = -p^2 = -s-u$ is held fixed. We use multiple superscripts $\mathcal{M}^{(i_1,\ldots,i_k)}$ to indicate a sequence of similar expressions involving the amplitudes $\mathcal{M}^{(i_1)}, \ldots, \mathcal{M}^{(i_k)}$. For odd $k > 1$, there are 10 independent sum rules:

$$B_k(p^2) = \oint_\infty \frac{ds}{4\pi i} \Big\{ \tfrac{\mathcal{M}^{(2,5,8)-}(s,t)}{(-su)^{\frac{k-3}{2}}}, \tfrac{\mathcal{M}^{(3,7)-}(s,t)}{(-su)^{\frac{k-1}{2}}}, \tfrac{(s-u)\mathcal{M}^{(4,7)+}(s,t)}{(-su)^{\frac{k-1}{2}}}, \tfrac{(s-u)\mathcal{M}^{(5)+}(s,u)}{(-su)^{\frac{k-1}{2}}}, \tfrac{(s-u)\mathcal{M}^{(9)}(s,u)}{(-su)^{\frac{k-1}{2}}}, \tfrac{(s-u)\mathcal{M}^{(4)}(s,u)}{(-su)^{\frac{k+1}{2}}} \Big\} = 0 \,. \tag{C.2}$$

The Regge bound (5.10) implies that these sum rules converge for $k > 1$.

C.1.2 Sum rules in lower dimensions

In lower dimensions $D \leq 7$, there are two novelties for local modules as noted in [185]. First, new identities can reduce the number of parity-even generators of the local module. This does not occur in $D = 7$. However, in $D = 6$ the generator $\mathcal{G}$ does not exist, thus we must remove the parity-even sum rules involving $\mathcal{M}^{(1)}(s,u)$. Similarly in $D = 5$, we simply remove the parity-even sum rules involving $\mathcal{M}^{(1,6,7)}(s,u)$.

The second novelty in lower dimensions is that new parity-odd structures appear. Following [185], we organize them into multiplets under permutations. In $D = 7$, there is one parity-odd singlet and two parity-odd triplets:

$$\begin{aligned}
\text{singlets}: &\; iS\ \epsilon(\varepsilon_1,\varepsilon_2,\varepsilon_3,\varepsilon_4,p_1,p_2,p_4)\mathcal{M}^{(13)}(s,u),\\
\text{triplets}: &\; iH_{14}H_{23}\,\epsilon(\varepsilon_1,\varepsilon_2,\varepsilon_3,\varepsilon_4,p_1,p_2,p_4)\mathcal{M}^{(11)}(s,u), \qquad (D=7)\\
&\; iX_{1243}\epsilon(\varepsilon_1,\varepsilon_2,\varepsilon_3,\varepsilon_4,p_1,p_2,p_4)\mathcal{M}^{(12)}(s,u).
\end{aligned} \tag{C.3}$$

Correspondingly, we can construct more sum rules

$$\begin{aligned}
B_k(p^2) &= \oint \frac{ds}{4\pi i}\left\{\frac{\mathcal{M}^{(11)-}(s,t)}{(-su)^{\frac{k-2}{2}}}, \frac{(s-u)\mathcal{M}^{(12)}(s,u)}{(-su)^{\frac{k}{2}}}\right\} = 0 \qquad (\text{even } k,\ D=7),\\
B_k(p^2) &= \oint \frac{ds}{4\pi i}\left\{\frac{\mathcal{M}^{(12)-}(s,t)}{(-su)^{\frac{k-1}{2}}}, \frac{(s-u)\mathcal{M}^{(11,12)+}(s,t)}{(-su)^{\frac{k-1}{2}}}, \frac{(s-u)\mathcal{M}^{(13)}(s,u)}{(-su)^{\frac{k-1}{2}}}\right\} = 0 \quad (\text{odd } k,\ D=7)\,.
\end{aligned} \tag{C.4}$$

In $D = 6$, there are three parity-odd triplets:

$$\begin{aligned}
&H_{14}H_{23}\sigma_{1234}\cdot(V_1\epsilon(\varepsilon_2,\varepsilon_3,\varepsilon_4,p_2,p_3,p_4))\mathcal{M}^{(10)}(s,u),\\
&\sigma^{14}_{23}\cdot\big(\sigma^{34}_{12}\cdot(H_{24}H_{34}V_1\epsilon(\varepsilon_1,\varepsilon_2,\varepsilon_3,p_1,p_2,p_3))\big)\mathcal{M}^{(11)}(s,u),\\
&\sigma^{34}_{12}\cdot\big((H_{234}V_1 - H_{123}V_4)\big(-p_2\cdot p_3\epsilon(\varepsilon_1,\varepsilon_2,\varepsilon_3,\varepsilon_4,p_1,p_4) + (p_3\leftrightarrow\varepsilon_3) - (p_2\leftrightarrow\varepsilon_2)\\
&+(p_{2,3}\leftrightarrow\varepsilon_{2,3})\big)\big)\mathcal{M}^{(12)}(s,u).
\end{aligned} \tag{C.5}$$

Here, we have introduced permutation operators σ to simplify the expressions:

$$\sigma_{1234} \cdot A_{1234} \equiv A_{1234} - A_{2341} + A_{3412} - A_{4123},$$
$$\sigma_{ij}^{kl} \cdot A_{1234} \equiv A_{1234} + (i \leftrightarrow j, k \leftrightarrow l)\,. \tag{C.6}$$

The corresponding parity-odd sum rules in $D = 6$ are given by

$$B_k(p^2) = \oint \frac{ds}{4\pi i}\left\{\tfrac{(s-u)\mathcal{M}^{(10)+}(s,t)}{(-su)^{\frac{k-2}{2}}}, \tfrac{\mathcal{M}^{(11)-}(s,u)}{(-su)^{\frac{k-2}{2}}}, \tfrac{\mathcal{M}^{(12)}(s,u)}{(-su)^{\frac{k-2}{2}}}\right\} = 0 \qquad (\text{even } k,\ D = 6)\,,$$
$$B_k(p^2) = \oint_\infty \frac{ds}{4\pi i}\left\{\tfrac{\mathcal{M}^{(11)}(s,u)}{(-su)^{\frac{k-3}{2}}}, \tfrac{\mathcal{M}^{(10,12)-}(t,s)}{(-su)^{\frac{k-3}{2}}}, \tfrac{\mathcal{M}^{(8)}(s,u)}{(-su)^{\frac{k-1}{2}}},, \tfrac{(s-u)\mathcal{M}^{(10,12)+}(t,s)}{(-su)^{\frac{k-1}{2}}}\right\} = 0 \quad (\text{odd } k,\ D = 6)\,. \tag{C.7}$$

Finally, in $D = 5$ there is one parity-odd triplet

$$-i\sigma_{12}^{34} \cdot \big(\sigma_{14} \cdot (H_{23}H_{234}V_1\epsilon(\varepsilon_1, \varepsilon_4, p_1, p_2, p_4))\big)\mathcal{M}^{(8)}(s,u), \qquad (D = 5) \tag{C.8}$$

which gives rise to three independent sum rules:

$$B_k(p^2) = \oint_\infty \frac{ds}{4\pi i}\left\{\tfrac{(s-u)\mathcal{M}^{(8)-}(t,s)}{(-su)^{\frac{k-2}{2}}}, \tfrac{\mathcal{M}^{(8)}(s,u)}{(-su)^{\frac{k-2}{2}}}\right\} = 0 \qquad (\text{even } k,\ D = 5)\,,$$
$$B_k(p^2) = \oint_\infty \frac{ds}{4\pi i}\left\{\tfrac{\mathcal{M}^{(8)-}(t,s)}{(-su)^{\frac{k-3}{2}}}\right\} = 0 \qquad (\text{odd } k,\ D = 5)\,. \tag{C.9}$$

C.1.3 Improved sum rules

Eqs. (C.1)-(C.9) provide complete sets of dispersive sum rules in the considered dimensions. By "complete" we mean that any sum rule with spin-k convergence can be expressed as finite sum of the $B_{\leq k}$ up to corrections that vanish faster than spin-k at high energies. Generically, the action of $B_k(p^2)$ on the low-energy amplitude (C.40) yields an infinite series of contact interactions. Following the method in [130], all but a finite number of contacts can be removed by adding an infinite series of higher-spin sum rules $B_{>k}^{(n)}(0)$ expanded around the forward limit. As further discussed in [5], while it is not allowed to expand $k = 2$ sum rules in the forward limit (due to the graviton pole), there are no analogous problems for $k > 2$. Explicit formulas for the resulting $B_k^{\text{imp}}(p^2)$ sum rules are recorded in ancillary files.

C.2 Vertices in lower dimensions

In the main text, we described three-point vertices for two gravitons and a massive state in dimensions $D \geq 8$. In lower spacetime dimensions, the counting of three-point structures is modified, and we must take into account additional ingredients in the representation theory of the little group $\mathrm{SO}(d)$ (where $d = D-1$). In this section, we describe these ingredients, and then discuss the individual cases $D = 7, 6, 5$ in turn. Detailed expressions can be found in the ancillary files included with this work.

C.2.1 Representation theory ingredients

C.2.1.1 Self-duality and ϵ-symbols

When $d = 2n$ is even, representations with full-height Young diagrams split into self-dual or anti-self-dual cases, according to whether m_n is positive or negative. Let us explain how to account for this in our index-free formalism. Recall that the polarization vectors w_i satisfy the orthogonality conditions and gauge redundancies (5.18). When d is even, the variety defined by these conditions (called a “flag variety") splits into two irreducible components $V_\pm$, distinguished by whether $w_1 \wedge \cdots \wedge w_n$ is self-dual or anti-self-dual. Specifically, we have

$$\frac{i^n}{n!}\epsilon_{\nu_1\cdots\nu_n}{}^{\mu_1\cdots\mu_n} w_1^{\nu_1}\cdots w_n^{\nu_n} = \pm w_1^{[\mu_1}\cdots w_n^{\mu_n]} \quad \text{on } V_\pm. \tag{C.10}$$

To see why there are two components $V_\pm$, we can recursively solve the orthogonality conditions $w_i \cdot w_j = 0$. First, we use $\mathrm{SO}(d)$-invariance and rescaling to set $w_1 = (1, i, 0, \ldots, 0)$. Using gauge-redundancies and $w_1 \cdot w_i = 0$, the remaining w_i must have the form $w_i = (0, 0, w_i^\perp)$, where $w_i^\perp \in \mathbb{C}^{d-2}$ are null vectors. The $w_i^\perp$ satisfy precisely the conditions and gauge redundancies for the flag variety of $\mathrm{SO}(d-2)$. Repeating this process for the $w_i^\perp$'s, we eventually arrive at the flag variety for $\mathrm{SO}(2)$, parametrized by a single null vector $w_n^{\perp\cdots\perp} \in \mathbb{C}^2$. Up to $\mathrm{SO}(2)$ transformations and rescaling, there are two possible null vectors $w_n^{\perp\cdots\perp} = (1, \pm i)$, corresponding to the two components.

The following combinations thus project the polynomial (5.19) associated with a tableau onto its self-dual (anti-self-dual) part:

$$\begin{array}{|c|}\hline a_1 \\ \hline \vdots \\ \hline a_n \\ \hline \end{array}_{\,\pm} = \begin{array}{|c|}\hline a_1 \\ \hline \vdots \\ \hline a_n \\ \hline \end{array} \pm i^n \epsilon(w_1, \ldots, w_n, a_1, \ldots, a_n). \tag{C.11}$$

Furthermore, the product of (C.11) with any polynomial in the w_i's is also self-dual (anti-self-dual), since it vanishes on V_- (V_+). In general, we define a tableau with chirality $\pm$ by adding an ϵ term to any full-height column, for example:

$$\begin{array}{|c|c|c|}\hline a & d & g \\ \hline b & e & \multicolumn{1}{c}{} \\ \cline{1-2} c & f & \multicolumn{1}{c}{} \\ \cline{1-2} \end{array}_{\,\pm} = \left(\begin{array}{|c|}\hline a \\ \hline b \\ \hline c \\ \hline \end{array}_{\,\pm} \right) \begin{array}{|c|c|}\hline d & g \\ \hline e & \multicolumn{1}{c}{} \\ \cline{1-1} f & \multicolumn{1}{c}{} \\ \cline{1-1} \end{array}. \tag{C.12}$$

Note that it doesn't matter which full-height column we choose — the resulting polynomial is the same since it agrees on both components V_+ and V_-; this can be verified explicitly with Gram determinant identities.

C.2.1.2 Counting three-point structures

Using the methods of [117, 118], one can show that possible three-point vertices for the representation ρ are classified by the following formula:

$$\begin{aligned} \text{odd } D \text{ or } D \geq 8 : &\begin{cases} (\mathrm{S}^2 \square\!\square_{d-1} \otimes \rho)^\bullet & \text{if } |\rho| \text{ is even} \\ (\wedge^2 \square\!\square_{d-1} \otimes \rho)^\bullet & \text{if } |\rho| \text{ is odd} \end{cases} \\ \text{even } D : &\ (\mathrm{S}^2 \square\!\square_{d-1} \otimes \rho)^\bullet_{(-1)^{|\rho|}} \oplus (\wedge^2 \square\!\square_{d-1} \otimes \rho)^\bullet_{(-1)^{|\rho|+1}}. \end{aligned} \tag{C.13}$$

Here, $\square\!\square_{d-1}$ denotes the spin-2 representation of $\mathrm{SO}(d-1)$. When we tensor an $\mathrm{SO}(d-1)$ representation with ρ, we implicitly dimensionally reduce ρ to an $\mathrm{SO}(d-1)$ representation. The notation $(\lambda)^\bullet$ denotes the $\mathrm{SO}(d-1)$-singlet subspace of λ, and $(\lambda)^\bullet_\pm$ denotes the $\mathrm{SO}(d-1)$ singlet subspace with parity $\pm$. Finally, $|\rho|$ is the number of boxes in the Young diagram of ρ. The formula (C.13) is useful for detecting linear dependencies between Young tableau in various spacetime dimensions.

C.2.1.3 Implications of CRT

CRT symmetry relates the $\mathrm{SO}(d)$ representation ρ to the dual reflected representation $(\rho^R)^*$. When $d \equiv 1, 2$, or $3 \mod 4$, we have simply $(\rho^R)^* = \rho$. In this case, we can choose conventions where three-point couplings for graviton-graviton-ρ vertices are real, simply by making the couplings invariant under $p_j^\mu \mapsto -p_j^\mu, i \mapsto -i$. In particular, when computing positivity bounds, we impose that the contribution of each type of partial wave to a sum rule is a positive-definite real symmetric matrix.

Meanwhile, when $d \equiv 0 \mod 4$, dual reflection changes the sign of the weight m_n, and hence exchanges self-dual and anti-self-dual representations $\rho_+ \leftrightarrow \rho_-$. In this case, CRT implies that three-point coefficients of ρ_+ and ρ_- are complex conjugates of each other. We discuss the implications of this for positivity bounds in $D = 5$ below.

C.2.2 Vertices in $D = 7$ ($d = 6$)

Because $d = 6$ is even, representations with height-3 Young diagrams split into self-dual and anti-self-dual cases. The only effect is to double the number of height-3 tableaux in table 5.2 by adding a $\pm$ chirality to each.

Let us denote a self-dual (anti-self-dual) representation by ρ_+ (ρ_-). In the absence of parity symmetry, the three-point amplitudes $g_{gg\rho_\pm}$ between two gravitons and states in ρ_+ or ρ_- need not be related. Consequently, we must sum over partial waves for each type of representation ρ_+ and ρ_- independently. In bootstrap calculations, this requires including separate positivity conditions for ρ_+-exchange and ρ_--exchange.

However, the contributions of ρ_+-exchange and ρ_--exchange to parity-even sum rules are identical. Thus, when computing bounds using parity-even sum rules (such as our bounds on α_2 and α_4), positivity conditions associated to ρ_+ and ρ_- are redundant, and it suffices to include only one of them (say ρ_+).

C.2.3 Vertices in $D = 6$ $(d = 5)$

In spacetime dimension $D = 6$, SO(5) Young tableaux can have at most two rows. Since vertices are functions of five vectors (w_1, w_2, e_1, e_2, n), there is a unique way to use the Levi-Civita tensor. It is convenient to write it as a height-3 column:

$$\begin{array}{|c|}\hline e_1 \\ \hline e_2 \\ \hline n \\ \hline \end{array} \equiv \epsilon(w_1, w_2, e_1, e_2, n) \qquad \text{for SO(5)}. \tag{C.14}$$

At most one column can have height 3, due to a Gram determinant identity. With this convention, the only change to table 5.2 is to remove the tableau for $(J, 2, 2)$, and to reinterpret the tableaux for $(J, 1, 1)$, $(J, 2, 1)$, and $(J, 3, 1)$ as parity-odd vertices for $(J, 1)$, $(J, 2)$, and $(J, 3)$ respectively.

C.2.4 Vertices in $D = 5$ $(d = 4)$

In spacetime dimension $D = 5$, SO(4) tableaux with two rows can have chirality $\pm$. In addition, we can use the Levi-Civita tensor in the form $\epsilon(w_1, a, b, c)$. Due to Gram determinant identities, this term can never be used if two-row columns are present, and it cannot be used twice. It is again convenient to draw it as a 3-row column:

$$\begin{array}{|c|}\hline e_1 \\ \hline e_2 \\ \hline n \\ \hline \end{array} \equiv \epsilon(w_1, e_1, e_2, n) \qquad \text{for SO(4)}. \tag{C.15}$$

With this convention, the tableau with row lengths $(J, 1, 1)$ get reinterpreted as a parity-odd coupling for the representation $\rho = (J)$. Note also that the counting formula (C.13) implies that there are only two linearly-independent vertices for the representations $(J, \pm 2)$ with even J. Overall, the possible vertices in $D = 5$ are given in table (C.1).

As discussed in section C.2.1.3, when $d = 4$, CRT implies that three-point coefficients of ρ_+ and ρ_- are complex conjugates of each other. Given a pair of representations ρ_+, ρ_- with opposite chirality, let us denote the corresponding partial waves by π_+, π_-. The $\pi_\pm$ are Hermitian matrices indexed by vertex labels i, j. Exploiting fact that generators of the local module are invariant under the $Z_2 \times Z_2$ symmetry which

$\ytableaushort{{\bullet}{\bullet}}\ (e_1{\cdot}e_2)^2$ $\ytableaushort{{e_1}{e_2}{\bullet}{\bullet}}\ e_1{\cdot}e_2$ $\ytableaushort{{e_1}{e_1}{e_2}{e_2}{\bullet}{\bullet}}$	$\ytableaushort{{e_1}{n}{\bullet}{\bullet},{e_2}}\ \pm\, e_1{\cdot}e_2$ $\ytableaushort{{e_1}{e_1}{e_2}{n}{\bullet}{\bullet},{e_2}}\ \pm$	$(1{+}S)\ \ytableaushort{{e_1}{e_2}{n}{\bullet}{\bullet},{n}}\ \pm\, e_1{\cdot}e_2$ $(1{+}S)\ \ytableaushort{{e_1}{e_2}{e_1}{e_2}{n}{\bullet}{\bullet},{n}}\ \pm$	$\ytableaushort{{e_1}{\bullet}{\bullet},{e_2},{n}}\ e_1{\cdot}e_2$ $\ytableaushort{{e_1}{e_1}{e_2}{\bullet}{\bullet},{e_2},{n}}$	$\ytableaushort{{e_1}{e_2}{\bullet}{\bullet},{n}{n}}\ \pm\, e_1{\cdot}e_2$ $\ytableaushort{{e_1}{e_2}{e_1}{e_2}{\bullet}{\bullet},{n}{n}}\ \pm$
$(1{+}S)\ \ytableaushort{{e_1}{e_1}{e_2}{\bullet}{\bullet},{e_2}{n}}\ \pm$	$\ytableaushort{{e_1}{e_1}{e_2}{n}{\bullet}{\bullet},{e_2}{n}{n}}\ \pm$	$(1{+}S)\ \ytableaushort{{e_1}{e_1}{e_2}{e_2}{n}{\bullet}{\bullet},{n}{n}{n}}\ \pm$	$\ytableaushort{{e_1}{e_1}{e_2}{e_2}{\bullet}{\bullet},{n}{n}{n}{n}}\ \pm$	

Table C.1: The graviton-graviton-massive couplings in $D = 5$, as Young tableau for SO(4). We use the same notation as in table 5.2. The meaning of the height-3 column is given in (C.15).

includes the interchange between initial and final states, we can choose conventions where

$$\pi_+ = \pi_-^* = \pi_-^T. \tag{C.16}$$

By choosing generators of the local module to be invariant under $p_j \mapsto -p_j, i \mapsto -i$, these relations automatically hold for all the coefficients of the projector on that basis. A contribution from ρ_+-exchange to the discontinuity of the amplitude takes the form

$$\mathrm{Tr}(M\pi_+), \tag{C.17}$$

where $M = g_+ g_+^\dagger$ is a Hermitian matrix built from a vector of three-point couplings g_+. The three-point couplings for ρ_- are complex-conjugate to g_+ and can be grouped into the matrix $g_- g_-^\dagger = g_+^* g_+^T = M^* = M^T$. Together, ρ_+ and ρ_--exchange thus contribute

$$\mathrm{Tr}(M\pi_+) + \mathrm{Tr}(M^T\pi_-) = \mathrm{Tr}(M(\pi_+ + \pi_-^T)) = 2\mathrm{Tr}(M\pi_+). \tag{C.18}$$

So, summing the two opposite-chirality irreps simply gives a factor of 2. In parity-even sum rules, only the real-symmetric part of M and π contributes, while for parity-odd sum rules, only the imaginary part of both contributes. Thus, when computing bounds using parity-even sum rules (as we do in this work), we can essentially pretend that the three-point couplings are real and symmetrical. Furthermore, we need only include positivity conditions for one chirality (say ρ_+), since the contributions from ρ_- are redundant.

C.3 Details on the partial wave decomposition

In this appendix, we derive the properly normalized partial wave decomposition (5.13) and illustrate it for scalars and gravitons.

C.3.1 Normalized partial wave expansion

It is helpful to view the two-particle Hilbert space as a direct integral over total momentum $P = p_1 + p_2$ of Hilbert spaces $\mathcal{H}_P$ with fixed P. Because the S-matrix preserves momentum, it acts within each $\mathcal{H}_P$. When $P = (E, \vec{0})$, $\mathcal{H}_P$ is spanned by states $|n\rangle$ such that $p_1 = \frac{E}{2}(1, n)$ and $p_2 = \frac{E}{2}(1, -n)$, where n is a unit vector. Let us momentarily suppress the spin of the external particles, i.e. consider scalars. The inner product on $\mathcal{H}_P$ is a ratio of the two-particle inner product and a momentum-conserving δ-function:

$$\langle n'|n\rangle = \frac{\langle p_3|p_1\rangle\langle p_4|p_2\rangle + \langle p_3|p_2\rangle\langle p_4|p_3\rangle}{(2\pi)^D \delta^D(p_1 + p_2 - p_3 - p_4)} = \frac{2^d (2\pi)^{d-1}}{s^{\frac{D-4}{2}}} \left(\delta(n, n') + \delta(n, -n')\right), \quad \text{(C.19)}$$

where $D = d + 1$ and we have used the standard single-particle inner product

$$\langle p_3|p_1\rangle = 2E_1 (2\pi)^{D-1} \delta^{D-1}(\vec{p}_1 - \vec{p}_3). \quad \text{(C.20)}$$

In (C.19), $\delta(n, n')$ is a δ-function on the sphere S^{d-1}, and $s = E^2$. The inner product (C.19) yields a corresponding completeness relation in $\mathcal{H}_P$:

$$1 = \frac{s^{\frac{D-4}{2}}}{2^d (2\pi)^{d-1}} \frac{1}{2} \int_{S^{d-1}} dn |n\rangle\langle n|, \quad \text{(C.21)}$$

where the factor of $\frac{1}{2}$ reflects Bose symmetry $|n\rangle = |-n\rangle$. Using this relation it will be straightforward to correctly normalize the partial wave amplitudes.

For scalar scattering, $\mathcal{H}_P$ decomposes into a direct sum of irreducible representations ρ of SO(d), where only even-spin traceless symmetric tensors $\rho = (J)$ appear, each with multiplicity one. In the case of graviton scattering, the states $\mathcal{H}_P$ acquire extra polarization labels $|n, e_1, e_2\rangle$, where e_1, e_2 are defined by (5.14), which adds corresponding Kronecker deltas added to the above. More general irreps ρ can appear in the decomposition of $\mathcal{H}_P$, and furthermore they can have nontrivial multiplicity.

For each ρ, we can choose basis vectors $|i, a\rangle$ where a is an SO(d)-index for ρ and i is a multiplicity label. The vertices $v^{i,a}(n, e_1, e_2)$ are proportional to the overlap of $|i, a\rangle$ with $|n, e_1, e_2\rangle$:

$$\langle i, a|n, e_1, e_2\rangle \equiv \left(s^{\frac{4-D}{2}} n_\rho^{(D)}\right)^{\frac{1}{2}} v^{i,a}(n, e_1, e_2), \tag{C.22}$$

where the constants out front have been introduced for later convenience. We can choose the basis to be orthonormal, $\langle i, a|j, b\rangle = \delta^{ij} g^{ab}$ where g^{ab} is an SO(d)-invariant metric. Projectors on ρ are then

$$\Pi_\rho^{ij} \equiv |i, a\rangle g_{ab} \langle j, b| \,, \tag{C.23}$$

where g_{ab} is the inverse to g^{ab}. As an operator on $\mathcal{H}_P$, the $2 \to 2$ S-matrix can be expanded as a sum of projectors:

$$S\big|_{2\to 2} = \sum_\rho \sum_{ij} (S_\rho(s))_{ji} \Pi_\rho^{ij}. \tag{C.24}$$

Unitarity of S implies that each $S_\rho(s)$ is separately a unitary matrix $S_\rho(s) S_\rho(s)^\dagger = 1$. Taking a matrix element of $\mathcal{M} = -i(S-1)$ in the basis states $|n, e_1, e_2\rangle$, we obtain the partial wave decomposition of the gravity amplitudes (5.13):

$$\begin{aligned} \mathcal{M} = \langle n', e_3^*, e_4^*|{-i}(S-1)|n, e_1, e_2\rangle &= \sum_\rho \sum_{ij} (a_\rho(s))_{ji} \langle n', e_3^*, e_4^*|\Pi_\rho^{ij}|n, e_1, e_2\rangle \\ &= s^{\frac{4-D}{2}} \sum_\rho n_\rho^{(D)} \sum_{ij} (a_\rho(s))_{ji} \pi_\rho^{ij}, \end{aligned} \tag{C.25}$$

where $\pi_\rho^{ij} = \bar{v}^{i,b} g_{ba} v^{j,a} \equiv (\bar{v}^i, v^j)$ and $S_\rho(s) = 1 + i a_\rho(s)$.

From this derivation, the normalization can be fixed simply by taking the trace of (C.23) and using the completeness relation (C.21):

$$\delta^{ij} \dim \rho = \frac{n_\rho^{(D)}}{2^{d+1}(2\pi)^{d-1}} \int_{S^{d-1}} dn \, \mathrm{Tr}\,(\bar{v}^i(n), v^j(n)) = \frac{n_\rho^{(D)} \operatorname{vol} S^{d-1}}{2^{d+1}(2\pi)^{d-1}} \mathrm{Tr}\,(\bar{v}^i(n), v^j(n)), \tag{C.26}$$

where we have used rotational-invariance to perform the integral over n, and Tr indicates a sum over polarization states. (We detail the precise meaning of Tr for gravitons below in (C.33).) We choose to normalize the vertices so that

$$\mathrm{Tr}\,(\bar{v}^i(n), v^j(n)) = \delta^{ij}. \tag{C.27}$$

The normalization coefficient $n_\rho^{(D)}$ is thus fixed to be $\dim \rho$ divided by essentially the phase space volume:

$$n_\rho^{(D)} = \frac{2^{d+1}(2\pi)^{d-1} \dim \rho}{\operatorname{vol} S^{d-1}}. \tag{C.28}$$

The dimension $\dim \rho$ can be computed from standard formulas, see e.g. [188, 141]. For spin-J traceless symmetric tensors, we have simply

$$\dim (J) = \frac{(2J + d - 2)\Gamma(d + J - 2)}{\Gamma(d - 1)\Gamma(J + 1)}\,. \tag{C.29}$$

C.3.2 Scalar scattering

Let us determine the precise expression for π_ρ in the case of scalar scattering. Since each $\rho = (J)$ appears with multiplicity 1, there is a unique vertex function

$$v(n) = k_J \boxed{\bullet} = k_J (n \cdot w_1)^J, \tag{C.30}$$

up to a constant k_J that we determine shortly. The partial waves are given by

$$\pi_J(n',n) = k_J^2(n'_{\mu_1}\cdots n'_{\mu_J} - \text{traces})(n^{\mu_1}\cdots n^{\mu_J} - \text{traces}) = k_J^2\frac{(d-2)_J}{2^J(\frac{d-2}{2})_J}\mathcal{P}_J(x), \tag{C.31}$$

where $x = n\cdot n' = 1+\frac{2t}{s}$, $(a)_n$ is the Pochhammer symbol, and $\mathcal{P}_J(x)$ is a Gegenbauer polynomial given by

$$\mathcal{P}_J(x) = {}_2F_1(-J, J+d-2, \tfrac{d-1}{2}, \tfrac{1-x}{2}). \tag{C.32}$$

Our normalization condition on vertices is equivalent to $\pi_J(n,n) = 1$, which fixes $k_J = \left(\frac{(d-2)_J}{2^J(\frac{d-2}{2})_J}\right)^{-1/2}$ since $\mathcal{P}_J(1) = 1$. We finally obtain $\pi_J(n',n) = \mathcal{P}_J(x)$, and (C.25) recovers the familiar partial wave expansion for scalars, see e.g. [119].

C.3.3 Graviton scattering

In the case of graviton scattering, the orthonormality condition used in (C.28) can be expanded as

$$\delta^{ij} = \mathrm{Tr}\,(\bar{v}^i, v^j) = \sum_{e_1,e_2}\left(v^i(n,e_1,e_2)^*, v^j(n,e_1,e_2)\right), \tag{C.33}$$

where $\sum_{e_1,e_2}$ denotes a sum over an orthonormal basis of polarization states, and $(u,v) = u^b g_{ba} v^a$ as before. Concretely, the sum over polarizations can be performed by replacing

$$e_1^{*\mu}e_1^{*\nu}e_1^{\rho}e_1^{\sigma} \to \frac{1}{2}(\widehat{g}^{\mu\rho}\widehat{g}^{\nu\sigma}+\widehat{g}^{\nu\rho}\widehat{g}^{\mu\sigma}) - \frac{1}{D-2}\widehat{g}^{\mu\nu}\widehat{g}^{\rho\sigma}\,, \quad \widehat{g}^{\mu\nu} \equiv \delta^{\mu\nu} - n^\mu n^\nu, \tag{C.34}$$

where μ,ν, etc. are SO(d) indices, and making a similar replacement for e_2. In practice, to obtain the vertices in the ancillary files, we began with the basis of vertices in table 5.2 (and the analogous bases in $D\le 7$), and applied the Gram Schmidt procedure using the pairing (C.33).

Let us illustrate some examples of graviton partial waves for the representation

$\rho = (J,1,1)$ in spacetime dimension $D \geq 8$. As shown in Table 5.2, there are two linearly-independent vertices for $(J,1,1)$. An orthonormal basis with respect to the pairing (C.33) is given by

$$
\begin{aligned}
v_1 &= \frac{iJ}{\sqrt{D}(J+2)} \begin{array}{|c|c|c|}\hline e_1 & \bullet & \bullet \\ \hline e_2 \\ \cline{1-1} n \\ \cline{1-1}\end{array}_{\,e_1\cdot e_2}\,, \\
v_2 &= \frac{iJ}{J+2}\sqrt{\frac{(J)_2 D}{(D-1)(J+D-2)_2}}\Bigg(\frac{1}{D} \begin{array}{|c|c|c|}\hline e_1 & \bullet & \bullet \\ \hline e_2 \\ \cline{1-1} n \\ \cline{1-1}\end{array}_{\,e_1\cdot e_2} + \begin{array}{|c|c|c|c|c|}\hline e_1 & e_1 & e_2 & \bullet & \bullet \\ \hline e_2 \\ \cline{1-1} n \\ \cline{1-1}\end{array}\Bigg)\,.
\end{aligned}
\tag{C.35}
$$

Gluing these vertices, we can construct partial waves, which are 2-by-2 matrices indexed by the vertex labels. For brevity, we record here only the top-left corner of this matrix π_ρ^{11}, obtained by gluing v_1 to itself. We furthermore write the result in terms of contributions $\pi_\rho^{11,(i)}(s,u)$ to each of the 29 scalar amplitudes defined in (5.8) through the 10 generators $\mathcal{M}^{(i)}(s,u)$ and their permutations. We find that s-channel exchange of $(J,1,1)$ produces

$$
\begin{aligned}
\pi^{11,(2)}_{(J,1,1)}(t,u) &= \frac{2(D-4)\mathcal{P}_J'(x)}{D(J+2)(J+D-5)m^8}, \quad \pi^{11,(4)}_{(J,1,1)}(u,t) = \frac{8\big((D-4)\mathcal{P}_J'(x) + x\mathcal{P}_J''(x)\big)}{D(J+2)(J+D-5)m^8}\,, \\
\pi^{11,(5)}_{(J,1,1)}(s,u) &= \frac{8\big((D-4)\mathcal{P}_J'(x) + (x+1)\mathcal{P}_J''(x)\big)}{D(J+2)(J+D-5)m^8}, \\
\pi^{11,(5)}_{(J,1,1)}(s,t) &= \frac{8\big((D-4)\mathcal{P}_J'(x) + (x-1)\mathcal{P}_J''(x)\big)}{D(J+2)(J+D-5)m^8},
\end{aligned}
\tag{C.36}
$$

and all other $\pi^{11,(i)}_{(J,1,1)}$ vanish. As before, $x = 1 + \frac{2t}{s}$. For additional expressions for partial waves, we refer the reader to the ancillary files included with this work.

C.4 Low-energy amplitudes

C.4.1 Tree-level graviton amplitudes

The higher-derivative interactions entering the action (5.1) are defined as:

$$
\begin{aligned}
&C^2 \equiv C_{\mu\nu\rho\sigma}C^{\mu\nu\rho\sigma}\,, \quad C^3 \equiv 3C_{\mu\nu\rho\sigma}C^{\rho\sigma}{}_{\alpha\beta}C^{\alpha\beta\mu\nu} - 4C_{\mu\nu\rho\sigma}C^{\nu\alpha\sigma\beta}C_{\alpha}{}^{\mu}{}_{\beta}{}^{\rho}\,, \\
&C'^3 \equiv -C_{\mu\nu\rho\sigma}C^{\rho\sigma}{}_{\alpha\beta}C^{\alpha\beta\mu\nu} + 2C_{\mu\nu\rho\sigma}C^{\nu\alpha\sigma\beta}C_{\alpha}{}^{\mu}{}_{\beta}{}^{\rho}\,.
\end{aligned}
\tag{C.37}
$$

where $C_{\mu\nu\sigma\rho}$ is the Weyl tensor (traceless part of the curvature tensor $R_{\mu\nu\sigma\rho}$). The Weyl tensor is convenient for writing low-energy effective actions since, as mentioned in the text, the Ricci tensor and scalar can be removed using equations of motion and do not affect our bounds (see also [238]). Thus C^2 is equivalent to the Gauss-Bonnet density (whose coefficient is sometimes called $\alpha_2 = \lambda_{\mathrm{GB}}$), and C'^3 is effectively proportional to the third Lovelock density. The normalizations in (5.1) have been chosen so that the on-shell three-graviton vertex agrees with [77]:

$$\mathcal{M}(123) = \sqrt{32\pi G}(\mathcal{A}_1^2 + \alpha_2\mathcal{A}_1\mathcal{A}_2 + \alpha_4\mathcal{A}_2^2), \tag{C.38}$$

where

$$\mathcal{A}_1 \equiv p_1 \cdot \varepsilon_3\ \varepsilon_1 \cdot \varepsilon_2 + p_3 \cdot \varepsilon_2\ \varepsilon_1 \cdot \varepsilon_3 + p_2 \cdot \varepsilon_1\ \varepsilon_2 \cdot \varepsilon_3, \quad \mathcal{A}_2 \equiv p_1 \cdot \varepsilon_3\ p_2 \cdot \varepsilon_1\ p_3 \cdot \varepsilon_2. \tag{C.39}$$

To illustrate scattering amplitudes in the local module, we now give explicit expressions for the 10 generating amplitudes $\mathcal{M}^{(i)}$ entering (5.8) for tree-level gravity in generic dimension $D \geq 8$. We include here higher-derivative couplings α_2, α_4 to linear order, and the unique 6-derivative interaction α_4' which yields a contact term:

$$\begin{aligned}
&\mathcal{M}^{(1)}(s,u) = 8\pi G\alpha_4' + \dots, && \mathcal{M}^{(2)}(s,u) = \tfrac{8\pi G}{stu} + \dots\,, \\
&\mathcal{M}^{(3)}(s,u) = \tfrac{8\pi G}{stu}(2 - \tfrac{t^2\alpha_4}{2}) + \dots\,, && \mathcal{M}^{(4)}(s,u) = \tfrac{8\pi G}{stu}(4 - 2t\alpha_2 - 4su\alpha_4) + \dots\,, \\
&\mathcal{M}^{(5)}(s,u) = \tfrac{8\pi G}{stu}(8 + 2\alpha_2 u) + \dots\,, && \mathcal{M}^{(6)}(s,u) = \tfrac{8\pi G}{stu}(4 - 4\alpha_2 t) + \dots\,, \\
&\mathcal{M}^{(7)}(s,u) = \tfrac{8\pi G}{stu}(8 + 4\alpha_2 t) + \dots\,, && \mathcal{M}^{(8)}(s,u) = \tfrac{8\pi G}{stu}(-2\alpha_2) + \dots\,, \\
&\mathcal{M}^{(9)}(s,u) = \tfrac{8\pi G}{stu}(-4\alpha_2 + 8\alpha_4 t) + \dots\,, && \mathcal{M}^{(10)}(s,u) = \tfrac{8\pi G}{stu}(4\alpha_4) + \dots\,.
\end{aligned} \tag{C.40}$$

All omitted terms are either quadratic in the α_2, α_4 or involve higher derivative contacts, which are simply polynomials in Mandelstam invariants subject to the symmetries of the corresponding $\mathcal{M}^{(i)}$. Complete expressions, including for lower dimensions, are recorded in ancillary files.

C.4.2 Kaluza-Klein and other light exchanges

In our bounds, we allow for tree-level exchanges of massive particles that are part of the low-energy EFT — i.e. whose masses are below the cutoff scale M. We refer to such particles as light; they could arise, for example, from Kaluza-Klein reduction. However, we do not actually assume anything about the existence of extra dimensions. We do however, make a choice about which types of light states to consider, and we include all representations with $J = m_1 \leq 2$. These include symmetric tensors with spin ≤ 2, and k-forms of any degree, which are the possible massless string modes in string theory. It would be interesting to consider other possible EFT matter content; we leave this problem for future work.

Given the partial waves, it is straightforward to determine the amplitudes for light exchanges. We look for meromorphic functions $\mathcal{M}^{(i)}(s,u)$ with the appropriate symmetry properties under crossing, and possessing simple poles in Mandelstam variables whose residues match the partial waves. As an example, consider the possible KK-mode representation $\rho = (1,1,1)$ (a 3-form). The partial waves expressions (C.36) predict that only the following amplitudes have s-channel poles:

$$4\mathcal{M}^{(2)}_{(1,1,1)}(t,u) = \mathcal{M}^{(4)}_{(1,1,1)}(t,u) = \mathcal{M}^{(5)}_{(1,1,1)}(s,u) = \mathcal{M}^{(5)}_{(1,1,1)}(s,t) = \frac{8}{3Dm^8(m^2-s)} + \text{no } s\text{-poles.} \tag{C.41}$$

We then fill in the t- and u-channel poles using symmetries. Since $\mathcal{M}^{(2,4)}$ are symmetric in their two arguments, and $\mathcal{M}^{(5)}$ has no symmetry, there is in fact nothing to add. That is, 3-form exchanges in all channels are accounted for by setting the function $\mathcal{M}^{(4)}_{(1,1,1)}(s,u) \equiv \frac{8}{3Dm^8(m^2+s+u)}$, etc.

The light amplitudes constructed via this procedure naturally have polynomial ambiguities, which represent four-point contact interactions. Following [5], we fix these ambiguities by demanding that light states contribute to sum rules with the minimal possible spin k. The contribution of light exchanges to various sum rules is then obtained by performing the appropriate contour integrals (e.g. (C.1)) on these amplitudes. Our full expressions for light exchange amplitudes, and their contributions to various sum rules, can be found in the ancillary files.

When computing bounds, we demand that the contribution of each possible light exchange is sign-definite, so that the resulting bounds are true independently of the light content of the EFT.

C.5 Details of numerical implementation and ancillary files

Figure 5.1 was produced by numerically searching for combinations of the $B_k^{\text{imp}}(p^2)$ sum rules whose action on every unknown state is positive, following the strategy detailed in [5]. The sum rules are integrated against wavepackets that are polynomials in p over $p \in [0, M]$, where we typically use 5 or 6 different exponents of p for each sum rules and reach up to Regge spin $k = 5$ or $k = 7$. Our search space thus contains between 200 and 400 trial sum rules.

To test positivity, we sample the action of these sum rules on a large number of heavy states with $m \geq M$ (and light states with $J \leq 2$), which are distributed in spin up to $J = 400$. We typically sample their action on between 10000 and 200000 states that have spin up to $J = 400$. We also include constraints from the $m \to \infty$ scaling limit with various $b = \frac{2J}{m}$. For the $k = 2$ sum rules, which dominate at $m \to \infty$, it is important that the wavepackets include an overall factor $p^{\alpha}(M - p)$ so the sum rules decay at large impact parameters (like $\sim 1/b^3$ in $D = 5$). We use the SDPB solver [49, 239] to search for linear combinations of the trial sum rules which are positive on all states and establish optimal bounds on the radial distance from the origin along various rays in the (α_2, α_4) plane. Since the functionals depend quadratically on the α_j, we converge toward the boundary by optimizing a sequence of linearized quantities.

In practice, we fix the set of functionals and increase the number of states until the bounds do not change, keeping only those sets of functionals for which such convergence could be achieved. In going from 5 to 6 exponents, the bounds improved by no more than a few percent. We thus expect that the recorded bounds are conservatively correct, and likely within 5% of being optimal.

We anticipate that the partial waves computed in this work will serve in many other studies. We have thus prepared “process files” which contain the complete information used to bootstrap each of the graviton scattering process studied in this letter: `GGGG5.txt`, `GGGG6.txt`, `GGGG7.txt`, `GGGGd.txt`, for $D = 5, 6, 7$ and $D \geq 8$ respectively, as well as a file `GGGG4.txt`, which characterizes the $D = 4$ case studied in our earlier paper [5]. Each file contains, in a native `Mathematica` notation:

- The basis `localbasis[GGGG[d]]` of polarization structures used throughout the file, i.e. the L elements generated from (5.8) where $L = 29$ for $D \geq 8$, written in terms of the H, V, X, S and $\mathcal{G}$ structures defined in section 5.2 (the latter two are denoted `HS` and `HGram` in the files).

- A list `vertices[GG[d]]` of three-point couplings v_i between two gravitons and a massive state, written in the Young Tableau notation of sections 5.3 and C.2 and divided by the scalar factor k_J of (C.31) (and e_i denoted `ep[i]`).

- On-shell three-graviton vertices `amplow[GGG[d]]`, which define higher-derivative corrections like α_2, α_4.

- Low-energy amplitudes `amplow[GGGG[d]]`, which including tree-level graviton exchanges keeping the α_k, as well as contact interactions `g[p,...]` that contribute up to relatively high power p in Mandelstam invariants. The coefficient $8\pi G\alpha_4'$ in the main text is given by `g[3,0,{GGGG[d],1}]` in the process files.

- Partial waves `partialwaves[GG[d], GG[d]]` which list, for each possible SO(d) irrep, an entry `exchange[irrep,{amplitude,channel,x},normalizations,matrix]` with typically `channel`$=s$ and `x`$= 1 + \frac{2t}{s}$. If an irrep allows n independent vertices, `normalizations` is an $n \times n$ matrix and `matrix` is $n \times n \times L$, such that their entry-wise product express the projector π^{ij} in `localbasis[amplitude]`. The the a'th derivative $\mathcal{P}_J^{(a)}(x)$ with respect to x of the Gegenbauer polynomial (C.32) is denoted as `pj[J,x,D,a]`. Irreps are denoted from the row lengths of the Young Tableau with a formal integer $m \geq 0$; for example $\{2m+3,1\}$ denotes the family of representations $(J,1)$ where $J \geq 3$ is odd. Non-generic irreps with low spin, for which some vertex structures disappear and the matrix becomes smaller, are explicitly separated.

- Light exchanges `ampKK[GG[d],GG[d]]`, similarly written as lists of `exchange[irrep,matrix]` for each irrep, where the $n \times n \times L$ `matrix` gives explicit functions of Mandelstam invariants.

- Improved sum rules `sumrules[bkimp[GGGG[d],k]]`, which give $B_k^{\rm imp}$ derived from (C.1), in terms of amplitude labels `M[...][s,-t]` entering `localbasis[GGGG[d]]`, with arguments $[s,-t]$ that indicate which Mandelstam invariants get mapped to the independent variables m^2, p^2 (sum rules are then m^2 integrals at fixed p^2).

- The actions `sumruleslow[bkimp[GGGG[d],k]]` and `sumrulesKK[bkimp[GGGG[d],k]]` of sum rules on the `amplow` and `ampKK` low-energy data.

This constitutes the full information from which the bootstrap problem can be implemented in an automated way.

C.6 Weight-shifting as a combinatorial operation

In general, the weight-shifting operator $\mathcal{D}^{(h)\mu}$ lets one "integrate-by-parts" inside an SO(d)-invariant pairing to remove a box from the left factor and replace it with $\mathcal{D}^{(h)\mu}$ acting on the right factor. Specifically, we have

$$(w_1^{[\mu_1} \cdots w_h^{\mu_h]} g, f) = \frac{1}{m_h}(w_1^{[\mu_1} \cdots w_{h-1}^{\mu_{h-1}} g, \mathcal{D}^{(h)\mu_h]} f), \tag{C.42}$$

where the Young diagram for f has height h. This is the generalization of (5.26) in the main text. In practice, this lets us remove a box from any of the tallest columns in a pairing of Young tableau.

Given (C.42), we should look for an efficient way to apply $\mathcal{D}^{(h)\mu}$ to a Young tableau. This can be accomplished with the help of the following observation:

- When acting on a polynomial defined via a tableau, the derivative in the i'th parenthesis in (5.24) acts *only* on columns with height exactly i.

This leads to a simple formula for applying $\mathcal{D}^{(h)\mu}$ to a Young tableau. To state it, we first define some simple operations on columns of height k:

$$
\begin{aligned}
S[k]^{\mu\nu}\begin{array}{|c|}\hline a_1\\\hline a_2\\\hline \vdots\\\hline a_k\\\hline\end{array} &= a_1^{\nu}\begin{array}{|c|}\hline \mu\\\hline a_2\\\hline \vdots\\\hline a_k\\\hline\end{array} + a_2^{\nu}\begin{array}{|c|}\hline a_1\\\hline \mu\\\hline \vdots\\\hline a_k\\\hline\end{array} + \cdots + a_k^{\nu}\begin{array}{|c|}\hline a_1\\\hline a_2\\\hline \vdots\\\hline \mu\\\hline\end{array}, \\
T[k]^{\mu}\begin{array}{|c|}\hline a_1\\\hline a_2\\\hline \vdots\\\hline a_k\\\hline\end{array} &= (-1)^{k-1}a_1^{\mu}\begin{array}{|c|}\hline a_2\\\hline \vdots\\\hline a_k\\\hline\end{array} + (-1)^{k-2}a_2^{\mu}\begin{array}{|c|}\hline a_1\\\hline \vdots\\\hline a_k\\\hline\end{array} + \cdots + a_k^{\mu}\begin{array}{|c|}\hline a_1\\\hline a_2\\\hline \vdots\\\hline\end{array}.
\end{aligned}
\tag{C.43}
$$

We define $S[k]$ and $T[k]$ to give zero when acting on columns with height $k' \neq k$. We furthermore extend them to derivations on the algebra generated by columns, so that they are linear and satisfy Leibniz rules:

$$
S[k]^{\mu\nu}(xy) = (S[k]^{\mu\nu}x)y + x(S[k]^{\mu\nu}y), \quad T[k]^{\mu}(xy) = (T[k]^{\mu}x)y + x(T[k]^{\mu}y). \tag{C.44}
$$

Finally, given a tableau Y, let $Y^{[k]}$ denote the product of all columns of Y with height k. In particular, Y can be decomposed as $Y = \prod_{k=1}^{h} Y^{[k]}$, where h is the height of Y. We claim that the action of $\mathcal{D}^{(h)}$ on Y is given by

$$
\begin{aligned}
\mathcal{D}^{(h)\mu_0}Y = &\left(\left(\delta^{\mu_0}_{\mu_1} - \frac{S[1]^{\mu_0}{}_{\mu_1}}{N_1^{(h)}}\right)Y^{[1]}\right)\left(\left(\delta^{\mu_1}_{\mu_2} - \frac{S[2]^{\mu_1}{}_{\mu_2}}{N_2^{(h)}}\right)Y^{[2]}\right)\cdots \\
&\left(\left(\delta^{\mu_{h-1}}_{\mu_h} - \frac{S[h]^{\mu_{h-1}}{}_{\mu_h}}{N_h^{(h)}-1}\right)T[h]^{\mu_h}Y^{[h]}\right).
\end{aligned}
\tag{C.45}
$$

The virtue of (C.45) is that it works symbolically within the algebra generated by

Young tableaux. For example, we have

$$
\begin{aligned}
v\cdot\mathcal{D}^{(3)} \begin{ytableau} a & d \\ b & e \\ c & f \end{ytableau} &= \left(v\cdot T[3] - \frac{1}{N_3^{(3)}-1} v\cdot S[3]\cdot T[3] \right) \begin{ytableau} a & d \\ b & e \\ c & f \end{ytableau} \\
&= v\cdot f \begin{ytableau} a & d \\ b & e \\ c \end{ytableau} - v\cdot e \begin{ytableau} a & d \\ b & f \\ c \end{ytableau} + v\cdot d \begin{ytableau} a & e \\ b & f \\ c \end{ytableau} + v\cdot c \begin{ytableau} d & a \\ e & b \\ f \end{ytableau} - v\cdot b \begin{ytableau} d & a \\ e & c \\ f \end{ytableau} \\
&+ v\cdot a \begin{ytableau} d & b \\ e & c \\ f \end{ytableau} \frac{1}{d-4} \left[c\cdot f \left(\begin{ytableau} a & d \\ b & e \\ v \end{ytableau} + \begin{ytableau} d & a \\ e & b \\ v \end{ytableau} \right) \pm \text{permutations} \right] .
\end{aligned}
\tag{C.46}
$$

The first line comes from applying $v\cdot T[3]$ and simply sums all the ways of erasing one box, while the second line comes from applying $v\cdot S[3]\cdot T[3]$. After including permutations, it contains 9 pairs of terms similar to the shown pair (with c replaced by a or b, or f replaced by d or e). If we add boxes with a vector n to the first row, then (C.45) implies

$$
\begin{aligned}
v\cdot\mathcal{D}^{(3)} \begin{ytableau} a & d & n & \cdots & n \\ b & e \\ c & f \end{ytableau} &= \left[v\cdot\mathcal{D}^{(3)} \begin{ytableau} a & d \\ b & e \\ c & f \end{ytableau} \right]^{\begin{ytableau} n & \cdots & n \end{ytableau}} \\
&- \frac{m_1-2}{d-3+m_1} \left[n\cdot\mathcal{D}^{(3)} \begin{ytableau} a & d \\ b & e \\ c & f \end{ytableau} \right]^{\begin{ytableau} v & \cdots & n \end{ytableau}} ,
\end{aligned}
\tag{C.47}
$$

where each square bracket is given by eq. (C.46).

Appendix D

Appendices for Chapter 5

D.1 Power counting in conformal correlators

We elaborate on the discussion in section 6.2 in this appendix. We start by considering the three-point functions of conserved currents. There are, in general, two parity-even OPE structures. These two three-point structures can be accounted by AdS YM three-point vertex (6.6) and a higher derivative cubic term arises in AdS EFTs

$$\mathcal{L} = -\frac{f^{abc}}{3g_{\rm YM}^3} g_H F_\mu{}^{\nu a} F_\nu{}^{\rho b} F_\rho{}^{\mu c} \,. \tag{D.1}$$

Using the bulk-to-boundary propagator of the gluon (6.8), we can explicitly evaluate the resulting three-point functions by performing the integrals over AdS

$$\begin{aligned}
\mathcal{M}_{3,\rm YM} &\propto \frac{(2d-3)\,(H_{23}V_1 + H_{13}V_2) + V_3\,((2d-3)H_{12} + 3(d-2)V_1V_2)}{(-2X_1\cdot X_2)^{d/2}\,(-2X_1\cdot X_3)^{d/2}\,(-2X_2\cdot X_3)^{d/2}}\,,\\
\mathcal{M}_{3,\rm cub} &\propto \frac{V_3\,((d+2)V_1V_2 + H_{12}) + H_{23}V_1 + H_{13}V_2}{(-2X_1\cdot X_2)^{d/2}\,(-2X_1\cdot X_3)^{d/2}\,(-2X_2\cdot X_3)^{d/2}}\,,
\end{aligned} \tag{D.2}$$

where the definitions of H_{ij} and V_i are

$$\begin{aligned}
H_{ij} &= 2\big((X_i\cdot Z_j)(Z_j\cdot X_i) - (X_i\cdot X_j)(Z_i\cdot Z_j)\big)\,,\\
V_i := V_{i,jk} &= \frac{(X_i\cdot X_k)(Z_i\cdot X_j) - (X_i\cdot X_j)(Z_i\cdot X_k)}{X_j\cdot X_k}\,.
\end{aligned} \tag{D.3}$$

See [47] for more details of this convention. We do not specify the overall coefficients in (D.2), as they can be absorbed into the OPE coefficients. In holographic CFTs, the OPE associated with $\mathcal{M}_{3,\text{cub}}$ should be suppressed by a large gap $\Delta_{\text{gap}} \gg 1$ [77]. However, staring at the LHS of (D.2) cannot tell which AdS vertices are their origins, making the power counting of OPE coefficients in terms of $1/\Delta_{\text{gap}}$ vague. This is in contrast to the flat-space EFT amplitudes, where it is easy to figure out that higher power of the momentum comes with higher suppression of the UV scale $1/M$.

Now as the differential operators $\mathcal{P}$ and $\mathcal{E}$ allow to uplift the flat-space amplitudes, the issue of the power counting in CFT can be resolved. We can show that $\mathcal{M}_{3,\text{cub}}$ can also be uplifted from flat-space three-point amplitudes produced by (D.1)

$$\widehat{\mathcal{M}_{3,\text{cub}}} \propto \mathcal{T}_{\mathcal{O}}\Big(\widehat{F}_{1\mu}{}^{\nu}\widehat{F}_{2\nu}{}^{\rho}\widehat{F}_{3\rho}{}^{\mu}\Big) + \text{perm}\,, \quad \widehat{F}_{i\mu\nu} = \mathcal{E}_{i\nu}\mathcal{P}_{i\mu} - \mathcal{E}_{i\mu}\mathcal{P}_{i\nu}\,. \tag{D.4}$$

It is then apparent that more $\mathcal{P}$ come with higher orders of $1/\Delta_{\text{gap}}$ in holographic CFTs. It is worth noting that this flat-space structure persists even beyond holographic CFTs because three-point structures (not including the OPE) are general objects as they are essentially fixed by conformal symmetry. This makes the helicity structures of CFT_3 [2] (i.e., the orthogonality of three-point structures) manifest by uplifting flat-space amplitudes.

We expect a similar uplift to work for three-point functions where the third operator is non-conserved. Such uplifts may diagonalize OPE matrix of mean field theory (MFT) in general dimensions, as one did for CFT_3 [2]. Using the bootstrap idea, the diagonal MFT OPE could pave the way for constraining spinning correlation functions (beyond holographic CFTs).

The same arguments apply to the power counting in four-point correlators. For example, the low-lying terms in the four-point function of conserved currents from contact diagrams follow precisely as flat-space amplitudes (for the sharp power counting in flat-space where the gravity is dynamical, see [200])

$$\widehat{\mathcal{M}}^{\rm ct}_{4V} \propto \frac{c_1}{C_T\Delta^2_{\rm gap}}\Big[\mathcal{T}_{\mathcal{O}}\Big(\widehat{F}_{1\mu\nu}\widehat{F}_2^{\mu\nu}\widehat{F}_{3\rho\sigma}\widehat{F}_4^{\rho\sigma}\Big)+{\rm perm}\Big]+\frac{c_2}{C_T\Delta^2_{\rm gap}}\Big[\mathcal{T}_{\mathcal{O}}\Big(\widehat{F}_{1\mu}{}^{\nu}\widehat{F}_{2\nu}{}^{\rho}\widehat{F}_{3\rho}{}^{\sigma}\widehat{F}_{4\sigma}{}^{\mu}\Big)\Big]+\cdots\,, \tag{D.5}$$

where C_T is the central charge appearing as the coefficient of the stress-tensor two-point function. For holographic CFTs, we have the hierarchy $C_T \gg \Delta^{d-1}_{\rm gap} \gg 1$.

Although we focus on spin-1 conserved current in this appendix, the same principle should apply to three and four-point stress tensor correlators.

D.2 Graviton vertices in AdS

In this appendix, we provide three and four-point vertices for Einstein gravity in AdS

$$S=\frac{1}{16\pi G}\int d^{d+1}x\sqrt{g}(R-2\Lambda)\,, \tag{D.6}$$

where $\Lambda=-(d-1)(d-2)/(2R^2_{\rm AdS})$. To compute vertices, we expand the metric around the AdS background

$$g_{\mu\nu}=g^{\rm AdS}_{\mu\nu}+\sqrt{32\pi G}h_{\mu\nu}\,, \tag{D.7}$$

and then expand the action up to the fourth order. For the three-point vertex, we perform (6.5) for two gravitons to give $\delta_{1,2}h$ while leaving the third one "off-shell". We vary off the off-shell graviton to give the three-point vertex function; for the four-point vertex, which gives rise to four-point contact amplitude, we use (6.5) to end up with the final answer. As in the main text, when it does not confuse, we slip off the superscript "AdS" and remember $g_{\mu\nu}$ is the AdS metric. We performed the calculations using the xAcT Mathematica package [240].

D.2.1 Three-point vertex

The external on-shell gravitons are computed by the bulk-to-boundary propagators, which satisfy

$$\delta_i h^\mu_\mu = \nabla_\mu \delta_i h^{\mu\nu} = 0\,, \quad \Big(\nabla^2 + \frac{2}{R^2_{\mathrm{AdS}}}\Big)\delta_i h_{\mu\nu} = 0\,, \tag{D.8}$$

Then we find the three-point vertex can be written by

$$V^{\mu\nu}_{h,12} = \widehat{V}^{\mu\nu}_{h,12} - \frac{1}{2}\widehat{V}_{h,12} g^{\mu\nu}\,, \tag{D.9}$$

where $\widehat{V}_{h,12}$ is the trace of $\widehat{V}^{\mu\nu}_{h,12}$

$$\begin{aligned}\widehat{V}^{\mu\nu}_{h,12} = \sqrt{8\pi G}\Big(&- \nabla^\nu \delta_2 h^{\rho\sigma}\nabla^\mu \delta_1 h_{\rho\sigma} - \nabla^\mu \delta_2 h^{\rho\sigma}\nabla^\nu \delta_1 h_{\rho\sigma} - 2\delta_1 h_{\rho\sigma}\nabla^\sigma\nabla^\rho \delta_2 h^{\mu\nu} \\ &+ 2\delta_1 h_{\rho\sigma}\nabla^\sigma\nabla^\nu\delta_2 h^{\mu\rho} + 2\delta_1 h_{\rho\sigma}\nabla^\sigma\nabla^\mu\delta_2 h^{\nu\rho} - 2\delta_1 h_{\rho\sigma}\nabla^\nu\nabla^\mu\delta_2 h^{\rho\sigma} - 2h_{2,\rho\sigma}\nabla^\sigma\nabla^\rho\delta_1 h^{\mu\nu} \\ &+ 2h_{2,\rho\sigma}\nabla^\sigma\nabla^\nu\delta_1 h^{\mu\rho} + 2h_{2,\rho\sigma}\nabla^\sigma\nabla^\mu\delta_1 h^{\nu\rho} - 2h_{2,\rho\sigma}\nabla^\nu\nabla^\mu\delta_1 h^{\rho\sigma} - 2\nabla_\sigma\delta_1 h^\mu_\rho\nabla^\sigma\delta_2 h^{\nu\rho} \\ &+ 2\nabla_\sigma\delta_1 h^\mu_\rho\nabla^\rho\delta_2 h^{\nu\sigma} - 2\nabla^\sigma\delta_2 h^{\mu\rho}\nabla_\sigma\delta_1 h^\nu_\rho + 2\nabla^\rho\delta_2 h^{\mu\sigma}\nabla_\sigma\delta_1 h^\nu_\rho\Big)\,. \end{aligned} \tag{D.10}$$

D.2.2 Four-point vertex

Four-point vertex can be calculated similarly. We present the four-point vertex with ordering (1234) below

$$
\begin{aligned}
V_{1234,h} = 4\pi G\Big[&\delta_1 h_{\mu\rho}\Big(2\delta_2 h^{\mu\rho}\nabla_\nu\delta_4 h^{\gamma\sigma}\nabla_\gamma\delta_3 h_{\nu\sigma} - 3\delta_2 h^{\mu\rho}\nabla_\gamma\delta_4 h^{\nu\sigma}\nabla_\gamma\delta_3 h_{\nu\sigma} \\
&- 16\delta_2 h^\mu_\sigma\nabla_\gamma\delta_4 h^{\nu\sigma}\nabla_\rho\delta_3 h_{\gamma\nu} + 12\delta_2 h^\mu_\sigma\nabla_\rho\delta_4 h^{\gamma\nu}\nabla_\sigma\delta_3 h_{\gamma\nu} - 4\delta_2 h_{\nu\sigma}\nabla_\gamma\delta_4 h^{\mu\rho}\nabla_\gamma\delta_3 h^{\nu\sigma} \\
&+ 12\delta_2 h_{\nu\sigma}\nabla_\gamma\delta_3 h^{\mu\sigma}\nabla_\gamma\delta_4 h^{\nu\rho} - 16\delta_2 h_{\nu\sigma}\nabla_\rho\delta_3 h^\mu_\gamma\nabla_\nu\delta_4 h^{\gamma\sigma} + 24\delta_2 h_{\nu\sigma}\nabla_\sigma\delta_3 h^\mu_\gamma\nabla_\nu\delta_4 h^{\gamma\rho} \\
&- 16\delta_2 h_{\nu\sigma}\nabla_\sigma\delta_3 h^\mu_\gamma\nabla_\gamma\delta_4 h^{\nu\rho} - 8\delta_2 h_{\nu\sigma}\nabla^\mu\delta_3 h^\sigma_\gamma\nabla_\nu\delta_4 h^{\gamma\rho} + 16\delta_2 h_{\nu\sigma}\nabla_\gamma\delta_4 h^{\mu\rho}\nabla_\nu\delta_3 h^\sigma_\gamma \\
&+ 16\delta_2 h^\mu_\sigma\delta_3 h_{\gamma\nu}\nabla_\sigma\nabla_\rho\delta_4 h^{\gamma\nu} - 32\delta_2 h^\mu_\sigma\delta_3 h_{\gamma\nu}\nabla_\gamma\nabla_\rho\delta_4 h^{\nu\sigma} + 16\delta_2 h^\mu_\sigma\delta_3 h_{\gamma\nu}\nabla_\gamma\nabla_\nu\delta_4 h^{\rho\sigma} \\
&- 8\delta_2 h^\mu_\sigma\nabla_\gamma\delta_3 h^\rho_\nu\nabla_\nu\delta_4 h^{\gamma\sigma} + 24\delta_2 h^\mu_\sigma\nabla_\gamma\delta_3 h^\rho_\nu\nabla_\gamma\delta_4 h^{\nu\sigma}\Big) + \frac{\delta_1 h_{\mu\rho}}{R^2_{\text{AdS}}}\Big(- d\delta_2 h^{\mu\rho}\delta_4 h^{\nu\sigma}\delta_3 h_{\nu\sigma} \\
&+ 20\delta_2 h^{\mu\rho}\delta_4 h^{\nu\sigma}\delta_3 h_{\nu\sigma} + 4d\delta_2 h^\mu_\sigma\delta_4 h^{\nu\rho}\delta_3 h^\sigma_\nu - 32\delta_2 h^\mu_\sigma\delta_3 h^\rho_\nu\delta_4 h^{\nu\sigma} + 16\delta_2 h^\mu_\sigma\delta_4 h^{\nu\rho}\delta_3 h^\sigma_\nu\Big)\Big]\,.
\end{aligned}
\tag{D.11}
$$

The corresponding four-point contact diagram is then evaluated by

$$
\mathcal{M}^{\text{ct}}_{4,\text{grav}} = \int D^{d+1}Y\big(V_{1234,h}(Y) + \text{perm}\big)\,. \tag{D.12}
$$

D.3 On the graviton bulk-to-boundary propagator

In this appendix, we complete the differential representation for bulk-to-boundary propagators (6.15). We provide detailed identities for contracting bulk-to-boundary propagators when deriving the differential representation.

The complete version of (6.15) is

$$
\begin{aligned}
&\delta_i h_{\mu\nu} = \mathcal{E}_{i,\mu}\mathcal{E}_{i,\nu}\delta_i\phi_d\,, \\
&\nabla_\mu\delta_i h_{\nu\rho} = \mathcal{E}_{i,\nu}\mathcal{E}_{i,\rho}\mathcal{P}_{i\mu}\delta_i\phi_{d-1} - \big(Y_\rho\mathcal{E}_{i\mu}\mathcal{E}_{i\nu}\delta_i\phi_d + Y_\nu\mathcal{E}_{i\mu}\mathcal{E}_{i\rho}\delta_i\phi_d\big)\,, \\
&\nabla_\mu\nabla_\nu\delta_i h_{\rho\sigma} = \mathcal{E}_{i,\rho}\mathcal{E}_{i,\sigma}\mathcal{P}_{i\mu}\mathcal{P}_{i\nu}\delta_i\phi_{d-2} - Y_\sigma\mathcal{E}_{i\nu}\mathcal{E}_{i\rho}\mathcal{P}_{i\mu}\delta_i\phi_{d-1} - Y_\mu\big(\mathcal{E}_{i\rho}\mathcal{E}_{i\sigma}\mathcal{P}_{i\nu}\delta_i\phi_{d-1} + Y_\sigma\mathcal{E}_{i\nu}\mathcal{E}_{i\rho}\delta_i\phi_d\big) \\
&- Y_\rho\big(\mathcal{E}_{i\nu}\mathcal{E}_{i\sigma}\mathcal{P}_{i\mu}\delta_i\phi_{d-1} + Y_\mu\mathcal{E}_{i\nu}\mathcal{E}_{i\sigma}\delta_i\phi_d\big) - \delta_{\mu\rho}\mathcal{E}_{i\nu}\mathcal{E}_{i\sigma}\delta_i\phi_d - \delta_{\sigma\mu}\mathcal{E}_{i\nu}\mathcal{E}_{i\rho}\delta_i\phi_d\,.
\end{aligned}
\tag{D.13}
$$

To arrive at differential representation exhibiting flat-space structure, we should prove identities with the spirit of transverse-traceless and on-shell conditions in flat-space. We find

$$\mathcal{E}_i \cdot \mathcal{E}_i \,\mathcal{P}_{i\mu}\mathcal{P}_{i\nu}\delta_i\phi_{d-2} = \mathcal{E}_i \cdot \mathcal{E}_i\delta_i\phi_d = \mathcal{P}_i \cdot \mathcal{P}_i\delta_i\phi_{d-2} = \mathcal{E}_i \cdot \mathcal{P}_i \,\mathcal{P}_{i\mu}\delta_i\phi_{d-2} = \mathcal{E}_i \cdot \mathcal{P}_i\delta_i\phi_{d-1} = 0\,, \tag{D.14}$$

For those terms $\mathcal{O}(Y), \mathcal{O}(Y, g)$, we prove a set of identities that can help us get rid of Y in the final representation so that the differential representation is well-defined even from perspective pure CFT

$$\begin{aligned}
&Y \cdot \mathcal{P}_i\delta_i\phi_{d-1} = (Y \cdot \mathcal{P}_i)^2\delta_i\phi_{d-2} = Y \cdot \mathcal{E}_i\delta_i\phi_d = (Y \cdot \mathcal{E}_i)^2\delta_i\phi_d = (Y \cdot \mathcal{E}_i)^2 \,\mathcal{P}_{i,\mu}\delta_i\phi_{d-1} = 0\,,\\
&Y \cdot \mathcal{P}_i \,\mathcal{P}_{i,\mu}\delta_i\phi_{d-2} = -\mathcal{P}_{i,\mu}\delta_i\phi_{d-1}\,, \quad (Y \cdot \mathcal{E}_i)^2 \,\mathcal{P}_{i,\mu}\mathcal{P}_{i,\nu}\delta_i\phi_{d-2} = 2\mathcal{E}_{i,\mu}\mathcal{E}_{i,\nu}\delta_i\phi_d\,,\\
&Y \cdot \mathcal{E}_i \,\mathcal{P}_{i,\mu}\delta_i\phi_{d-1} = -\mathcal{E}_{i,\mu}\delta_i\phi_d\,, \quad Y \cdot \mathcal{E}_i \,\mathcal{P}_{i,\mu}\mathcal{P}_{i,\nu}\delta_i\phi_{d-2} = -\mathcal{E}_{i,(\mu}\mathcal{P}_{i,\nu)}\delta_i\phi_{d-1}\,.
\end{aligned} \tag{D.15}$$

D.4 On the graviton bulk-to-bulk propagator

In this appendix, we show in detail how we derive (6.28) by following the lines of [7, 211]. For simplicity, we take the de-Donder gauge for the propagating graviton. It is useful to decompose the graviton into the traceless part and the trace part

$$h_{\mu\nu} = \tilde{h}_{\mu\nu} + \frac{1}{d+1} h g_{\mu\nu}\,, \quad \tilde{h} \equiv 0\,. \tag{D.16}$$

The basic idea is to treat $\tilde{h}_{\mu\nu}$ and h independently.They give rise to three different bulk-to-bulk propagators by the Wick contractions that satisfy different equations. To see this, we consider the equation of motion of graviton in the de-Donder gauge

$$(\nabla^2_{Y_1} + 2)\left\langle h_{\mu\nu}(Y_1)h_{\rho\sigma}(Y_2)\right\rangle - 2g_{\mu\nu}\left\langle h(Y_1)h_{\rho\sigma}(Y_2)\right\rangle = \frac{1}{2}\big(g_{\mu\rho}g_{\nu\sigma} + g_{\mu\sigma}g_{\nu\rho} - \frac{2g_{\mu\nu}g_{\rho\sigma}}{d-1}\big)\delta(Y_1 - Y_2)\,. \tag{D.17}$$

It is easy to find that upon the trace decomposition (D.22) we have

$$
\begin{aligned}
&(\nabla^2_{Y_1}+2)\left\langle \tilde{h}_{\mu\nu}(Y_1)\tilde{h}_{\rho\sigma}(Y_2)\right\rangle=\frac{1}{2}\big(g_{\mu\rho}g_{\nu\sigma}+g_{\mu\sigma}g_{\nu\rho}-\frac{2g_{\mu\nu}g_{\rho\sigma}}{d+1}\big)\delta(Y_1-Y_2)\,,\\
&(\nabla^2_{Y_1}-2d)\left\langle h(Y_1)h(Y_2)\right\rangle=\frac{2(d+1)}{d-1}\delta(Y_1-Y_2)\,,\\
&(\nabla^2_{Y_1}-2d)\left\langle h(Y_1)\tilde{h}_{\mu\nu}(Y_2)\right\rangle=(\nabla^2_{Y_1}+2)\left\langle h_{\mu\nu}(Y_1)h(Y_2)\right\rangle=0\,.
\end{aligned}
\tag{D.18}
$$

Besides, any vertex functions coupled to the stress-tensor are now naturally decomposed into traceless and trace part

$$
V_{\mu\nu}h^{\mu\nu}=\tilde{V}_{\mu\nu}\tilde{h}^{\mu\nu}+\frac{1}{d+1}\mathrm{Tr}\,V\,h\,. \tag{D.19}
$$

With all these ingredients in mind, we can rewrite the graviton exchange amplitudes eq: graviton exchange diagram as

$$
\begin{aligned}
\mathcal{M}^{(s)}_{4\mathrm{ex,grav}}=&16\times 8\pi G\int D^{d+2}Y_1D^{d+2}Y_2\,\Big(\tilde{V}^{\mu\nu}_{h,12}\left\langle \tilde{h}_{\mu\nu}(Y_1)\tilde{h}_{\rho\sigma}(Y_2)\right\rangle\tilde{V}^{\rho\sigma}_{h,34}\\
&+\frac{1}{(d+1)^2}\mathrm{Tr}\,V_{h,12}\left\langle h(Y_1)h(Y_2)\right\rangle\mathrm{Tr}\,V_{h,34}+\frac{1}{d+1}\mathrm{Tr}\,V_{h,12}\left\langle h(Y_1)\tilde{h}_{\rho\sigma}(Y_2)\right\rangle\tilde{V}^{\rho\sigma}_{34,h}\\
&+\frac{1}{d+1}\tilde{V}^{\mu\nu}_{h,12}\left\langle \tilde{h}_{\mu\nu}(Y_1)h(Y_2)\right\rangle\mathrm{Tr}\,V_{h,34}\Big)\,.
\end{aligned}
\tag{D.20}
$$

Using the AdS embedding formalism for the bulk-to-boundary propagator (6.14), we can easily prove the following identities

$$
\mathcal{C}_{12}\tilde{V}^{\mu\nu}_{h,12}=\big(\nabla^2_{Y_1}+2(d+1)\big)\tilde{V}^{\mu\nu}_{h,12}\,,\quad \mathcal{C}_{12}\mathrm{Tr}\,V_{h,12}=\nabla^2_{Y_1}\mathrm{Tr}\,V_{h,12}\,. \tag{D.21}
$$

Therefore, we find

$$
\begin{aligned}
&\mathcal{D}^{d,2}_{12}\mathcal{M}_{4\mathrm{ex,grav}}=\int D^{d+2}Y_1D^{d+2}Y_2\times\\
&\Big(\tilde{V}^{\mu\nu}_{h,12}(\nabla^2_{Y_1}+2)\left\langle \tilde{h}_{\mu\nu}(Y_1)\tilde{h}_{\rho\sigma}(Y_2)\right\rangle\tilde{V}^{\rho\sigma}_{h,34}+\frac{1}{(d+1)^2}\mathrm{Tr}\,V_{h,12}(\nabla^2_{Y_1}-2d)\left\langle h(Y_1)h(Y_2)\right\rangle\mathrm{Tr}\,V_{h,34}\\
&+\frac{1}{d+1}\mathrm{Tr}\,V_{h,12}(\nabla^2_{Y_1}-2d)\left\langle h(Y_1)\tilde{h}_{\rho\sigma}(Y_2)\right\rangle\tilde{V}^{\rho\sigma}_{h,34}+\frac{1}{d+1}\tilde{V}^{\mu\nu}_{h,12}(\nabla^2_{Y_1}+2)\left\langle \tilde{h}_{\mu\nu}(Y_1)h(Y_2)\right\rangle\mathrm{Tr}\,V_{h,34}\Big)\,.
\end{aligned}
\tag{D.22}
$$

Plugging (D.18) into (D.22), we prove (6.28).

Bibliography

[1] Y.-Z. Li, *Notes on flat-space limit of AdS/CFT*, *JHEP* **09** (2021) 027, [2106.04606].

[2] S. Caron-Huot and Y.-Z. Li, *Helicity basis for three-dimensional conformal field theory*, *JHEP* **06** (2021) 041, [2102.08160].

[3] S. Komatsu, M. F. Paulos, B. C. Van Rees and X. Zhao, *Landau diagrams in AdS and S-matrices from conformal correlators*, *JHEP* **11** (2020) 046, [2007.13745].

[4] S. Caron-Huot, Y.-Z. Li, J. Parra-Martinez and D. Simmons-Duffin, *Graviton partial waves and causality in higher dimensions*, 2205.01495.

[5] S. Caron-Huot, Y.-Z. Li, J. Parra-Martinez and D. Simmons-Duffin, *Causality constraints on corrections to Einstein gravity*, 2201.06602.

[6] Y.-Z. Li, *Flat-space structure of gluon and graviton in AdS*, 2212.13195.

[7] A. Herderschee, R. Roiban and F. Teng, *On the differential representation and color-kinematics duality of AdS boundary correlators*, *JHEP* **05** (2022) 026, [2201.05067].

[8] S. Weinberg, *The Quantum theory of fields. Vol. 1: Foundations.* Cambridge University Press, 6, 2005.

[9] J. M. Maldacena, *The Large N limit of superconformal field theories and supergravity*, *Adv. Theor. Math. Phys.* **2** (1998) 231–252, [hep-th/9711200].

[10] E. Witten, *Anti-de Sitter space and holography*, *Adv. Theor. Math. Phys.* **2** (1998) 253–291, [hep-th/9802150].

[11] S. S. Gubser, I. R. Klebanov and A. M. Polyakov, *Gauge theory correlators from noncritical string theory*, *Phys. Lett. B* **428** (1998) 105–114, [hep-th/9802109].

[12] T. Hartman, D. Mazac, D. Simmons-Duffin and A. Zhiboedov, *Snowmass White Paper: The Analytic Conformal Bootstrap*, in *2022 Snowmass Summer Study*, 2, 2022, 2202.11012.

[13] A. Bissi, A. Sinha and X. Zhou, *Selected topics in analytic conformal bootstrap: A guided journey*, *Phys. Rept.* **991** (2022) 1–89, [2202.08475].

[14] J. Polchinski, *S matrices from AdS space-time*, hep-th/9901076.

[15] S. B. Giddings, *Flat space scattering and bulk locality in the AdS / CFT correspondence*, *Phys. Rev. D* **61** (2000) 106008, [hep-th/9907129].

[16] M. Gary, S. B. Giddings and J. Penedones, *Local bulk S-matrix elements and CFT singularities*, *Phys. Rev. D* **80** (2009) 085005, [0903.4437].

[17] M. Gary and S. B. Giddings, *The Flat space S-matrix from the AdS/CFT correspondence?*, *Phys. Rev. D* **80** (2009) 046008, [0904.3544].

[18] I. Heemskerk, J. Penedones, J. Polchinski and J. Sully, *Holography from Conformal Field Theory*, *JHEP* **10** (2009) 079, [0907.0151].

[19] A. L. Fitzpatrick, E. Katz, D. Poland and D. Simmons-Duffin, *Effective Conformal Theory and the Flat-Space Limit of AdS*, *JHEP* **07** (2011) 023, [1007.2412].

[20] A. L. Fitzpatrick and J. Kaplan, *Scattering States in AdS/CFT*, 1104.2597.

[21] T. Okuda and J. Penedones, *String scattering in flat space and a scaling limit of Yang-Mills correlators*, *Phys. Rev. D* **83** (2011) 086001, [1002.2641].

[22] J. Penedones, *Writing CFT correlation functions as AdS scattering amplitudes*, *JHEP* **03** (2011) 025, [1011.1485].

[23] A. L. Fitzpatrick and J. Kaplan, *Analyticity and the Holographic S-Matrix*, *JHEP* **10** (2012) 127, [1111.6972].

[24] J. Maldacena, D. Simmons-Duffin and A. Zhiboedov, *Looking for a bulk point*, *JHEP* **01** (2017) 013, [1509.03612].

[25] M. F. Paulos, J. Penedones, J. Toledo, B. C. van Rees and P. Vieira, *The S-matrix bootstrap. Part I: QFT in AdS*, *JHEP* **11** (2017) 133, [1607.06109].

[26] S. Raju, *New Recursion Relations and a Flat Space Limit for AdS/CFT Correlators*, *Phys. Rev. D* **85** (2012) 126009, [1201.6449].

[27] B. C. van Rees and X. Zhao, *QFT in AdS instead of LSZ*, 2210.15683.

[28] H. Epstein, *Some analytic properties of scattering amplitudes in quantum field theory*, in *8th Brandeis University Summer Institute in Theoretical Physics: Particle symmetries and axiomatic field theory*, pp. 1–128, 1966.

[29] L. Eberhardt, S. Komatsu and S. Mizera, *Scattering equations in AdS: scalar correlators in arbitrary dimensions*, *JHEP* **11** (2020) 158, [2007.06574].

[30] K. Roehrig and D. Skinner, *Ambitwistor strings and the scattering equations on $AdS_3 \times S^3$*, *JHEP* **02** (2022) 073, [2007.07234].

[31] P. Diwakar, A. Herderschee, R. Roiban and F. Teng, *BCJ amplitude relations for Anti-de Sitter boundary correlators in embedding space*, *JHEP* **10** (2021) 141, [2106.10822].

[32] C. Cheung, J. Parra-Martinez and A. Sivaramakrishnan, *On-shell correlators and color-kinematics duality in curved symmetric spacetimes*, *JHEP* **05** (2022) 027, [2201.05147].

[33] S. Caron-Huot, D. Mazac, L. Rastelli and D. Simmons-Duffin, *AdS bulk locality from sharp CFT bounds*, *JHEP* **11** (2021) 164, [2106.10274].

[34] A. M. Polyakov, *Conformal symmetry of critical fluctuations*, *JETP Lett.* **12** (1970) 381–383.

[35] J. Cardy, *Scaling and renormalization in statistical physics*, vol. 5. Cambridge university press, 1996.

[36] S. Ferrara, A. F. Grillo and R. Gatto, *Tensor representations of conformal algebra and conformally covariant operator product expansion*, *Annals Phys.* **76** (1973) 161–188.

[37] A. M. Polyakov, *Nonhamiltonian approach to conformal quantum field theory*, *Zh. Eksp. Teor. Fiz.* **66** (1974) 23–42.

[38] R. Rattazzi, V. S. Rychkov, E. Tonni and A. Vichi, *Bounding scalar operator dimensions in 4D CFT*, *JHEP* **12** (2008) 031, [0807.0004].

[39] D. Poland, S. Rychkov and A. Vichi, *The Conformal Bootstrap: Theory, Numerical Techniques, and Applications*, *Rev. Mod. Phys.* **91** (2019) 015002, [1805.04405].

[40] A. L. Fitzpatrick, J. Kaplan, D. Poland and D. Simmons-Duffin, *The Analytic Bootstrap and AdS Superhorizon Locality*, *JHEP* **12** (2013) 004, [1212.3616].

[41] Z. Komargodski and A. Zhiboedov, *Convexity and Liberation at Large Spin*, *JHEP* **11** (2013) 140, [1212.4103].

[42] L. F. Alday, *Large Spin Perturbation Theory for Conformal Field Theories*, *Phys. Rev. Lett.* **119** (2017) 111601, [1611.01500].

[43] S. Caron-Huot, *Analyticity in Spin in Conformal Theories*, *JHEP* **09** (2017) 078, [1703.00278].

[44] A. B. Zamolodchikov, *Irreversibility of the Flux of the Renormalization Group in a 2D Field Theory*, *JETP Lett.* **43** (1986) 730–732.

[45] J. Polchinski, *Scale and Conformal Invariance in Quantum Field Theory*, *Nucl. Phys. B* **303** (1988) 226–236.

[46] Y. Nakayama, *Scale invariance vs conformal invariance*, *Phys. Rept.* **569** (2015) 1–93, [1302.0884].

[47] M. S. Costa, J. Penedones, D. Poland and S. Rychkov, *Spinning Conformal Correlators*, *JHEP* **11** (2011) 071, [1107.3554].

[48] S. Minwalla, *Restrictions imposed by superconformal invariance on quantum field theories*, *Adv. Theor. Math. Phys.* **2** (1998) 783–851, [hep-th/9712074].

[49] D. Simmons-Duffin, *A Semidefinite Program Solver for the Conformal Bootstrap*, *JHEP* **06** (2015) 174, [1502.02033].

[50] S. El-Showk, M. F. Paulos, D. Poland, S. Rychkov, D. Simmons-Duffin and A. Vichi, *Solving the 3D Ising Model with the Conformal Bootstrap*, *Phys. Rev. D* **86** (2012) 025022, [1203.6064].

[51] F. Kos, D. Poland, D. Simmons-Duffin and A. Vichi, *Precision Islands in the Ising and $O(N)$ Models*, *JHEP* **08** (2016) 036, [1603.04436].

[52] M. Hasenbusch, *Finite size scaling study of lattice models in the three-dimensional Ising universality class*, *Phys. Rev. B* **82** (2010) 174433, [1004.4486].

[53] A. L. Fitzpatrick and J. Kaplan, *Unitarity and the Holographic S-Matrix*, *JHEP* **10** (2012) 032, [1112.4845].

[54] A. Kaviraj, K. Sen and A. Sinha, *Analytic bootstrap at large spin*, *JHEP* **11** (2015) 083, [1502.01437].

[55] L. F. Alday, A. Bissi and T. Lukowski, *Large spin systematics in CFT*, *JHEP* **11** (2015) 101, [1502.07707].

[56] A. Kaviraj, K. Sen and A. Sinha, *Universal anomalous dimensions at large spin and large twist*, *JHEP* **07** (2015) 026, [1504.00772].

[57] L. F. Alday and A. Zhiboedov, *An Algebraic Approach to the Analytic Bootstrap*, *JHEP* **04** (2017) 157, [1510.08091].

[58] S. Pal, J. Qiao and S. Rychkov, *Twist accumulation in conformal field theory. A rigorous approach to the lightcone bootstrap*, 2212.04893.

[59] L. F. Alday and A. Zhiboedov, *Conformal Bootstrap With Slightly Broken Higher Spin Symmetry*, *JHEP* **06** (2016) 091, [1506.04659].

[60] D. Simmons-Duffin, *The Lightcone Bootstrap and the Spectrum of the 3d Ising CFT*, *JHEP* **03** (2017) 086, [1612.08471].

[61] D. Simmons-Duffin, D. Stanford and E. Witten, *A spacetime derivation of the Lorentzian OPE inversion formula*, *JHEP* **07** (2018) 085, [1711.03816].

[62] P. Kravchuk and D. Simmons-Duffin, *Light-ray operators in conformal field theory*, *JHEP* **11** (2018) 102, [1805.00098].

[63] M. Henningson and K. Skenderis, *The Holographic Weyl anomaly*, *JHEP* **07** (1998) 023, [hep-th/9806087].

[64] M. Henningson and K. Skenderis, *Holography and the Weyl anomaly*, *Fortsch. Phys.* **48** (2000) 125–128, [hep-th/9812032].

[65] S. de Haro, S. N. Solodukhin and K. Skenderis, *Holographic reconstruction of space-time and renormalization in the AdS / CFT correspondence*, *Commun. Math. Phys.* **217** (2001) 595–622, [hep-th/0002230].

[66] K. Skenderis, *Asymptotically Anti-de Sitter space-times and their stress energy tensor*, *Int. J. Mod. Phys. A* **16** (2001) 740–749, [hep-th/0010138].

[67] G. Hooft, *Dimensional reduction in quantum gravity*, *arXiv preprint gr-qc/9310026* (1993) .

[68] L. Susskind, *The world as a hologram (1994)*, *arXiv preprint hep-th/9409089* (1994) .

[69] J. D. Bekenstein, *Black holes and entropy*, *Physical Review D* **7** (1973) 2333.

[70] G. W. Gibbons and S. W. Hawking, *Action integrals and partition functions in quantum gravity*, *Physical Review D* **15** (1977) 2752.

[71] O. Aharony, S. S. Gubser, J. Maldacena, H. Ooguri and Y. Oz, *Large n field theories, string theory and gravity*, *Physics Reports* **323** (2000) 183–386.

[72] S. Lee, S. Minwalla, M. Rangamani and N. Seiberg, *Three point functions of chiral operators in D = 4, N=4 SYM at large N*, *Adv. Theor. Math. Phys.* **2** (1998) 697–718, [hep-th/9806074].

[73] V. Pestun, *Localization of gauge theory on a four-sphere and supersymmetric Wilson loops*, *Commun. Math. Phys.* **313** (2012) 71–129, [0712.2824].

[74] J. K. Erickson, G. W. Semenoff and K. Zarembo, *Wilson loops in N=4 supersymmetric Yang-Mills theory*, *Nucl. Phys. B* **582** (2000) 155–175, [hep-th/0003055].

[75] N. Beisert et al., *Review of AdS/CFT Integrability: An Overview*, *Lett. Math. Phys.* **99** (2012) 3–32, [1012.3982].

[76] R. C. Myers and A. Sinha, *Seeing a c-theorem with holography*, *Physical Review D* **82** (2010) 046006.

[77] X. O. Camanho, J. D. Edelstein, J. Maldacena and A. Zhiboedov, *Causality Constraints on Corrections to the Graviton Three-Point Coupling*, *JHEP* **02** (2016) 020, [1407.5597].

[78] T. Hartman, S. Jain and S. Kundu, *Causality Constraints in Conformal Field Theory*, *JHEP* **05** (2016) 099, [1509.00014].

[79] N. Afkhami-Jeddi, T. Hartman, S. Kundu and A. Tajdini, *Einstein gravity 3-point functions from conformal field theory*, *JHEP* **12** (2017) 049, [1610.09378].

[80] C. de Rham, S. Melville, A. J. Tolley and S.-Y. Zhou, *Positivity bounds for scalar field theories*, *Phys. Rev. D* **96** (2017) 081702, [1702.06134].

[81] A. Adams, N. Arkani-Hamed, S. Dubovsky, A. Nicolis and R. Rattazzi, *Causality, analyticity and an IR obstruction to UV completion*, *JHEP* **10** (2006) 014, [hep-th/0602178].

[82] S. Caron-Huot and V. Van Duong, *Extremal Effective Field Theories*, *JHEP* **05** (2021) 280, [2011.02957].

[83] A. J. Tolley, Z.-Y. Wang and S.-Y. Zhou, *New positivity bounds from full crossing symmetry*, *JHEP* **05** (2021) 255, [2011.02400].

[84] L.-Y. Chiang, Y.-t. Huang, W. Li, L. Rodina and H.-C. Weng, *Into the EFThedron and UV constraints from IR consistency*, 2105.02862.

[85] L.-Y. Chiang, Y.-t. Huang, W. Li, L. Rodina and H.-C. Weng, *(Non)-projective bounds on gravitational EFT*, 2201.07177.

[86] N. Arkani-Hamed, T.-C. Huang and Y.-T. Huang, *The EFT-Hedron*, *JHEP* **05** (2021) 259, [2012.15849].

[87] B. Bellazzini, J. Elias Miró, R. Rattazzi, M. Riembau and F. Riva, *Positive Moments for Scattering Amplitudes*, 2011.00037.

[88] A. Sinha and A. Zahed, *Crossing Symmetric Dispersion Relations in QFTs*, *Phys. Rev. Lett.* **126** (2021) 181601, [2012.04877].

[89] S. Caron-Huot, D. Mazac, L. Rastelli and D. Simmons-Duffin, *Dispersive CFT Sum Rules*, *JHEP* **05** (2021) 243, [2008.04931].

[90] A. Bagchi, R. Basu, A. Kakkar and A. Mehra, *Flat Holography: Aspects of the dual field theory*, *JHEP* **12** (2016) 147, [1609.06203].

[91] A. Hamilton, D. N. Kabat, G. Lifschytz and D. A. Lowe, *Local bulk operators in AdS/CFT: A Boundary view of horizons and locality*, *Phys. Rev. D* **73** (2006) 086003, [hep-th/0506118].

[92] A. Hamilton, D. N. Kabat, G. Lifschytz and D. A. Lowe, *Holographic representation of local bulk operators*, *Phys. Rev. D* **74** (2006) 066009, [hep-th/0606141].

[93] E. Hijano, *Flat space physics from AdS/CFT*, *JHEP* **07** (2019) 132, [1905.02729].

[94] R. Bousso, S. Leichenauer and V. Rosenhaus, *Light-sheets and AdS/CFT*, *Phys. Rev. D* **86** (2012) 046009, [1203.6619].

[95] B. Czech, J. L. Karczmarek, F. Nogueira and M. Van Raamsdonk, *The Gravity Dual of a Density Matrix*, *Class. Quant. Grav.* **29** (2012) 155009, [1204.1330].

[96] R. Bousso, B. Freivogel, S. Leichenauer, V. Rosenhaus and C. Zukowski, *Null Geodesics, Local CFT Operators and AdS/CFT for Subregions*, *Phys. Rev. D* **88** (2013) 064057, [1209.4641].

[97] D. Harlow, *The Ryu–Takayanagi Formula from Quantum Error Correction*, *Commun. Math. Phys.* **354** (2017) 865–912, [1607.03901].

[98] L. F. Alday and X. Zhou, *Simplicity of AdS Supergravity at One Loop*, *JHEP* **09** (2020) 008, [1912.02663].

[99] L. F. Alday and X. Zhou, *All Tree-Level Correlators for M-theory on* $AdS_7 \times S^4$, *Phys. Rev. Lett.* **125** (2020) 131604, [2006.06653].

[100] F. Aprile, J. M. Drummond, H. Paul and M. Santagata, *The Virasoro-Shapiro amplitude in* $AdS_5 \times S^5$ *and level splitting of 10d conformal symmetry*, 2012.12092.

[101] L. F. Alday, C. Behan, P. Ferrero and X. Zhou, *Gluon Scattering in AdS from CFT*, *JHEP* **06** (2021) 020, [2103.15830].

[102] F. Aprile and P. Vieira, *Large p explorations. From SUGRA to big STRINGS in Mellin space*, *JHEP* **12** (2020) 206, [2007.09176].

[103] C. Wen and S.-Q. Zhang, *Notes on gravity multiplet correlators in $AdS_3 \times S^3$*, 2106.03499.

[104] T. Abl, P. Heslop and A. E. Lipstein, *Towards the Virasoro-Shapiro amplitude in $AdS_5 \times S^5$*, *JHEP* **04** (2021) 237, [2012.12091].

[105] C. Cardona, *Correlation functions at the bulk point singularity from the gravitational eikonal S-matrix*, *JHEP* **11** (2019) 044, [1906.08734].

[106] L. F. Alday and S. Caron-Huot, *Gravitational S-matrix from CFT dispersion relations*, *JHEP* **12** (2018) 017, [1711.02031].

[107] G. Mack, *D-independent representation of Conformal Field Theories in D dimensions via transformation to auxiliary Dual Resonance Models. Scalar amplitudes*, 0907.2407.

[108] G. Mack, *D-dimensional Conformal Field Theories with anomalous dimensions as Dual Resonance Models*, *Bulg. J. Phys.* **36** (2009) 214–226, [0909.1024].

[109] A. L. Fitzpatrick, J. Kaplan, J. Penedones, S. Raju and B. C. van Rees, *A Natural Language for AdS/CFT Correlators*, *JHEP* **11** (2011) 095, [1107.1499].

[110] J. Penedones, J. A. Silva and A. Zhiboedov, *Nonperturbative Mellin Amplitudes: Existence, Properties, Applications*, *JHEP* **08** (2020) 031, [1912.11100].

[111] P. Kravchuk, J. Qiao and S. Rychkov, *Distributions in CFT II. Minkowski Space*, 2104.02090.

[112] M. Hogervorst and S. Rychkov, *Radial Coordinates for Conformal Blocks*, *Phys. Rev. D* **87** (2013) 106004, [1303.1111].

[113] F. Kos, D. Poland and D. Simmons-Duffin, *Bootstrapping the $O(N)$ vector models*, *JHEP* **06** (2014) 091, [1307.6856].

[114] A. May, G. Penington and J. Sorce, *Holographic scattering requires a connected entanglement wedge*, *JHEP* **08** (2020) 132, [1912.05649].

[115] D. Simmons-Duffin, *The Conformal Bootstrap*, in *Proceedings, Theoretical Advanced Study Institute in Elementary Particle Physics: New Frontiers in Fields and Strings (TASI 2015): Boulder, CO, USA, June 1-26, 2015*, pp. 1–74, 2017, 1602.07982, DOI.

[116] V. K. Dobrev, V. B. Petkova, S. G. Petrova and I. T. Todorov, *Dynamical Derivation of Vacuum Operator Product Expansion in Euclidean Conformal Quantum Field Theory*, *Phys. Rev. D* **13** (1976) 887.

[117] P. Kravchuk and D. Simmons-Duffin, *Counting Conformal Correlators*, *JHEP* **02** (2018) 096, [1612.08987].

[118] S. Chakraborty, S. D. Chowdhury, T. Gopalka, S. Kundu, S. Minwalla and A. Mishra, *Classification of all 3 particle S-matrices quadratic in photons or gravitons*, *JHEP* **04** (2020) 110, [2001.07117].

[119] M. Correia, A. Sever and A. Zhiboedov, *An Analytical Toolkit for the S-matrix Bootstrap*, 2006.08221.

[120] D. Carmi and S. Caron-Huot, *A Conformal Dispersion Relation: Correlations from Absorption*, *JHEP* **09** (2020) 009, [1910.12123].

[121] D. Meltzer, E. Perlmutter and A. Sivaramakrishnan, *Unitarity Methods in AdS/CFT*, *JHEP* **03** (2020) 061, [1912.09521].

[122] D. Meltzer and A. Sivaramakrishnan, *CFT unitarity and the AdS Cutkosky rules*, *JHEP* **11** (2020) 073, [2008.11730].

[123] D. Meltzer, *Dispersion Formulas in QFTs, CFTs, and Holography*, *JHEP* **05** (2021) 098, [2103.15839].

[124] D. Ponomarev, *From bulk loops to boundary large-N expansion*, *JHEP* **01** (2020) 154, [1908.03974].

[125] X. Z. B. C. Van Rees, *Flar-space limit of Non-perturbative Conformal Correlators*, *to appear* .

[126] L. Cornalba, M. S. Costa, J. Penedones and R. Schiappa, *Eikonal Approximation in AdS/CFT: From Shock Waves to Four-Point Functions*, *JHEP* **08** (2007) 019, [hep-th/0611122].

[127] M. S. Costa, V. Goncalves and J. Penedones, *Conformal Regge theory*, *JHEP* **12** (2012) 091, [1209.4355].

[128] A. Antunes, M. S. Costa, T. Hansen, A. Salgarkar and S. Sarkar, *The perturbative CFT optical theorem and high-energy string scattering in AdS at one loop*, *JHEP* **04** (2021) 088, [2012.01515].

[129] S. Kundu, *Swampland Conditions for Higher Derivative Couplings from CFT*, 2104.11238.

[130] S. Caron-Huot, D. Mazac, L. Rastelli and D. Simmons-Duffin, *Sharp Boundaries for the Swampland*, *JHEP* **07** (2021) 110, [2102.08951].

[131] E. Hijano and D. Neuenfeld, *Soft photon theorems from CFT Ward identites in the flat limit of AdS/CFT*, *JHEP* **11** (2020) 009, [2005.03667].

[132] D. Chandorkar, S. D. Chowdhury, S. Kundu and S. Minwalla, *Bounds on Regge growth of flat space scattering from bounds on chaos*, *JHEP* **05** (2021) 143, [2102.03122].

[133] H. Kawai, D. C. Lewellen and S. H. H. Tye, *A Relation Between Tree Amplitudes of Closed and Open Strings*, *Nucl. Phys. B* **269** (1986) 1–23.

[134] Z. Bern, J. J. M. Carrasco and H. Johansson, *New Relations for Gauge-Theory Amplitudes*, *Phys. Rev. D* **78** (2008) 085011, [0805.3993].

[135] C. Armstrong, A. E. Lipstein and J. Mei, *Color/kinematics duality in AdS_4*, *JHEP* **02** (2021) 194, [2012.02059].

[136] S. Albayrak, S. Kharel and D. Meltzer, *On duality of color and kinematics in (A)dS momentum space*, *JHEP* **03** (2021) 249, [2012.10460].

[137] S. Jain, R. R. John, A. Mehta, A. A. Nizami and A. Suresh, *Momentum space parity-odd CFT 3-point functions*, 2101.11635.

[138] S. Jain, R. Rajan, A. Mehta, A. A. Nizami and A. Suresh, *Double copy structure of parity-violating CFT correlators*, 2104.12803.

[139] S. Pasterski, S.-H. Shao and A. Strominger, *Gluon Amplitudes as 2d Conformal Correlators*, *Phys. Rev. D* **96** (2017) 085006, [1706.03917].

[140] H. T. Lam and S.-H. Shao, *Conformal Basis, Optical Theorem, and the Bulk Point Singularity*, *Phys. Rev. D* **98** (2018) 025020, [1711.06138].

[141] D. Karateev, P. Kravchuk and D. Simmons-Duffin, *Harmonic Analysis and Mean Field Theory*, *JHEP* **10** (2019) 217, [1809.05111].

[142] S. Albayrak, D. Meltzer and D. Poland, *More Analytic Bootstrap: Nonperturbative Effects and Fermions*, *JHEP* **08** (2019) 040, [1904.00032].

[143] L. Iliesiu, F. Kos, D. Poland, S. S. Pufu and D. Simmons-Duffin, *Bootstrapping 3D Fermions with Global Symmetries*, *JHEP* **01** (2018) 036, [1705.03484].

[144] A. Dymarsky, F. Kos, P. Kravchuk, D. Poland and D. Simmons-Duffin, *The 3d Stress-Tensor Bootstrap*, *JHEP* **02** (2018) 164, [1708.05718].

[145] D. Karateev, P. Kravchuk, M. Serone and A. Vichi, *Fermion Conformal Bootstrap in 4d*, *JHEP* **06** (2019) 088, [1902.05969].

[146] R. S. Erramilli, L. V. Iliesiu, P. Kravchuk, W. Landry, D. Poland and D. Simmons-Duffin, *blocks_3d: Software for general 3d conformal blocks*, 2011.01959.

[147] M. S. Costa, J. Penedones, D. Poland and S. Rychkov, *Spinning Conformal Blocks*, *JHEP* **11** (2011) 154, [1109.6321].

[148] D. Karateev, P. Kravchuk and D. Simmons-Duffin, *Weight Shifting Operators and Conformal Blocks*, *JHEP* **02** (2018) 081, [1706.07813].

[149] M. S. Costa, T. Hansen and J. Penedones, *Bounds for OPE coefficients on the Regge trajectory*, *JHEP* **10** (2017) 197, [1707.07689].

[150] C. Sleight and M. Taronna, *Spinning Mellin Bootstrap: Conformal Partial Waves, Crossing Kernels and Applications*, *Fortsch. Phys.* **66** (2018) 1800038, [1804.09334].

[151] M. Kulaxizi, A. Parnachev and A. Zhiboedov, *Bulk Phase Shift, CFT Regge Limit and Einstein Gravity*, *JHEP* **06** (2018) 121, [1705.02934].

[152] M. Kologlu, P. Kravchuk, D. Simmons-Duffin and A. Zhiboedov, *Shocks, Superconvergence, and a Stringy Equivalence Principle*, *JHEP* **11** (2020) 096, [1904.05905].

[153] M. Kologlu, P. Kravchuk, D. Simmons-Duffin and A. Zhiboedov, *The light-ray OPE and conformal colliders*, *JHEP* **01** (2021) 128, [1905.01311].

[154] S. Weinberg, *Infrared photons and gravitons*, *Phys. Rev.* **140** (1965) B516–B524.

[155] R. Britto, F. Cachazo and B. Feng, *New recursion relations for tree amplitudes of gluons*, *Nucl. Phys. B* **715** (2005) 499–522, [hep-th/0412308].

[156] R. Britto, F. Cachazo, B. Feng and E. Witten, *Direct proof of tree-level recursion relation in Yang-Mills theory*, *Phys. Rev. Lett.* **94** (2005) 181602, [hep-th/0501052].

[157] A. Bzowski, P. McFadden and K. Skenderis, *Implications of conformal invariance in momentum space*, *JHEP* **03** (2014) 111, [1304.7760].

[158] M. S. Costa and T. Hansen, *Conformal correlators of mixed-symmetry tensors*, *JHEP* **02** (2015) 151, [1411.7351].

[159] A. Bzowski, P. McFadden and K. Skenderis, *Renormalised 3-point functions of stress tensors and conserved currents in CFT*, *JHEP* **11** (2018) 153, [1711.09105].

[160] A. Bzowski, P. McFadden and K. Skenderis, *Renormalised CFT 3-point functions of scalars, currents and stress tensors*, *JHEP* **11** (2018) 159, [1805.12100].

[161] J. M. Maldacena and G. L. Pimentel, *On graviton non-Gaussianities during inflation*, *JHEP* **09** (2011) 045, [1104.2846].

[162] D. Baumann, C. Duaso Pueyo, A. Joyce, H. Lee and G. L. Pimentel, *The Cosmological Bootstrap: Spinning Correlators from Symmetries and Factorization*, 2005.04234.

[163] S. Raju, *Four Point Functions of the Stress Tensor and Conserved Currents in AdS_4/CFT_3*, *Phys. Rev. D* **85** (2012) 126008, [1201.6452].

[164] E. Skvortsov, *Light-Front Bootstrap for Chern-Simons Matter Theories*, *JHEP* **06** (2019) 058, [1811.12333].

[165] B. Nagaraj and D. Ponomarev, *Spinor-Helicity Formalism for Massless Fields in AdS_4*, *Phys. Rev. Lett.* **122** (2019) 101602, [1811.08438].

[166] C. Closset, T. T. Dumitrescu, G. Festuccia, Z. Komargodski and N. Seiberg, *Comments on Chern-Simons Contact Terms in Three Dimensions*, *JHEP* **09** (2012) 091, [1206.5218].

[167] M. S. Costa, T. Hansen, J. a. Penedones and E. Trevisani, *Radial expansion for spinning conformal blocks*, *JHEP* **07** (2016) 057, [1603.05552].

[168] J.-F. Fortin, V. Prilepina and W. Skiba, *Conformal Four-Point Correlation Functions from the Operator Product Expansion*, *JHEP* **08** (2020) 115, [1907.10506].

[169] R. S. Erramilli, L. V. Iliesiu and P. Kravchuk, *Recursion relation for general 3d blocks*, *JHEP* **12** (2019) 116, [1907.11247].

[170] D. Simmons-Duffin, *Projectors, Shadows, and Conformal Blocks*, *JHEP* **04** (2014) 146, [1204.3894].

[171] S. Caron-Huot and A.-K. Trinh, *All tree-level correlators in $AdS_5 x S_5$ supergravity: hidden ten-dimensional conformal symmetry*, *JHEP* **01** (2019) 196, [1809.09173].

[172] H. Isono, T. Noumi and G. Shiu, *Momentum space approach to crossing symmetric CFT correlators*, *JHEP* **07** (2018) 136, [1805.11107].

[173] J. Liu, E. Perlmutter, V. Rosenhaus and D. Simmons-Duffin, *d-dimensional SYK, AdS Loops, and $6j$ Symbols*, *JHEP* **03** (2019) 052, [1808.00612].

[174] D. J. Binder, D. Z. Freedman and S. S. Pufu, *A bispinor formalism for spinning Witten diagrams*, *JHEP* **02** (2022) 040, [2003.07448].

[175] S. Albayrak and S. Kharel, *Towards the higher point holographic momentum space amplitudes*, *JHEP* **02** (2019) 040, [1810.12459].

[176] S. Albayrak, C. Chowdhury and S. Kharel, *New relation for Witten diagrams*, *JHEP* **10** (2019) 274, [1904.10043].

[177] Y.-Z. Li, *Notes on flat-space limit of AdS/CFT*, *work in progress* .

[178] H. Elvang and Y.-t. Huang, *Scattering Amplitudes*, 1308.1697.

[179] N. Arkani-Hamed, T.-C. Huang and Y.-t. Huang, *Scattering amplitudes for all masses and spins*, *JHEP* **11** (2021) 070, [1709.04891].

[180] S. Caron-Huot and M. Wilhelm, *Renormalization group coefficients and the S-matrix*, *JHEP* **12** (2016) 010, [1607.06448].

[181] B. I. Zwiebel, *From Scattering Amplitudes to the Dilatation Generator in N=4 SYM*, *J. Phys. A* **45** (2012) 115401, [1111.0083].

[182] T. He and P. Mitra, *Covariant Phase Space and Soft Factorization in Non-Abelian Gauge Theories*, 2009.14334.

[183] S. Weinberg, *Photons and gravitons in perturbation theory: Derivation of Maxwell's and Einstein's equations*, *Phys. Rev.* **138** (1965) B988–B1002.

[184] B. Bellazzini, C. Cheung and G. N. Remmen, *Quantum Gravity Constraints from Unitarity and Analyticity*, *Phys. Rev. D* **93** (2016) 064076, [1509.00851].

[185] S. D. Chowdhury, A. Gadde, T. Gopalka, I. Halder, L. Janagal and S. Minwalla, *Classifying and constraining local four photon and four graviton S-matrices*, *JHEP* **02** (2020) 114, [1910.14392].

[186] K. Häring and A. Zhiboedov, *Gravitational Regge bounds*, 2202.08280.

[187] V. K. Dobrev, G. Mack, V. B. Petkova, S. G. Petrova and I. T. Todorov, *Harmonic Analysis on the n-Dimensional Lorentz Group and Its Application to Conformal Quantum Field Theory*, vol. 63. 1977, 10.1007/BFb0009678.

[188] P. Kravchuk, *Casimir recursion relations for general conformal blocks*, *JHEP* **02** (2018) 011, [1709.05347].

[189] M. S. Costa, T. Hansen, J. a. Penedones and E. Trevisani, *Projectors and seed conformal blocks for traceless mixed-symmetry tensors*, *JHEP* **07** (2016) 018, [1603.05551].

[190] M. K. N. Balasubramanian, R. Patil and A. Rudra, *Spinning amplitudes from scalar amplitudes*, *JHEP* **11** (2021) 151, [2106.05301].

[191] Z. Bern, E. Herrmann, D. Kosmopoulos and R. Roiban, *Effective Field Theory Islands from Perturbative and Nonperturbative Four-Graviton Amplitudes to appear*, .

[192] G. Dvali, *Black Holes and Large N Species Solution to the Hierarchy Problem*, *Fortsch. Phys.* **58** (2010) 528–536, [0706.2050].

[193] M. J. Duff, *Observations on Conformal Anomalies*, *Nucl. Phys. B* **125** (1977) 334–348.

[194] Y.-Z. Li, H. Lu and L. Ma, *Hidden relations of central charges and OPEs in holographic CFT*, *JHEP* **11** (2021) 135, [2108.05384].

[195] D. M. Hofman and J. Maldacena, *Conformal collider physics: Energy and charge correlations*, *JHEP* **05** (2008) 012, [0803.1467].

[196] A. Buchel, R. C. Myers and A. Sinha, *Beyond eta/s = 1/4 pi*, *JHEP* **03** (2009) 084, [0812.2521].

[197] J. Albert and L. Rastelli, *Bootstrapping Pions at Large N*, 2203.11950.

[198] L.-Y. Chiang, Y.-t. Huang, L. Rodina and H.-C. Weng, *De-projecting the EFThedron*, 2204.07140.

[199] Z. Bern, D. Kosmopoulos and A. Zhiboedov, *Gravitational effective field theory islands, low-spin dominance, and the four-graviton amplitude*, *J. Phys. A* **54** (2021) 344002, [2103.12728].

[200] J. Henriksson, B. McPeak, F. Russo and A. Vichi, *Bounding Violations of the Weak Gravity Conjecture*, 2203.08164.

[201] H. Kawai, D. Lewellen and S.-H. Tye, *A relation between tree amplitudes of closed and open strings*, *Nuclear Physics B* **269** (1986) 1–23.

[202] Z. Bern, J. J. M. Carrasco and H. Johansson, *Perturbative Quantum Gravity as a Double Copy of Gauge Theory*, *Phys. Rev. Lett.* **105** (2010) 061602, [1004.0476].

[203] Z. Bern, J. J. Carrasco, M. Chiodaroli, H. Johansson and R. Roiban, *The Duality Between Color and Kinematics and its Applications*, 1909.01358.

[204] C. Sleight and M. Taronna, *From AdS to dS exchanges: Spectral representation, Mellin amplitudes, and crossing*, *Phys. Rev. D* **104** (2021) L081902, [2007.09993].

[205] M. Hogervorst, J. a. Penedones and K. S. Vaziri, *Towards the non-perturbative cosmological bootstrap*, 2107.13871.

[206] H. Gomez, R. L. Jusinskas and A. Lipstein, *Cosmological Scattering Equations*, *Phys. Rev. Lett.* **127** (2021) 251604, [2106.11903].

[207] H. Gomez, R. Lipinski Jusinskas and A. Lipstein, *Cosmological scattering equations at tree-level and one-loop*, *JHEP* **07** (2022) 004, [2112.12695].

[208] J. M. Maldacena, *Non-Gaussian features of primordial fluctuations in single field inflationary models*, *JHEP* **05** (2003) 013, [astro-ph/0210603].

[209] H. Lee and X. Wang, *Cosmological Double-Copy Relations*, 2212.11282.

[210] M. S. Costa, V. Goncalves and J. a. Penedones, *Spinning AdS Propagators*, *JHEP* **09** (2014) 064, [1404.5625].

[211] Y.-Z. Li and J. Mei, *Toward higher point AdS amplitudes in Mellin space*, *to appear* .

[212] J. A. Farrow, A. E. Lipstein and P. McFadden, *Double copy structure of CFT correlators*, *JHEP* **02** (2019) 130, [1812.11129].

[213] C. Armstrong, H. Gomez, R. Lipinski Jusinskas, A. Lipstein and J. Mei, *New recursion relations for tree-level correlators in anti–de Sitter spacetime*, *Phys. Rev. D* **106** (2022) L121701, [2209.02709].

[214] C. Armstrong, H. Gomez, R. Lipinski Jusinskas, A. Lipstein and J. Mei, *Effective field theories and cosmological scattering equations*, *JHEP* **08** (2022) 054, [2204.08931].

[215] X. Zhou, *Double Copy Relation in AdS Space*, *Phys. Rev. Lett.* **127** (2021) 141601, [2106.07651].

[216] A. Bissi, G. Fardelli, A. Manenti and X. Zhou, *Spinning correlators in $\mathcal{N} = 2$ SCFTs: Superspace and AdS amplitudes*, 2209.01204.

[217] C. Sleight and M. Taronna, *From dS to AdS and back*, *JHEP* **12** (2021) 074, [2109.02725].

[218] D. Baumann, D. Green, A. Joyce, E. Pajer, G. L. Pimentel, C. Sleight et al., *Snowmass White Paper: The Cosmological Bootstrap*, in *2022 Snowmass Summer Study*, 3, 2022, 2203.08121.

[219] C. Sleight, *A Mellin Space Approach to Cosmological Correlators*, *JHEP* **01** (2020) 090, [1906.12302].

[220] N. Arkani-Hamed, D. Baumann, H. Lee and G. L. Pimentel, *The Cosmological Bootstrap: Inflationary Correlators from Symmetries and Singularities*, *JHEP* **04** (2020) 105, [1811.00024].

[221] D. Baumann, C. Duaso Pueyo, A. Joyce, H. Lee and G. L. Pimentel, *The cosmological bootstrap: weight-shifting operators and scalar seeds*, *JHEP* **12** (2020) 204, [1910.14051].

[222] D. Baumann, C. Duaso Pueyo and A. Joyce, *Bootstrapping Cosmological Correlations*, *AAPPS Bull.* **30** (2020) 2–9.

[223] V. Goncalves, J. Penedones and E. Trevisani, *Factorization of Mellin amplitudes*, *JHEP* **10** (2015) 040, [1410.4185].

[224] S. Duary, E. Hijano and M. Patra, *Towards an IR finite S-matrix in the flat limit of AdS/CFT*, 2211.13711.

[225] S. Duary, *AdS correction to the Faddeev-Kulish state: Migrating from the Flat Peninsula*, 2212.09509.

[226] R. J. Eden, P. V. Landshoff, D. I. Olive and J. C. Polkinghorne, *The analytic S-matrix*. Cambridge Univ. Press, Cambridge, 1966.

[227] Z. Bern, E. Herrmann, D. Kosmopoulos and R. Roiban, *Effective Field Theory islands from perturbative and nonperturbative four-graviton amplitudes*, *JHEP* **01** (2023) 113, [2205.01655].

[228] J. Qiao, *Classification of Convergent OPE Channels for Lorentzian CFT Four-Point Functions*, *SciPost Phys.* **13** (2022) 093, [2005.09105].

[229] E. D'Hoker, D. Z. Freedman, S. D. Mathur, A. Matusis and L. Rastelli, *Graviton exchange and complete four point functions in the AdS / CFT correspondence*, *Nucl. Phys. B* **562** (1999) 353–394, [hep-th/9903196].

[230] F. A. Dolan and H. Osborn, *Conformal partial waves and the operator product expansion*, *Nucl. Phys. B* **678** (2004) 491–507, [hep-th/0309180].

[231] F. A. Dolan and H. Osborn, *Conformal four point functions and the operator product expansion*, *Nucl. Phys. B* **599** (2001) 459–496, [hep-th/0011040].

[232] S. Caron-Huot, Y. Gobeil and Z. Zahraee, *The leading trajectory in the 2+1D Ising CFT*, 2007.11647.

[233] E. Hijano, P. Kraus, E. Perlmutter and R. Snively, *Witten Diagrams Revisited: The AdS Geometry of Conformal Blocks*, *JHEP* **01** (2016) 146, [1508.00501].

[234] Y.-Z. Li and H.-Y. Zhang, *More on heavy-light bootstrap up to double-stress-tensor*, *JHEP* **10** (2020) 055, [2004.04758].

[235] W. Li, *Closed-form expression for cross-channel conformal blocks near the lightcone*, *JHEP* **01** (2020) 055, [1906.00707].

[236] W. Li, *Lightcone expansions of conformal blocks in closed form*, *JHEP* **06** (2020) 105, [1912.01168].

[237] W. Li, *Factorized lightcone expansion of conformal blocks*, 2012.09710.

[238] J. D. Edelstein, R. Ghosh, A. Laddha and S. Sarkar, *Causality constraints in Quadratic Gravity*, *JHEP* **09** (2021) 150, [2107.07424].

[239] W. Landry and D. Simmons-Duffin, *Scaling the semidefinite program solver SDPB*, 1909.09745.

[240] J. M. Martin-Garcia, *xact: Efficient tensor computer algebra for mathematica*, *http://xact.es/* .